

# Taxonomy, Phylogeny and Paleobiogeography of the Cassiduloid Echinoids

By

Camilla Alves Souto

A dissertation submitted in partial satisfaction of the

requirements for the degree of

Doctor of Philosophy

in

Integrative Biology

in the

Graduate Division

of the

University of California, Berkeley

Committee in charge:

Professor Charles R. Marshall, Chair

Professor Rauri Bowie

Professor Kipling Will

Professor Richard Mooi

Fall 2018

Taxonomy, Phylogeny and Paleobiogeography of the Cassiduloid Echinoids

Copyright 2018  
by  
Camilla Alves Souto

## Abstract

### Taxonomy, Phylogeny and Paleobiogeography of the Cassiduloid Echinoids

By

Camilla Alves Souto

Doctor of Philosophy in Integrative Biology

University of California, Berkeley

Professor Charles R. Marshall, Chair

Cassiduloids are rare and poorly known irregular echinoids, which include the sand dollars and heart urchins, that typically live buried in the sediment, where they feed on small organic particles. Cassiduloids evolved during the Marine Mesozoic Revolution, but despite their rich fossil record, species richness (diversity) is very low. The goal of this thesis is to improve our taxonomic knowledge of the group, propose hypotheses of relationship among its representatives and analyze their patterns of geographic distribution through time, thereby contributing to our understanding of their evolutionary history.

In the first chapter<sup>1</sup>, I used synchrotron radiation-based micro-computed tomography (SR $\mu$ CT) images of type specimens to describe a new *Cassidulus* species and a new cassiduloid genus that could not have been discovered with traditional techniques. I also designate a neotype for the type species of the genus *Cassidulus*, *Cassidulus caribaeorum*, provide remarks on the taxonomic history of each taxon, a diagnostic table of all living cassidulid species, and extend the known geographic and bathymetric range of two species. Besides rendering novel morphological data, the SR $\mu$ CT images provided significant insights in the evolution of bourrelets of these cassiduloid echinoids. However, determining how the bourrelets have evolved, as well as the evolution of all the cassiduloid traits, requires a phylogenetic framework of the group.

Therefore, in the second chapter, I reconstructed the phylogeny of the cassidulids using morphological characters and inferred their patterns of geographical distribution through time. Because morphological and geographic histories are erased by extinctions, unraveling phylogenetic relationships and biogeographic patterns based on only the living species can be challenging, especially for groups that have experienced extensive extinction such as the cassiduloids. Studies have shown that fossil taxa generally improve phylogenetic resolution because of their unique morphological information that have often been modified in Recent species. Thus, inclusion of fossils can be critical to addressing evolutionary questions. Surprisingly for marine invertebrates, there are relatively few studies that have included fossils in their phylogenetic and biogeographic analyses. I performed a cladistic analysis of 45 cassidulids based on 98 characters, which resulted in 24 most-parsimonious trees. The monophyly of the family Cassidulidae was not supported because the genera *Eurhodia* and *Glossaster* were placed within the family Faujasiidae. Analyses to determine the sensitivity of the resulting clades to missing data

did not result in significantly different topologies or resolution of the tree, but the coding of partial uncertainties changed the relationship within some subclades (particularly within genera). The taxonomic implications of these results and the evolution of some morphological features are discussed. The evolutionary history of the cassiduloids has been dominated by high levels of homoplasy and a dearth of unique novel traits. The cassiduloids (as defined in this study) most likely originated in the Early Cretaceous (oldest records from the Aptian), and no conspicuous novelties were added during their evolution. Biogeographically, a time-stratified DEC model with range constraints indicates that the cassidulids had a south Tethyan and northwest Atlantic origin probably dating back to the Late Cretaceous (Campanian–Maastrichtian) or Paleocene. Most cassiduloids are endemic to small regions and their evolution has mostly been influenced by dispersal rather than vicariant events. Speciation occurred mainly within the northwest Atlantic during the Late Paleocene to the early Eocene. Despite their high diversity during the Paleogene, cassidulids and faujasiids have only seven extant species, and three of them are relicts of lineages that date back to the Eocene. Future studies of the biology of these poorly known species, some of which brood their young, will yield further insights into the evolutionary history of this group.

While the first two chapters focused on cassiduloids, the third chapter is a broader macroevolutionary study of the echinoids. Specifically, I performed an analysis of how their genus richness (diversity) has changed since their appearance in the fossil record and estimated the turnover rates (origination and extinction) throughout their evolutionary history. The ability to document macroevolutionary trends has been accelerated by the development of free-access online databases. However, despite their undeniable benefit to research, these databases are not free from error and their data need to be checked on a regular basis. Therefore, with the goal of analyzing the echinoid's diversity dynamics since their appearance in the fossil record, I assess the quality of the echinoid entries in the Paleobiology Database (PBDB), correct errors and improve the dataset by including missing information. Assessments of data quality included cross-referencing classifications and checking stratigraphic ranges and synonymies against the literature. The entries in the PBDB were derived from 1,100 references and include ~9,500 occurrences representing 445 genera, about 65% of all valid echinoid genera. Fifty percent of the occurrences were from Europe and the USA, and 41% percent were from the Cretaceous. Genus classifications were mostly outdated and some species were misclassified. Diversity curves were then generated using three different methods to account for preservation and sampling biases. Overall, the echinoid data from the PDBD reflected major trends known for the evolution of the class (e.g. increased diversification during the Marine Mesozoic Revolution) and recovered extinction events that have affected all marine biota (e.g. the end-Cretaceous mass extinction). However, spatial, temporal and taxonomic biases exist, so we need to be mindful of these when analyzing the data. The fossil record of the echinoids dates back to the Middle Ordovician. Although affected by mass extinctions, the group's diversity has been steadily increasing since the origin of the irregular echinoids in the Mesozoic. In addition to the echinoid diversity curve and turnover rates, contrasting and similar diversity trajectories for closely related major echinoid clades are also presented.

---

<sup>1</sup> This work is already published and is included in this dissertation with permission from my sole co-author. The citation is as follows: Souto, C. & Martins, L. 2018. Synchrotron micro-CT scanning leads to the discovery of a new genus of morphologically conserved echinoid (Echinodermata: Cassiduloida). *Zootaxa*, 4457(1), 70–92.

To my families, biological and otherwise,  
for the encouragement, support, patience and unconditional love;

To my mentors,  
for provoking in me thought and acquisition of knowledge;

To everyone who has gifted me with a thought,  
for opening my mind and enriching the way I think about the world;

To trailblazing women who move the world forward by their daring attitudes,  
rolled-up-sleeves work ethic, and blatant disregard for norms.

## Table of Contents

List of Figures	iii
List of Tables	v
Introduction	vi
1. Synchrotron micro-CT scanning leads to the discovery of a new genus of morphologically conserved echinoid (Echinodermata: Cassiduloida)	1
2. Homoplasy, endemism, and extinction: phylogeny and biogeography of the cassidulid echinoids (Echinodermata)	26
3. Estimating echinoid diversity dynamics from open-access databases: pitfalls and evolutionary trends	69
Bibliography	83
Appendices	97

## List of Figures

1.1. <i>Cassidulus briareus</i> sp. nov.: images of the test of holotype and of paratype .....	5
1.2. <i>Cassidulus briareus</i> sp. nov.: SR $\mu$ CT-based volume renderings of apical system, petals and phyllodes; and drawings of phyllodes, ambulacrum and periproct .....	6
1.3. <i>Cassidulus caribaeorum</i> (?): images of the test and drawings of phyllodes and petal.....	9
1.4. <i>Cassidulus caribaeorum</i> : images of the test of neotype and SR $\mu$ CT-based volume renderings of apical system, phyllodes and periproct.....	12
1.5. <i>Cassidulus caribaeorum</i> : SEM images of juveniles, spines and sphaeridia.....	13
1.6. <i>Cassidulus caribaeorum</i> : SEM images of pedicellariae.....	14
1.7. <i>Kassandrina malayana</i> comb. nov.: images of the test of syntype; and <i>Kassandrina florescens</i> comb. nov.: images of the test .....	17
1.8. <i>Kassandrina malayana</i> comb. nov.: SR $\mu$ CT-based volume renderings of oral region of test, apical system, petal, phyllodes, ambulacrum and periproct; and drawings of phyllodes.....	18
1.9. <i>Kassandrina malayana</i> comb. nov.: SEM images of pedicellariae and spine.....	19
1.10. SR $\mu$ CT-based volume renderings of bourrelets from <i>Cassidulus briareus</i> sp. nov. and from <i>Kassandrina malayana</i> comb. nov.....	21
2.1. Previous morphology-based phylogenetic hypotheses of relationship within cassidulids, and among cassidulids, faujasiids and neolampadids .....	28
2.2. Outline drawings of cassiduloid tests depicting differences in shape.....	38
2.3. Drawings of a petal showing measurements for characters 21 and 23, and character states for petal shape (character 25).....	40
2.4. Drawings of the ambulacral plates beyond the posterior petals .....	41
2.5. Drawing of the posterior ambulacrum showing the measurements for characters 34 and 36, and outline drawings of tests showing different ambulacral expansion types.....	42
2.6. Outline drawings of the cross-section of the test along the anterior-posterior axis, $\mu$ CT image of the periproct of <i>Oligopodia epigonus</i> in internal view, and drawings of the different periproctal plate arrangements and placement of anal opening.....	44
2.7. Drawings of the adoral region of the test.....	46
2.8. Drawings of phyllopores and of posterior phyllodes.....	47
2.9. Drawings of ophicephalous and tridentate pedicellariae .....	48
2.10. Strict consensus of 24 MPTs recovered by Analysis 1 .....	56
2.11. Preferred tree topology with best stratigraphic congruence from A1 and proposed designation for the families Cassidulidae and Faujasiidae .....	57
2.12. 50% majority-rule consensus of 24 MPTs recovered by Analysis 1 and Analysis; and 20 MPTs recovered by Analysis .....	58

2.13. Plot with the consistency and retention indexes for characters in A1 .....	60
2.14. Mirrored trees depicting the Maximum Parsimony optimization of “Periproct position” and “Minimum number of plates on I5, between the basicoronal plate and the base of the periproct” .....	61
2.15. Mirrored trees depicting the Maximum Parsimony optimization of “Periproct orientation” and “Minimum number of plates framing the periproct” .....	62
2.16. 50% majority-rule consensus of 4 MPTs recovered by Analysis 4.....	63
2.17. Ancestral area reconstruction of clade F inferred by the dispersal-extinction-cladogenesis (DEC) model with range and time-stratified dispersal constraints .....	67
2.18. Ancestral area reconstruction of clade I inferred by the dispersal-extinction-cladogenesis (DEC) model with range and time-stratified dispersal constraints .....	68
3.1. Workflow followed to retrieve and assess the Paleobiology Database echinoid dataset .....	71
3.2. Number of Paleobiology Database entries per year.....	73
3.3. Phylogenetic coverage of the echinoid Paleobiology Database (PBDB) occurrences .....	74
3.4. Comparison among echinoid diversity curves derived from the PBDB dataset, the modified dataset and the final dataset .....	77
3.5. Comparison among diversity curves of major echinoid groups derived from the PBDB dataset, the modified dataset and the final dataset.....	77
3.6. Echinoid diversity curve through time.....	78
3.7. Echinoid per-capita origination and extinction rates through time.....	79
3.8. Comparison between diversity trajectories of major echinoid groups derived from the final dataset .....	81



## List of Tables

1.1. Information about the specimens analyzed using SR $\mu$ CT .....	3
1.2. Diagnostic morphological traits distinguishing the extant cassidulid species. Numbers in parentheses indicate rare occurrences .....	24
2.1. Classification of the selected ingroup genera according to previous and hypotheses of present study .....	27
2.2. List of taxa included in the phylogenetic analyses and used for the phylogenetic calibration, their stratigraphic range, geographic distribution, and the character coding completeness for each species.....	32
2.3. Status of the known cassidulid taxa prior to analysis .....	36
2.4. List of taxa chosen <i>a posteriori</i> to aid phylogenetic calibration, their stratigraphic range, geographic distribution, clade assigned and characters used for assignment .....	51
3.1. Characteristics of the echinoid dataset downloaded from the Paleobiology Database.....	75

## Introduction

My curiosity about the cassiduloids started when I was an undergraduate student at the Federal University of Bahia, in Brazil. Among the regular urchins and sand dollars at our local zoology museum, there were also enigmatic irregular echinoids (cassiduloids) I had never seen before; and they had been collected just a few miles away. While the species was first described (poorly) as *Cassidulus infidus* by Theodor Mortensen in 1948, my research soon revealed how little we knew about it, and indeed the whole group. For example, *C. infidus* was known only from the holotype, a denuded test free of spines or pedicellariae; as a result, in the only phylogeny that included this species, published by Sherman Sutter in 1994, there were missing data for characters related to these structures and the resulting topology included a trichotomy with the three Atlantic *Cassidulus* species. The sister taxon to this clade was *Rhyncholampas pacificus* Agassiz from the East Pacific, and the sister taxon to the (Atlantic *Cassidulus* + *R. pacificus*) clade was the other extant *Cassidulus* known at the time, *C. malayanus* Mortensen, from Indonesia. So, I decided to re-describe *C. infidus* and reanalyze its morphology to see if the new traits would improve the phylogenetic resolution. The paraphyly of *Cassidulus* was another interesting problem that I had to set aside until I had access to specimens and resources; Chapters 1 and 2 revealed why Sherman's results were not mistaken.

In addition to being interested in the phylogenetic relationships within the group, I was also curious about their geographic distribution. Cassiduloids live mostly in warm shallow water and they are often restricted to small regions and bathymetries. To make it even more interesting, cassiduloids have a great fossil record, which means their evolutionary history has been well preserved. I wanted to find out if the fossil record could explain the disjunct distribution of the extant *Cassidulus* species and give insights about their divergence from their sister genus, *Rhyncholampas*, often considered synonymous with *Cassidulus*. Analyzing the phylogeny and biogeography of the genera *Cassidulus* and *Rhyncholampas* was the goal of my Master's thesis, which, after one year, proved to be an impossible task to be completed in such a short time.

As a neontologist, I had no idea of what a "rich fossil record" meant, nor that our knowledge of the fossil record was so disorganized. My literature search revealed that both genera were composed of dozens of species, most of them probably not valid; but because of their poor descriptions, a morphological analysis of the specimens was necessary to unravel the history of the group. After analyzing almost 250 papers, this species list is yet to be completed.

So for my Master's, I took a step back and decided to analyze the relationships within the family Cassidulidae, composed of five genera including *Cassidulus* and *Rhyncholampas*. I was pleased to notice that although the literature on fossil cassidulids was overwhelmingly large and complex, the fossil specimens were often amazingly well preserved. With the short time I had left to complete my Master's, I developed a cassidulid phylogeny that showed me that "much was hidden under the tree of the living species" and only the fossil record could reveal the group's history. Once again, I realized that I needed to take a step back and broaden the scope of the phylogenetic analysis.

Cassiduloids have a very interesting evolutionary history. In addition to their puzzling geographic distribution, they show a variety of reproductive modes (though their biology is severely understudied), from planktotrophic species to brooders with a marsupium, and their morphology is very boring. And yes, boring is quite interesting! Boring groups are destined to fail; nevertheless, cassiduloid are still among us and doing biologically interesting things such as caring for their young, being functional while completely buried in sediment and escaping voracious

gastropods. Finding morphological differences among congeneric species is not an easy task and when differences are found, most often related to shape, describing them and converting them into characters is challenging. Genetics, development, bad luck; for whatever reason, cassiduloids have not evolved many novel traits in tens of millions of years (although some could argue that cassiduloids in the broad Porter Kier's sense are the dinosaurs and sand dollars are the birds, I here refer to the cassiduloids in the strict sense presented in Chapter 2 and also partially supported by Kroh & Smith's [2010] phylogeny; and in any case, the disparity in non-avian dinosaurs swamps the disparity of birds, while even the cassiduloids sensu Kier are much less disparate than the sand dollars). However, three-dimensional images produced by x-ray micro-computed tomography ( $\mu$ CT) proved to be great resources to analyze and describe the cassiduloid's morphological uniformity.

The echinoid test is composed of numerous calcified plates, bound together by connective tissue, forming a compact body. The first great advantage of the  $\mu$ CT images was that they allowed me to analyze the internal part of the test. Breaking the compact echinoid test is not welcomed by museum curators, especially when specimens are rare, like the cassiduloids. Also, their test is very fragile. Many specimens I analyzed were broken into small pieces and making a sense of where each plate should go was not always straightforward. In addition,  $\mu$ CT images revealed each individual plate, allowing me to describe and compare them, instead of trying to describe the body shape as a whole. Although I have not included most of the  $\mu$ CT data that I generated in this dissertation (because it turns out that getting enough contrast to generate  $\mu$ CT images from fossil echinoids that fed on calcareous sediment is not viable), I present in Chapter 1 some discoveries I made using this approach: the description of a new species of *Cassidulus* and of a new cassidulid genus. The new genus, in special, revealing an amazing case of convergence within the cassiduloids: the multiple independent formation of the bourrelets. These are mounds formed around the echinoid mouth, which contain many specialized spines that serves as cutlery, sorting, grabbing and bringing sediment into the mouth. All cassiduloids (in the strict sense) have bourrelets; some are poorly developed, others are large and pointy. However, looking from the inside of the test, I noticed that these mounds may be formed in two different ways: by the accretion of stereom (carbonate) on the outside of the test or by the depression of the plate from the inside, which projects it outwards. In addition to revealing the new genus, this discovery also played a major role in the phylogenetic analyses performed in Chapter 2, although I could not analyze the bourrelets in all fossil species.

My second attempt to reconstruct the phylogeny of the cassidulids after my Master's work included three times as many ingroup species, four times as many outgroups, and three times as many characters. The results were unexpected, although not too surprising. The cassidulid genera were separated into lineages that did not share a common cassidulid ancestor. Two genera remained, together with other species that should be in different, maybe even undescribed, genera. The analyses also revealed that the "boring" cassiduloid morphology results from the fact that they have been re-evolving the same character states over and over, and that the extant cassiduloids are relicts of ancient lineages whose diversity have been sharply reduced since the Oligocene. Chapter 2 also includes a paleobiogeographic analysis, with hypotheses for the origin and geographic expansion of the group throughout their history. Surprisingly, although extant cassidulids are brooders and endemic to small regions, their ancestors crossed oceans multiple times. More phylogenetic and paleobiogeographic studies of the cassiduloids should follow. Hopefully, by the time they are done, additional data on the population biology and ecology of the cassiduloids will allow for thorough analyses of their evolutionary history.

Although currently depauperate, the species richness of the cassiduloids was once very high; according to Kier's counts, they composed 40% of all echinoids in the Eocene. To understand the reasons why the group's diversity has been decreasing, I wanted first to analyze when that happened. Also, was the decrease gradual or abrupt? Was it geographically biased? To approach these questions, I decided to analyze the change in cassiduloid diversity through time using the most complete database for paleontological data: the Paleobiology Database (PBDB). While analyzing the PBDB data, I noticed that the number of cassiduloid occurrences was too low to allow for robust results. Also, the taxonomy of many entries needed revision. Therefore, I changed the scope of my analysis to include all echinoids. And to increase the confidence level of the results, I first assessed the quality of the data entered in the PBDB and also detected genera and stratigraphic intervals with missing information. Chapter 3 presents these results in addition to an analysis of the echinoid diversity dynamics. Future work will include adding the missing information to the PBDB to reanalyzing the diversity curve of the group as a whole and, ultimately, of the cassiduloids.

## Acknowledgements

My journey so far has taken me to many places, but these last seven years in the Bay Area were probably the most intense and rewarding. So much, diversity, so many flavors, so many opportunities. Though overwhelming at times, I'm happy to have embraced as many opportunities as I could. Professionally, these include activities in research, teaching and outreach; for each, I'm grateful for having received support from amazing people, including:

My supervisor, Charles Marshall, whose support has been unconditional and generous; I appreciate the encouragement, advice, discussions, last minute comments on writings, and, of course, the good humor and the willingness to allow me host the soccer world cup in the lab. My co-supervisor Rich Mooi, to whom I am grateful for timeless discussions (mostly about echinoids), for providing interesting specimens, encouragement and careful revisions of manuscripts, for letting me borrow his precious books, and for believing in my potential. And the other members of my dissertation committee, Rauri Bowie and Kip Will, for valuable comments on my writings and encouragement.

My lab peers who were literally by my side all these years at Cal. I'm grateful not only for the interesting and thoughtful discussions we've had in so many varied topics but also for their company during out-of-science activities. Also thankful to Daniel Varajão de Latorre for making me realize that *baianês* is a different language, to Jun Ying Lim for biogeographic discussions that improved Chapter 2, Ashley Poust for amusing me with very interesting curiosities (many of them about echinoderms), Mathias Pires (unfortunately for a brief period) for being my personal trainer, and especially Lucy Chang for keeping me sane around "the boys" and for her immense help with the R analyses presented in Chapter 3.

The UCB faculty, often with open doors to graduate students; discussions with them broadened my scope about evolutionary biology, especially those with David Lindberg, Ivo Duijnste, Seth Finnegan and Nipam Patel. The UCMP community for the support; also, the Fossil Coffee talks, the Fossil Fuel gatherings and Seth's field trips were enriching and memorable. I'm also grateful for having had the opportunity to learn from my 363 Cal students. The CalAcademy IZG community that received me with open arms as one of their own and provided me with space, access to collections and specimen numbers: Christina Piotrowski, Elizabeth Kools, Kelly Markelo, Jean DeMouthe (*in memoriam*) and Christine Garcia. Dula Parkinson and Harold Barnard (ALS-LNBL; Beamline 8.3.2) provided technical support to generate the SR $\mu$ CT imagery. Lydia Smith for her patience with walking me through DNA library preparation and for her dedication to making my samples work (I'm still hoping it will!).

Alexander Ziegler and Dula Parkinson provided interesting comments for Chapter 1, Cynthia Manso and Angela Zanata provided interesting comments for an early version of Chapter 2, and Andreas Kroh provided thoughtful comments to both chapters and has given great support to my research.

Friends and Cal peers for keeping me sane and cheerful all these years, especially Renske Kirchholtes (who still owes me personal training sessions), Eric Armstrong, Deise Cruz and my Milvinian roomies.

Finally, I'm eternally grateful to have a powerful support system and to be surrounded by joy, encouragement and love, which often crosses oceans and forests bringing me courage and strength: from my family, who has always believed and cheered for me even though they might have never understood what I was doing (and I'm sure I've never explained it properly); from my extended family, Luciana Martins and Wagner Magalhães, for being there for me throughout my

entire journey and whose connection has been a precious gift; and from my wife, Rina Bhagat, who has been nothing but supportive, understanding, and loving even during stressful moments of graduate student life.

My research was facilitated by dedicated museum curators and collection managers who granted me access to scientific collections and/or sent me specimens on loan and/or sent me images of specimens: Stephen Keable and Ross Pogson (AM), Gordon Hendler and Cathy Groves (LACM), Austin Hendy and Kathryn Estes-Smargiassi (LACMIP), Emese Bodor, Zoltán Lantos and Palotás Klára (MBFSZ), Adam J. Baldinger and Gonzalo Giribet (MCZ), Pierre-Alain Proz and Lionel Cavin (MHNG GEPI), Jean Mariaux (MHNG INVE), Marc Eleaume, Anouchka Sato, Sylvain Charbonnier and Jocelyn Falconnet (MNHN), Renato Ventura (MNRJ), Jolanta Jurkowska (MP MNHWU), Tim O'Hara, Melanie Mackenzie, David Holloway and Frank Holmes (MV), Andrew Cabrinovic and Timothy A.M. Ewin (NHMUK), Andreas Kroh (NHMW), Walter Etter (NMB), Jon Norenburg, Chad Walter, Jennifer Strotman, Kathy Hollis and Mark Florence (NMNH), Sabine Stöhr (SMNH), Roger W. Portell, John D. Slapcinsky, Gustav Paulay (UF), Carla Menegola (UFBA), Cynthia Manso (UFISITAB), Joke Bleeker (Naturalis Biodiversity Center), Carsten Lüter, (ZMB), Jørgen Olesen and Tom Schiøtte (ZMUC), and Michela Borges (ZUEC).

Also, I would not have been able to visit many of these institutions without the financial support I received from the Leeper Fund, the Robert and Nancy Beim Endowed Graduate Field Research Fund, and the Dissertation Completion Award (Department of Integrative Biology, University of California, Berkeley); the UCMP Annie Alexander Fund and the Palmer Fund (UCMP); the Systematics Research Fund (the Systematics Association and the Linnean Society of London); the Berkeley Chapter of Sigma Xi; the Vokes Grants-in-Aid Program (UF); and the 2016 NHM IP Collections Study Grant (LACMIP). My work also benefited from a grant of the French state managed by the Agence nationale de la Recherche via the programme "Investissements d'avenir" (ANR-11-INBS-0004-RECOLNAT), and used resources of the Advanced Light Source, which is a DOE Office of Science User Facility under contract number DE-AC02-05CH11231.

# CHAPTER 1

## **Synchrotron micro-CT scanning leads to the discovery of a new genus of morphologically conserved echinoid (Echinodermata: Cassiduloidea)**

### **Introduction**

The taxonomic treatment of the genus *Cassidulus* dates back to Lamarck (1801). Upon describing *Cassidulus*, Lamarck provided a brief and broad description of the genus and included three species, two of which are *nomina nuda* (*Cassidulus belgicus* Lamarck, 1801, which was later included in the synonymy list of *Procassidulus lapiscancri* (Leske, 1778) by Lamarck [1837, p. 516], and *Cassidulus scutellatus* Lamarck, 1801), and one, *Cassidulus caribaeorum* Lamarck, 1801, is valid. Since then, *C. caribaeorum* has been recognized as the type species of the genus even though to our knowledge, no formal designation has ever been done. As early as 1830 Blainville recognized the possibility that this genus was not a natural unit. A. Agassiz (1869) attempted to reclassify its extant species, but he deliberately excluded fossil species. Descriptions of cassiduloid species (both extinct and extant) and genera remained vague throughout the 1800s and early 1900s, partly because the morphology of the group is conserved (Wagner 2000) but also because the original diagnoses are vague. Rates of morphological change in cassiduloids appear to be very low and differences among species are mostly related to slight changes in shape rather than differences in numeric traits, or to the evolution of novel traits (see high levels of homoplasy reported by Suter [1994a,b]). As a result, taxonomic assignments have lacked explicit justifications, and the genus *Cassidulus*, the type genus of the order Cassiduloidea, became a repository of species of unknown phylogenetic placement, especially for fossils. Echinoid workers have recognized this issue and at least 80 fossil *Cassidulus* species have now been transferred to other genera (e.g. Bittner 1892; Cooke 1959; Kier 1962). Nonetheless, there is still much taxonomic work to be done.

In this paper, we use synchrotron radiation-based micro-computed tomography (SR $\mu$ CT) images to provide thorough morphological descriptions and generate hypotheses of relationships for three cassiduloid species. Specifically, we describe a new genus to accommodate the species *Cassidulus malayanus* and *Australanthus florescens*, a new species of *Cassidulus* from Australia, and designate a neotype for *Cassidulus caribaeorum*. We also synthesize the taxonomic history of each taxon, extend the known geographic and bathymetric range of *C. caribaeorum* and *C. malayanus*, and provide SR $\mu$ CT images depicting the plate patterns of the new taxa. In addition, a diagnostic table that includes all living cassidulid species is provided.

Micro-computed tomography, together with magnetic resonance imaging (MRI), has proven to be a valuable tool for taxonomic studies by providing an immense amount of morphological data without damaging the specimens (Ziegler 2012; Faulwetter et al. 2013; Zamora et al. 2015; Carbayo et al. 2016; Okanishi et al. 2017). Indeed, the discovery of the genus described herein would not have been possible without the analysis of the internal architecture of the specimen, enabled by SR $\mu$ CT images.

## Materials and Methods

Abbreviations: scanning electron microscopy (SEM), length (L), width (W), test height (TH), test length (TL), test width (TW), holotype (H), neotype (N), paratype (P), syntype (S), limestone (Lst), formation (Fm). Acronyms: Advanced Light Source, Lawrence Berkeley National Laboratory, Berkeley, U.S.A. (ALS-LBNL); Australian Museum, Sydney, Australia (AM); California Academy of Sciences, San Francisco, U.S.A. (CAS; Invertebrate Zoology collections, CASIZ; Geology collections, CASG); Los Angeles County, Natural History Museum, Los Angeles, U.S.A. (LACMIP); Muséum National d'Histoire Naturelle, Paris, France (MNHN); Museu Nacional, Rio de Janeiro, Brazil (MNRJ); Muzeum Przyrodnicze Uniwersytetu Wrocławskiego, Wrocław, Poland (MP MNHWU); Museum Victoria, Melbourne, Australia (MV); Natural History Museum, London, United Kingdom (NHM-UK); National Museum of Natural History, Washington D.C., U.S.A. (NMNH); Swedish Museum of Natural History, Stockholm, Sweden (SMNH); University of California, Museum of Paleontology, Berkeley, U.S.A. (UCMP); Florida Museum of Natural History, Gainesville, U.S.A. (UF); Museu de Zoologia, Universidade Federal da Bahia, Salvador, Brazil (UFBA); Zoological Museum, University of Copenhagen, Denmark (ZMUC); Museu de Zoologia da Universidade Estadual de Campinas, Campinas, Brazil (ZUEC).

The plate patterns of the living taxa were visualized using SR $\mu$ CT images obtained at the ALS-LBNL (beamline 8.3.2). Synchrotrons can produce X-ray beams with extremely high flux and thus they have high penetrating ability. The number of synchrotron facilities worldwide is limited compared to lab-based  $\mu$ CT systems, but when access is possible, there are advantages to SR $\mu$ CT. For instance, the scanning time is reduced, allowing high resolution images in much shorter times. Also, a monochromatic portion of the X-ray beam can be selected, leading to higher contrast and higher quality images without beam hardening artifacts. Finally, although not used here, the relatively high coherence of the X-ray beams allows phase contrast imaging, which facilitates visualization of structures that would otherwise be invisible because they have very similar X-ray absorption. For more information about  $\mu$ CT systems and applications, see Stock (2009) and Ziegler & Menze (2014).

Specimens in ethanol were air-dried prior to scanning, individually placed between two small rectangular sheets of styrofoam (one flat to fit the oral region, and one carved to accommodate the concavity of the aboral region) held together using conventional tape and attached to the metal sample holder using double-sided tape. We then let sample accommodate for at least 10 min before scanning. This technique was preferred to using clay to fix the specimen to the holder because clay and the calcified echinoid plates have similar density. Further, specimens need to be pressed against the clay to facilitate optimum adhesion and this process can be damaging to fragile specimens.

Specimens were scanned in monochromatic light mode (beam current 500 mA, energy 30 kV) using a 1x lens. Images were reconstructed in Fiji (Schindelin et al. 2012) using an algorithm developed at the ALS-LBNL and visualized in Avizo Standard software 8.0.1 (FEI Visualization Sciences Group, Burlington, MA). Screenshots of some structures were taken and drawings were made digitally in Adobe Illustrator CS6 using a Wacom Intuos tablet. The SR $\mu$ CT images generated in this study were deposited in MorphoBank (O'Leary & Kaufman 2012) and are publicly available online at <http://morphobank.org/permalink/?P2730> (Table 1.1).



**Table 1.1.** Information about the specimens analyzed using SR $\mu$ CT (images uploaded to MorphoBank, project ID 2730).

Species name	Test length (mm)	Museum deposition number	Scan time	Voxel size ( $\mu$ m)	File type	File size (Gb)	MorphoBank media number
<i>Cassidulus briareus</i> sp. nov.	18.53	MP 1267 Holotype MNHWU	00:34:35	8.4	TIF	0.74	M452514
	18.30	MP 1267 Paratype MNHWU	00:34:57	8.4	TIF	0.66	M452515
<i>Cassidulus caribaeorum</i>	17.95	CASIZ 112683A	00:30:15	8.4	TIF	0.56	M452516
	19.36	CASIZ 112683B	00:25:48	8.4	TIF	1.04	M565543
<i>Kassandrina malayana</i> comb. nov.	25.10	ZMUC 236	01:15:55	8.4	TIF	1.15	M452517

The pedicellariae and spines were disarticulated using household bleach (*ca.* 5% sodium hypochlorite solution) for 3–5 minutes, washed using three changes of distilled water, and kept in absolute ethanol. They were then placed on metal stubs with double-sided carbon tape using a dropper, separated from each other using a thin needle, set aside to air-dry, and finally analyzed with a Hitachi TM-1000 SEM.

Light photographs of specimens were taken using a Canon EOS Rebel T3i digital camera with a Canon EF 50 mm Lens coupled to a Beseler photo stand and a Cognisys StackShot (<http://www.cognisys-inc.com>); images were then stacked using the Helicon Focus 6 software ([www.heliconsoft.com](http://www.heliconsoft.com)).

Terminology for morphological descriptions follows Kroh & Smith (2010) and plate columns and individual plates are labeled according to Lovén’s system (Lovén 1874). Taxonomic assignments follow Kroh & Mooi (2017).

## Results

First, we describe a new species of *Cassidulus* based on specimens previously identified as *Cassidulus australis* and provide a discussion about the taxonomic history of the species starting with the initial description by Lamarck. Because the taxonomic history indicates instability regarding the definition of *Cassidulus caribaeorum*, we then designate a neotype for this species to stabilize its taxonomic status. Further, we describe a new cassidulid genus to accommodate the species *Cassidulus malayanus* and *Australanthus florescens*. The phylogenetic placement of the new genus based on published phylogenies and the evolution of the bourrelets within cassiduloids are discussed. Finally, we provide a diagnostic table for all extant cassiduloid species that possess a naked zone.

### **Class Echinoidea Leske, 1778**

#### **Order Cassiduloidea L. Agassiz & Desor, 1847**

#### **Family Cassidulidae L. Agassiz & Desor, 1847**

#### **Genus *Cassidulus* Lamarck, 1801**

#### ***Cassidulus briareus* sp. nov.**

(Figs. 1.1–1.2, 1.10)

**Type Material.** Holotype: Australia (Neuholland), collected by Salmin (probably Carl Ludwig Salmin), 18.36 mm TL (MP 1267 Holotype MNHWU). Paratype: same collection data as H, 18.20 mm TL (MP 1267 Paratype MNHWU).

**Comparative material of other species examined.** *Cassidulus caribaeorum?* Lamarck, 1801: possibly Caribbean Sea (MNHN-IE-2013-10590 [Syntype?]); Anegada, British Virgin Islands, TL 18–30 mm (CASIZ 112633, 112638, 112683A–B). *Cassidulus infidus* Mortensen, 1948b: Salvador–BA, Brazil, TL 7.5–13 mm (SMNH 4859 [H], UFBA 314, 757). *Cassidulus mitis* Krau, 1954: Rio de Janeiro–RJ, Brazil, TL 26–46 mm (CASIZ 116110, MNRJ 3673–3674, ZUEC 11–12).

**Diagnosis.** Test arched in cross section, greatest height at apical disc. Anterior region of test very inflated. Paired petals with unequal columns of respiratory podia. Naked zone along oral midline developed and pitted. Phyllodes without occluded plates. Peristome and periproct transverse. Three interambulacral plates on each side of periproct. Basicoronal plate 5 narrow and elongated.

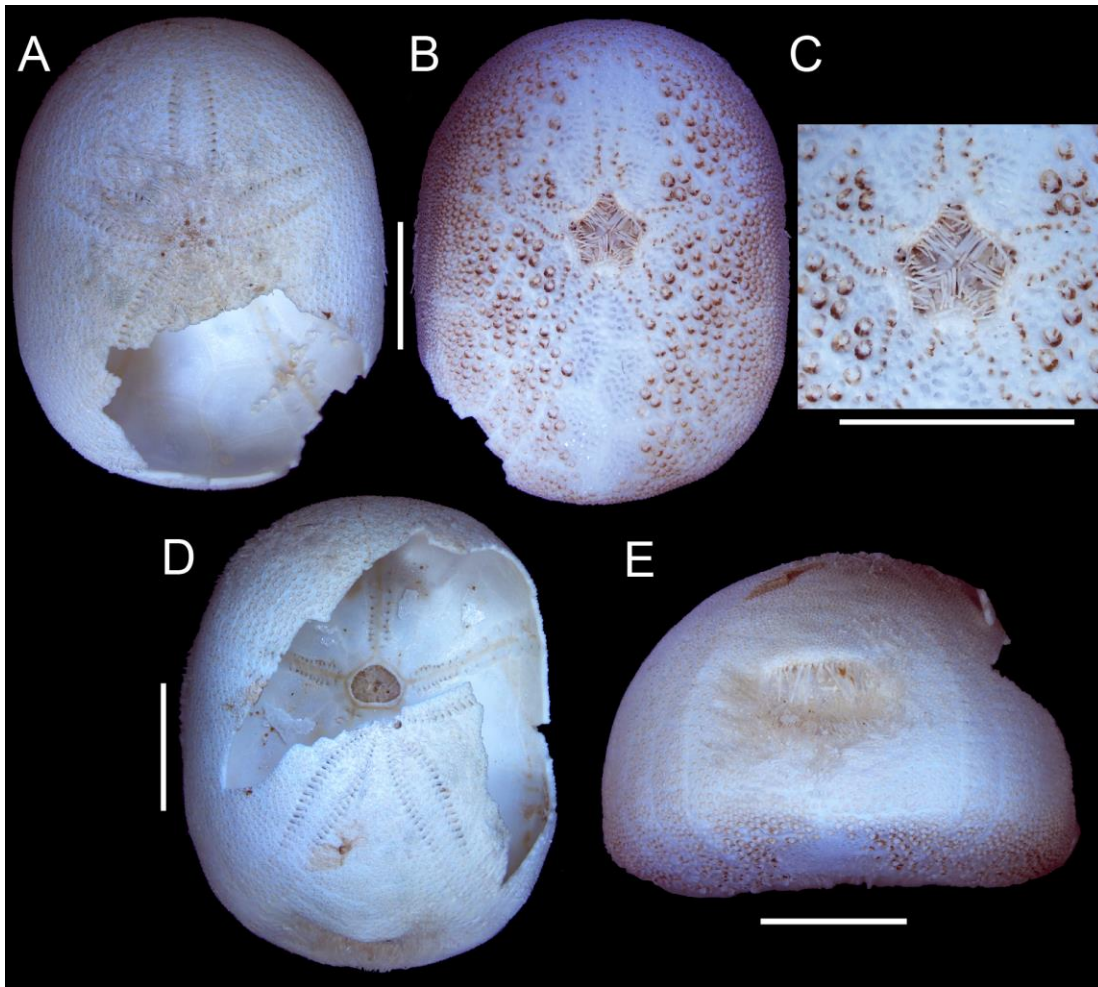
**Etymology.** Named after Briareus, the Greek God of violent sea storms, in reference to the turbulent taxonomic history related to the specimens described herein (see taxonomic history below).

**Description.** Test oval (TW 79% of TL), lateral edges straight, anterior and posterior margins round; anterior and posterior regions of aboral region inflated with greatest height at apical disc, transverse cross section domed; oral region concave along the midline of the anterior-posterior axis. Test measurements (TL \* TW \* TH in mm): 18.36 \* 14.52 \* 10.4 (H) (Fig. 1.1A–B) and 18.2 \* *ca.* 14.3 \* *ca.* 10.4 (P) (Fig. 1.1D–E).

Apical disc anterior, monobasal, *ca.* 9.5% of TL, flat, with four gonopores on disc edge; hydropores abundant and spread across plate (Fig. 1.2A). Anterior ocular plates between their adjacent gonopores; posterior ocular plates large and slightly posterior to gonopores 1 and 4; posterior region of apical disc slightly bulging towards interambulacrum.

Petalodium about 75% of TL. Petals roughly with same L and W, broad in the middle and narrow distally, but not closing (Fig. 1.2B–D); inner and outer columns of respiratory podia bowed; poriferous zone narrow, pores slightly conjugated; outer pores elongated, inner pores round and smaller than outer. Columns *a* and *b* of posterior petals differ by 2 pore-pairs (number of respiratory podia in P: petal I, 21/23; petal V, 24/22), of anterior paired petals differ by 1–2 pore-pairs (number of respiratory podia in H: petal II, 21/20; petal IV, 18/20), anterior petal is equal (H: petal III, 21/21 respiratory podia). Primary tubercles present in poriferous zone; 3, sometimes 4 primary tubercles per petal plate. No occluded plates in petals. Ambulacra beyond petals increase 60–90% in relation to end-petal W; unipores in plates beyond petals: aboral plates wider than long, pores on suture, between adradial edge and middle of plate (Fig. 1.2E), and oral plates about 2x longer than wide, pores on middle of plate suture (Fig. 1.2I).

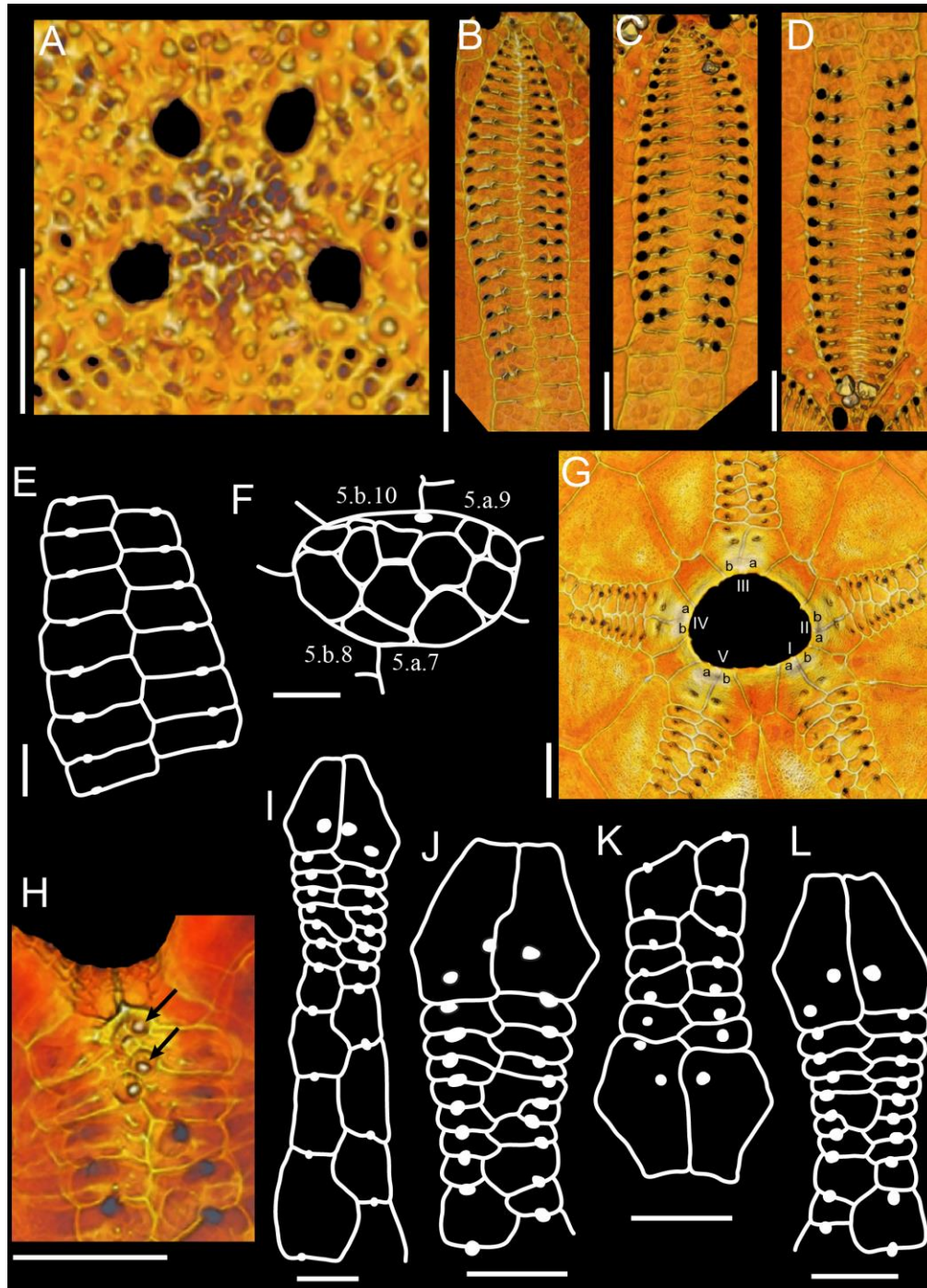
Phyllodes with unipores, with only one column of pores on each half (number of phyllopores per half: anterior phyllode 5–6, paired phyllodes 7–9) (Fig. 1.2G–L). Plates sometimes unequal in size and shape; pyrinoïd plate present on phyllode II, between plates 5 and 6 (Fig. 1.2G, J). Columns slightly bowed proximally and W narrows down distally. Pores usually aligned in a uniform column. Buccal pores same size as phyllopores. Ambulacral basicoronal plates pierced by buccal pore and one per ambulacrum also pierced by a phyllopore in the sequence a, a, b, a, b from phyllode I to V (Fig. 1.2G). Four to 5 sphaeridia in large and enclosed pits near buccal pores (Fig. 1.2H).



**Figure 1.1.** *Cassidulus briareus* sp. nov. (MP 1267 MNHWU): test of holotype in (A) aboral and (B) oral view, and (C) detail of peristome and phyllodes; and test of paratype in (D) aboral and (E) posterior view. Scale bars: A–E, 5 mm.

Peristome anterior (34% TL from anterior region), deep (basicoronal plates extend further towards the inside of the test), slightly transverse (L 78–81% of W), pentagonal on the outside and subpentagonal on the inside (Fig. 1.1C). Mouth opening in center of peristomial membrane. Bourrelets slightly developed as mounds mostly towards the inside of the peristome (Fig. 1.10A–B). Cross-section of bourrelet with *ca.* 8 spines (Fig. 1.10B).

Columns *a* and *b* of interambulacrum 5 with 7 and 8 plates between basicoronal plate and base of periproct, respectively, and 2 until adapical region of periproct (i.e. periproct is framed by 3 plates on each side). Interambulacral basicoronal plates 1 and 4 very narrow (much reduced and occluded in one specimen), 2 and 3 broadest, 5 intermediate in size (Fig. 1.2G). Second and third oral plates on interambulacrum 5 are much longer than wide. Naked zone well-developed throughout midline of test on interambulacrum 5 and ambulacrum III (W 22–25% of TW) (Fig. 1.1B). Deep pits present in oral region, mostly on naked zone.



**Figure 1.2.** *Cassidulus briareus* sp. nov. (MP 1267 MNHWU; all from holotype except B, F–H): (A–D, G–H) SR $\mu$ CT-based volume renderings and (E–F, I–L) drawings showing (A) apical disc, (B–D) internal view of petals I–III, respectively, (E) plates beyond ambulacrum V, (F) periproct (internal view; solid white region indicates anal opening), (G) internal view of peristome and phyllodes, (H) longitudinal section of phyllode III (arrows indicate sphaeridia), and (I–L) internal views of the phyllodes V, II–IV, respectively. Scale bars: A–L, 1 mm.

Periproct marginal and transverse (L 46% of W), beyond posterior petals; aboral plates form a prominent lip, oral and lateral plates do not bend inside the periproct (Fig. 1.1E). Periproct framed adorally by plates 5.a.7 and 5.b.8, and adapically by plates 5.a.9 and 5.b.10. Periproctal membrane with 2 rows of 4 large plates; smaller plates scattered in aboral region near anus (Fig. 1.2F). Anus opening aborally, on center of periproctal membrane.

Primary tubercles perforate and slightly crenulate. Oral primary tubercles with mamelon displaced in the opposite direction of the spine (usually anteriorly from center of bosses) and *ca.* 2.5x as large as aboral tubercles. Bourrelet spines curved and with thick tip, oral spines long and straight, aboral spines short and straight, spines on periproct thin, straight, and intermediate in size between oral and aboral spines. Miliary tubercles all over the test. Few tridentate pedicellariae on stalks (valves 220–225  $\mu\text{m}$  L) on periproct. Because very little soft tissue was preserved on available specimens, ophicephalous pedicellariae and tube foot ossicles were not observed.

**Remarks.** *Cassidulus briareus* sp. nov. differs from its congeners (i.e. *C. caribaeorum*, *C. infidus* and *C. mitis*) (Table 1.2) by having the anterior region of the test very inflated (versus gradual height increase towards apical disc); a narrow and elongated basicoronal plate 5 (versus squarish shape); a subpentagonal to triangular peristome, from the inside of the test (versus subpentagonal to pentagonal); and a reduced number of plates framing the periproct (3 versus 4 in the others [but rarely 3 plates on *b* column]). In addition, it differs from *C. caribaeorum* by having an arched test in cross section of the adult (versus triangular shape), shorter periproct, and more developed phyllodes with 2–3 more phyllopores than *C. caribaeorum*; from *C. mitis* by having a uniform row of pores in the phyllodes (versus disorganized row in which some pores are displaced forming an apparent inner series), and from *C. infidus* by having the greatest height at the apical disc (versus posterior to the apical disc).

### ***Cassidulus briareus* sp. nov. and its historical context within the genus *Cassidulus***

The specimens described herein were formerly identified as *Cassidulus australis* Blv. To our knowledge, Blainville did not describe any living species of *Cassidulus* and in his papers, he acknowledged Lamarck as author of *C. australis* (see Blainville 1830, p. 192; 1834, p. 210). This species was described by Lamarck (1816) but later considered to be invalid (Gray 1855, p. 34; A. Agassiz 1872–1874, p. 153; Mortensen 1948a, p. 209–210). Here we provide information on the taxonomic history of the genus *Cassidulus* that was pertinent in the decision to describe the new species.

Lamarck (1801, p. 348–349) described *C. caribaeorum* together with the genus *Cassidulus*, without recording the repository of the holotype or the type locality of the species. The latter was assumed to be the Caribbean, given the name of the species and also because Lamarck mentioned Spanish Town (near Kingston, Jamaica) in a later publication (Lamarck 1816, p. 35). He (1801, p. 349) also made reference to Bruguière et al. (1827, pl. 143, fig. 8–10), which includes illustrations of the specimen that, although of poor quality and lacking detail, captured the triangular shape of the test in cross section and the shape of the periproct and peristome.

In 1816 (p. 35), Lamarck described *C. australis*, based on specimens supposedly collected by Charles Alexandre Lesueur and François Péron during the Baudin Expedition (1801–1803) in Shark’s Bay, Western Australia (as “baie des Chiens marins, Nouvelle-Hollande”). This description was slightly different from the description of *C. caribaeorum*; however, Lamarck mentioned that *C. australis* also occurred in the Caribbean and included in his

synonymy list Bruguière et al. (1827, pl. 143, fig. 8–10), which means this species and *C. caribaeorum* are synonyms. Again, he failed to record where the specimen was deposited.

Shortly afterwards, Lamouroux et al. (1824, p. 174) synonymized *C. caribaeorum* with *C. australis* and redescribed the species. They also suggested re-naming the species *C. richardi*, in honor of the person who had collected the type of *C. caribaeorum*, and mentioned that it was not clear that the specimen collected by Péron and Lesueur was the same as the one described by Lamarck (1816). Their description stated that the specimen was “rather convex above”, which matches the shape of *Cassidulus briareus* sp. nov., but the test shape in the illustration is more similar to that of *C. caribaeorum* (triangular shape seen in large specimens).

All subsequent publications involving the genus *Cassidulus* (including the ones by Lamarck) accepted the synonymy proposed by Lamouroux et al. (1824), although any of the three names (*C. caribaeorum*, *C. australis* and *C. richardi*) was used for the species (e.g. Eichwald 1829; Blainville 1830; 1834; Lamarck 1837; 1840; Des Moulins 1835–1837; A. Agassiz 1869; Mortensen 1948b; Mooi 1990b). The occurrence of the species in Australia was often disregarded even though Lamarck kept including this locality in his papers.

L. Agassiz & Desor (1847, p. 157) finally indicated that there was a specimen of *C. australis* (possibly the holotype) in the MNHN; and Mortensen (1948b, p. 209–210) suggested that the occurrence of the species in Australia was probably a result of “erroneous labeling”. His reasoning was that if the species occurred in Australia, more specimens would have been collected during the intervening 150 years; logic that makes sense for many taxa. This species, however, appears to be less common than expected.

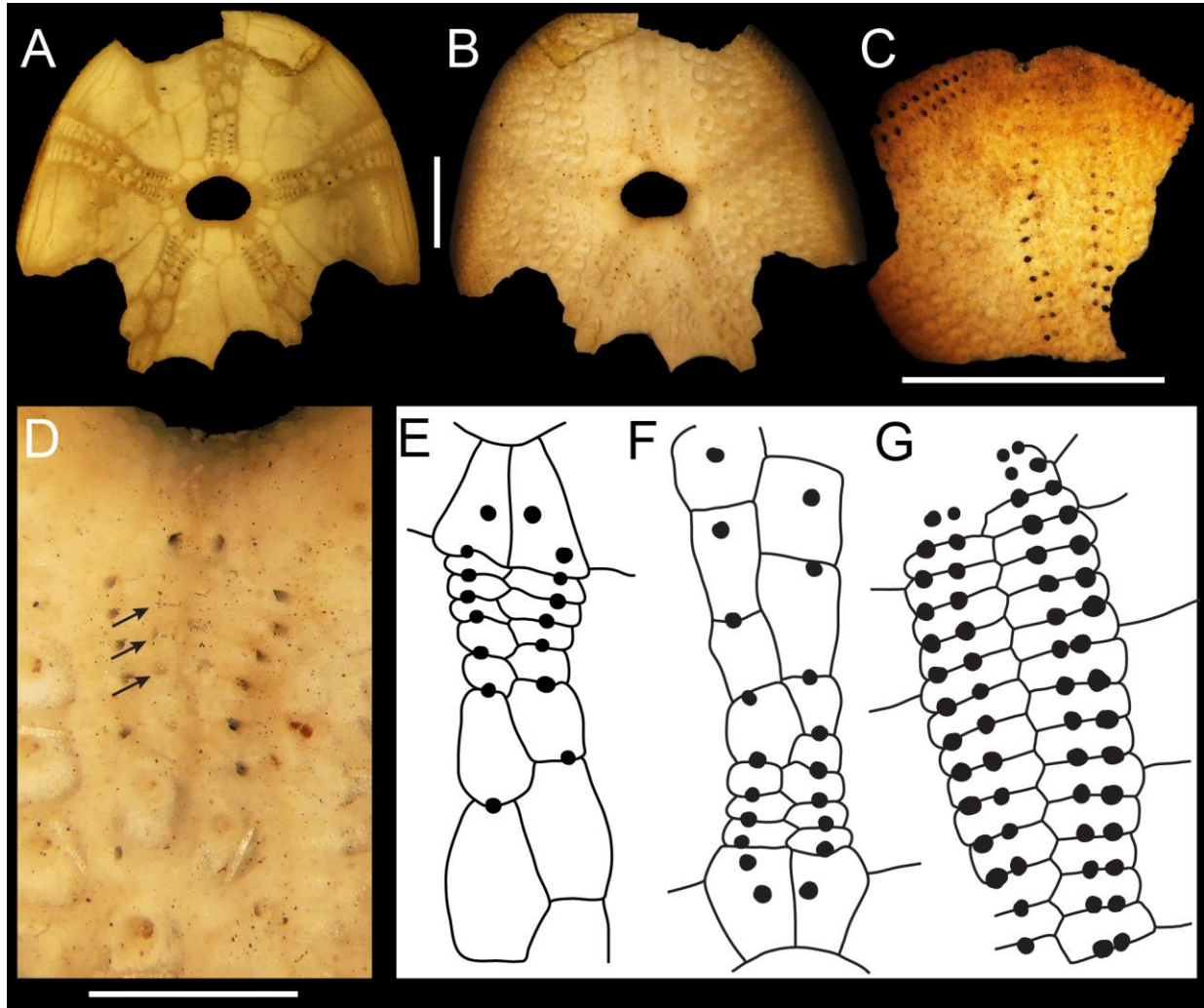
Vadon et al. (1984) mentioned that they did not find the type of *C. caribaeorum* in the MNHN and that Lamarck probably described the same specimen twice. The label retained the name used last, i.e. *C. australis*. However, Lamarck (1816) clearly mentioned that they were specimens from different localities. In addition, Lamarck’s descriptions of *C. caribaeorum* and of *C. australis* were slightly different, although both were somewhat imprecise.

**Possible type specimen of *C. caribaeorum* at the MNHN.** Following up on this debate, we believe that the vial identified as *C. caribaeorum* in the MNHN (Fig. 1.3, MNHN-IE-2013-10590 [Syntype ?]; previously as EcEs 5040) might contain the type of one of the species described by Lamarck or perhaps even of both species. Two labels in the vial provide different identifications: one is identified as *C. australis* and the other (label apparently younger and written by A. Agassiz) is identified as *Rhyncholampas caribaeorum*, with *C. australis* and *Nucleolites richardi* as synonyms. Also, both labels refer to the “Voyage de Péron & Lesueur 1801”, which indicates the material was from Australia rather than the Caribbean (MNHN 2017).

This vial contains broken pieces of two specimens as indicated by the fact that there are six complete phyllodes (one entire set and an additional broken phyllode). The following traits characterize them as *Cassidulus*: petal unequal in length (only one present, not sure if anterior or posterior; Fig. 1.3C, G), peristome transverse and subpentagonal (W 3.39 mm, L 2.18 mm), buccal pores present, sphaeridia in enclosed pits (Fig. 1.3D), phyllodes with a single column of phyllopores per half (Fig. 1.3D–F), naked zone developed and deeply pitted, mamelons of oral primary tubercles displaced from center. Additional characteristics are: posterior phyllodes and phyllode III with 5–6 pores, anterior paired phyllodes with 6–7 pores, plates beyond phyllodes longer than wide.

Basicoronal plate 5 seems more elongated than in specimens of *C. caribaeorum* preserved in the CASIZ collection (CASIZ 112633, 112683A) but not as narrow as in *Cassidulus briareus* sp. nov. (Fig. 1.3A), and the number of phyllopores also overlaps both species.

Therefore, identifying the broken pieces based on these traits is not reliable, nor would be any assertion that they belong to one or two species. Also, the illustrations in Bruguière et al. (1827, pl. 143, fig. 8–10) are very poor and only capture the overall shape of the specimen, making it impossible to determine if they correspond to the broken specimens in the vial at the MNHN.



**Figure 1.3.** *Cassidulus caribaeorum* (?) (MNHN-IE-2013-10590 [syntype?]): photos of (A) internal and (B) external view of oral region of carapace; (C) part of the aboral region of carapace showing petal II or V (according to the position of smaller column of pore-pairs); (D) detail of phyllode I, arrows indicate sphaeridia in enclosed pits; and drawings of internal view of phyllodes (E) V and (F) III, and (G) petal depicted in (C). Scale bars: A–C, 5 mm; D, 2 mm.

#### Decision to describe a new species

According to the synonymy list provided by Lamarck (1816), *C. australis* is a subjective junior synonym of *C. caribaeorum*. In addition, since *C. australis* was poorly described, it is impossible to determine if any subsequently collected Australian *Cassidulus* specimens are

conspecific. The type specimen is probably lost, unidentifiable, or lacking diagnostic features, leading to much confusion in the literature regarding its validity. Therefore, it is not possible to determine that the material collected by Salmin is the same as Lamarck's *C. australis*, and we elected to describe a new species while at the same time stabilizing the nomenclature within the genus *Cassidulus*.

#### **Prediction of the type locality of *C. briareus* sp. nov.**

C.L. Salmin was a trader in Hamburg, Germany, who collected and sold specimens during the 1860s–1870s without taking much care in recording details regarding sampling locality (Holthuis 2002). The only record we found in the literature documenting a collection of Australian echinoderms made by him is of holothuroids, collected in Cape York, Queensland (Samyn et al. 2013). However, museum registries also indicate that he has collected marine fish in Victoria, suggesting that the specimens described herein could have been collected in other places along the Australian coast.

If “*C. australis*” was indeed collected by Péron and Lesueur in Australia, it is possible that *C. briareus* sp. nov. lived in the same region (i.e. Shark’s Bay, Western Australia).

#### **Decision to designate a neotype for *Cassidulus caribaeorum* Lamarck**

As the type material of this species cannot be reliably identified and the illustrations provided by Bruguière et al. (1827, pl. 143, fig. 8–10) do not contain diagnostic characteristics, a neotype designation for *C. caribaeorum* is necessary to objectively define this species name (ICZN 1999, articles 75.1 and 75.3.4), and also to clarify the taxonomic status of the higher taxonomic ranks in which this species serves as the type species.

#### ***Cassidulus caribaeorum* Lamarck, 1801**

(Figs. 1.4–1.6)

*Cassidulus cariboeorum* Lamarck, 1801: 348–349.

*Rhyncholampas caribaeorum* — A. Agassiz, 1869:270–271.

*Rhynchopygus caribaeorum* — A. Agassiz, 1872–1874:153, 343, pl. 15.

*Rhyncholampas cariboeorum* — H.L. Clark, 1917:106, pl. 144.

*Cassidulus caribaeorum* — Mortensen, 1948a: 205–210, pls. 2, 11; Gray, 1855:34; Mooi, 1990b: 80.

*Cassidulus cariboeorum* — Kier, 1962: 176–178, pl. 26.

**Type Material.** Neotype (designated herein): Caribbean Sea, British Virgin Islands, Anegada, Loblolly Bay, 0.5–1 m, collected by R. Mooi and M. Telford, 01.IV.1986, 26.68 mm TL (CASIZ 222205).

**Neotype choice.** In the absence of specimens from the type locality, we chose an adult specimen from one of the few well-studied populations of *C. caribaeorum*. The specimen agrees with the original description of the species and is in great condition (i.e. test is intact and still has spines and pedicellariae).

**Comparative material examined.** *Cassidulus caribaeorum* Bahamas, TL 17 mm (NHM-UK 87.6.27.7); British Virgin Islands, Anegada, TL 9–30 mm (CASIZ 112632, 112633, 112637, 112638, 112683A); and French Antilles, TL 8–20 mm (UF 11786–11788, 11797–11798, 11825, 11892, 11933).



**Description.** Test oval (TW *ca.* 85% of TL), lateral edges straight, anterior and posterior margins round; greatest height at apical disc, test height decreases sharply from apical disc to periproct; transverse cross section triangular; oral region concave along the midline of the anterior-posterior axis. Test measurements (TL \* TW \* TH in mm): 26.68 \* 22.65 \* 11.71 (Fig. 1.4A–B, D–E).

Apical disc anterior, monobasal, *ca.* 11% of TL, flat, with four elongated gonopores on disc edge; anterior gonopores closer together, posterior gonopores further apart (Fig. 1.4A; 1.4F, not from N); hydropores abundant and spread across plate. Anterior ocular plates between their adjacent gonopores; posterior ocular plates near distal edge of gonopores 1 and 4.

Petalodium system about 74% of TL. Posterior petals longer than others; anterior petals wider than posterior petals. Anterior petals broad in the middle and narrow distally (not closing), and with bowed columns of respiratory podia. Posterior petals roughly with same width throughout; columns of respiratory podia curved outwards towards test edge. Poriferous zone of petals narrow, pores slightly conjugated; outer pores slightly elongated, inner pores round and smaller than outer. Columns *a* and *b* of posterior petals differ by 3–5 pore-pairs (number of respiratory podia: petal I, 27/30; petal V, 27/32), of anterior paired petals differ by 3–4 pore-pairs (number of respiratory podia: petal II, 20/23; petal IV, 20/24), anterior petal is equal (petal III, 25/25 respiratory podia). Primary tubercles present in poriferous zone; 2, sometimes 3 primary tubercles per petal plate. No occluded plates in petals. Ambulacra beyond petals increase 55% in relation to end-petal W; unipores in plates beyond petals: aboral plates wider than long, pores on suture, between adradial edge and middle of plate.

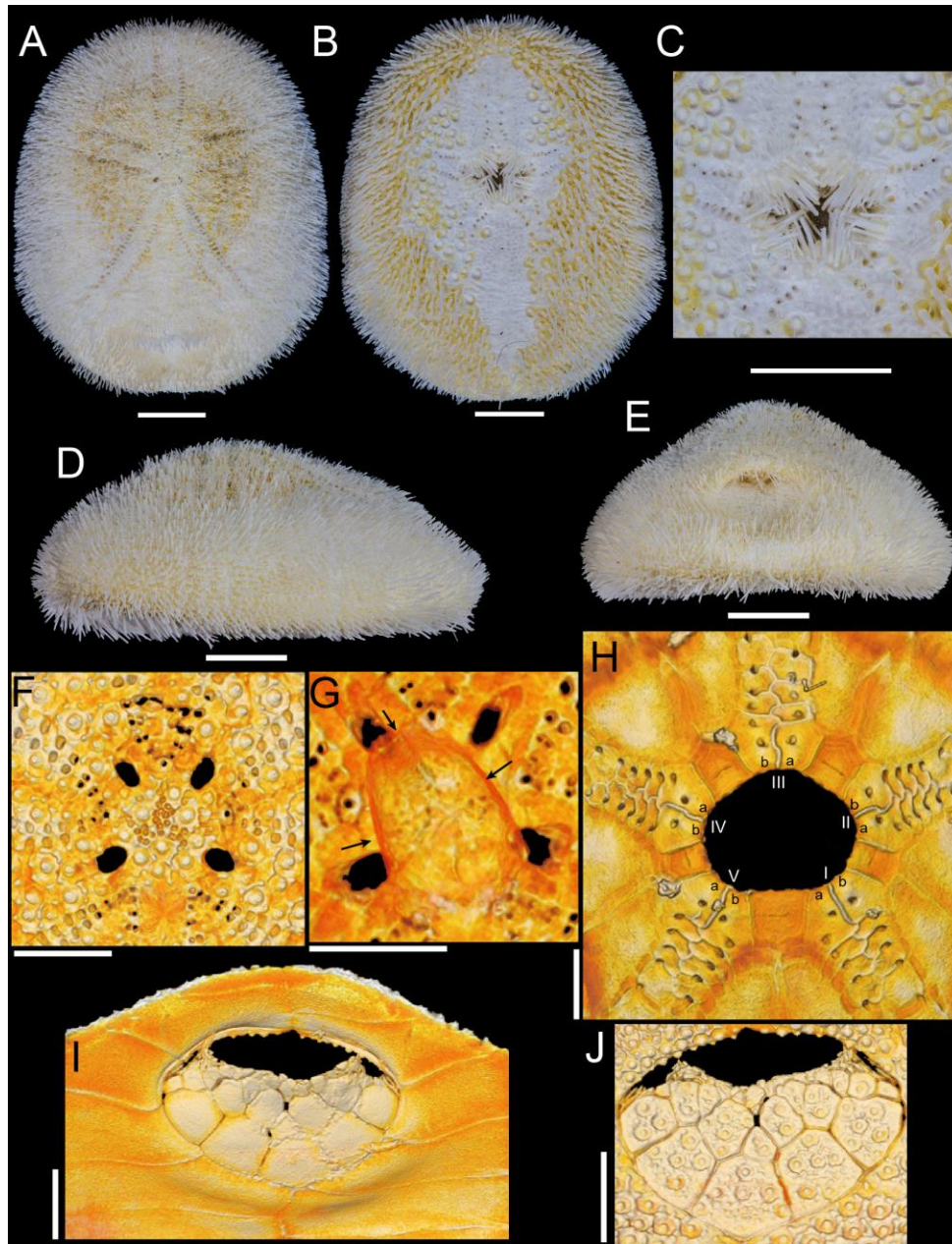
Phyllodes with unipores, with only one column of pores on each half (number of phyllopores: phyllodes 1 and 5, 4/5; phyllodes 2 and 4, 6/6; phyllode 3, 6/5) (Fig. 1.4C). Columns mostly straight, largest W adorally and phyllodes narrow down distally. Buccal pores same size as phyllopores. Four to 6 sphaeridia (109–116  $\mu$ m L; Fig. 1.5L) in large and enclosed pits near buccal pores.

Peristome anterior (34% TL from anterior region), slightly transverse (L 68% of W), pentagonal. Mouth opening in center of peristomial membrane. Bourrelets slightly developed as mounds mostly towards the inside of the peristome.

Naked zone well-developed throughout midline of test on interambulacrum 5 and ambulacrum III, wider anteriorly than posteriorly (W 22% of TW). Deep pits present in oral region, mostly on naked zone. One primary tubercle present on naked zone, adjacent to phyllode 1.

Periproct marginal and transverse (L 70% of W), beyond posterior petals; aboral plates form a prominent lip, oral and lateral plates do not bend inside the periproct (Fig. 1.4E; 1.4I–J, not from N). Periproctal membrane with 2 rows of 5–6 medium- to large-sized plates; smaller plates scattered in aboral region near anus (Fig. 1.4I–J, not from N). Anus opening aborally, on center of periproctal membrane and surrounded by elongated papillae.

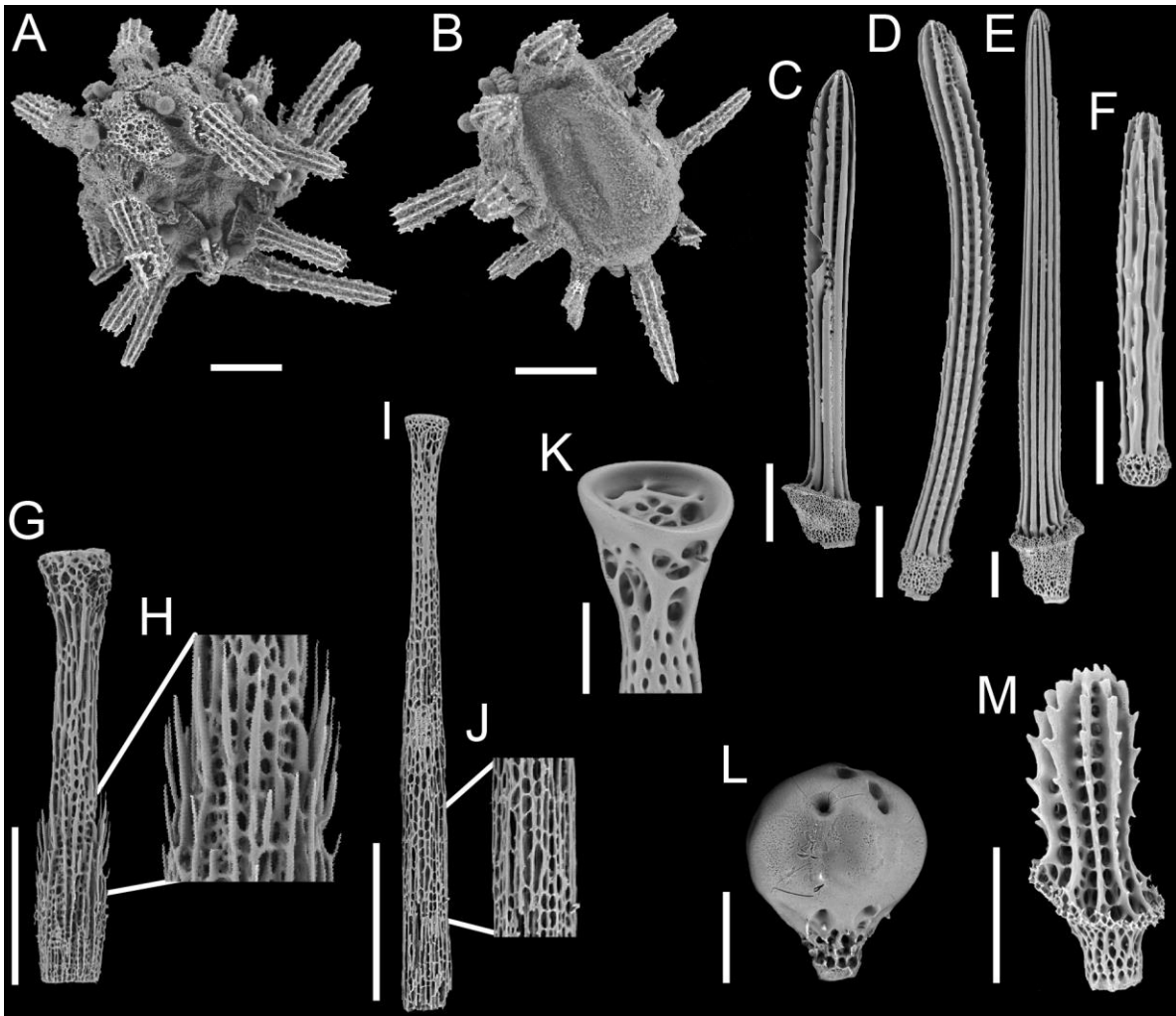
Primary tubercles perforate and slightly crenulate. Oral primary tubercles with mamelon displaced in the opposite direction of the spine (usually anteriorly from center of bosses) and 2.25x as large as aboral tubercles. Aboral spines short, straight, apex thicker than base, shaft serrated (Fig. 1.5C); bourrelet spines curved, shaft serrated, base short (Fig. 1.5D); oral spines long, straight, thicker at the base than at the apex, shaft mostly smooth (Fig. 1.5E; not from N); spines on lip above periproct thin, straight, intermediate in size between oral and aboral spines, shaft slightly serrated on both extremities. Miliary spines abundant, short, straight, thickness uniform, tip crown-shaped, shaft serrated (Fig. 1.5F, not from N).



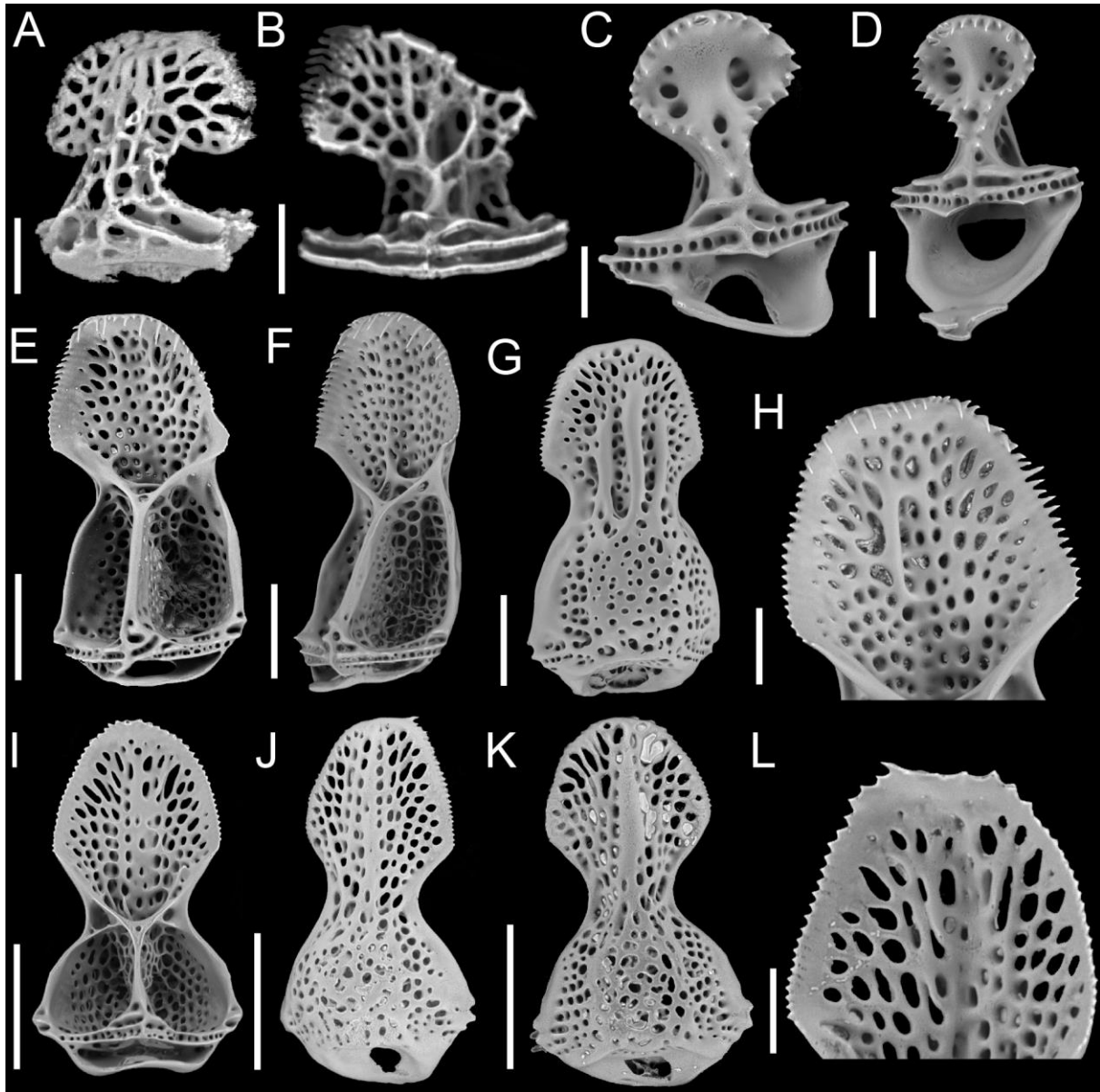
**Figure 1.4.** *Cassidulus caribaeorum* Lamarck, 1801 (CASIZ 222205 [neotype] [A–E]; CASIZ 112683B [F–G, I–J]; CASIZ 112683A [H]): photos of test in (A) aboral and (B) oral view, (C) detail of peristome and phyllodes, and test in (D) side and (E) posterior view; SR $\mu$ CT-based volume renderings of apical disc in (F) external and (G) internal view (arrows indicate calcareous ridges beneath madreporic plate), (H) of peristome in internal view, and of periproct in (I) internal and (J) external view. Scale bars: A–E, 5 mm; F–J, 1 mm.

Periproctal and peristomial membranes with small ossicles. Triphyllous pedicellariae small and apparently abundant near aboral ambulacra. Valves short and broad (45–56  $\mu$ m L; Fig. 1.6A–B) with delicate teeth along whole blade margin. Ophicephalous pedicellariae small and

rare. Valves (135–181  $\mu\text{m}$  L; Fig. 1.6C–D) with coarse teeth along whole blade margin (open row, U-shaped). Hinge broad, handles conspicuous. Two types of tridentate pedicellariae found. Large type found near posterior petals and periproct; valves (302–407  $\mu\text{m}$  L; Fig. 1.6E–H) broad and robust; blade with thin teeth along whole margin, teeth on distal margin numerous and very long; region between blade and basal region wide, basal region tall; stalk (494–553  $\mu\text{m}$  L; Fig. 1.5G) robust, proximal region thicker than distal region and with pointy upward projections (Fig. 1.5H), no neck present. Small type found around apical disc where embryos and young (Fig. 1.5A–B) are; valves (228–302  $\mu\text{m}$  L; Fig. 1.6I–L) broad; blade with coarse teeth along whole margin, teeth on distal margin larger; region between blade and basal region narrow, basal region short and spineless; stalk (610–767 [broken]  $\mu\text{m}$  L; Fig. 1.5I) long and thin, base thicker than apex, stereom thin and intricate (Fig. 1.5J), neck present.



**Figure 1.5.** *Cassidulus caribaeorum* Lamarck, 1801 (CASIZ 222205 [neotype] [A–D, I–L]; CASIZ 112638 [E–G, M]), SEM images: (A–B) juveniles attached to the test; (C) aboral, (D) bourelet, (E) oral and (F) miliary spines; stalk of (G) large tridentate pedicellariae (detail of projections in H), (I) small tridentate pedicellariae (detail of stereom in J), and of (K) ophicephalous pedicellariae; (L) sphaeridium; and (M) young spine. Scale bars: A–B, M, 100  $\mu\text{m}$ ; C–I, 200  $\mu\text{m}$ ; K–L, 50  $\mu\text{m}$ .



**Figure 1.6.** *Cassidulus caribaeorum* Lamarck, 1801 (CASIZ 222205 [neotype] [B–E, J–L]; CASIZ 112638 [A, F–I]), SEM images: valves of (A–B) triphyllous pedicellariae, (C–D) ophicephalous pedicellariae, (E–G) large tridentate pedicellariae ([H] detail of valve head), and (I–K) small tridentate pedicellariae ([L] detail of valve head). Scale bars: A–B, 15  $\mu\text{m}$ ; C–D, H, L, 30  $\mu\text{m}$ ; E–G, I–K, 100  $\mu\text{m}$ .

**Additional information based on comparative material and literature.** Posterior region of apical disc slightly bulged towards interambulacrum. Oral plates beyond petals about 1.15–1.60x longer than wide, pores near the distal edge of plate suture. Plates on phyllodes sometimes unequal in size and shape; pyrinoïd plates not present. Phyllopores usually aligned in a uniform column. Ambulacral basicoronal plates pierced by buccal pore and one per ambulacrum also pierced by a phyllopore in the sequence a, b, a, b, b from phylloïde I to V (Fig.

1.4H). Columns *a* and *b* of interambulacrum 5 with 6–7 plates between basicoronal plate and base of periproct and 3 (rarely 4) until adapical region of periproct (i.e. periproct is framed by 4 [rarely 3] plates on each side). Interambulacral basicoronal plates 1 and 4 narrower than others, 5 the broadest, 2 and 3 intermediate in size. Second and third oral plates on interambulacrum 5 are much longer than wide. Periproct framed adorally by plates 5.a.6 (or 5.a.7) and 5.b.7, and adapically by plates 5.a.10 (or 5.a.9) and 5.b.10.

Gastric caecum highly reduced (Ziegler et al. 2008). Anterior stomach located in ambulacrum III, where it joins the short esophagus, and in interambulacrum 3; a cluster of 4–6 smooth, finger-like pouches at the junction of esophagus and anterior stomach, and further subdivided into two smaller clusters directed laterally towards interambulacra 2 and 3 (Ziegler et al. 2010). Color *in vivo*: white (Kier 1975).

**Intraspecific variability.** Besides the difference in the number of plates on oral interambulacrum 5, other differences were observed between specimens. For instance, the difference in the number of respiratory podia between the columns *a* and *b* of anterior paired petals varies from 2–4 pore-pairs. Also, the number of phyllopores varies from 4–5 in phyllodes I, III and V, and from 5–7 in phyllodes II and IV; and although most specimens have deep pits in the naked region, a few others have shallow and small pits.

**Bathymetric and geographic distribution.** *Cassidulus caribaeorum* has been recorded in Belize, the British Virgin Islands, Jamaica, Mexico, Panama and Puerto Rico (Lamarck 1801; Gladfelter 1978; Kier 1975; Tzompantzi et al. 1999; Alvarado et al. 2008; Rodríguez-Barreras et al. 2012), Bahamas and French Antilles (extended herein). The NHM-UK database holds occurrences from Antigua and Barbuda. Occurrence of the species in the Dominican Republic has been indicated by Alvarado (2011), but we have not been able to find the original reference for the occurrence nor a record in museum databases.

This species occurs in shallow water, up to 18 m of depth (Mooi 1990b; extended herein). A. Agassiz's (1872–1874, p. 343) record of specimens living at 106 fathoms (*ca.* 194 m) of depth is probably wrong.

**Natural history notes.** Even though *C. caribaeorum* was described more than 200 years ago and is fairly well-distributed in shallow Caribbean waters, information about this species is still scarce. The specimens analyzed herein were collected from 10–100 mm beneath the surface of the sediment, which was composed of clean calcareous sand. This specific population migrates with changes in season and the density of individuals varies between 5–25 individuals/m<sup>2</sup> (Gladfelter 1978).

Some cassiduloids are known to brood their young (Mortensen 1948a), sometimes in brooding pouches or among the aboral spines, as is the case for *C. caribaeorum*. The neotype described herein has several embryos and young in the aboral region (see dark yellow patch around apical disc on Fig. 1.4A). Gladfelter (1978) suggested that fertilization in this species may be internal and he also did not rule out the possibility of parthenogenesis; both hypotheses remain to be tested. Sexual dimorphism in gonopore size is not as apparent as in other cassiduloids (e.g. *Neolampas rostellata* A. Agassiz, 1869) but because of the presence of embryos on the test, the neotype is most likely a female. Sexual maturity was observed in individuals larger than 10 mm in TL.

See Gladfelter (1978) and Telford & Mooi (1996) for additional information on the natural history of *C. caribaeorum*.

*Incertae familiae*

*Kassandrina* gen. nov.

(Figs. 1.7–1.10)

*Cassidulus* (*pars*) — Gregory, 1892: 435–436; Mooi, 1990b: 81 (*pars*); Holmes, 1999: 53.

*Procassidulus* (*pars*) — Mortensen, 1948a: 223–226; Mortensen, 1948b: 1.

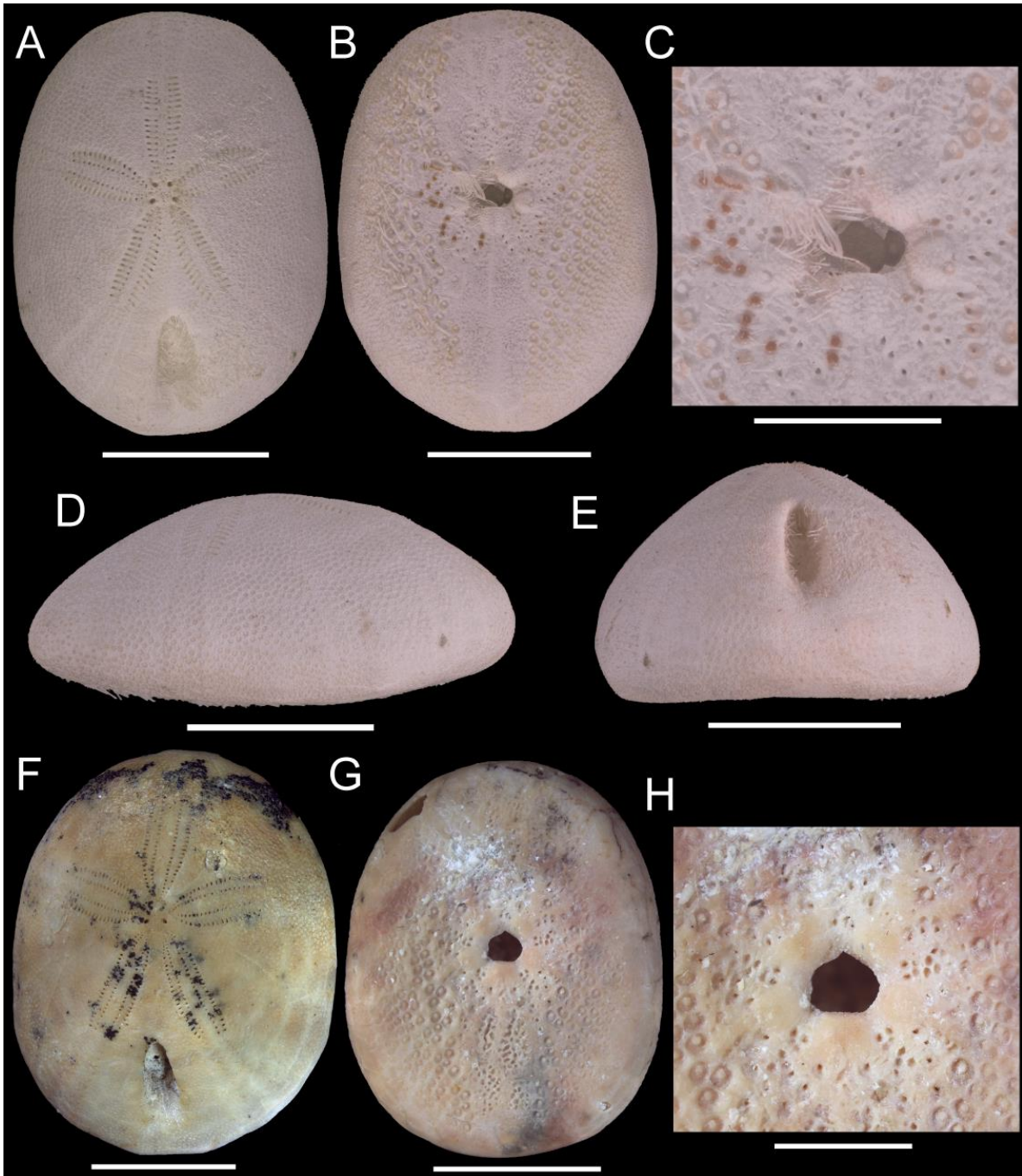
**Type species.** *Procassidulus malayanus* Mortensen, 1948b; here designated.

**Diagnosis.** Apical disc monobasal with 4 gonopores. Petals with equal columns of respiratory podia. Ambulacral plates beyond petals with pores running along the middle. Interambulacrum 5 with 11–12 plates between basicoronal 5 and aboral edge of periproct. Naked zone along oral midline developed and pitted. Phyllodes short and with few occluded plates. Peristome transverse and pentagonal. Bourrelets bulged outwards because of internal depression on the basicoronal plates. Periproct aboral, longitudinal, and narrow.

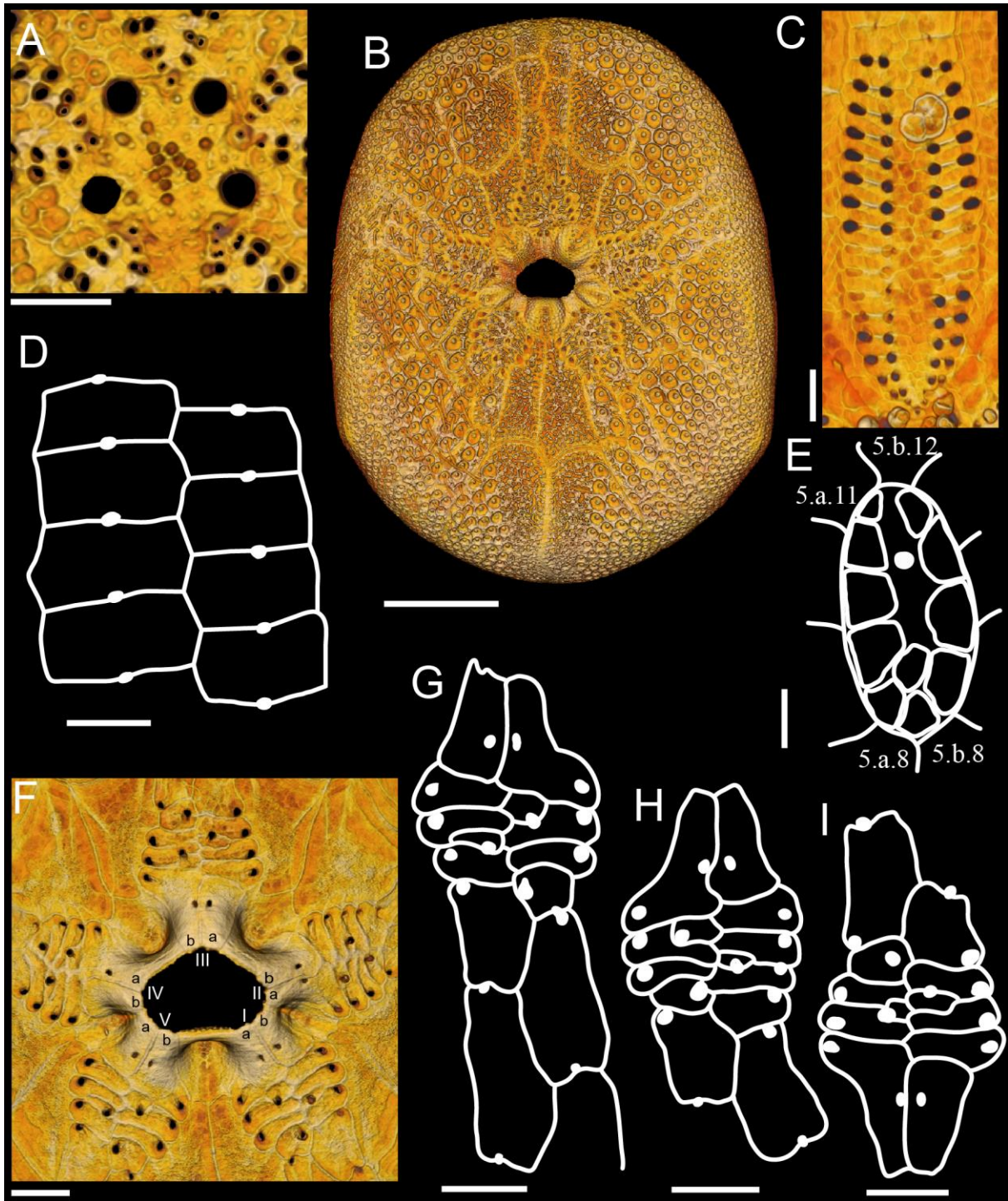
**Description.** Test oval (TW 70–80% TL), aboral region arched and not much inflated, oral region concave (Fig. 1.7). Apical disc anterior, monobasal with 4 gonopores (Fig. 1.8A); hydropores few and restricted to the center of the plate or numerous and widespread.

Petals short, not tapering, with roughly same L and W (Figs. 1.7A, F; 1.8C); columns of respiratory podia equal, pore-pairs conjugated, inner pore round and outer pore elongated. Inner columns of pores straight or slightly bowed; outer columns straight or slightly bowed on posterior petals, and always bowed on anterior petals. Two to 3 primary tubercles per plate, at least one of them in poriferous zone. Ambulacra beyond petals increase 125–175% in relation to end-petal W; unipores in plates beyond petals: aboral plates wider than long (cubic in small specimens), pores on plate suture, in the middle of plate (Fig. 1.8D), and oral ambulacral plates longer than wide, pores on middle of plate suture (Fig. 1.8G). Phyllodes with unipores, short (usually 4 pores per half), with 1–2 (rarely 3) occluded plates, not sunken, broad, greatest W proximally (Figs. 1.7C, H; 1.8F–I). Inner pores usually straight, outer pores piercing at an angle (i.e. phyllodes are narrower on the inside). Pore on last plate displaced inwards (i.e. not in an occluded plate). Ambulacral basicoronal plates pierced by large buccal pore and one per ambulacrum also pierced by a phyllopore in the sequence a, a, b, a, b from phyllode I–V (Fig. 1.8F). Buccal pores near phyllodes, facing upwards. Phyllodes with 6–7 round sphaeridia in open pits near buccal pores (Fig. 1.7C).

Peristome transverse and pentagonal (Fig. 1.7C, H). Mouth opening in center of peristomial membrane. Bourrelets bulged outwards because of internal depression on the interambulacral basicoronal plates (Fig. 1.10C–F); bourrelets 1 and 4 narrower and least developed. Basicoronal plates elongated. Interambulacrum 5 with 11–12 plates between basicoronal plate and aboral edge of periproct; plates 2 and 3 much longer than wide. Naked zone along oral midline developed and pitted (Figs. 1.7B, G, 1.8B). Periproct aboral, longitudinal and narrow (Fig. 1.7E); surrounding plates bend, forming a groove. Periproct framed adorally by 7<sup>th</sup>–9<sup>th</sup> plates, and adapically by 11<sup>th</sup>–13<sup>th</sup> plates. Periproctal membrane with one row of large plates forming a U and anus sitting on center of adapical region (Fig. 1.8E). A second large plate and smaller plates may be also present inside.



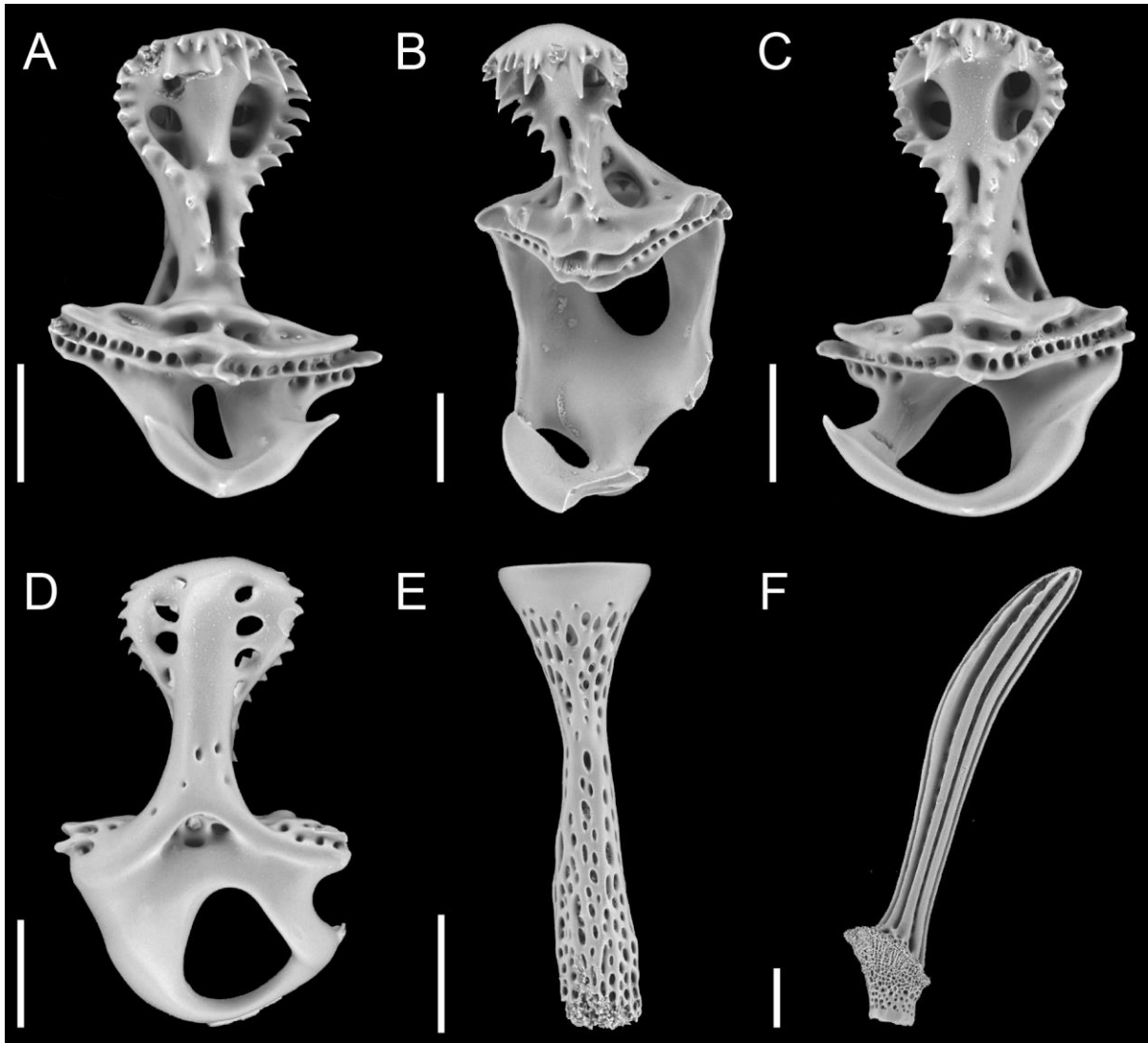
**Figure 1.7.** *Kassandrina malayana* comb. nov. (Mortensen, 1948b) (ZMUC 236 [syntype]): photos of test in (A) aboral and (B) oral view, (C) detail of peristome and phyllodes, and test in (D) side and (E) posterior view. *Kassandrina florescens* comb. nov. (CASIZ 71853): test in (F) aboral and (G) oral view, and (H) detail of peristome and phyllodes. Scale bars: A–B, D–G, 10 mm; C, H, 5 mm.



**Figure 1.8.** *Kassandrina malayana* comb. nov. (Mortensen, 1948b) (ZMUC 236 [sytype]): (A–C, F) SR $\mu$ CT-based volume renderings and (D–E, G–I) drawings showing (A) apical disc, (B) oral view of test, (C) internal view of petal III (light-colored pores in the middle are not open on the outside of the test), (D) plates beyond ambulacrum I, (E) periproct (external view; solid white region indicates anal opening), (F) internal view of peristome and phyllodes, and (G–I) internal views of the phyllodes V, II and III, respectively. Scale bars: A, C–I, 1 mm; B, 5 mm.



Primary tubercles perforate and slightly crenulate. Ophicephalous pedicellariae numerous at ambitus. Valves (198–267  $\mu\text{m}$  L; Fig. 1.9A–D) with coarse teeth along whole blade margin; tip of blade with two series of teeth: upper series with small teeth, lower series with large, thick teeth. Hinge broad, handles conspicuous. Stem (380–390  $\mu\text{m}$  L; Fig. 1.9E) thin with broad cup. Tridentate pedicellariae small, in periproct groove. Oral tubercles with displaced mamelon and larger than aboral tubercles. Spines (Fig. 1.9F) hollow, shaft serrated along entire length or only distally, aboral spines short and straight, spines on lip above periproct and oral spines long and thin, bourrelet spines thin and curved.



**Figure 1.9.** *Kassandrina malayana* comb. nov. (Mortensen, 1948b) (ZMUC 236 [S]), SEM images: (A–D) valves and (E) stem of ophicephalous pedicellariae, and (F) spine from bourrelet. Scale bars: A–D, 50  $\mu\text{m}$ ; E–F, 100  $\mu\text{m}$ .

**Etymology.** Named after Cassandra of Troy, depicted in the myth of Hecuba and Priam’s family as the odd sibling. *Kassandrina malayana* comb. nov. is an odd *Cassidulus*. Spelled with

an initial “K” so that the type species abbreviation can be distinguished from the old combination. Gender feminine.

**Material examined (included species).** *Kassandrina malayana* comb. nov. (Mortensen, 1948b): Kei Islands, Indonesia, 250–290 m, 10–12.V.1922, TL 13.5–25 mm (ZMUC 236 [S], ZMUC 521 [S]); Off Bedwell Island, Western Australia, 439 m, 18.VI.2007, TL 15 mm (AM J.24441).

*Kassandrina florescens* (Gregory) comb. nov. (*Cassidulus florescens* Gregory, 1892): Point Addis Lst., Late Oligocene–Early Miocene, Fyansford Hill, South Australia (NHM-UK E3772–3773 [Syntypes, TL 20–22 mm]). Point Addis Fm., Late Oligocene, Point Addis and Airey’s Inlet, South Australia (CASG 71853 [TL 22–32 mm], LACMIP 42070.1 [TL 22–30 mm]). Janjukian Fm., Oligocene, Airey’s Inlet, South Australia (MV P82080).

**Comparative material of other species examined.** *Australanthus longianus* (Gregory, 1890): Tortachilla Lst., Middle–Late Eocene, South Australia (NHM-UK E42428 [Syntype, TL 46 mm], MV P19225 [TL 58 mm], MV P19229 [TL 47 mm], MV P20197, NMNH 460548 [TL 39 mm]). Janjukian Fm., Late Eocene, Aldinga, South Australia (NMNH 96252 [TL 47 mm]). Kingscote Lst., Eocene–Oligocene, Kangaroo Island, Australia (MV P146827 [TL 54 mm], MV P146451–146462 [TL 54–74 mm]). Miocene (?), Thompson’s Beach, South Australia (UCMP 318988 [TL 31–35 mm]).

**Current distribution (extended herein).** Western Australia and Kei Island, 250–439 m deep. **Fossil record.** Oligocene to Early Miocene of South Australia.

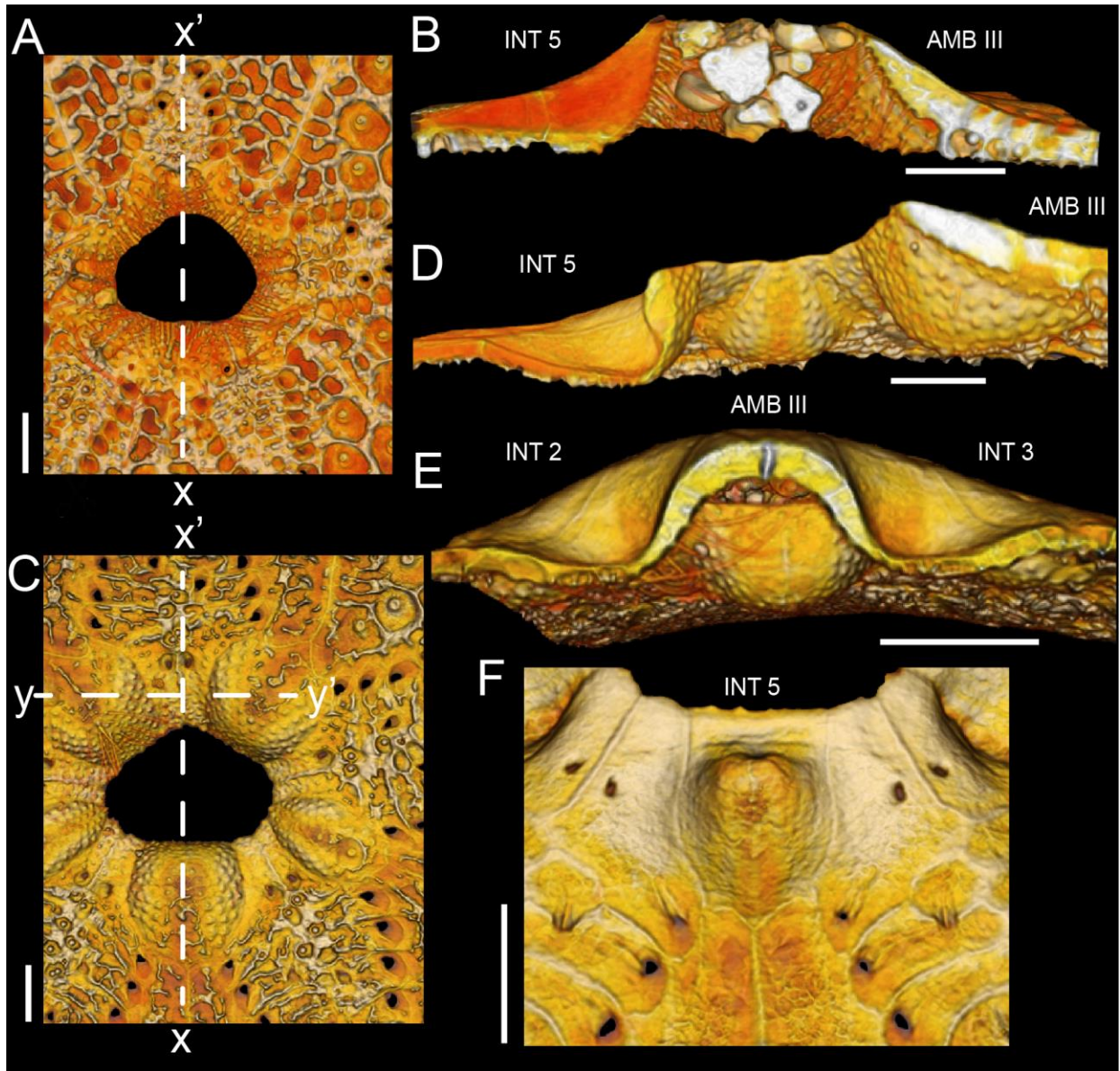
**Biological note.** Females of *K. florescens* comb. nov. have larger gonopores than the males. More specimens of *K. malayana* comb. nov. are needed to check whether this slight sexual dimorphism is characteristic of the genus.

**Note on type specimens of *K. malayana* comb. nov.** The original description of *K. malayana* comb. nov. was very poor and Mortensen (1948b) mentioned only the H, even though he included data from two specimens within the bathymetric range. He later provided a thorough description in his *Monograph of the Echinoidea* (Mortensen 1948a) and mentioned that there were two specimens: a larger specimen (the type) and a smaller specimen he designated as the co-type (considered here as the P).

### **The morphology of the bourrelets, and the classification and composition of the new genus**

A major difference between the families Cassidulidae and Faujasiidae is the shape of the bourrelets, which are round mounds in the former and tooth-like in the latter. However, there are intermediate states between these two forms, and some genera classified as faujasiids, such as *Petalobrissus* and *Australanthus*, do not always have tooth-like bourrelets. SR $\mu$ CT images of the taxa described herein have shown that bourrelets in cassiduloids are built in different ways. Bourrelets seen externally as mounds may be formed by an accretion of stereom on the interambulacral basicoronal plates, as seen in *Cassidulus* (Fig. 1.10B), or by a depression on the interior surface of the basicoronal plate, which makes these plates project outwards (Fig. 1.10D–F). The outer surface of the bourrelets of *K. malayana* comb. nov. is similar to that of *Cassidulus* (i.e. round mounds), and this may be the reason why this species has remained within the cassidulids rather than the faujasiids. However, our analyses show that the bourrelets of *K. malayana* comb. nov. was formed by a depression on the basicoronal plate, which means this species does not belong in the genus *Cassidulus* nor in any of the other extant cassiduloid genera *sensu* Kier (1962). We also looked extensively for an extinct genus whose diagnosis would

include *K. malayana* comb. nov.; however, we did not find a genus that conformed to the species description.



**Figure 1.10.** SR $\mu$ CT-based volume renderings of bourrelets from (A–B) *Cassidulus briareus* sp. nov. (MP 1267 MNHWU [paratype]) and (C–F) *Kassandrina malayana* comb. nov. (Mortensen, 1948b) (ZMUC 236 [syntype]): (A, C) oral view of test showing the peristome and part of the phyllodes I, III–V; dotted lines indicate region depicted in (B) and (D), i.e. cross section (x – x' axis) of bourrelet 5 on the left, and of phyllode III on the right (the inside of the test is towards the top of the page); (E) frontal cross section (y – y' axis) of test showing depression on bourrelets 2 and 3; and (F) internal view of test showing phyllodes I and V, and basicoronal 5 between them. AMB, ambulacrum; INT, interambulacrum. Scale bars: A–F, 1 mm.

Amongst the valid cassiduloid genera *sensu* Kier (1962), only *K. florescens* comb. nov. fits the description of the new genus. Although apparently common in the fossil record (based on the number of specimens deposited together in museum collections), there is not much information about this species in the literature. *Kassandrina florescens* comb. nov. was described in the genus *Cassidulus*, but Holmes (1999) implied that the genus classification could be wrong. Sullivan (2007) placed this genus in the genus *Australanthus* although no justification was given. However, the type species of *Australanthus*, *A. longianus*, has tooth-like bourrelets rather than round mounds as in *K. florescens* comb. nov.

Our analyses also showed that a depression is also present on the interior surface of the basicoronal plate of some faujasiids, such as *Faujasia* and *Hardouinia*, and it may be of phylogenetic importance. Cladistic analyses are necessary to test this hypothesis; until these are performed, we have decided to leave the genus unclassified (*incertae familiae*) instead of arbitrarily choosing the family that *K. malayana* comb. nov. or *K. florescens* comb. nov. are currently classified under (i.e. Cassidulidae and Faujasiidae, respectively). Also, because the uncertainty in the phylogenetic placement of this genus, we decided to provide a more detailed and broader diagnosis.

### **Taxonomic history of *K. malayana* comb. nov. and genus-level relationships**

Mortensen (1948a) described *K. malayana* comb. nov. in the genus *Procassidulus*, unaware that this genus had a tetrabasal apical disc. The periproct position and groove were also quite different, but Mortensen did not consider them of generic importance. Kier (1962) finally described the apical disc of *Procassidulus lapiscancri* as tetrabasal, leading Mooi (1990b) to place “*P. malayanus*” temporarily in the genus *Cassidulus*. Suter (1994b) tested this classification in a phylogenetic framework and the preferred phylogeny revealed that “*C. malayanus*” was sister taxon to the genera *Rhyncholampas* and *Cassidulus*. Suter (1994b) indicated that this species did not fit Kier’s description of the genus *Cassidulus*. However, he emphasized the need to analyze the fossil species before attempting to reclassify it. Indeed, *Cassidulus* contains many fossil species (see Lambert & Thiéry 1909–1925; Kier & Lawson 1978; Kroh 2010), but most of them have been mistakenly placed in this genus. In addition, morphological characters supporting the new genus are numerous, among them the longitudinal and aboral periproct, the absence of a lip above the periproct, equal *a* and *b* columns of respiratory podia, sphaeridia placed in open pits, internally depressed basicoronal plate, and phyllodes with occluded plates.

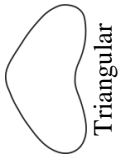
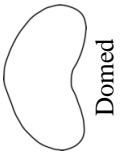
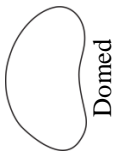

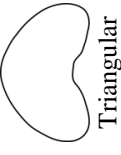
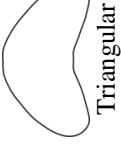
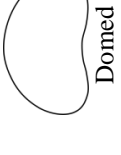












According to Suter (1994b), *Kassandrina* gen. nov. is the sister taxon to the clade composed of *Cassidulus* and *Rhyncholampas*. Synapomorphies that supported the clade (*Kassandrina* gen. nov. (*Cassidulus*, *Rhyncholampas*)) were: transverse peristome, phyllode W expanded beyond bourrelets, and ophicephalous pedicellariae with smooth neck.

### **Comparison among genera**

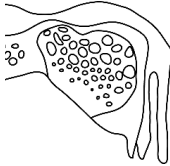
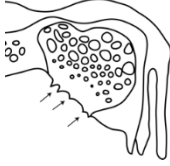

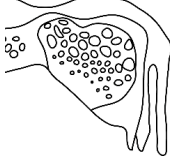
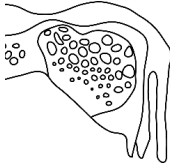
*Kassandrina* gen. nov. differs from *Cassidulus*, *Rhyncholampas* and *Paralampas* by having a longitudinal periproct; from *Eurhodia*, *Glossaster* and *Oligopodia* by having a transverse peristome; from *Petalobrissus*, *Procassidulus* and *Rhynchopygus* by having a monobasal apical disc; and from *Australanthus* by having occluded plates in the phyllodes (versus absence of occluded plates; inner pore is displaced from edge of plate), large sphaeridial pits by themselves or in double rows (versus tiny sphaeridial pits in groups of 2–4), pores of respiratory podia in the outer edge of the ambulacral plate at the end of the posterior petals

(versus pore-pairs migrate towards the middle of the plate at the end of the posterior petals), small expansion of the ambulacra W between the end of the petal and the ambitus (2–2.5 versus 3–4.5 times the W at end-petal), and bulging, but not tooth-like phyllodes (versus tooth-like phyllodes). Table 1.2 depicts the main morphological differences between the living cassiduloid species possessing a complete naked zone: *C. caribaeorum*, *C. mitis*, *C. infidus*, *C. briareus* sp. nov., *Rhyncholampas pacificus* (A. Agassiz, 1863), *K. malayana* comb. nov., and *Eurhodia relictata* Mooi, 1990a.

**Table 1.2.** Diagnostic morphological traits distinguishing the extant cassidulid species. Numbers in parentheses indicate rare occurrences.

	<i>Cassidulus caribaeorum</i> Lamarck	<i>Cassidulus mitis</i> Krau	<i>Cassidulus infidus</i> Mortensen	<i>Cassidulus briareus</i> sp. nov.	<i>Rhyncholampas pacificus</i> (A. Agassiz)	<i>Kassandrina malayana</i> comb. nov. (Mortensen)	<i>Eurhodia relicta</i> Mooi
Transversal cross-section of adult test <sup>1</sup>	 Triangular	 Domed	 Domed	 Domed	 Triangular	 Triangular	 Domed
Longitudinal cross-section of adult test <sup>1</sup>							
Greatest height of test	At apical disc	At apical disc	Posterior to apical disc	At apical disc	At apical disc	At apical disc	At apical disc
Occluded plates in phyllodes	Absent	Absent	Absent	Absent	Present	Present	Present
Outer row of phyllopores organized in a column	Yes	No	Yes	No	No	Yes	Yes
Organization of large plates in periproctal membrane	2 rows	2 rows	2 rows	2 rows	2 rows	1 row	1 row
Columns of respiratory podia in paired petals	Differ by more than 1 pore-pair	Differ by more than 1 pore-pair	Differ by more than 1 pore-pair	Differ by more than 1 pore-pair	Differ by more than 1 pore-pair	Equal	Equal
Number of plates framing periproct	8[9]	[7]8	?	6	[7]8-9	9	6
Periproct orientation	Wider than long	Wider than long	Wider than long	Wider than long	Wider than long	Longer than wide	Wider than long
Peristome orientation	Wider than long	Wider than long	Wider than long	Wider than long	Wider than long	Wider than long	Longer than wide
Teeth on base of blade of ophicephalous pedicellariae	 2 rows	 1 row	 1 row	?	 2 rows	 2 rows	?

**Table 1.2.** Continued.

Large tridentate pedicellariae	Present	Not found	Not found	?	Present	Not found	?
Blade of narrow tridentate pedicellariae	Wide	Narrow	Narrow	?	Narrow	Narrow	?
Teeth on base of narrow tridentate pedicellariae				?			Absent

<sup>1</sup>Drawings were based on  $\mu$ CT images of the cross-section of the test along the center of the peristome, except for *C. infidus* and *E. relicta*, whose drawings were based on photographs and peristome opening could not be drawn.

## CHAPTER 2

# Homoplasy, endemism, and extinction: phylogeny and biogeography of the cassidulid echinoids (Echinodermata)

### Introduction

Cassiduloids (from here onwards sensu Kier [1962], unless stated otherwise) are irregular echinoids that originated in the midst of the Marine Mesozoic Revolution (Kier 1974; Vermeij 1977), when the evolution of traits that permitted infaunalization (e.g. migration of the periproct away from the apical system, bilateralization, evolution of petals) opened up possibilities of avoiding epifaunal predation and for exploring a new ecological space (Boivin et al. 2018). Their rich fossil record indicates that the cassiduloids thrived early in their evolution and survived the end-Cretaceous mass extinction (Smith & Jeffery 1998), reaching their highest taxonomic diversity during the Eocene (*ca.* 56–40 Mya), when they comprised more than 40% of all echinoids (Kier 1974). Since then, their diversity has been declining and today they represent only 3% (about 30 species) of all living echinoids (Mooi 1990b). Explanations for this demise have included the lack of morphological innovation, competition with clypeasteroids and spatangoids, Cenozoic cooling, and stochastic events (Suter 1988; McKinney & Oyen 1989; Wagner 2000).

Taxonomically, the order Cassiduloidea has traditionally been a “trash can” among the irregular echinoids. The lack of unifying characteristics (synapomorphies) means that almost any irregular echinoid without a plastron or a clypeasteroid shape could be assigned to the group. As a result, proposed classification schemes comprise artificial families, sometimes even explicitly acknowledged as such by their authors (e.g. Cassidulidae and Echinobrissidae [Mortensen 1948a], and Pliolampadidae [Kier 1962]). Kier’s (1962) monograph was a great advance for cassiduloid studies, but subsequent phylogenetic analyses have shown that nearly all ten families proposed by him are not monophyletic, nor is the order Cassiduloidea itself monophyletic (Suter 1994a, b; Wilkinson et al. 1996; Smith 2001; Saucède & Néraudeau 2006).

The cassiduloid phylogenetic analysis performed by Suter (1994a) was the most complete and included all living and many fossil genera. However, possibly because of problems with character exhaustion (Wagner 2000) and consequent high similarity among groups, Suter (1994a) ended up with many most parsimonious hypotheses to choose from and weak support for the cassiduloid families. These results led Kroh and Smith (2010) to dismember the order and propose a new classification, elevating the valid families to the status of order and removing several genera from the Cassiduloidea altogether. The order Cassiduloidea sensu Kroh and Smith (2010) consists of just three families, Cassidulidae, Neolampadidae and Pliolampadidae; but the relationships among the cassiduloids was very poorly supported and no convincing synapomorphies have been identified to support even this smaller grouping.

The composition of the family Cassidulidae — “true cassiduloids” — has changed a great deal since Mortensen’s (1948) monograph (Table 2.1). As it retains the name of the family (and of the order Cassiduloidea), *Cassidulus* Lamarek, 1801 is the only genus that has always been classified as a cassidulid, together with *Rhyncholampas* A. Agassiz, 1869. In addition to these taxa, over 20 other genera have been considered members of the cassidulid group at one time or



another. However, most classifications (Table 2.1) and phylogenies published to date (Fig. 2.1) agree that five genera are included in this family: *Cassidulus*, *Rhyncholampas*, *Eurhodia*, *Glossaster* and *Paralampas* (Kroh & Mooi 2018). Although Suter's phylogenies had good taxonomic coverage, his goal was to analyze the relationships at the order level and few cassidulids were included in the analyses (Suter 1994a, b). Therefore, relationships among the cassidulid genera and their delimitations were not robust. Also, there remains a need to explain, in a phylogenetic framework, the origin of the cassidulids, their diversification during the Eocene and their near-complete demise as they approached the present.

As a first step towards this understanding, this study aimed to: 1) propose a time-calibrated phylogenetic hypothesis of relationships among the cassidulid genera and their contained species; 2) test the taxonomic assignments to date and discuss the taxonomic implications resulting from the phylogeny; 3) propose a paleogeographic scenario for the evolutionary history of the family Cassidulidae; and 4) analyze the impact of missing data and partial uncertainties in parsimony-based phylogenetic reconstruction.

**Table 2.1.** Classification of the selected ingroup genera according to previous and hypotheses of present study. Endnotes include taxa considered as cassidulids in previous studies, and the reason why they were considered outgroups (O) or not included in the present analyses. Abbreviations are: C, family Cassidulidae; E, family Echinobrissidae; Nu, family Nucleolitidae; P; family Pliolampadidae; I, *incertae sedis*.

Genera	Mortensen (1948a) <sup>1</sup>	Kier (1962) <sup>2</sup>	Mooi (1990b)	Smith & Jeffery (2000)	WoRMS (2018b)	This Study
<i>Cassidulus</i>	C	C	C	C	C	C
<i>Eurhodia</i>	C	P	C	C	C	C
<i>Glossaster</i>	C <sup>3</sup>	C <sup>4</sup>	–	–	C	C
<i>Kassandrina</i> <sup>5</sup>	C	–	C	–	I	I
<i>Paralampas</i>	C	C <sup>6</sup>	–	Nu <sup>7</sup>	C	C
<i>Rhyncholampas</i>	C <sup>4</sup>	C	C	C	C	C

<sup>1</sup> Mortensen (1948a) — genera with a tetrabasal apical disc: *Astrolampas* Pomel, *Fauraster* Lambert & Thiery, *Lefortia* Cossman, *Procassidulus* (O), *Pygurostoma* Cotteau & Gauthier, *Rhynchopygus* (O), and *Vologesia* Cotteau & Gauthier. Genera lacking a complete naked zone running along the oral midline of the test: *Clypeanthus* Cotteau, *Ilarionia* Dames, *Galerolampas* Cotteau, *Gitolampas* Gauthier, *Haimea* Michelin, *Neocatopygus* Duncan & Sladen, *Oligopodia* (O), *Oligopygus* de Loriol, *Pliolampas* Pomel, *Stigmatopygus* (O), *Studeria* (O), and *Zuffardia* Checchia-Rispoli. Genera with tooth-like bourrelets: *Hypsopygaster* Bajarunas and *Australanthus* (O). Others: *Protolampas* Lambert (inframarginal periproct), *Echinanthus* Leske (*nomen dubium*), *Microlampas* Cotteau (synonym with *Echinolampas*).

<sup>2</sup> Kier (1962) — genera with a tetrabasal apical disc: *Nucleopygus* Agassiz, *Ochetes* Pomel.

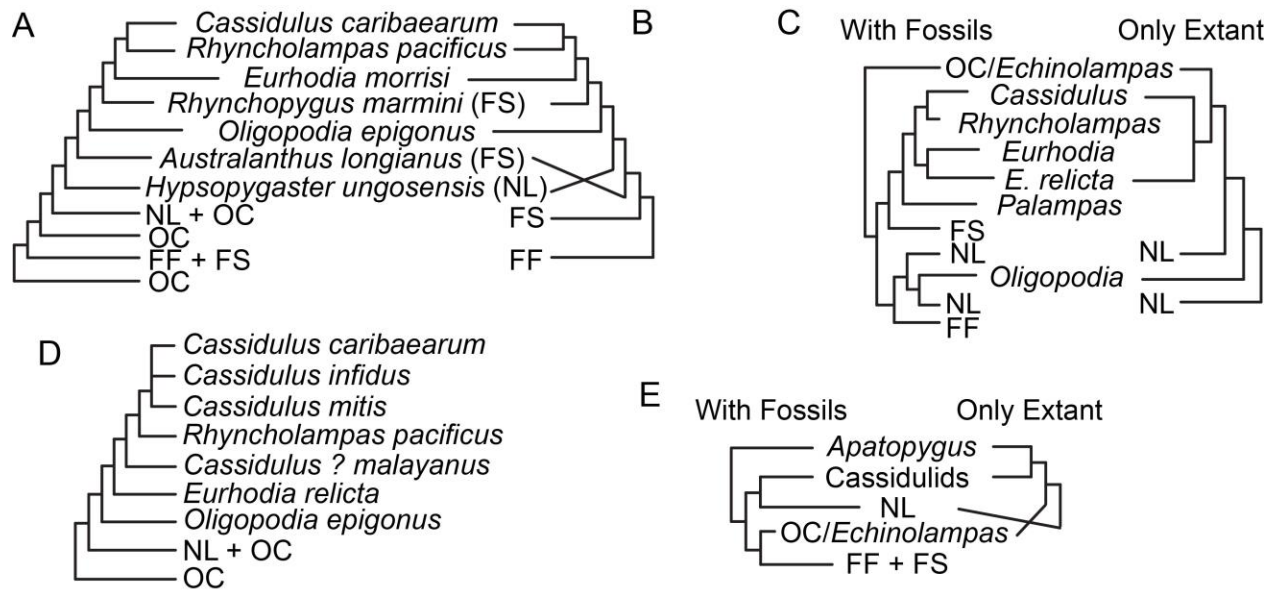
<sup>3</sup> Suggested synonymy with *Procassidulus*.

<sup>4</sup> Synonym with *Cassidulus*.

<sup>5</sup> The species *Kassandrina malayana* was previously placed in *Procassidulus* by Mortensen (1948a) and *Cassidulus* by Mooi (1990b).

<sup>6</sup> Suggested synonymy with *Rhynchopygus*.

<sup>7</sup> Subgenus of *Petalobrissus* Lambert.



**Figure 2.1.** Previous morphology-based phylogenetic hypotheses of relationship within cassidulids, and among cassidulids, faujasiids and neolampadids. (A) Suter (1994a), (B) Saucède & Néraudeau (2006), (C) Smith (2001), (D) Suter (1994b), (E) Kroh & Smith (2010). Abbreviations following WoRMS's (2018b) classification are: FF, Faujasiinae; FS, Stigmatopyginae; NL, Neolampadina; OC, other cassiduloids.

## Material and Methods

**Acronyms.** Australian Museum, Sydney, Australia (AM); California Academy of Sciences, San Francisco, U.S.A. (CAS; Invertebrate Zoology collections, CASIZ; Geology collections CASG); Los Angeles County, Natural History Museum, Los Angeles, U.S.A. (LACM; Invertebrate Zoology collections, LACM; Invertebrate Paleontology collections, LACMIP); Department of Geological and Geophysical Collections of the Mining and Geological Survey of Hungary, Budapest, Hungary (MBFSZ); Museum of Comparative Zoology, Harvard, U.S.A. (MCZ); Muséum National d'Histoire Naturelle, Paris, France (MNHN); Museu Nacional, Rio de Janeiro, Brazil (MNRJ); Muzeum Przyrodnicze Uniwersytetu Wrocławskiego, Wrocław, Poland (MP MNHWU); Museum Victoria, Melbourne, Australia (MV); Natural History Museum, London, United Kingdom (NHMUK); Naturhistorisches Museum Wien, Austria (NHMW); Naturhistorisches Museum, Basel, Switzerland (NMB); Department of Geology and Palaeontology, Museum d'Histoire Naturelle Genève, Switzerland (MHNG GEPI); National Museum of Natural History, Washington D.C., U.S.A. (NMNH); Swedish Museum of Natural History, Stockholm, Sweden (SMNH); University of California, Museum of Paleontology, Berkeley, U.S.A. (UCMP); Florida Museum of Natural History, Gainesville, U.S.A. (UF); Museu de Zoologia, Universidade Federal da Bahia, Salvador, Brazil (UFBA); Echinoderm Collection, Universidade Federal de Sergipe, Itabaiana, Brazil (UFISITAB); Naturalis Biodiversity Center, Leiden, Amsterdam (ZMA); Museum für Naturkunde, Berlin, Germany (ZMB); Zoological Museum, University of Copenhagen, Denmark (ZMUC); Museu de Zoologia da Universidade Estadual de Campinas, Brazil (ZUEC).

**Abbreviations.** **CI**, consistency index; **FAD**, first appearance datum; **I5**, interambulacrum 5; **LAD**, last appearance datum; **Mya**, millions of years ago; **MPT**, most parsimonious tree; **RI**, retention index; **TH**, test height; **TL**, test length; **TW**, test width. Numbering of plates, i.e. Arabic numerals for interambulacral plates and Roman numerals for ambulacral plates, follows Lovén's system (Lovén 1874).

### **Taxon Sampling**

**Ingroup Taxa.** Phylogenetic reconstructions of the cassiduloids have generally agreed that the monophyly of the family Cassidulidae is supported by a complete and pitted naked zone running along the oral I5 and ambulacrum III (Fig. 2.1). Ancestral traits that also characterize current members of this family (Kroh & Mooi 2018) are a monobasal apical system and a marginal periproct. At least 30 genera have been considered members of the cassidulid group, however, its classification has been unstable (see Table 2.1) and there is no widely accepted work of sufficiently comprehensive taxon sampling to serve as a standard for the group. Therefore, I used the traits listed above to define the ingroup.

The type and all extant species of each genus were included in the analyses. Fossil species were included whenever accessible specimens with good preservation were available. A total of 45 species (six extant and 39 extinct) from five genera were included (Table 2.2). Table 2.3 provides a summary with the taxonomic status of the species contained in each of these genera.

Genus *Cassidulus* Lamarck, 1801 — The family Cassidulidae (and concomitantly, the order Cassiduloidea) was based on this genus. Probably as a result of being the first genus and of its broad description, over 75 cassidulid-like species (and even cassiduloid-like ones) were erroneously placed in this genus (Souto *et al.* 2011b). Nine species (four extant and five extinct) were included in the analyses: the type, *C. caribaeorum* Lamarck, 1801; *C. briareus* Souto & Martins, 2018); *C. californicus* Anderson, 1905; *C. ellipticus* Kew, 1920; *C. falconensis* (Jeanett, 1928); *C. infidus* Mortensen, 1948b; *C. kieri* Adegoke, 1977; *C. mitis* Krau, 1954; *C. trojanus* Cooke, 1942. Carter & Beisel (1987) suggested that *C. trojanus* should be transferred to the genus *Eurhodia*; however, the traits they used to justify this change (i.e. deep pits in the naked zone and concave oral surface) are not present in the type species of *Eurhodia*.

Genus *Eurhodia* d'Archiac & Haime, 1853 — Kier (1962) described the family Pliolampadidae and placed *Eurhodia* within it, probably due to the presence of a longitudinally elongate peristome. However, pliolampadids do not have a naked zone in oral I5 and Mooi (1990b) reclassified *Eurhodia* within the cassidulids. Twelve species (one extant and 11 extinct) were included in my analyses: the type, *E. morrisoni* d'Archiac & Haime, 1853; *E. australiae* (Duncan, 1877); *E. baumi* Kier, 1980; *E. calderi* d'Archiac & Haime, 1853; *E. cravenensis* (Kellum, 1926); *E. holmesi* (Twitchell in Clark & Twitchell, 1915); *E. matleyi* (Hawkins in Arnold & Clark, 1927); *E. navillei* (de Loriol, 1880); *E. patelliformis* (Bouvé, 1851); *E. relictata* Mooi, 1990a; and *E. rugosa* (Ravenel, 1848), *E. thebensis* (de Loriol, 1880). *Eurhodia relictata* is the only representative of this genus since the Late Eocene (*ca.* 37.8 Mya). Mooi (1990a) included *E. relictata* within *Eurhodia* because of its resemblance to *E. holmesi* even though he also highlighted its great resemblance to *Oligopodia epigonus* (von Martens, 1865). Other species with questionable status are *E. cravenensis*, considered synonymous with *E. holmesi* by Cooke (1942) and Kier (1980), *E. calderi* and *E. thebensis*, considered synonymous with *E. navillei* by Roman & Strougo (1994). My decision to keep all three species was based on differences noticed in my morphological analyses.

Genus *Glossaster* Lambert, 1918 — This is the oldest known cassidulid genus, with the first occurrences dating back to the Campanian (*ca.* 83.6 Mya, Late Cretaceous). Its fossil record indicates that this genus went extinct in the Middle Eocene (*ca.* 37.8 Mya). The original description of *Glossaster* was brief and it was unclear whether Lambert (1918) was describing a new genus (as on p. 18 he mentions eight genera in the tribe Rhynchopyginae Lambert, and *Glossaster* was listed among the genera on p. 39) or a subgenus (as he mentions in the footnote 2 on p. 39). *Glossaster* has been considered a synonym of *Procassidulus* (Mortensen 1948a) and of *Cassidulus* (Kier 1962), but Kier & Lawson (1978) considered *Glossaster* a genus on its own. Three species were included in my analyses, even though their classification has been unstable (see Néraudeau *et al.* 1997; Smith & Jeffery 2000): the type, *G. sorigneti* (Michelin in Goubert, 1859), *G. vasseuri* (Cotteau, 1888) and *G. welschi* Gauthier in Lambert, 1931.

Genus *Paralampas* Duncan & Sladen, 1882 — *Paralampas* is also an extinct cassidulid genus, with a fossil record ranging from the Maastrichtian to the Eocene (*ca.* 72.1–33.9 Mya). To my knowledge, there are seven species of *Paralampas* widely distributed. Although Smith & Jeffery (2000) considered *Paralampas* a subgenus of *Petalobrissus*, the latter has a tetrabasal apical system and a longitudinal periproct. Two species were included in my analyses: the type, *P. pileus* Duncan & Sladen, 1882 and *P. rancureli* Tessier & Roman, 1973.

Genus *Rhyncholampas* Agassiz, 1869 — This genus was described to include *C. caribaeorum* (the former type species designated upon original description of the genus) and *Rhyncholampas pacificus* (Agassiz, 1863) because the genus *Cassidulus* was thought to be pre-occupied. After analyzing some fossil specimens, Agassiz (1872, p. 153, 342) synonymized *Rhyncholampas* with *Rhynchopygus* d'Orbigny, 1856, even though he was compelled to separate these genera in 1869 (Agassiz 1869, p. 270). *Rhyncholampas* is the sister taxon to *Cassidulus* (Fig. 2.1) and some authors (e.g. Mortensen 1948a) have considered them to be synonymous. Kier (1962, p. 18) mentioned that both genera include species with intermediate characteristics making these difficult to allocate unequivocally to either genus. In this regard, I analyzed all species available to test the monophyly of these genera. Eighteen species (one extant and 17 extinct) were included in the analyses: the type, *R. pacificus*; *R. alabamensis* (Twitchell in Clark & Twitchell, 1915); *R. anceps* Lambert, 1933; *R. ayresi* Kier, 1963; *R. carolinensis* (Twitchell in Clark & Twitchell, 1915); *R. chipolanus* Oyen & Portell, 1996; *R. conradi* (Conrad, 1850); *R. daradensis* (M. Lambert in Meunier, 1906); *R. ericsoni* (Fisher, 1951); *R. evergladensis* (Mansfield, 1932); *R. globosus* (Fisher, 1951); *R. gouldii* (Bouvé, 1846); *R. grignonensis* (Defrance, 1825); *R. mexicanus* (Kew, 1920); *R. riveroi* (Sánchez-Roig, 1949); *R. rodriguezii* Lambert & Sánchez-Roig in Sánchez-Roig 1926 (its type specimen could not be analyzed but two morphotypes were observed, therefore, both were included in the analyses: *R. rodriguezii\_A* and *R. rodriguezii\_R*); *R. sabistonensis* (Kellum, 1926); *R. tuderii* Lambert, 1937. A few *Rhyncholampas* species had already been synonymized by Cooke (1959), for example, *R. evergladensis* with *sabistonensis* and *R. alabamensis* with *R. gouldii* (but see Osborn and Ciampaglio [2014] for a revalidation of *R. alabamensis*). Most American species are very similar and their differences are often related to size and overall test shape; therefore, it is possible that challenges in comparing specimens with similar body size from different countries and formations have resulted in taxonomic oversplitting.

**Outgroup selection.** Outgroups (*sensu* Nixon & Carpenter 1993) were considered as terminal taxa to verify the relationships among the cassidulid genera. Twenty-one species, 15 extinct and six extant, were chosen as outgroup taxa (Table 2.2). I sampled outgroups across the various

cassiduloid groups, but I gave priority to extinct species with available material in good condition, thereby avoiding having to account for large amounts of missing data in the matrix. Also, some outgroups that diverged very early in the history of the cassiduloids (i.e. *Nucleolites scutatus* Lamarck, 1816 and *Apatopygus recens* [Milne Edwards in Cuvier, 1836]) were chosen in an attempt to minimize homoplasy and problems of character exhaustion common within the cassiduloids (Huelsenbeck 1991; Wagner 2000; Smith 2001).

The superfamily Neolampadina is the sister group to the cassidulids (Kroh & Smith 2010) and was represented by two extant and one extinct species: *Neolampas rostellata* Agassiz, 1869; *Pliolampas elegantula* (Cotteau, 1883); and *Studeria recens* (Agassiz, 1879). The Neolampadina live in deeper waters (Mooi 1990b) and probably evolved through paedomorphosis (Philip 1963) that resulted in poor development or even loss of petaloids.

The relationship between cassidulids and faujasiids has been controversial (Suter 1994a; Smith 2000; Kroh & Smith 2010). The Faujasiidae is an extinct group and many of its species have been classified as cassidulids at some point in their taxonomic history (e.g. *Australanthus longianus* (Gregory, 1890), *Procassidulus lapiscancris* (Leske, 1778), *Petalobrissus cubensis* (Weisbord, 1934), *Rhynchopygus marmeni* (Desor in Agassiz & Desor, 1847), and vice-versa (e.g. *G. welschi*). In addition to these four faujasiid species, I included eight faujasiid outgroups in the analyses, according to availability of material: *Petalobrissus setifensis* (Coquand in Cotteau, 1866), *Rhynchopygus arumaensis* Kier, 1972, *Rhynchopygus macari* Smiser, 1935, *Stigmatopygus pulchelus* Smith, 1995, *Hardouinia mortonis* (Michelin, 1850), *Hardouinia bassleri* (Twitchell in Clark & Twitchell, 1915), *Faujasia apicalis* (Desor in Agassiz & Desor, 1847), and *Faujasia rancheriana* Cooke, 1955.

I also chose two genera (*Oligopodia* Duncan, 1889 and *Kassandrina* Souto & Martins, 2018) that include extant species previously considered cassidulids and whose taxonomic status remains poorly established. *Oligopodia epigonus* (von Martens, 1865) was classified within the cassidulids by Mortensen (1948a) and Mooi (1990b), while others considered this species *incertae sedis* (e.g. Kier & Lawson 1978). Phylogenetic hypotheses have suggested that this genus is a cassidulid (Suter 1994a, b; Saucède & Néraudeau 2006); however, in these studies *O. epigonus* was coded as having a wide naked zone in the oral midline, an aboral lip above the periproct and a pentagonal peristome, features not present in the holotype. Smith (2001) placed *O. epigonus* within the neolampadids.

The other *incertae sedis* genus, *Kassandrina*, was recently described to include the species *K. malayana* (Mortensen, 1948b) and *K. florescens* (Gregory, 1892). Mooi (1990b) temporarily placed *K. malayana* in the genus *Cassidulus* but this species has an aboral and longitudinal periproct rather than posterior and transverse. Because of the presence of exclusive characteristics belonging to cassidulids (e.g. pitted naked zone) and faujasiids (e.g. basicoronal plates internally depressed), Souto & Martins (2018) decided to leave this genus unclassified rather than choosing one of these families arbitrarily. All three *incertae sedis* species mentioned here were included as outgroups in my analyses.

Finally, I included an extant Echinolampadidae (*Echinolampas depressa* [Gray, 1851]) as an outgroup. Because my goal was to reconstruct the relationships within the cassidulids, the clypeasteroids were not included.

**Table 2.2.** List of taxa included in the phylogenetic analyses and used for the phylogenetic calibration, their stratigraphic range, geographic distribution, and the character coding completeness (CCC) for each species. Type species of genera in bold; genera and family classification following WoRMS (2018b). Uncertain age between [].

Taxon	Estimated Age (Ma) <sup>1</sup>	Reference for Age Assignment <sup>2</sup>	Geographic Distribution	CCC (%) <sup>3</sup>
Family Apatopygidae				
<i>Apatopygus recens</i>	0.01–0	N/A	New Zealand	100
<i>Nucleolites scutatus</i>	163.5–145	Kier 1962	Western Europe	92
Order Cassiduloidea				
Family Cassidulidae				
<i>Cassidulus britareus</i>	0.01–0	N/A	Australia	96
<i>Cassidulus californicus</i>	56–37.8	Squires & Demettrion 1995	USA (CA)	83–85
<b><i>Cassidulus caribaeorum</i></b>	0.01–0	N/A	Caribbean Sea	100
<i>Cassidulus ellipticus</i>	56–37.8	Squires & Demettrion 1995	Mexico (BC) to USA (CA)	79–82
<i>Cassidulus falconensis</i>	[15.97–5.33]–2.58 <sup>4</sup>	Cooke 1961, Mihaljević et al. 2010, UCMP	Venezuela	92
<i>Cassidulus infidus</i>	0.01–0	N/A	Brazil (BA)	100
<i>Cassidulus kieri</i>	66–56	Adegoke 1977	Nigeria	94
<i>Cassidulus mitis</i>	0.01–0	N/A	Brazil (RJ, SP)	100
<i>Cassidulus trojanus</i>	37.8–33.9	Osborn et al. 2016	USA (FL)	92
<i>Eurhodia australiae</i>	47.8–33.9	Holmes 2004	Australia (SA)	92
<i>Eurhodia baumi</i>	47.8–37.8	Osborn et al. 2016	USA (SC, NC)	91
<i>Eurhodia calderi</i>	59.2–47.8	Duncan & Sladen 1886, Afzal et al. 2009, UCMP	Pakistan	93
<i>Eurhodia cravenensis</i>	47.8–37.8	Kier 1980	USA (NC)	89–90
<i>Eurhodia holmesi</i>	47.8–37.8	Osborn et al. 2016	USA (SC, NC)	93
<i>Eurhodia matleyi</i>	47.8–33.9	Donovan 2004	Jamaica	91
<b><i>Eurhodia morrissi</i></b>	59.2–47.8	Smith & Jeffery 2000, Afzal et al. 2009	Pakistan	93
<i>Eurhodia navillei</i>	56–41.2	Roman & Strougo 1994, Tawadros 2012	Egypt and Senegal	88–90
<i>Eurhodia patelliformis</i>	37.8–33.9	Osborn et al. 2016	USA (FL)	91
<i>Eurhodia relicta</i>	0.01–0	N/A	Venezuela and Suriname	98
<i>Eurhodia rugosa</i>	47.8–37.8	Osborn et al. 2016	USA (SC, NC)	94
<i>Eurhodia thebensis</i>	47.8–41.2	Fourtau 1913, Tawadros 2012	Egypt	82–85

**Table 2.2.** Continued.

Taxon	Estimated Age (Ma) <sup>1</sup>	Reference for Age Assignment <sup>2</sup>	Geographic Distribution	CCC (%) <sup>3</sup>
<i>Glossaster sorigneti</i>	47.8–41.2	Néraudeau et al. 1997	France	81–82
<i>Glossaster vasseuri</i>	47.8–37.8	Cotteau 1885–1889	France	92–93
<i>Glossaster welschi</i>	83.6–66	MINHN Syntype	Algeria	74–75
<i>Paralampas pileus</i>	59.2–47.8	Duncan & Sladen 1886, Afzal et al. 2009, UCMF	Pakistan	92–93
<i>Paralampas rancureli</i>	59.2–56	Smith & Jeffery 2000	Ivory Coast	86
<i>Rhyncholampas alabamensis</i>	27.82–23.03	Osborn & Ciampaglio 2014	USA (AL, MS)	90–92
<i>Rhyncholampas anceps</i>	56–47.8	Lambert 1933	Madagascar	85–87
<i>Rhyncholampas ayresi</i>	3.6–0.01	Oyen & Portell 2002	USA (FL)	91
<i>Rhyncholampas carolinensis</i>	47.8–37.8	Osborn et al. 2016	USA (NC)	91
<i>Rhyncholampas chipolanus</i>	23.03–15.97	Oyen & Portell 2002	USA (FL)	88–89
<i>Rhyncholampas conradi</i>	37.8–33.9	Osborn et al. 2016	USA (FL)	91
<i>Rhyncholampas daradensis</i>	47.8–41.2	Roman & Gorodiski 1959	Senegal	92
<i>Rhyncholampas ericsoni</i>	[47.8–37.8]–33.9	Osborn et al. 2016	USA (FL)	88–89
<i>Rhyncholampas evergladensis</i>	5.33–2.58	Oyen & Portell 2002	USA (FL)	93
<i>Rhyncholampas globosus</i>	47.8–33.9	Fischer 1951, UF	USA (FL)	90
<i>Rhyncholampas gouldii</i>	33.9–23.03	Oyen & Portell 2002	USA (FL)	92
<i>Rhyncholampas grignonensis</i>	47.8–37.8	Néraudeau et al. 1997, Carrasco 2016	Western Europe	90
<i>Rhyncholampas mexicanus</i>	15.97–7.25	Kew 1920, Coates 1999	Mexico (BC)	88
<i>Rhyncholampas pacificus</i>	0.01–0	N/A	Mexico (BC) to Panama, Galapagos island	100
<i>Rhyncholampas riveroi</i>	27.82–23.03	Sanchez Roig 1949	Cuba	75–77
<i>Rhyncholampas rodriguezi_A</i>	23.03–15.97	Sanchez Roig 1949	Cuba	87
<i>Rhyncholampas rodriguezi_R</i>	23.03–15.97	Sanchez Roig 1949	Cuba	90–91
<i>Rhyncholampas sabistonensis</i>	47.8–37.8 <sup>5</sup>	Kellum 1926	USA (NC)	88–91
<i>Rhyncholampas tuderi</i>	56–37.8	Lambert 1937, MNHN	Morocco	88–89

**Table 2.2.** Continued.

Taxon	Estimated Age (Ma) <sup>1</sup>	Reference for Age Assignment <sup>2</sup>	Geographic Distribution	CCC (%) <sup>3</sup>
Family Neolampadidae				
<i>Neolampas rostellata</i>	0.01–0	N/A	Florida, Gulf of Mexico, NE Atlantic	100
<i>Studeria recens</i>	0.01–0	N/A	Indo-Pacific	94
Family Pliolampadidae				
<i>Pliolampas elegantula</i>	[23.03–]15.97– 11.63[–5.33]	Kier 1962, MNHN	France	93
Order Clypeasteroidea				
Family Faujasidae				
<i>Australanthus longianus</i>	[47.8–37.8]–33.9	Holmes 2004	Australia (SA)	93
<i>Faujasia apicalis</i>	72.1–66	Smith & Jeffery 2000	The Netherlands and Belgium	93
<i>Faujasia rancheriana</i>	113–100.5	Cooke 1955	Colombia	92
<i>Hardouinia mortonis</i>	72.1–66	Smith & Jeffery 2000	USA (NC, MS, TX), Cuba	94
<i>Hardouinia bassleri</i>	86.3–83.6	Cooke 1953	USA (AL)	83–84
<i>Petalobrius cubensis</i>	89.8–72.1	Weisbord 1934, Cooke 1953	Cuba, Mexico (CS), USA (TX)	94
<i>Petalobrius setifensis</i>	83.6–66	Smith & Jeffery 2000	Algeria, Tunisia, Lybia	90–91
<i>Proccassidulus lapiscancri</i>	72.1–66	Smith & Jeffery 2000	The Netherlands and Belgium	93
<i>Rhynchopygus arumaensis</i>	83.6–72.1	Kier 1972	Saudi Arabia	91
<i>Rhynchopygus macari</i>	72.1–66	Smith & Jeffery 2000	The Netherlands and Belgium	82–84
<i>Rhynchopygus marmini</i>	72.1–66	Smith & Jeffery 2000	Western Europe	88–89
<i>Stigmatopygus pulchellus</i>	72.1–66	Smith & Jeffery 2000	Oman, United Arab	90–91
Order Echinolampadoidea				
Family Echinolampadidae				
<i>Echinolampas depressa</i>	0.01–0	N/A	Colombia to USA (NC)	100
Order <i>sedis</i> and stem groups				
<i>Kassandrina florescens</i>	[33.9–27.82]– 15.97	Souto & Martins 2018	Australia (South)	92
<i>Kassandrina malayana</i>	0.01–0	N/A	Indo-Pacific	99
<i>Oligopodia epigonus</i>	0.01–0	N/A	Indo-Pacific	100



<sup>1</sup>According to Cohen et al. (2013; updated).

<sup>2</sup>Australian formations were checked against the Australian Stratigraphic Units Database, available at [http://dbforms.ga.gov.au/pls/www/geodx.strat\\_units.int](http://dbforms.ga.gov.au/pls/www/geodx.strat_units.int), on 15 August 2017; and the U.S.A. formations were checked against the National Geologic Map Database, available at <https://ngmdb.usgs.gov/Geolex/search>, on 15 August 2017.

<sup>3</sup>Lower values of completeness consider partial uncertainty as missing data.

<sup>4</sup>Jeanett (1928) assigned *C. falconensis* to the “serie Capadare”, in the upper part of “couches d’Ojo de Agua”, Middle Miocene (serie Caparade might refer to the Capadare formation). Cooke (1961, p. 5) mentioned that the section Jeannett (1928) called “d’Ojo de Agua” actually refers to two formations that range from the Middle to the Late Miocene. He also presented more information regarding the locality where the specimens were collected, Punta Gavilán; still, he also assigned *C. falconensis* to the Middle Miocene. Mihaljević et al. (2010) reported two records for this species: *Eurhodia falconensis*, as originally described by Jeannett (1928) placed in the original description; and *Cassidulus (Cassidulus) falconensis*, which was the classification proposed by Cooke (1961). Both records were assigned to the Middle Miocene. Lodeiros et al. (2013) interpreted “Punta Gavilán” as belonging to the Punta Gavilán formation, which is Pliocene in age. The UCMF holds specimens of *C. falconensis* from the San Gregorio formation (Pliocene). Because the age assignments have been challenging to interpret and the UCMF record was verified by us, we placed uncertainty in the Miocene range of the species.

<sup>5</sup>Age assignment for *R. sabistonensis* is very controversial. Cooke (1942) suggests this species occurs at the Trent Marl (Oligocene) and specimens at UF are from the Tamiami formation (Pliocene). Because the identification of *Rhyncholampas* species is challenging, we decided to use the age assignment presented in the original description of the species (i.e. Castle Hayne marl, Middle Eocene).

**Table 2.3.** Status of the known cassidulid taxa prior to analysis. “Species analyzed” are those species where I was able to examine specimens. Of those “Species not analyzed”, I made taxonomic calls based on the literature: “Probably valid” are species whose morphological description and/or images most closely fit the description of their assigned genus; “Uncertain status” refers to species that I did not have access to the literature or that had descriptions and images too poor to allow for confident identification and thus they need further morphological analysis; and “Misclassified” are species whose description and/or images clearly indicate they should be placed in a different genus. The percentage of the species in each cassidulid genus included in the phylogenetic analysis is given in the last column: lowest value = “Species analyzed” / (“Species analyzed” + “Probably valid” + “Uncertain status”); largest value = “Species analyzed” / (“Species analyzed” + “Probably valid”).

Genus	Species analyzed <sup>1</sup>	Species not analyzed			Species included in phylogenetic analysis
		Probably valid	Uncertain status	Misclassified	
<i>Cassidulus</i>	9	1	9	21	47–90%
<i>Eurhodia</i>	12	1	12	2	48–92%
<i>Glossaster</i>	3	1	2	0	50–75%
<i>Paralampas</i>	2	1	2	2	40–67%
<i>Rhyncholampas</i>	18	9	20 <sup>2</sup>	0	38–67%

<sup>1</sup> Indicate genus designations prior to the analyses. See section “Taxonomic assignment of cassiduloids analyzed in this study” for taxonomic assignments following the analysis.

<sup>2</sup> Many of these described as *Pygorhynchus* Agassiz, 1839.

### Data Collection, Characters and Coding

Data were collected from direct observation of specimens and from the literature (Appendix 2.1). Morphological analyses were performed using a stereo microscope attached to a camera lucida (if available during museum visits). Light application of ethanol with a paintbrush was used to highlight plate boundaries of dry specimens. When authorized by museum curators, fossils were cleaned and polished to reveal plate boundaries and ambulacral pores. Test measurements were taken with a digital caliper to the nearest 0.01 mm. Selected drawings were digitized and converted to high-resolution images in Adobe Illustrator CS6 using a Wacom Intuos tablet.

Tube foot ossicles, pedicellariae and sphaeridia were removed with thin needles, cleaned and disarticulated using household bleach (ca. 5% sodium hypochlorite solution) for 3–5 minutes, washed using three changes of distilled water, and kept in absolute ethanol. They were then placed on metal stubs with double-sided carbon tape using a dropper, separated from each other using a thin needle, set aside to air-dry, and imaged with a Hitachi TM-1000 SEM.

I selected 98 morphological features based on test shape (11 characters, 25 states), apical system (7 characters, 15 states), aboral ambulacra (20 characters, 54 states), periproct and I5 (19 characters, 54 states), peristome and basicoronal plates (20 characters, 43 states), oral ambulacra and sphaeridia (15 characters, 38 states), and tuberculation and pedicellariae (6 characters, 13 states). I did not exclude any character that had high homoplasy indices in previous studies, but characters related to the internal organs were not included because they are only available for a small subset of the extant species included here. For quantitative characters, only the largest specimens of each species were measured to reduce biases related to ontogenetic changes. Sixty-

four characters were binary and 34 multi-state, with a total of 242 character states. Four quantitative characters were ordered.

The following list applies to all phylogenetic analyses (see explanation in “Phylogenetic Analyses”). Ordered characters and characters excluded from A2 (taxa with missing information excluded) are indicated.

A) Test shape: aboral view

1. *Test outline: subquadrate or round* ( $TW > 0.90 TL$ ) (Fig. 2.2A–B) [0]; *oval* ( $TW 0.75–0.90 TL$ ) (Fig. 2.2C–D) [1]; *elongate* ( $TW < 0.75 TL$ ) (Fig. 2.2E) [2]. This character codes for the relationship between the test width and the test length.

2. *Test edge: uniform, nearly straight edges* (Fig. 2.2A, D) [0]; *curved, greatest in the middle or posteriorly* (Fig. 2.2B–C) [1].

3. *Test funneled posteriorly: no* [0]; *yes* (Fig. 2.2D–E) [1]. In tests with a funneled posterior region, the plates in interambulacra 1 and 4 are nearly straight and the width of the test decreases rapidly from widest point to the posterior region.

B) Test shape: frontal view

4. *Shape of the transverse cross-section of the test: triangular* (Fig. 2.2F–G) [0]; *dome-shaped* (Fig. 2.2H–I) [1]. This character coded for the relationship between test height and test width: triangular tests are slightly inflated and they increase in height while they diminish in width; domed tests are strongly inflated and they increase in height while they largely maintain their width.

5. *Acute peak at the apical system: absent* [0]; *present* (Fig. 2.2H) [1]. This character codes for an elevation at the apical system common in *Rhyncholampas* species, and is independent from the transverse cross-section of the test. For instance, *R. ericsoni* has a domed test and an acute peak at the apical system.

6. *Adoral contour of test edge: sharp* (Fig. 2.2F–H) [0]; *round* (Fig. 2.2I) [1]. In tests with sharp edges, the widest region is in the oral most 1/3 of the test; in tests with round edges, the widest region is near or at the middle of the test.

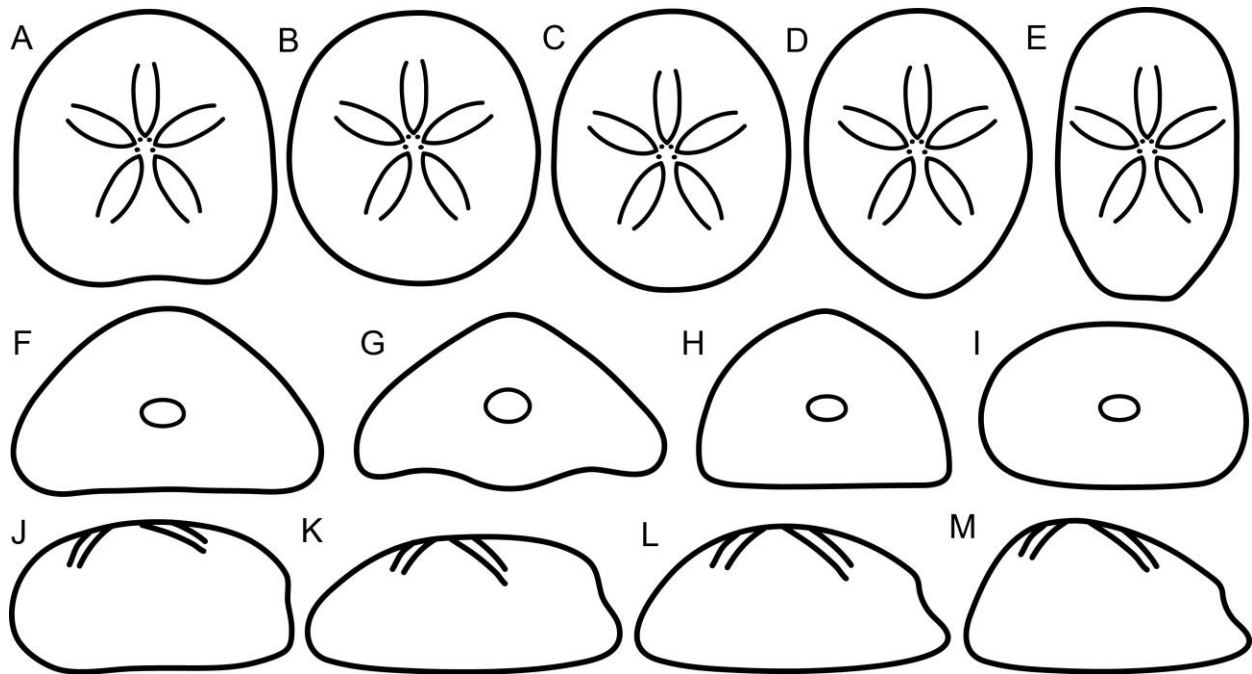
C) Test shape: posterior view

7. *Oral posterior I5 plates concave: no* [0]; *yes* [1]. Some cassiduloids have a curvature on the oral posterior I5 plates resulting in an interradial region projected downwards. In addition, there is a depression on the plates at the oral ambulacra 1 and 5 and instead of having an open midline throughout the test, these species have an ‘M-shaped’ bipartite channel (Fig. 2.2G). This condition is strongest in *Hardouinia* but is also present in other genera.

D) Test shape: lateral view

8. *Shape of the aboral region at a longitudinal cross-section: flat* (Fig. 2.2J–K) [0]; *slight posterior slope* (Fig. 2.2L) [1]; *sharp posterior slope* (Fig. 2.2M) [2]. Tests with flat aboral region have a roughly uniform height from the apical system to the periproct. In tests with a posterior slope, the test decreases in height towards the peristome so the greatest center of mass is in the anteriormost region of the test; the decrease may be slight or sharp.

9. *Posterior region of test truncated: no* (Fig. 2.2K–M) [0]; *yes* (Fig. 2.2J) [1]. Tests with truncated posterior region end abruptly.



**Figure 2.2.** Outline drawings of cassiduloid tests depicting differences in shape (characters 1–9). Aboral view: (A) subquadrate, (B) round, (C–D) oval, and (E) elongate outline; posterior view showing transverse cross-section of test: (F–G) triangular and (H–I) dome-shaped; side view: outline (J) mostly flat throughout, (K) flat posteriorly, and with (L) slight and (M) sharp aboral slope.

#### E) Test shape: oral view

10. Overall contour of oral region: nearly flat [0]; concavity only near the peristome [1]; concavity starting at test edge [2].

11. Oral region inflated: no [0]; yes [1]. This character codes for the presence of a swollen region in interambulacra 1, 4 and 5.

#### F) Apical System

12. Apical system monobasal in adults: no [0]; yes [1]. The apical system in *Apatopygus recens* is tetrabasal in juveniles and monobasal in adults, possibly because of the fusion of the genital plates. Because I do not have information about the ontogenetic changes in most fossil taxa, I chose to code this character for adults only.

13. Length of apical system in relation to the test length: large (over 8.5% of TL) [0]; medium-sized (6.5–8.5% of TL) [1]; small (less than 6.5% of TL) [2]. Measurements of apical system were taken from the anterior margin of ocular plate III to the posteriormost region of the apical system (posterior edge of madreporic plate or of ocular plates I and V). Only mature specimens (i.e. with all gonopores well developed) were measured. For species with strong sexual dimorphism in gonopore size (e.g. *S. recens*), only males were measured.

14. Number of gonopores: four [0]; three [1].

15. Symmetry among gonopores: symmetric [0]; asymmetric [1]. Gonopores are asymmetric when gonopores 1 and 2 are displaced distally and proximally, respectively, so that

the position of the gonopores in the left and right side of the apical system is asymmetric. For species with three gonopores, symmetry was based on the position of the posterior gonopores in relation to the center of the apical system.

16. *Location of ocular plates: between gonopores [0]; beyond gonopores [1].*

17. *Madreporic plate extended posteriorly: no [0]; yes [1].* In some species, the posterior region of the madreporic plate has an acute rather than a curved or flat edge, ending beyond gonopores 1 and 4.

18. *Hydropores: abundant, all over madreporic plate [0]; few (up to 15), confined to a small region in madreporic plate [1].*

#### G) Aboral ambulacra

*Neolampas rostellata* does not have developed petals and their ambulacral system is reduced to single and rudimentary pores, except for the phyllodes which are well developed. Characters 19–26, 28–30, 32 coded for features of the aboral ambulacra not applicable to this species.

19. *Largest petal of ambulacral system, in size and number of pore-pairs: I and III roughly same size [0]; petal I largest [1]; petal III largest [2].* In species with unequal columns of pore-pairs, I measured the longest column.

20. *Posterior paired petals very reduced: no [0]; yes [1].* Petals I and V were considered very reduced when their length was less than 90% the length of the other petals.

#### H) Aboral ambulacra: petal III

21. *Petal III — distal shape (Fig. 2.3A): wide ( $We/Wm > 0.70$ ) [0]; convergent ( $We/Wm = 0.40-0.70$ ) [1]; tapering ( $We/Wm < 0.40$ ) [2].* The ancestral state is a divergent petal, in which the pores at the end of the petal follow the growth in plate width and get more separated; while in tapering petals, the pores at the end of the petal are often positioned slightly closer to the midline of the petal, even with slight increases in plate width.

22. *Petal III — shape of columns of respiratory podia: both straight (Fig. 2.3B–C) [0]; inner straight and outer bowed (Fig. 2.3D) [1]; both bowed (Fig. 2.3E–F) [2].* This character codes for the change in width of the plates in the petal. Some have constant width throughout; others increase and then decrease in width.

23. *Petal III— width of poriferous zone in relation to interporiferous zone (Fig. 2.3A): very wide ( $Wr > Wm$ ) [0]; wide ( $Wm \geq Wr$  and  $Wm < 2Wr$ ) [1]; narrow ( $Wm > 2Wr$ ) [2].* This character codes for the relation between the region of the petal responsible for gas exchange (poriferous) and the region with more primary spine coverage (interporiferous). In some species, the region for gas exchange is very reduced and the area with primary spines is large; in others, the region for gas exchange takes up most of the petal area.

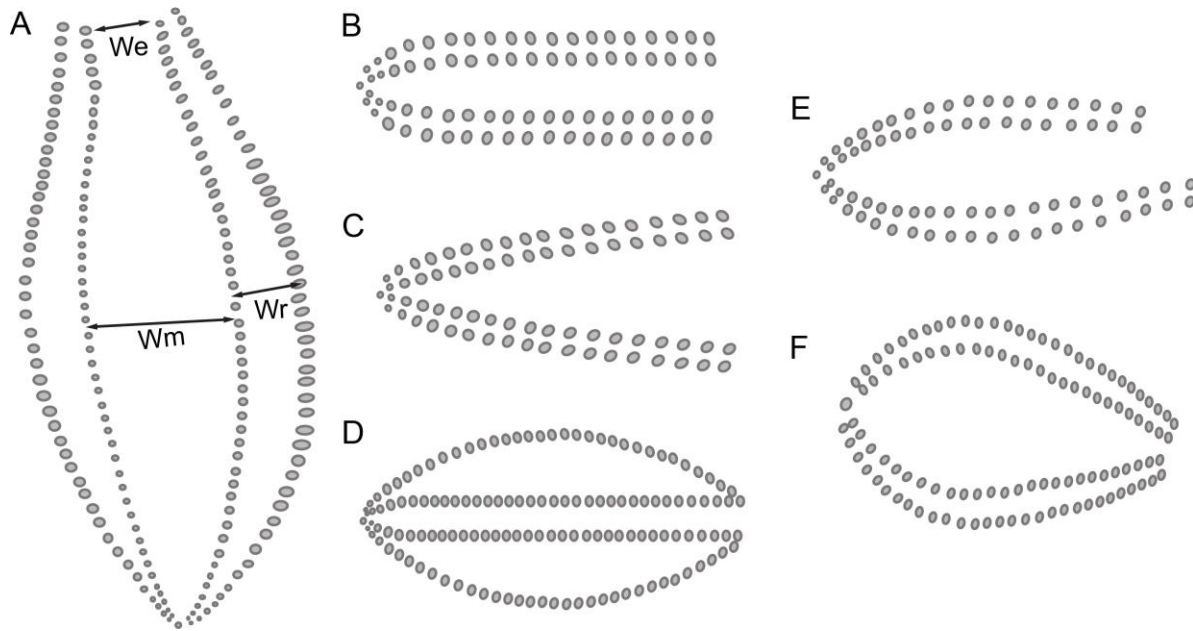
24. *Length of a and b columns of respiratory podia – petal III: equal or differ by one pore-pair [0]; differ by more than one pore-pair [1].*

#### I) Aboral ambulacra: petals II and IV

25. *Shape of anterior paired petals: straight (Fig. 2.3B) [0]; V-shaped (Fig. 2.3C) [1]; oval (Fig. 2.3D) [2]; tulip-shaped (Fig. 2.3E) [3]; leaf-shaped (Fig. 2.3F) [4].* These states are usually distinguished by the width of the ambulacral plates throughout the petal length and by the position of the inner pores. In straight petals, the ambulacral plates have roughly the same width and the columns of respiratory podia are straight and parallel. In the other petal shapes, the

ambulacral plates increase in width towards the middle of the petal. This increase may be continuous throughout the petal while the inner column is straight but not parallel, resulting in V-shaped petals; or the ambulacral plates decrease in width from the middle to the end of the petal, resulting in a bowed outer column of respiratory podia. Bowed outer columns: straight and parallel inner columns result in oval petals, bowed and open inner columns result in tulip-shaped petals, and bowed and tapering inner columns result in leaf-shaped petals.

26. Length of a and b columns of respiratory podia – paired anterior petals: equal or differ by one pore-pair [0]; differ by 2–4 pore-pairs [1]; differ by 5 or more pore-pairs [2].



**Figure 2.3.** Drawings of a petal showing (A) measurements for characters 21 and 23 (Wm, perradial zone width; We, distal [opening] width; and Wr, poriferous zone width), and character states for petal shape (character 25) defined as (B) straight, (C) V-shaped, (D) oval, (E) tulip-shaped, and (F) leaf-shaped. Images also refer to character 22.

#### J) Aboral ambulacra: petals I and V

27. Shape of the ambulacra at posterior paired petals: uniform [0]; bowed [1]. The shape was evaluated based on the difference between the widest region of the petal and the width of the plates at the end of the petal. In bowed petals, the width of the plates increases up to the middle of the petal and then it decreases by more than 25% towards the end.

28. Width of a and b columns of respiratory podia in posterior petals: not asymmetric [0]; strong asymmetry (width inner column < 80% width outer column) [1].

29. Length of a and b columns of respiratory podia – paired posterior petals: equal or differ by one pore-pair [0]; unequal differ by more than one pore-pair [1]. Most cassiduloids have columns of pore-pairs of the same size; however, in a few species the number of pore-pairs may be significantly different within a species (i.e. *R. pacificus*, whose columns may differ by three to seven pore-pairs). This condition appears early in the life of the echinoid because of different timing in the development of both columns and therefore, should not be influenced by the size of the specimen.

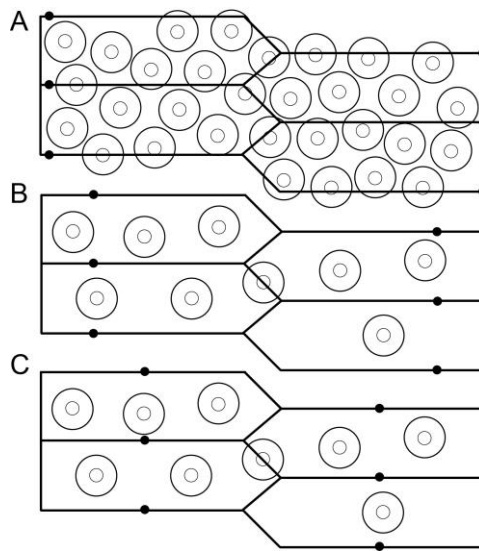
K) Aboral ambulacra: general characteristics of petals

30. *Shape of outer respiratory podia petals: slit-like [0]; elongated [1]; round [2].* In all species, the outer pores are round internally but in some cases these pores expand as they move to the surface of the test becoming elongated (width is kept) or slit-like. Only the largest specimens of each species were measured to avoid biases related to ontogenetic changes.

31. *Density of primary tubercles in interporiferous zone: high (Fig. 2.4A) [0]; low (Fig. 2.4B) [1].* Density of tubercles is high when there is no space among them, and low when primary tubercles are sparse and more tubercles could be accommodated among them.

32. *Tuberculation of poriferous zone: miliary tubercles only [0]; miliary and 1–2 sparse primary tubercles [1]; miliary and 3–5 often reduced primary tubercles [2]; 6 or more reduced primary tubercles [3].* Some species have small primary tubercles in the poriferous zones; although reduced in size, these are still larger than the miliary tubercles.

33. *Last inner pore of paired petals on occluded plate: no [0]; yes [1].*



**Figure 2.4.** (A–C) Drawings of the ambulacral plates beyond the posterior petals. Solid dots represent the pores and concentric circles represent the primary tubercles. Images refer to characters 31 and 38.

L) Aboral ambulacra: plates beyond petals

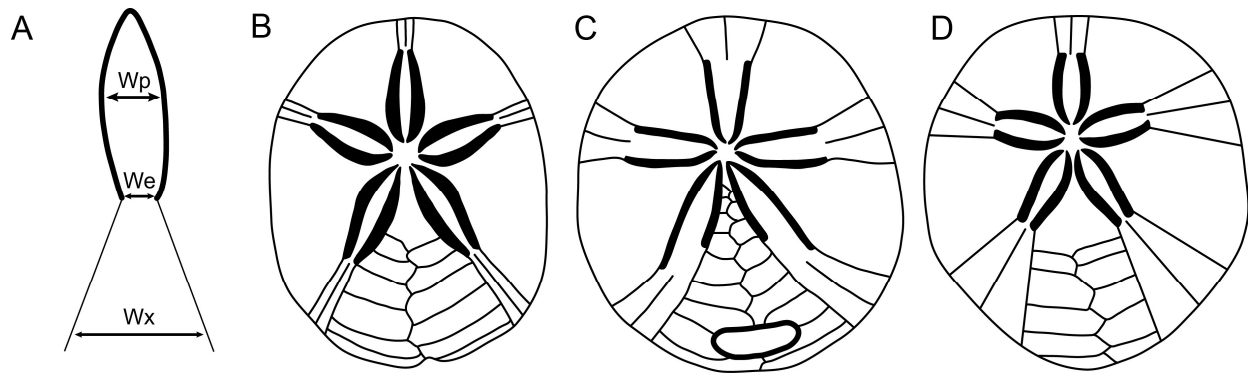
34. *Expansion of the posterior ambulacra beyond petals (Fig. 2.5A): uniform (Fig. 2.5B) [0]; slight expansion (Fig. 2.5C) [1]; strong expansion (Fig. 2.5D) [2].* Expansion ( $W_x$ ) was estimated in relation to the width of the plates at the end of the posterior petals ( $W_e$ ): slight expansion is an increase by up to 100% and strong expansion is an increase of more than 100%.

35. *Orientation of ambulacra beyond petals: curved anteriorly (Fig. 2.5C) [0]; straight expansion following ambulacra (Fig. 2.5D) [1].*

36. *Amount of expansion ( $W_x$ ) in relation to greatest width of posterior petals ( $W_p$ ) (Fig. 2.5A): petal more than 5% wider (Fig. 2.5B) [0]; same width (Fig. 2.5C) [1]; expansion more than 5% wider (Fig. 2.5D) [2].* This ratio apparently changed with ontogeny (i.e. expansion grows faster with ontogeny), therefore, only the larger specimens of each species were analyzed.

37. *Shape of ambulacral plates beyond posterior petals: rectangular, wider than long [0]; cubic or slightly longer than wide [1].* This character codes for the first four plates after the end of the petal. Rectangular plates are present when the ambulacrum is wide and the pores beyond petals are close to one another.

38. *Placement of pores beyond posterior petals: near or at adradial suture (Fig. 2.4A) [0]; between adradial suture and the middle of the plate (Fig. 2.4B) [1]; running thorough the midline of the plate (Fig. 2.4C) [2].* The pore may be displaced across the stereom. Therefore, this character coded for the position of the pore on the outside of the test.



**Figure 2.5.** (A) Drawing of the posterior ambulacrum showing the measurements for characters 34 and 36 (We, distal; Wp, petal [opening] width; and Wx, ambulacral expansion). Outline drawings of tests showing different ambulacral expansion types: (B) uniform, (C) slight, and (D) strong. Images also refer to character 35.

#### M) Periproct and interambulacrum 5

39. *Periproct position: on aboral surface [0]; marginal [1]; on oral surface [2].*

40. *Presence of a prominent aboral lip over periproct: no (Fig. 2.6A) [0]; yes (Fig. 2.6B) [1].* A lip is formed when the aboral plates framing the periproct curve and extend, forming a lip that covers the periproct opening from above.

41. *Shape of lateral plates framing periproct: bent inwards (Fig. 2.6C, E) [0]; straight (Fig. 2.6A–B, D) [1].* Initially, the periproct of the cassiduloids was placed in a groove, formed by the bending of the lateral plates framing it. But in many groups, the lateral plates do not bend and are narrower as a result.

42. *Lateral plates framing periproct supported internally by folds: no [0]; yes (Fig. 2.6F) [1].* The plates framing the periproct may be internally supported by an additional layer of stereom that connects them.

43. *Periproct with subanal shelf: no [0]; yes (Fig. 2.6B) [1].* A subanal shelf is formed by the inward and horizontal expansion of the adoral plates framing the periproct.

44. *Periproct orientation: longitudinal (width < length) [0]; equant (width = length) [1]; transverse (width > length) [2].* The lateral plates framing transverse periprocts are usually shorter and narrower than the lateral plates framing longitudinal periprocts.

45. *Periproct tear-shaped: no [0]; yes [1].* In a tear-shaped periproct, the width increases from aboral to oral region.



46. *Plates on periproctal membrane: one main row of medium-sized plates and many small plates (Fig. 2.6G) [0]; two rows of medium-sized plates and few small plates (Fig. 2.6H) [1]; one row with three large plates (Fig. 2.6I) [2].* Not included in A2.

47. *Anus placement in peristomial membrane: in the center (Fig. 2.6G) [0]; on the aboral edge (Fig. 2.6H–I) [1].* Not included in A2.

48. *Shape of interambulacral plates beneath periproct: concave, forming a groove [0]; convex [1].* This character is inapplicable to the taxa with a periproct near or in the oral surface.

49. *Minimum number of plates on I5, between the basicoronal plate and the base of the periproct: 11 or more [0]; 10 [1]; 9 [2]; 8 [3]; 7 [4]; 6 [5]; 5 [6].* This character coded for the position of the periproct with respect to specific plates within interambulacrum 5. The number of plates may undergo a slight variation within a species (usually by only one plate), but it does not vary with the size of the specimens. This number is also not related to the size of the species; for instance, *R. mexicanus* (TL = 70 mm) and *E. australiae* (TL = 26 mm) have the same number of plates. Ordered 0–1–2.

50. *Minimum number of plates framing the periproct: 10 or more [0]; 9 [1]; 8 [2]; 7 [3]; 6 [4]; 5 [5]; 4 [6].* The number of plates framing the periproct does not necessarily correlate with the size of the periproct given that the length of the plates may vary across taxa. Ordered 0–1–2–3–4–5–6.

51. *Presence of primary tubercles in distal region of I5 basicoronal plate and proximal region of plates 5.2: absent or few [0]; abundant (more than five tubercles) [1].* Some species have tubercles near the peristome regardless of the presence (and width) of a naked zone. The tubercles may be sparse, along the phyllodes or randomly distributed (variable within a species), or abundant along the phyllodes and in the middle of the plate.

52. *Naked zone running along oral I5: absent [0]; reduced [1]; developed [2].* A reduced naked zone has only a small reduction in tubercle density and it does not reach the posterior edge of the test.

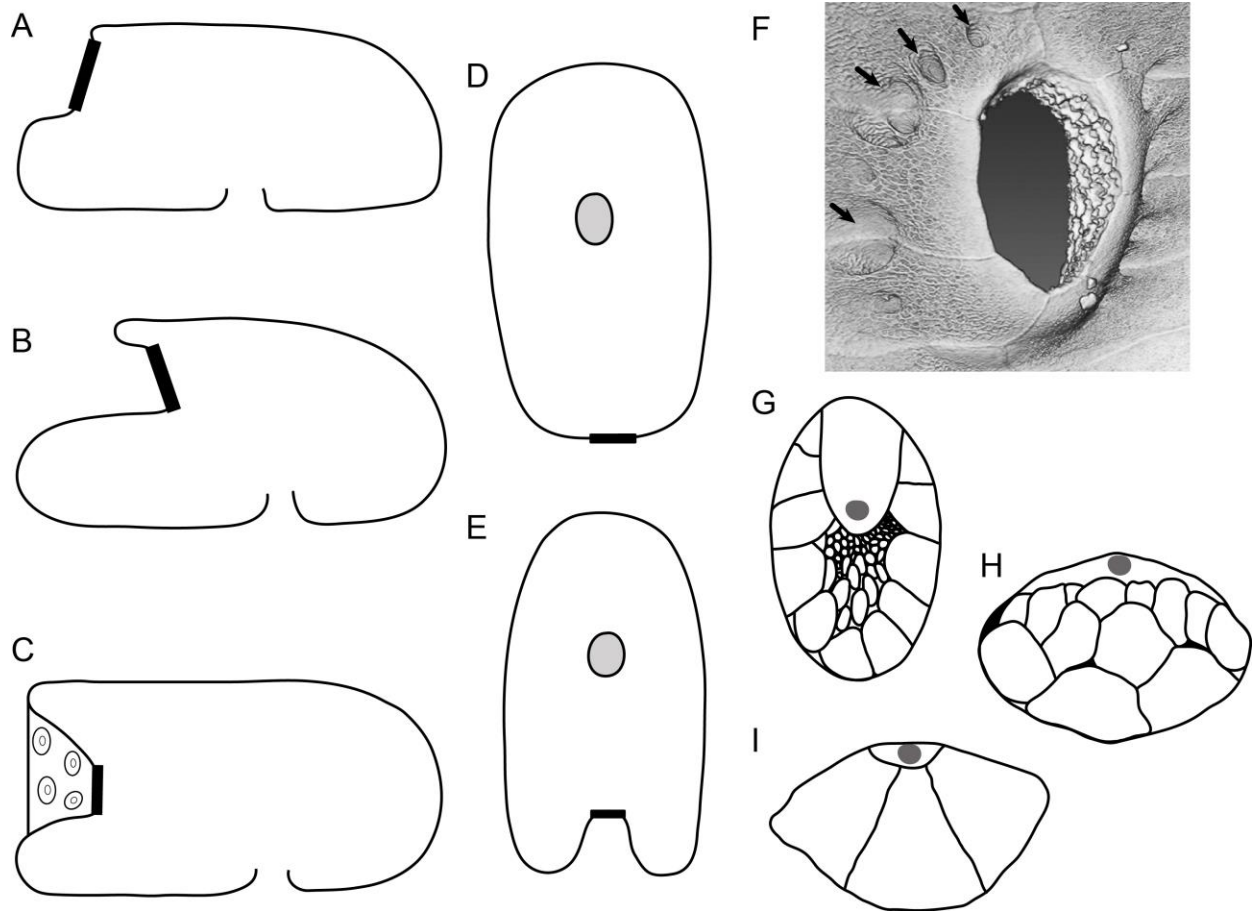
53. *Width of I5 naked zone in relation to the test width: narrow (less than 10% TW) [0]; wide (12% or more in TW) [1].* This character was coded based on the broadest region of the naked zone, usually in the middle.

54. *I5 granular: no [0]; yes [1].* Although the naked zone is free of primary spines, miliary spines are still present. In some species, there is an increased density of miliary tubercles, giving a granular appearance.

55. *Pits on I5: absent [0]; finely pitted [1]; deeply pitted [2].* The distribution of pits in the naked zone was very variable; therefore, I only coded for their size rather than their distribution.

56. *Pits on distal edge of interambulacral basicoronal plates: absent [0]; present [1].* Pits may be large and deep (as in some *Eurhodia*) or small and shallow (as in *A. longianus*), following the same pattern coded in character 60.

57. *Naked zone running along oral ambulacrum III: absent [0]; narrow [1]; wide [2].* The width of the naked zone in ambulacrum III was estimated based on the naked zone in I5. Naked zone III is usually larger, but in some species, it is narrower.



**Figure 2.6.** Outline drawings of the cross-section of the test along the anterior-posterior axis, showing the test outline in (A–C) side view and in (D–E) aboral view; peristome in light grey, solid rectangle represents placement of the periproctal membrane, which is inside of the test in (C) and (E) because of the bending of the interambulacral plates. (F)  $\mu$ CT image of the periproct of *Oligopodia epigonus* in internal view showing the peristomial folds. (G–I) Drawings of the different periproctal plate arrangements and placement of anal opening (in dark grey). Images refer to characters 40–43, 46, 47.

#### N) Peristome and basicoronal plates

58. *Peristome orientation*: transverse (width > 1.1 length) [0]; equant (width = 0.9 – 1.1 length) [1]; longitudinal (width < 0.9 length) [2].

59. *Shape of peristome*: (sub)pentagonal (Fig. 2.7B–E) [0]; oval (Fig. 2.7A) [1]; The peristome in some cassiduloids (i.e. *C. infidus*) develops from a circular to a pentagonal shape, passing through a subpentagonal stage when juvenile.

60. *Peristome position*: near the center or slightly anterior [0]; very anterior [1]. Peristomes were considered very anterior when their posterior edge was less than 41% of the TL from the anterior ambitus.

61. *Accretion of stereom on interambulacral basicoronal plates* (Souto & Martins 2018, fig. 10): absent or low [0]; high [1]. In some species, there is the accretion of a thick stereom layer on the basicoronal plates, forming solid bourrelets.

62. *Deep depression on interambulacral basicoronal plates (Souto & Martins 2018, fig. 10): absent [0]; present [1].*

63. *Bourrelet 5 bulged anteriorly: no (Fig. 2.7A) [0]; yes (Fig. 2.7B) [1].* In some species, the posterior region of the peristome is strongly convex adorally; in others, this anterior projection is weak or absent resulting in a nearly flat posterior edge.

64. *Bourrelets pointy: no [0]; yes [1].* Developed bourrelets are usually smoothly bulged, but sometimes they project outwards (towards the sediment), forming a pointed tip.

65. *Bourrelets tooth-like: no [0]; yes (Fig. 2.7C) [1].* In tooth-like bourrelets, the sides of the bourrelets are straight instead of round, and the distal region is wider than the proximal region.

66. *Bourrelet 5 poorly developed: no [0]; yes [1].* This character codes for the development of bourrelet 5 in relation to bourrelets 2 and 3. Despite being undeveloped, bourrelet 5 may still be slightly bulged, pointed or tooth-like.

67. *Basicoronal plates 1 and 4 narrower than basicoronal plate 5: no [0]; yes [1].*

68. *Oral surface of I5 basicoronal plate longer than wide: no, wider or equant (Fig. 2.7A–B) [0]; yes (Fig. 2.7D–E) [1].*

69. *Distal edge of I5 basicoronal plate expands beyond distal edge of ambulacrum V basicoronal plate: no (Fig. 2.7B) [0]; yes (Fig. 2.7D–E) [1].*

70. *Proximal edge of I5 basicoronal plate more than twice as wide as ambulacrum V basicoronal plate: yes (Fig. 2.7B, D) [0]; no (Fig. 2.7E) [1].*

71. *Size of ambulacral basicoronal plates along the perradial suture: short [0]; medium-sized [1]; enlarged [2].* The size was estimated based on the orientation and size of the second ambulacral plate. When the basicoronal is short, the second plate is diagonal to the midline of the phyllode (Fig. 2.7C); when it is medium-sized, the second plate is perpendicular to the midline of the phyllode (Fig. 2.7B); and when it is enlarged, the second plate is a demiplate (Fig. 2.7E).

72. *Shape of ambulacral basicoronal plates: flush or wall-like (Fig. 2.7F) [0]; bent (Fig. 2.7G) [1].* In bent plates, a great proportion of the plate is on the oral side. The shape of the plates apparently influences where the first pores are located: in flush plates, the pores start deep inside the peristome; in wall-like plates, the pores are placed at the oral region of the plate, often facing the inside of the peristome; and in bent plates, the pores are located distally, close to the phyllodes and facing outwards.

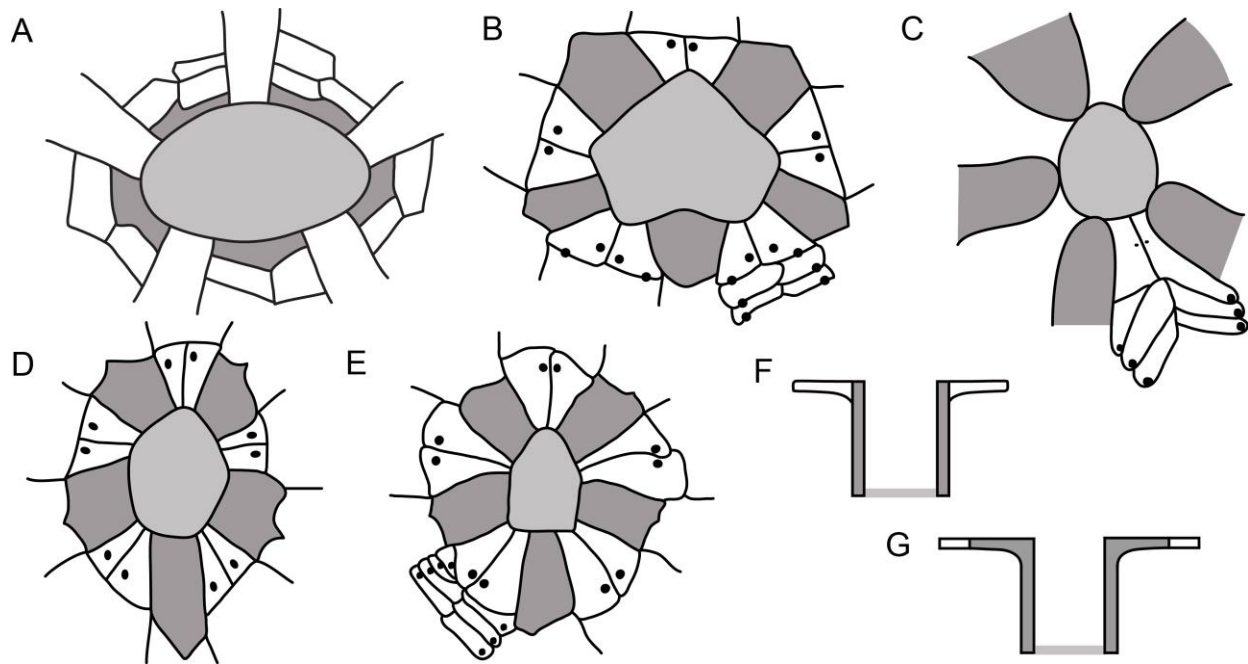
73. *Adoral region of ambulacral basicoronal plate depressed: no [0]; yes [1].* Depressed plates are often distally enlarged and their lowest region is usually lower than the peristomial opening.

74. *Ambulacral basicoronal plates pierced by more than two pores: no [0]; yes [1].*

75. *First pore in ambulacral basicoronal plate modified into a buccal pore: no (Fig. 2.8D) [0]; reduced (Fig. 2.8E) [1]; distinct (Fig. 2.8A–C, F) [2].*

76. *Distance between first and second ambulacral pores: near (Fig. 2.7B) [0]; far (Fig. 2.7C) [1].* When the pores are far from each other, there is a large and noticeable gap between them.

77. *Placement of second ambulacral pore: in the middle of the plate, often distally (Fig. 2.7B) [0]; distally and near the adradial suture (Fig. 2.7C) [1].* One plate on each pair of ambulacral basicoronal plates in cassiduloids is pierced by at least two pores. In species with only two pores, the second pore is always placed distally; however, in species with more than two pores, the placement of the pores along the anterior-posterior axis will vary according to the number of pores present.



**Figure 2.7.** Drawings of the adoral region of the test (A–E) seen from the outside (light grey represents the peristome, dark grey the interambulacral basicoronal plates, and black dots the buccal pores and phyllopores) and (F–G) in cross-section (interambulacral basicoronal plates in dark grey and post-basicoronal plates in white; peristome in light grey represents the region closest to the inside of the test). Images refer to characters 59, 63, 65, 68–72, 76, 77.

O) Oral ambulacra: phyllode III

78. *Shape of outer column of anterior phyllode: straight (Fig. 2.8A) [0]; barrel-shaped (Fig. 2.8B) [1]; triangular-shaped (Fig. 2.8C) [2].* Straight phyllodes have parallel columns of pores; barrel-shaped phyllodes have their greatest width in the middle; and triangular-shaped phyllodes have their greatest width adorally.

P) Oral ambulacra: phyllodes II and IV

79. *Arrangement of columns of paired anterior phyllodes: one column (inner column absent; Fig. 2.8A) [0]; scattered pores (Fig. 2.8C) [1]; two complete columns (inner column throughout phyllode; Fig. 2.8B, D) [2].* In phyllodes in which the inner column is complete, the outer column is usually composed only of demiplates.

80. *Shape of outer column of paired anterior phyllodes: rows of three (Fig. 2.8D) [0]; straight or barrel-shaped (Fig. 2.8A–B) [1]; tapering (Fig. 2.8E) [2].*

81. *Maximum number of normal plates in paired anterior phyllodes: eleven or more [0]; eight to ten [1]; five to seven [2]; up to four [3].* Character states were chosen based on intraspecific variability; for example, some species had specimens with five to seven or eight to ten pores but never outside of these ranges. Ordered 0–1–2–3.

Q) Oral ambulacra: phyllodes I and V

82. *Size of posterior phyllodes: long, last phyllopores distal to 2<sup>nd</sup> interambulacral plate [0]; short, last phyllopores proximal to 3<sup>rd</sup> interambulacral plate [1].*

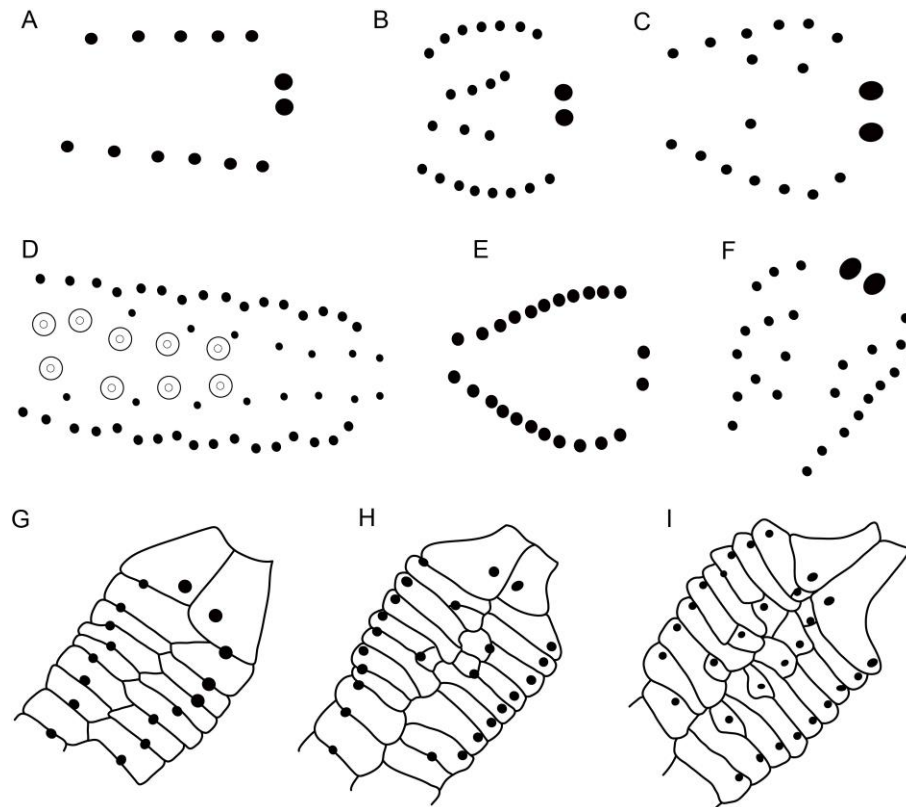
83. *Maximum number of normal plates in posterior phyllodes: twelve or more [0]; eight to eleven [1]; four to seven [2].* Character states were chosen based on intraspecific variability. Also, in phyllodes with up to seven pores, the pores are spaced out; but in phyllodes with twelve pores or more, the pores are close together and the phyllode is very developed. Ordered 0–1–2.

84. *Arrangement of outer phyllopores in external view: pores in a uniform column (Fig. 2.8E) [0]; pores scattered (Fig. 2.8F) [1].* Phyllopores are usually placed near the adradial suture, but in some species the phyllopores are also found in the middle of the plate or near the perradial suture. These pores were considered as part of the outer column because they are not homologous with pores in occluded plates.

85. *Phyllodes tapering: no [0]; yes (Fig. 2.8E) [1].* Phyllodes were considered tapering when the pores in the distal plates were displaced towards the perradial suture.

86. *Occluded plates in posterior phyllodes: absent or rare (Fig. 2.8G) [0]; few (Fig. 2.8H) [1]; many (Fig. 2.8I) [2].* The presence and number of occluded plates is usually conserved within a species. However, in some cases I found one or two specimens with one occluded plate. These occurrences were considered rare. Also, the concentration of occluded plates was assessed by taking into account the ratio between the number of occluded plates and the number of normal plates. In phyllodes with many occluded plates, at least 1/3 of the plates are occluded.

87. *Presence of primary tubercles on phyllodes: absent [0]; present distally (Fig. 2.8D) [1].*



**Figure 2.8.** Drawings of phyllopores from (A–E) the anterior paired and (F) the posterior phyllodes; buccal pores on the right, concentric circles represent primary tubercles. (G–I) Drawings of posterior phyllodes; basicoronal plates on the right. Images refer to characters 75, 78–80, 84–87.

R) Oral ambulacra: sphaeridia

88. *Location of sphaeridial pits in posterior phyllodes: near buccal pores only [0]; throughout phyllodes [1].* This character was coded as unknown for three species (*K. malayana*, *K. florescens* and *R. marmini*) because they have very short phyllodes making it challenging to assess if the sphaeridial pits are restricted to a small region near the peristome or if they would be widespread if the phyllodes were larger.

89. *Sphaeridia placement: in open pits [0]; concealed by a thin layer of stereom [1].*

90. *Sphaeridial pits greatly reduced: no [0]; yes [1].*

91. *Number of sphaeridial pits: seven or more [0]; up to six [1].*

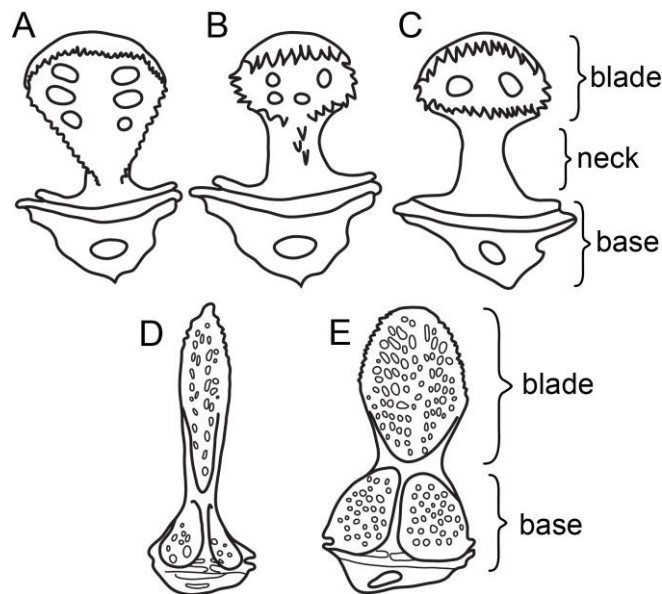
S) Oral ambulacra: plates beyond phyllodes

92. *Shape of ambulacral plates beyond phyllodes: transverse [0]; cubic [1]; longitudinal [2].* This character codes for the ambulacral plates in the oral region only.

T) Overall test tuberculation

93. *Tubercle size: aboral tubercles at least 60% as large as oral tubercles [0]; aboral tubercles less than 60% of oral tubercles [1]*

94. *Oral tubercles with bosses displaced from center: no [0]; yes [1].* Species with enlarged areoles have larger spines on the oral region of the test that aid in locomotion.



**Figure 2.9.** Drawings of (A–C) ophicephalous and (D–E) tridentate pedicellariae. Images refer to characters 95–97.

U) Pedicellariae

95. *Teeth on blade of ophicephalous pedicellariae: teeth form an open-U blade and run down on the edges of the neck (Fig. 2.9A) [0]; teeth form a semi-oval blade and run down in the middle of the neck (Fig. 2.9B) [1]; teeth form an oval blade and are absent in the neck (Fig. 2.9C) [2].* Not included in A2.

96. Size of teeth on distal region of ophicephalous pedicellariae: coarse (Fig. 2.9B–C) [0]; fine (Fig. 2.9A) [1]. Not included in A2.

97. Tridentate pedicellariae blade in relation to base: long and narrow (Fig. 2.9D) [0]; short and broad (Fig. 2.9C) [1]. Not included in A2.

98. Teeth on base of tridentate pedicellariae (Souto & Martins 2018, table 2): absent [0]; present [1]. Not included in A2.

A data matrix (Appendix 2.2) was constructed in Mesquite version 3.51 (Maddison & Maddison 2011). Phylogenetically uninformative characters were not included, polymorphic characters were kept. Inapplicable characters were coded as ‘–’, while missing data were coded as ‘?’. For some characters, I was able to exclude a subset of the character states for a particular taxon but I was unsure of the remaining character states; these partial uncertainties were included within curly brackets and not coded as missing data. I used the command ‘mstaxa=variable’ to differentiate partial uncertainty and polymorphism. Missing data often results in a high number of equally parsimonious solutions and reduced resolution; partial uncertainty should ameliorate these effects.

After coding the characters, I estimated the completeness of all fossil taxa (Table 2.2). Rowe (1988) defined completeness as the percentage of missing data (due to nonpreservation and inapplicability) in relation to the total number of characters in the matrix. In my estimation of completeness, only the characters with missing data due to nonpreservation were considered. I believe that inapplicability should not affect the estimation of completeness because if fossil preservation allowed for the detection on inapplicable characters, then the preservation for that character is good.

### Phylogenetic Analyses

Four cladistic analyses were conducted using the software PAUP\* version 4.0a163 (Swofford 2003) using the parsimony optimality criterion. In all of these, heuristic searches were performed using stepwise random addition sequences with 1000 replicates (start=stepwise addseq=random randomize=addseq nreps=100) followed by tree bisection-reconnection branch swapping (swap=tbr multrees=yes). Five trees were held at each step of stepwise addition (hold=5). Branches without unambiguous optimizations were collapsed (pset collapse=minbrlen). Trees with best score were retained (filter best=yes permdel=yes). Finally, strict consensus and 50% majority-rule consensus trees were generated. Clade support was determined with bootstrap resampling (1000 heuristic replicates [Felsenstein 1985]) and character changes were optimized using the "accelerated transformation" (ACCTRAN) option. Batch files with commands are available in Appendix 2.3 and in Morphobank (O’Leary & Kaufman 2012) project P3287.

*Nucleolites scutatus*, *A. recens* and *E. depressa* are the most distantly related taxa and hence were used to root the trees. All characters were treated as equally weighted and continuous characters not derived from ratios were ordered (an additional analysis with unordered characters was also performed). Analysis 1 (A1) included all ingroup (45) and outgroup taxa (21), all 98 characters, and coded for partial uncertainty. To analyze the effect of missing data on the resulting topology, characters coded for less than 20% of the species (n=6) were excluded from Analysis 2 (A2). In Analysis 3 (A3) partial uncertainties (n = 34) were converted into missing data (“?”), and Analysis 4 (A4) aimed to examine the influence of fossil taxa on the tree topology and hence included only extant taxa (six ingroup and six outgroups).

## Using stratigraphy to choose the best tree

Temporal data has been applied in parsimony-based phylogenetic reconstruction in two different ways: *a priori*, as discrete characters used to build phylogenies (e.g. stratocladistics methods [Bodenbender & Fisher 2001]), and *a posteriori*, as a separate dataset to test phylogenetic hypotheses (e.g. Day et al. 2016). Although many agree that temporal data should be used in association with phylogeny (Gauthier et al. 1988; Huelsenbeck 1994; Fox et al. 1999), stratocladistics has been severely criticized especially because the concept of homology does not apply to time, but also because of the way that time is binned into stratigraphic intervals (Smith 2000; Sumrall & Brochu 2003). Fisher (2008) reviewed the main concerns raised by critics and provided a discussion addressing them. However, most software does not support temporal data, making the implementation and testing of this method very challenging.

Here, I used temporal data *a posteriori* to calculate stratigraphic congruence metrics for each MPT and determine which MPT best fits stratigraphy. Different metrics of stratigraphic congruence and their refinements have been proposed, all assessing if the FAD of a taxon corresponds to its placement in the phylogeny and/or the length of the ghost lineages (for a description of the main methods, see Huelsenbeck 1994; Benton & Storrs 1994; Siddall 1998; Wills 1999; Pol & Norell 2001; Wills et al. 2008).

Tests were performed using the DatePhylo and StratPhyloCongruence functions of the “strap” R package (Bell & Lloyd 2015). Input files consisted of the MPTs and a list with the FAD and LAD of each taxon. I adopted a conservative approach and included uncertain ages in the temporal range of species (see Table 2.2). Analyses were performed using the “basic” dating method (Smith 1994), which sets the root length at 0 My. Polytomies were treated as hard (hard=TRUE), and outgroups and topologies were fixed. Because the temporal data comes from stratigraphic intervals rather than absolute ages, I treated FADs and LADs as uncertain and two values were randomly drawn from within the interval (randomly.sample.ages=TRUE; samp.perm=1000). Estimated p-values were then calculated for these metrics from 1000 randomly generated trees (rand.perm=1000).

## Tree Calibration

Stratigraphic ranges of species (Table 2.2) were obtained from the literature and museum records; absolute dates were not available. Additional extinct taxa were used to calibrate the phylogeny based on assignable synapomorphies *a posteriori* (e.g. node dating) (Table 2.4). For each cassidulid genus, I targeted the oldest species and species occurring in different geographic areas. However, I only included the five species whose literature data allowed for a reliable phylogenetic placement. These species were manually added to the best tree, which was then calibrated using the “basic” method and plotted against the geological time scale of the International Commission on Stratigraphy (2015).

## Historical Biogeography

I defined eight discrete biogeographic areas based on the occurrences and distribution of taxa in selected cassiduloid clades: Eastern Pacific (EPC), subcontinent India (IND; including India and modern day Pakistan); Indo-Pacific and Australia (IPA), Madagascar (MAD), North-western Atlantic (NWA), South-western Atlantic (SWA), North Tethys (NTH, comprises modern day Europe), and South Tethys (STH, comprises modern day North Africa and the Middle East).



**Table 2.4.** List of taxa chosen *a posteriori* to aid phylogenetic calibration, their stratigraphic range, geographic distribution, clade assigned and characters used for assignment. Genus and family classification following classification proposed herein. Uncertain age between “[ ]”, uncertain character states separated by “/”.

Taxon	Estimated Age (Ma) <sup>1</sup>	Reference for Age Assignment	Geographic Distribution	Clade	Diagnosable character states and characteristics
<b>Order Cassiduloidea</b>					
<i>Paralampas platisternus</i>	72.1–66	Smith & Jeffery 2000	Oman and United Arab Emirates	<i>Paralampas</i>	21(1), 34(2), 44(0/1), 79(1), 81(2)
<b>Family Cassidulidae</b>					
<i>Rhyncholampas cooki</i>	37.8–33.9	Sanchez-Roig 1952	Cuba	<i>R. tuderii</i>	26(1), 29(1), 27(0), 53(1)
<i>Rhyncholampas fontis</i>	[66–47.8]	Cooke 1942	USA (FL)	<i>R. alabamensis</i>	1(0), 4(0), 5(1), 10(0), 26(1), 29(1)
<i>Rhyncholampas smithi</i>	44–42.9	Srivastava et al. 2008	India	<i>R. rodriguezii_A</i>	1(0), 4(1), 5(1), 10(0), 26(1), 29(1), petal III short
<b>Family Faujasuidae</b>					
<i>Glossaster ? besairiei</i> <sup>2</sup>	56–47.8	Lambert 1929; Besaire & Lambert 1930	Madagascar	<i>Glossaster</i>	26(0), 58(2), 60(1)

<sup>1</sup> According to Cohen *et al.* (2013; updated).

<sup>2</sup> This species was originally described in the genus *Paralampas*; however, the species description and poor illustrations indicate that it has a longitudinal and anterior peristome, prominent bourrelets, and a broad and deeply pitted naked zone. These characteristics suggest that *P. besairiei* should be placed within *Glossaster* but analysis of the holotype is necessary to support this classification.

Reconstruction of ancestral distribution was performed using the dispersal-extinction-cladogenesis (DEC) likelihood model (Ree et al. 2005; Ree & Smith 2008) implemented in Reconstruct Ancestral State in Phylogenies (RASP) version 4.0 (Yu et al. 2015). I chose a reticulate instead of a hierarchical vicariance model because the fragmentation and isolation of areas in the ocean are less likely than on land. In particular, the DEC model allows for time-stratified analyses with different dispersal rates among areas to capture deep-time processes more realistically (Ree & Smith 2008). To explore the flexibility offered by DEC, I analyzed four different scenarios: 1) without any constraints, 2) with range constraints, 3) with dispersal constraints, 4) with range and dispersal constraints. Constraints took into consideration geographic distance and barriers resulting from the tectonic activity since the Late Cretaceous (Appendix 2.4–2.5). In the timeframe captured in this study, two significant geologic events were the formation of the Isthmus of Panama in the Pliocene (O’Dea et al. 2016) and the disruption of the circum-equatorial paleocurrent in the Late Oligocene (Stille et al. 1996). These events stratified the phylogeny into three time-slices, each with a specific Q-matrix of dispersal rates between areas. In addition to the range constraints, the maximum number of areas at each node was set to two given that extant and extinct cassiduloids are endemic to small geographic regions (except in rare situations in which taxonomic revision is required).

I performed a separate analysis with each major clade of the preferred tree and excluded outgroups to reduce biases caused by missing taxa resulting from poor preservation and incomplete sampling. I also resolved polytomies according to taxon age (i.e. oldest taxon with an early split) and geography (i.e. nearby species as sister taxa).

## Results and Discussion

The complete parsimony analysis including all species, characters and partial uncertainties (A1; Fig. 2.10) resulted in 24 MPTs of 750 steps (CI = 0.237, RI = 0.604) recovered from two tree-islands (for results with unordered characters, see Appendix 2.6). Low p-values for all stratigraphic congruence metrics (Appendix 2.7) indicate that the 24 MPTs have a better stratigraphic fit than the 1000 randomly generated trees. Three of the MPTs obtained the best fit for all four metrics; the only difference among them concerns the placement of *E. baumi* and its relationship to other *Eurhodia* species. The selected topology was the MPT with best stratigraphic fit and whose relationships were present in most MPTs (Fig. 2.11). When characters with a high percentage of missing data were removed (A2), 24 MPTs of 738 steps (CI = 0.230, RI = 0.602) were recovered. The topology of the majority-rule consensus did not change if compared to A1 (Fig. 2.12); therefore, the removal/inclusion of these characters had no impact on the topology recovered in A1.

About 33% of the taxa had characters coded as partial uncertainties, varying from one to three characters in each taxon (Table 2.2). When partial uncertainties were converted to missing data (A3), 20 MPTs of 746 steps (CI = 0.239, RI = 0.605) were recovered. Although the major structure of the topology did not change, the relationship within some subclades changed considerably (Fig. 2.12). These subclades comprise nine of the 22 taxa with partial uncertainties, including all taxa with three partial uncertainties. The nature of the characters also affected the topology because the two characters with the highest number of partial uncertainties were quantitative and ordered. In addition, Analysis 3 recovered fewer MPTs. Different from partial uncertainties or any coded character, missing data do not affect tree topology. Because most characters have a high homoplasy index and missing data are not counted towards homoplasies, partial uncertainties return more conflicting tree solutions than missing data. Nevertheless,

converting partial uncertainties into missing data removes information and should not be favored. In the cassidulid tree recovered here, Analysis 1 had slightly better resolution.

Overall, the branch support for most clades was low and did not change significantly among the four analyses.

### **Phylogenetic structure and taxonomic implications**

Eight unambiguous synapomorphies support the clade composed by cassidulids, neolampadids and faujasiids (clade A) (Appendix 2.8); five of them related to the reduction of the phyllodes. Three major clades are then defined in the strict consensus, with the faujasiids being more closely related to the cassidulids than the neolampadids (Fig. 2.10). These results contrast with the relationships found in previous studies (Fig. 2.1). In their analysis of the post-Paleozoic echinoids, Kroh & Smith (2010) initially found a similar result, with the faujasiids sister to the cassidulids; however, after revising their analyses, the faujasiids were placed outside their cassiduloid clade (see Kroh & Smith, 2010 figure 5 [pre-revision topology] *versus* figure 2 [post-revision topology; Andreas Kroh, pers. comm.]). Given the close relationship among cassidulids, faujasiids and neolampadids found here and in previous studies, my recommendation is to keep the faujasiids within the order Cassiduloidea.

Clade B is composed of the subfamily Neolampadina (neolampadids and pliolampadids) and *O. epigonus*. Six unambiguous synapomorphies support this clade, including the placement of the ocular plates beyond the gonopores, a longitudinal peristome, and further reduction of the phyllodes. The Neolampadina are then supported by eight unambiguous synapomorphies, including the funneled posterior region, the loss of gonopore 3, and the presence of six plates on I5 up to the plates framing the periproct. Despite the placement of *O. epigonus* as sister to the Neolampadina, an analysis with additional neolampadids and gitolampadids are necessary to better classify this species as a member of this subfamily or of another clade. For now, I rule out the possibility of *O. epigonus* being a cassidulid, but this species is likely a cassiduloid.

Clade C, composed of cassidulids and faujasiids, is supported by five unambiguous synapomorphies, including the shape of the ophicephalous pedicellaria — with teeth forming a semi-oval blade and running down the middle of the neck — and the presence of a developed naked zone in I5 and ambulacrum III. The monophyly of the family Cassidulidae was not supported because the genera *Eurhodia* and *Glossaster* were placed within the faujasiids.

The family Faujasiidae (clade D) is supported by seven unambiguous synapomorphies related to the size and shape of the basicoronal plate 5 and the number of occluded plates in the posterior phyllodes. Morphological data indicate that the Neognathostomata phyllode was initially composed of a single column of plates per half and with pores in triads (Fig. 2.8D). Long phyllodes with single columns are found in apatopygids and most echinolampadids, even though their phyllopores are not organized in a uniform column when looked from the outside of the test. At some point, occluded plates evolved, possibly with the reduction of plates in the triads. For instance, the plates in *A. recens* vary in size and shape, and some phyllopores are placed near the perradial suture. Faujasiids usually have many occluded plates in the phyllodes; cassidulids and neolampadids tend to have fewer.

Smith and Wright (2000) subdivided the faujasiids into two subfamilies mainly based on the position of the periproct: marginal to inframarginal in the Faujasiinae and supramarginal to aboral in the Stigmatopyginae. My analyses do not support the subfamily Stigmatopyginae because this subfamily is based on plesiomorphic characters and its members do not form a monophyletic group. For example, two basal dichotomies in clade D split *R. arumaensis* and

*Petalobrissus*, both Stigmatopyginae, from the remaining faujasiids. Previous studies are also discordant (Fig. 2.1). Regardless of the relationship among them, all the faujasiid species seem to belong together, including *A. longianus* and *R. marmini*, previously placed within the cassidulids (Fig. 2.1; but note that Suter [1994a] mistakenly coded the apical system of *R. marmini* as monobasal instead of tetrabasal). Unambiguous synapomorphies supporting the remaining faujasiids are a longitudinal peristome and reduction of bourrelet 5.

Clade E is composed by Stigmatopyginae and Faujasiinae species and supported by five unambiguous synapomorphies related to the adoral region, including the shape of the basicoronal plate 5 (i.e. proximally depressed and distally elongated), presence of tooth-like bourrelets, and reduction of the buccal pores. The former two synapomorphies are also present in *A. longianus*, placed within Clade G. Tooth-like bourrelets have been used to diagnose the family Faujasiidae; however, some faujasiids (e.g. *Petalobrissus* and *F. rancheriana*) do not possess this trait. Therefore, if this phylogeny is accurate, tooth-like bourrelets evolved twice within the faujasiids.

Five unambiguous synapomorphies support clade F, including having a monobasal apical system, pits on the interambulacral basicoronal plates and pointy bourrelets. In my preferred phylogeny, two subclades split from this clade, each supported by two unambiguous synapomorphies: clade G is composed by *A. longianus*, *E. australiae*, *Glossaster* and *Kassandrina*; and clade H (crown group Faujasiidae), composed of *C. ellipticus* and the other *Eurhodia* species. Some characteristics that tell them apart are, respectively, a longitudinal versus a transverse periproct, anterior paired petals oval versus leaf-shaped, and 8 or more versus 8 or fewer plates framing the periproct. The topology of clade F changed considerably when partial uncertainties were converted into missing data. While relationships within clade G did not change, clade H collapsed and support for the monophyly of the genus *Eurhodia* was lost.

The genus *Eurhodia* displays some of the greatest diversity in test shape within the cassiduloids (from here onwards sensu this paper, unless stated otherwise) and three genera have been described to separate its valid species: *Eurhodia*, for the species *Pygorhynchus morrissi*; *Ravenelia* McCrady, 1859, for the species *Pygorhynchus rugosus*; and *Gisopygus* Gauthier in Fourtau, 1899, for four Egyptian species described as *Rhynchopygus*, amongst them, *R. navillei* and *R. thebensis* (note also that Kier [1962] doubtfully considered this genus a synonym of *Rhyncholampas* even though he did not analyze any specimen). The results recovered here do not support any of these genera. Also, no other *Eurhodia* species strongly resembles the type species, *E. morrissi*, and few of the currently valid species were originally described in this genus. Despite the uniqueness of *E. morrissi* and the lack of non-homoplastic synapomorphies supporting clade H, I decided to maintain all species in this clade within the genus *Eurhodia* to keep its stability.

Several taxonomic implications stem from the relationships recovered in clade D. First, the genus *Rhynchopygus* is characterized by a prominent extension above the periproct that is absent in both *R. arumaensis* and *R. macari*. *Rhynchopygus arumaensis* split off from the faujasiids very early in the evolution of the clade and should be placed in a different genus. *Rhynchopygus macari* shares more characters with *P. lapiscancrici* than with *R. marmini*, suggesting that they could all belong to the same genus or to different genera. But an analysis of the other *Rhynchopygus* and *Procassidulus* species is needed to verify the variability within each of these genera before any conclusion is made. Second, although *F. apicalis* and *F. rancheriana* are sister taxa, there are many differences between them. The round bourrelets and tetrabasal apical system of *F. rancheriana* suggest that this species should be placed in the genus *Eurypetalum* Kier, 1962. Third, *E. australiae* is unlike any other species I analyzed and should

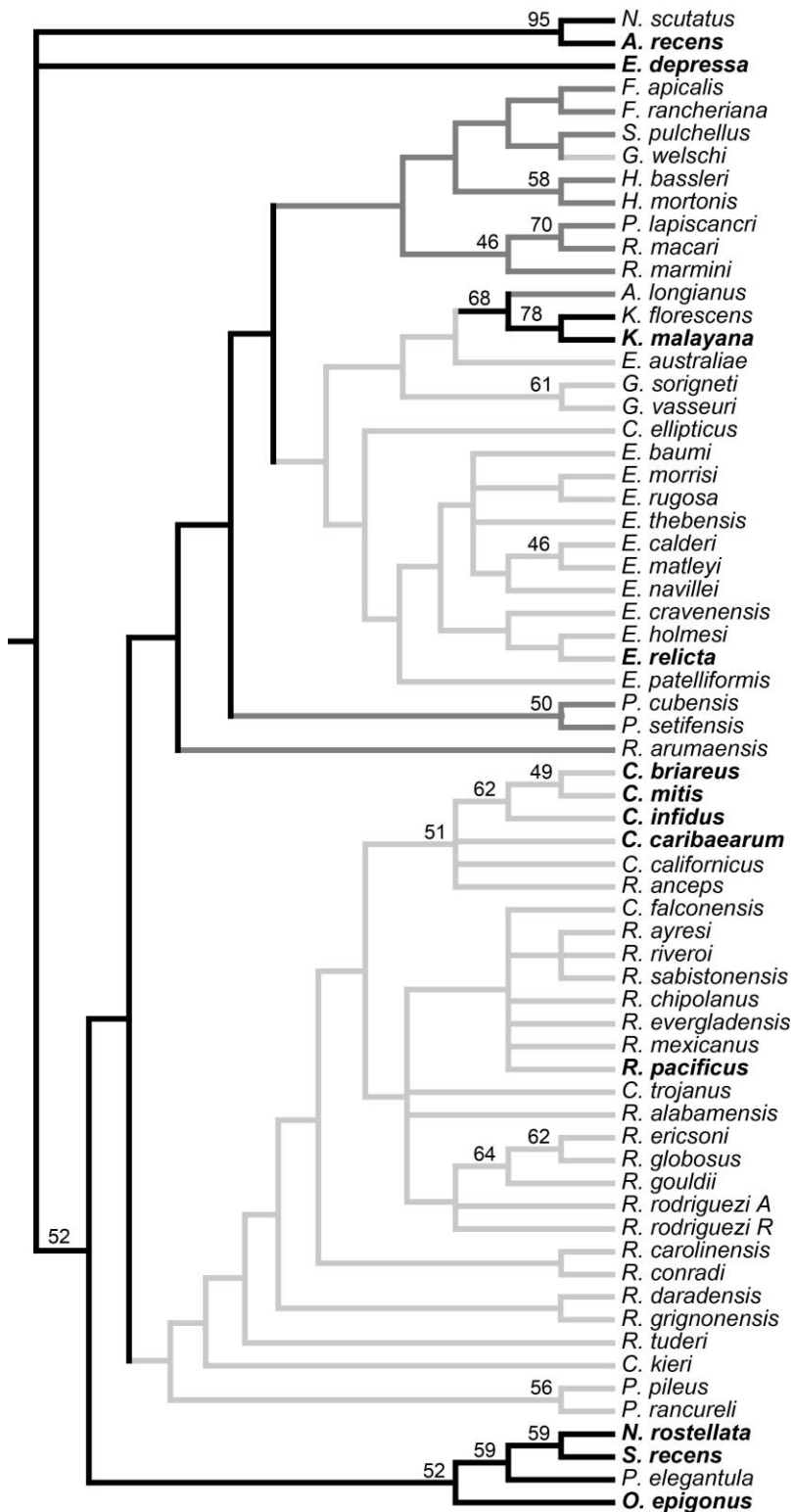
be placed in a different genus than the ones included in this phylogeny; alternatively, *C. ellipticus* should be transferred to *Eurhodia*. Finally, *G. welschii* does not belong in the genus *Glossaster* because its type species, *G. sorigneti*, is placed in a different clade. Smith & Jeffery (2000) transferred *G. welschii* to the genus *Stigmatopygus* and my analyses support this change.

The sister clade to the faujasiids (clade I) is supported by two unambiguous synapomorphies: plates framing the periproct do not bend inwards and basicoronal plates 1 and 4 are narrower than basicoronal plate 5. While they have historically been placed within the cassidulids (except by Smith & Jeffery [2000], who placed *Paralampas* as a subgenus of *Petalobrissus*) and form a monophyletic group with them, the synapomorphies supporting clade I are few and do not provide an unambiguous diagnosis for the family.

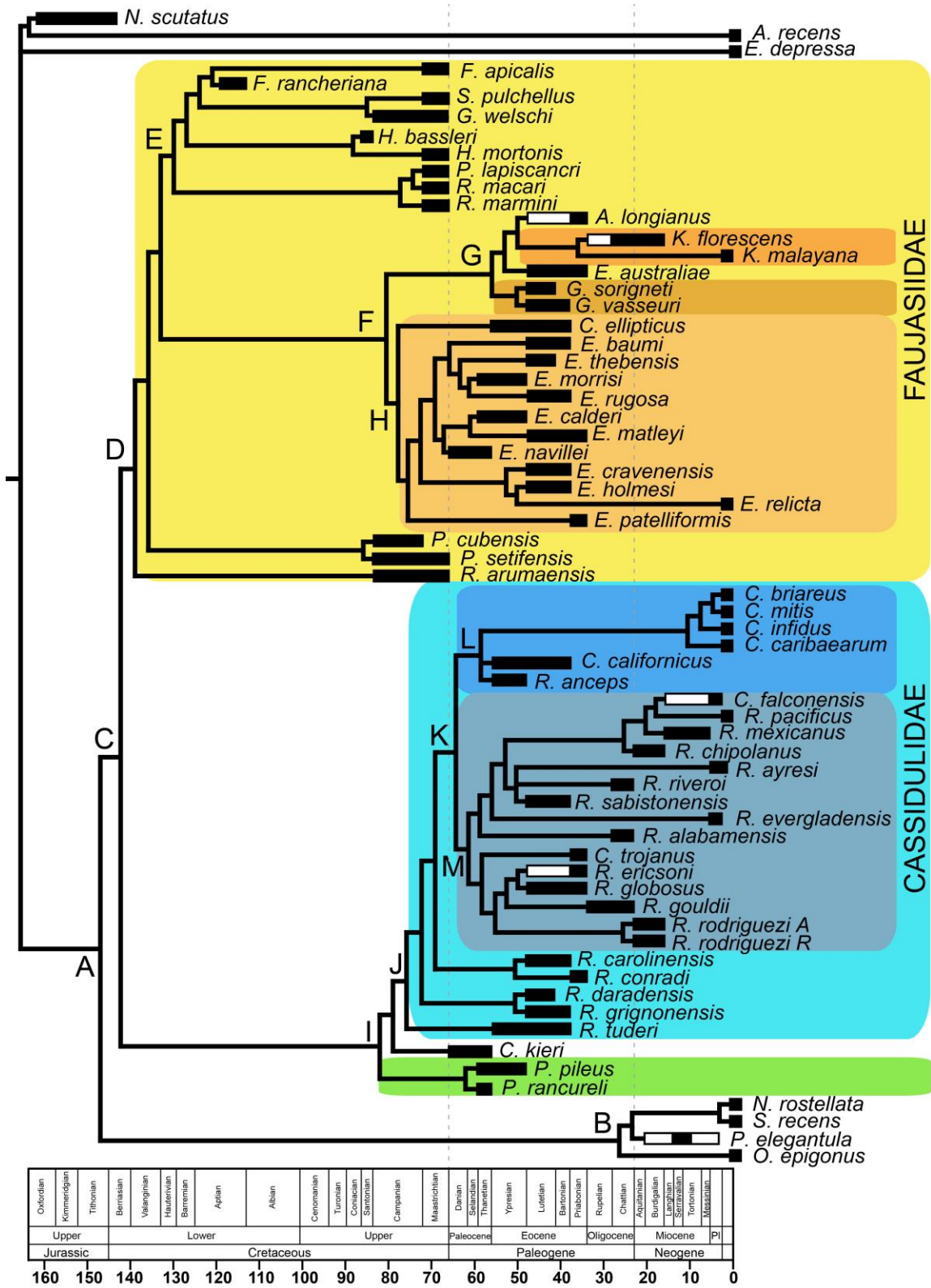
The family Cassidulidae (clade J) is supported by seven synapomorphies (five unambiguous): columns of anterior paired petals differ by up to four pore-pairs (non-homoplastic), posterior paired petals with unequal columns of pore-pairs, plates beyond petals with a horizontal shape, transverse periproct, plates below the periproct convex and not forming a groove, bourrelets formed by the accretion of stereom onto the basicoronals, and oral tubercles larger than adoral tubercles. Three basal dichotomies split the stem from the crown group Cassidulidae (clade K), which is composed by the genera *Cassidulus* (clade L) and *Rhyncholampas* (clade M). Crown Cassidulidae is supported by four synapomorphies (three unambiguous): posterior region of test not truncated, naked zone wide, basicoronal ambulacral plates bent, and enclosed sphaeridial pits. Two characters coded only for extant species also support this clade, although they could have evolved at any node between the clades C and K: periproctal membrane with two rows of medium-sized plates and anus placed on the aboral edge.

The genus *Cassidulus* (clade L) is supported by five unambiguous synapomorphies, mostly related to the reduction of the phyllodes that have few plates, none of them occluded. The genus *Rhyncholampas* is supported by four unambiguous synapomorphies, including having petals the same width as the ambulacra beyond petals and seven or more sphaeridia. *Rhyncholampas* is subdivided into two clades and the placement of *C. trojanus* and *R. alabamensis* was not the same in all MPTs. Also, the conversion of partial uncertainties into missing data destabilized the relationships within the clade.

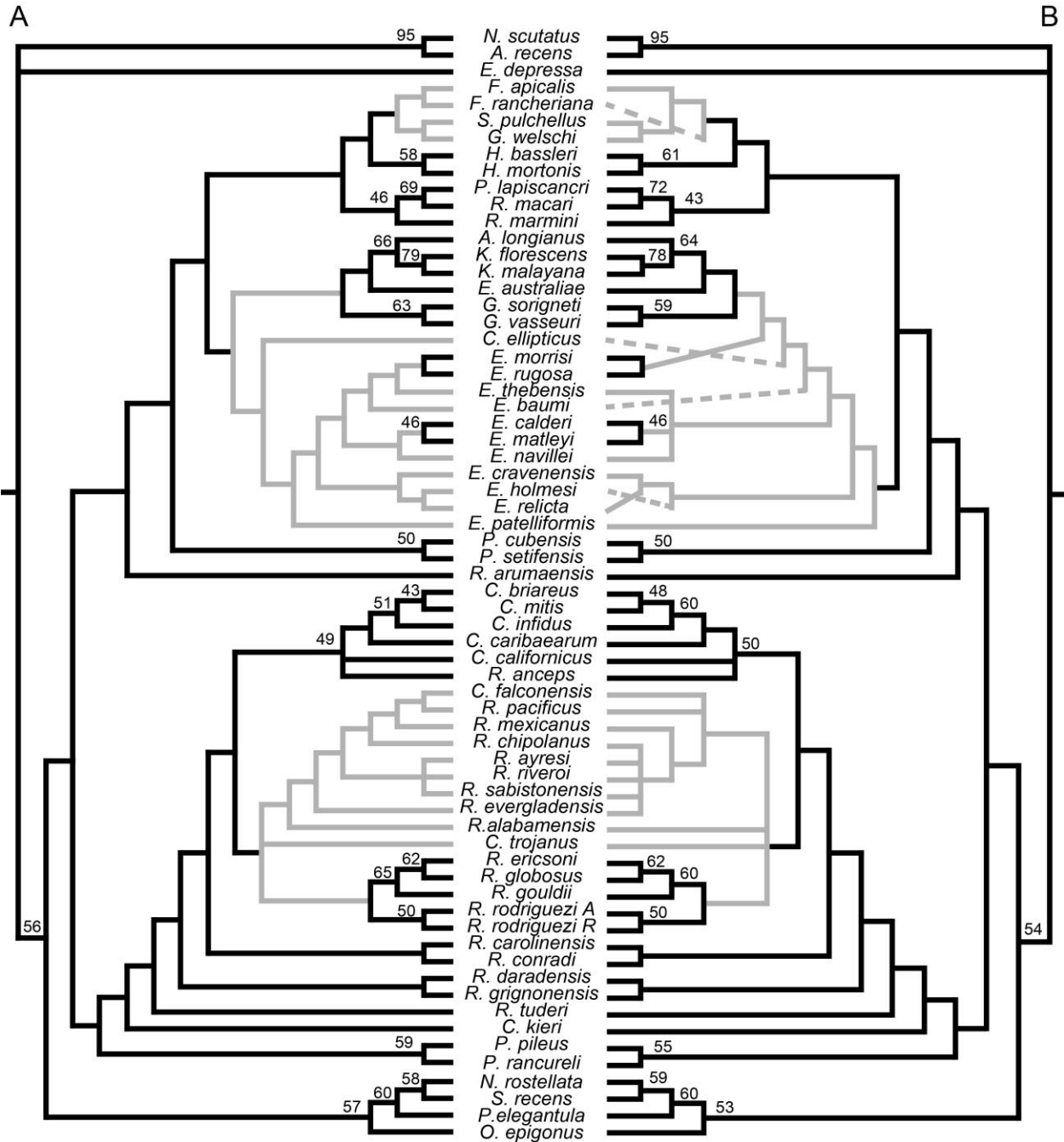
Morphological differences between the genera *Cassidulus* and *Rhyncholampas* are very slight, even though they diverged more than 60 Mya. Many *Rhyncholampas* species were originally placed in the genus *Cassidulus* and later transferred to *Rhyncholampas*; this analysis corroborates some of these taxonomic assignments (i.e. *R. alabamensis*, *R. ericsoni*, *R. evergladensis*, *R. globosus*, *R. mexicanus*, *R. riveroi*, *R. sabistonensis*) and includes *C. falconensis* and *C. trojanus*, which had been previously described as and placed in *Eurhodia*, respectively. These results also indicate that *R. anceps* should be placed in the genus *Cassidulus*, and the *Rhyncholampas* species outside of clade L and *C. kieri* should be placed in other genera.



**Figure 2.10.** Strict consensus of 24 MPTs recovered by Analysis 1 (including all taxa, all characters and partial uncertainty). Bootstrap values (1000 replicates) above 40% are shown near the nodes. Color in lineages represent: the cassidulids in light grey, the faujasiids in dark grey, and other taxa in black. Extant taxa in bold.



**Figure 2.11.** Preferred tree topology with best stratigraphic congruence from A1 and proposed designation for the families Cassidulidae and Faujasiidae. Clades discussed in the text are indicated by capital letters.



**Figure 2.12.** 50% majority-rule consensus of A) 24 MPTs recovered by Analysis 1 (including all taxa, all characters and partial uncertainty) and Analysis 2 (without characters with > 80% of missing data); and B) 20 MPTs recovered by Analysis 3 (partial uncertainties as missing data). Bootstrap values (1000 replicates) above 40% for analyses A2 and A3 are shown near the nodes. Differences between cladograms in light grey.



## Taxonomic assignment of cassiduloids analyzed in this study

### Order CASSIDULOIDA

Genus *Paralampas*: *P. pileus* (type species), *P. platisternus*, *P. rancureli*.

Not reassigned, misclassified cassiduloids: *C. kieri*, *E. australiae*, *R. arumaensis*, *R. carolinensis*, *R. conradi*, *R. daradensis*, *R. grignonensis*, *R. tuderii*.

### Family FAUJASIIDAE

Genus *Eurhodia*: *E. morrisoni* (type species), *E. baumi*, *E. calderi*, *E. cravenensis*, *E. elliptica* nov. comb., *E. holmesii*, *E. matleyi*, *E. navillei*, *E. patelliformis*, *E. relicta*, *E. rugosa*, *E. thebensis*.

Genus *Glossaster*: *G. sorigneti* (type species), *Glossaster* ? *besairiei* comb. nov., *G. vasseuri*.

### Family CASSIDULIDAE

Genus *Cassidulus*: *C. caribaeorum* (type species), *C. anceps* comb. nov., *C. briareus*, *C. californicus*, *C. infidus*, *C. mitis*.

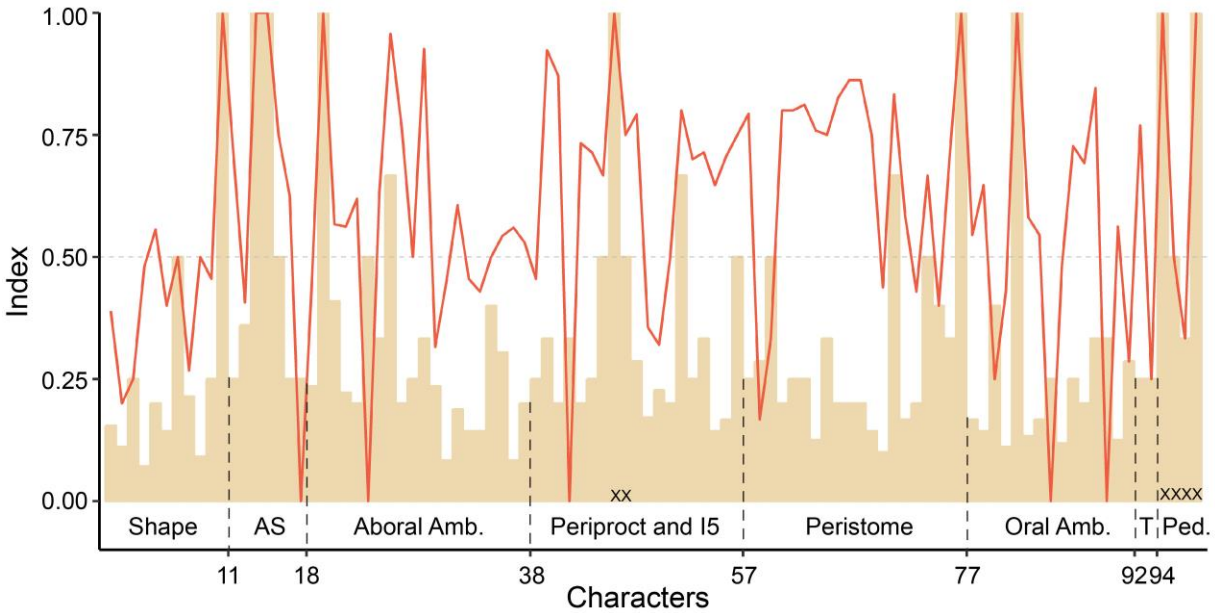
Genus *Rhyncholampas*: *R. pacificus* (type species), *R. alabamensis*, *R. ayresi*, *R. chipolanus*, *R. ericsoni*, *R. evergladensis*, *R. falconensis* comb. nov., *R. globosus*, *R. gouldii*, *R. mexicanus*, *R. riveroi*, *R. rodriguezii*, *R. sabistonensis*, *R. trojanus* comb. nov.

## Homoplasy and character evolution

Low CI and moderate RI (Fig. 2.13, Appendix 2.9) indicate that most characters were homoplastic, which helps to explain the low bootstrap values. A similar result was obtained by Smith (2001) and Kroh & Smith (2010) in their phylogeny of the post-Paleozoic echinoids, which suggests that the evolutionary history of the cassiduloids involves multiple shuffling of character states (shuffling here does not refer to lateral gene transfer, but to the constant character state changes as a result of homoplasy) rather than the evolution of novel traits (Smith 2001; present paper). Agreeing with Kier (1962), Suter (1994a) and Saucède & Néraudeau (2006) also attributed the high level of homoplasy, and consequently low phylogenetic resolution, to parallel evolution within the cassiduloids. In fact, parallelism and reversals are frequent among irregular echinoids that evolved to live in similar environments (e.g. Kier 1974; Smith 2001; Saucède et al. 2003).

The evolution of the apical system from four to one genital plate (i.e. tetrabasal versus monobasal) has been poorly studied and it is unclear if some genital plates reduced in size until they disappeared leaving a single enlarged plate or if the genital plates fused to form a solid plate, or some combination of these processes. In the cassiduloid clade defined here, the apical system changed from monobasal to tetrabasal in some faujasiids, and then apparently reverted to monobasal in *F. apicalis*.

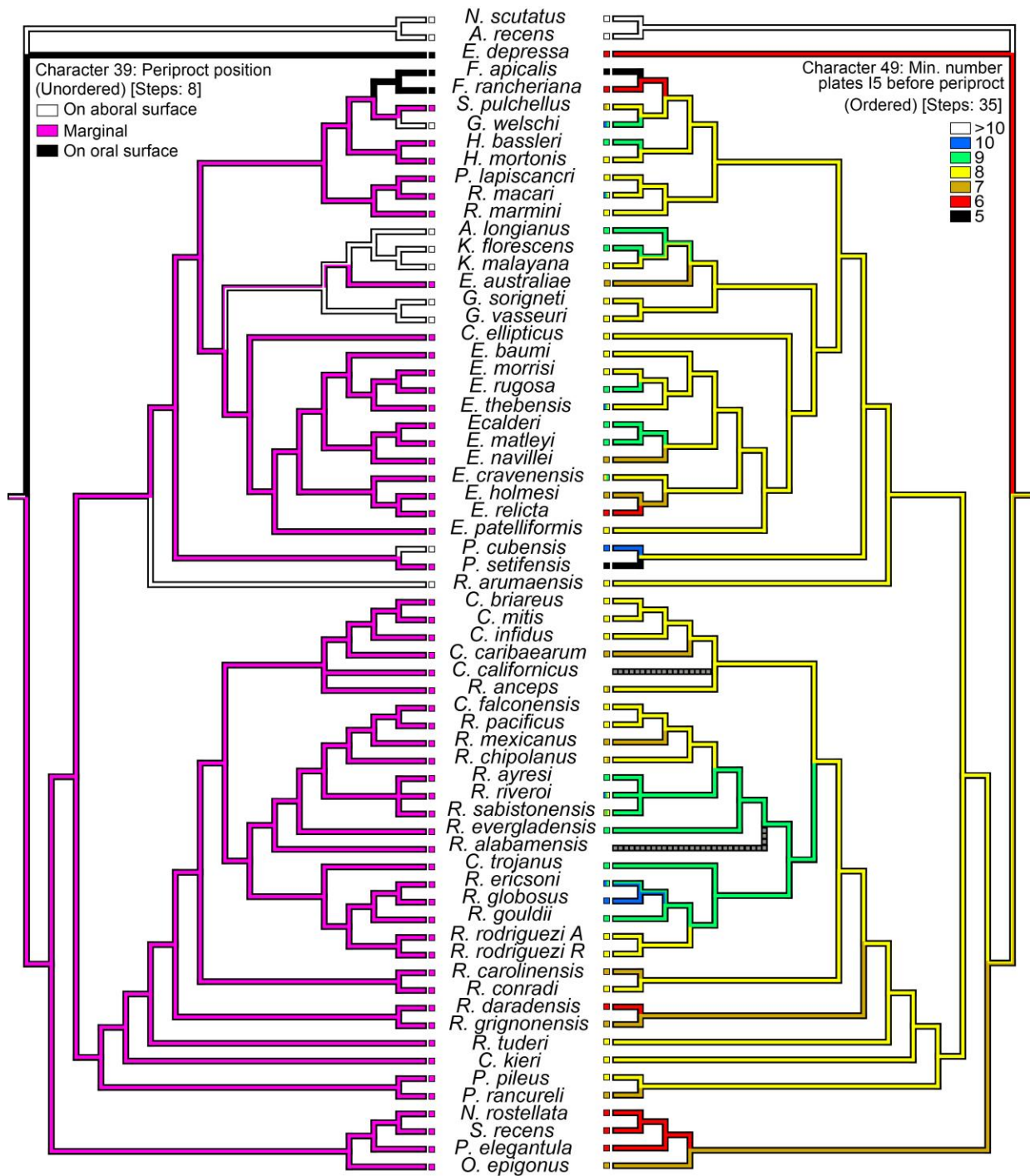
Other major transitions concern the peristome and periproct. In the reconstructed cassiduloid phylogeny, the orientation of the peristome changed from transverse to longitudinal and vice versa; the periproct position changed multiple times from marginal to aboral and once to oral (all within the faujasiids); and the orientation of the periproct changed multiple times from longitudinal to transverse. These transitions are probably affected by the rate and orientation of plate growth, and the rate of plate addition. Different lineages could be affected differently; for example, a transverse periproct is not necessarily framed by fewer plates than a longitudinal periproct, and the number of interambulacral plates from the peristome to the periproct is not necessarily higher if the periproct is aboral rather than marginal, although the number of plates tends to be lower in species whose periproct is oral (Figs. 2.14–2.15).



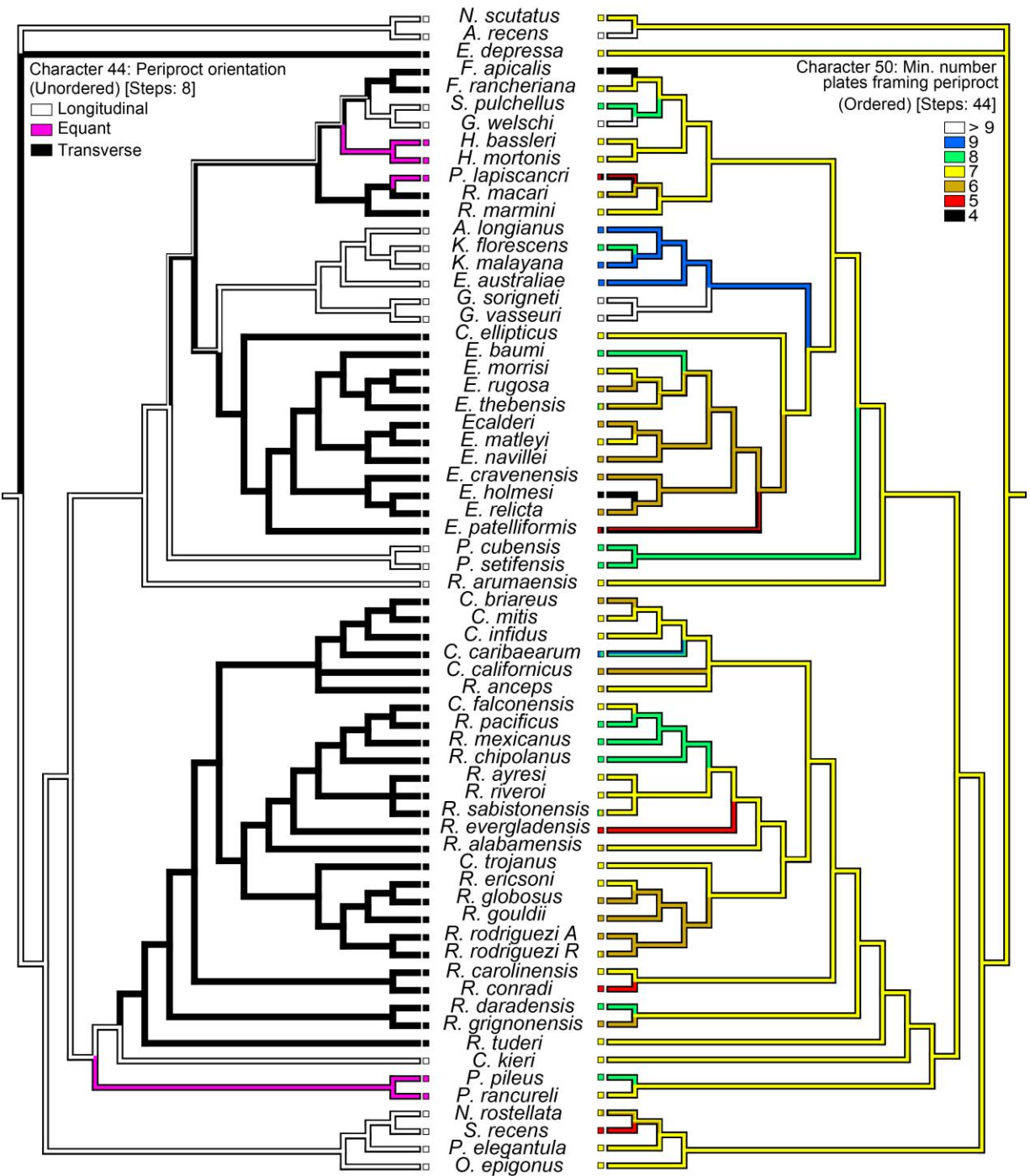
**Figure 2.13.** Plot with the consistency (bar plot) and retention (line plot) indexes for characters in A1. Dashed line separates the following categories of morphological characters: test shape, apical system (AS), aboral ambulacra, periproct and interambulacrum 5, peristome and basicoronal plates, oral ambulacra, test tuberculation (T) and pedicellariae (P). Characters removed from A2 because of amount of missing data marked with an “X”.

Souto & Martins (2018) showed that the bourrelets in cassiduloids may be formed by the accretion of stereom onto the basicoronal plates or by an internal depression on the basicoronal plates that project the bourrelets outwards. My morphological analyses indicate that these conditions can also co-occur. For example, *R. pacificus* has a slight depression in the interambulacral basicoronal plates and a thick accretion of stereom, while *K. florescens* has a deep depression in the interambulacral basicoronal plates and a slight accretion of stereom. Because slight depressions are very difficult to detect in fossils and unbroken extant species, I did not code for it. Whether both conditions co-occur or not, usually only one is responsible for the formation of the bourrelets. Usually, tooth-like and pointy bourrelets in faujasiids are formed by a deep depression in the plates, while the bulged and pointy bourrelets in cassidulids are formed by a strong accretion of stereom.

Micro-computed tomography provided insights about the different ways in which bourrelets are built (Souto & Martins, 2018), but there is still much to learn about other cassiduloid novelties, for example, the naked zone and apical system modifications. These novelties are usually coded for presence versus absence or tetrabasal versus monobasal, respectively, but without an examination of their ontogeny and deeper homologies we are likely missing important parts of the story that can lead to more nuanced coding schemes.



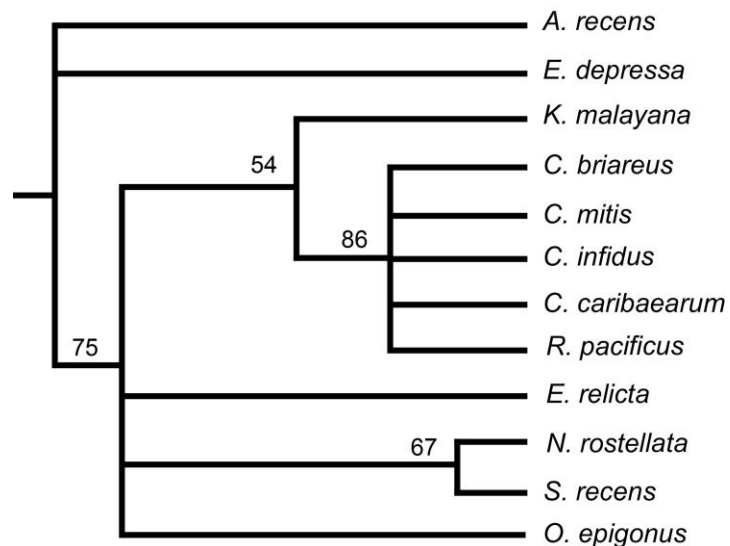
**Figure 2.14.** Mirrored trees depicting the Maximum Parsimony optimization of “Periproct position” on the left and “Minimum number of plates on I5, between the basicoronal plate and the base of the periproct” on the right. Branch color refers to inferred ancestral state.



**Figure 2.15.** Mirrored trees depicting the Maximum Parsimony optimization of “Periproct orientation” on the left and “Minimum number of plates framing the periproct” on the right. Branch color refers to inferred ancestral state.

## Using fossils to reconstruct phylogenies

Analysis 4 (extant taxa only) was based on 70 parsimony-informative characters and resulted in four MPTs of 203 steps (CI = 0.567, RI = 0.564; Fig. 2.15). The relationships among the extant species changed with the removal of fossil taxa, especially regarding the position of *O. epigonus* and *E. relictus*. Also, despite the higher CI, the topology restricted to extant taxa did not add much to our knowledge of the relationship among the cassiduloid genera. Accordingly, the inclusion of fossil species provided better resolution of phylogenetic relationships within the cassidulids, allowed for the delimitation of supraspecific taxa, and detected taxonomic inconsistencies that have not been assessed before. For example, *K. malayana* was classified within the cassidulids (Mooi 1990b; Suter 1994b) instead of the faujasiids, and many have considered *R. pacificus* congeneric with *C. caribaeorum* (e.g. Agassiz 1869; Mortensen 1948a), but the analyses performed here show that *Rhyncholampas* and *Cassidulus* have been separated for at least 60 million years. Characters responsible for this nesting include scattered arrangement of phyllopores in posterior phyllodes and convex shape of bourrelet 5, which is shared with *C. mitis* and *C. briareus*; and petals with narrow poriferous zone, high number of sphaeridia and naked zone with reduced pits, which is shared only with *C. mitis*.



**Figure 2.16.** 50% majority-rule consensus of 4 MPTs recovered by Analysis 4 (extant taxa only). Bootstrap values (1000 replicates) above 40% are shown near the nodes.

Smith (2001) and Kroh & Smith (2010) also recovered different results from phylogenies with and without fossils (Fig. 2.1C, E). Because of unique combinations of character states that have often been erased in Recent species, fossils generally improve phylogenetic resolution (Huelsenbeck 1994). However, this improvement will depend on trade-offs between the completeness and temporal position of the fossils; for example, young fossils with low completeness may worsen the phylogenetic resolution (Huelsenbeck 1991). In the phylogeny reconstructed here, completeness was relatively high (74–100%), but one of the species with lower completeness — *R. riveroi*, 75–77% complete — and dating back to the Late Oligocene resulted in a trichotomy; while a taxon from the Late Cretaceous with similar completeness — *G. welschi*, 74–75% complete — had a better resolution.

Fossils may not be as important when recovering the relationships of very closely related extant taxa. However, because cassiduloids have few extant species that descend from ancient lineages separated by tens of millions of years, adding fossils is necessary to recover the morphological information lost since those lineages split. Phylogenetic studies that include fossil invertebrates are still uncommon for numerous reasons, including the incompleteness of the fossil record, the lack of knowledge about it, and the physical separation of biological and paleontological collections. Also, although the resolution of the current analysis has not been diminished by the amount of missing data, their negative effect in phylogenetic resolution usually prevents the inclusion of fossil taxa in evolutionary studies (Donoghue et al. 1989). As observed here, the amount of missing data may be diluted if more characters are added (Wiens 2003; Prevosti & Chemisquy 2010), even if they are highly homoplastic. So whenever possible, the inclusion of fossil taxa should at least be considered.

### **Difference among DEC model scenarios**

The reconstruction of ancestral areas by the scenarios without range constraints resulted in unrealistic geographic distributions. For example, one of the probable areas for the “Clade F” ancestor comprises the Indo-Pacific, Australia and the Northwest Atlantic (IPA + NWA); and for the *Cassidulus* ancestor comprises Madagascar and the Northwest Atlantic (MAD + NWA). The extant cassiduloid species (sensu Kier 1962) live primarily burrowed in soft substrates and have a restricted geographic distribution, often confined to low latitude shallow-water environments (Kier 1962; Mooi 1990b). A wide distribution involving different oceans or disjunct areas have never been recorded in this group.

The DEC model with constrained scenarios resulted in 0–3 extinction events, while the unconstrained scenario had none. Also, the scenario with range and dispersal constraints resulted in more events than the other scenarios (Appendices 2.10–2.12), which is expected given the inflexibility imposed by these constraints. However, this scenario is more realistic. With the break-up of Pangea and redistribution of the land masses, the patterns in ocean circulation and, as a result, the connectivity among areas changed considerably. Therefore, I will focus on the fully constrained scenario (Appendix 2.13).

### **Ancestral area reconstruction**

Fossil evidence indicates that the family Cassidulidae and Clade F have a south Tethyan (mainly the Saharan epicontinental sea; Reyment 1980) and northwest Atlantic origin dating back to the Late Cretaceous (Figs. 2.17–2.18) when the oceans were connected by the Tethys and Central American seaways, providing a warm circum-equatorial current system (Bush 1997; Harzhauser et al. 2007). Marine regression and a northward movement of the Gondwanan continents resulting in the collision of Eurasia, Africa and India caused the interruption of this current system during the Miocene (Haq et al. 1987; Winterer 1991; Stille et al. 1996). As a result, lineages that moved away from STH often did not come back. The NWA, however, was the preferred area and where most sympatric speciation events took place.

The evolution of the cassidulids and of Clade F has mostly been influenced by dispersal rather than vicariant events, although vicariance has also played a major role especially considering that ancestors occupying adjacent areas often speciated in the extremes of their range, separated by a large body of water (e.g. NWA and STH). Dispersal was important in expanding the geographic range within each clade away from their center of origin. The DEC model also estimated that dispersal between areas was strongly asymmetric and mostly

eastwards, connecting the NWA to IND via the Tethys and from there to MAD and the IPA. However, most global paleocirculation models have agreed that the Tethyan circum-equatorial system had a strong westward flow (Gordon 1973; Follmi & Delamette 1990; Stille et al. 1996; Bush 1997), although small seasonal changes because of the Eurasian monsoons might have temporarily reversed this system locally (Bush 1997). Poulsen et al. (1998) suggested a more complex system with oceanic gyres, which seems to fit better the results recovered by the DEC model presented here.

I did not include any species within clade F *a posteriori* and to my knowledge, *E. navillei* is its oldest valid species. Many faujiids succumbed to the end-Cretaceous mass extinction, but Clade F descended from a surviving lineage whose diversification predated the Oligocene cooling. The DEC reconstructions indicate that Clade F probably originated (49%) in the NWA and STH. Speciation within clade H (*Eurhodia*) in these areas was prolific, with dead-end dispersal events to the EPA and IND. Clade G left the ancestral area to Australia (IPA), NTH and MAD; the last region a dead end. The center of origin was the major “exporter” of taxa. Speciation occurred mainly in sympatry, mostly within the NWA during the Paleocene to the Early Eocene, and then later within the IPA. The IPA clade has been isolated since the Early Eocene. Most vicariance events happened after a range expansion and were between disjunct areas; half of these between IND and the NWA, following a range expansion from STH. This clade left only two extant species, one species in the NWA and the other in the IPA.

The DEC reconstructions indicate that clade I probably originated (76.5%) in the NWA and STH with the early evolution of the clade occurring mostly in STH, the NWA playing a major role later. Speciation within clade K (*Rhyncholampas*) in the NWA was prolific throughout most of its evolution but clade K left only one Recent representative, *R. pacificus*, which is currently the cassidulid with widest geographic distribution, from Mexico (BJC) to Panama and the Galapagos islands. Interestingly, clade L (*Cassidulus*), at least three times less diverse than clade K (considering the whole diversity of both genera), left four extant species and has occupied a broader geographic range by leaving its ancestral area (NWA+STH [37%] or NWA [33%]) and dispersing worldwide. The NWA was the major exporter of taxa and the EPA the major importer. Dispersal events to the IPA, MAD, NTH and IND were dead ends. Speciation occurred mainly in sympatry, mostly within the NWA during the Late Paleocene to Early Eocene. Different from the pattern observed within Clade F, most vicariant events occurred between adjacent areas, two of these involving the EPA and the NWA. Also, only half of the vicariant events followed a range extension, and these were usually to adjacent areas, not going through the Tethys Ocean.

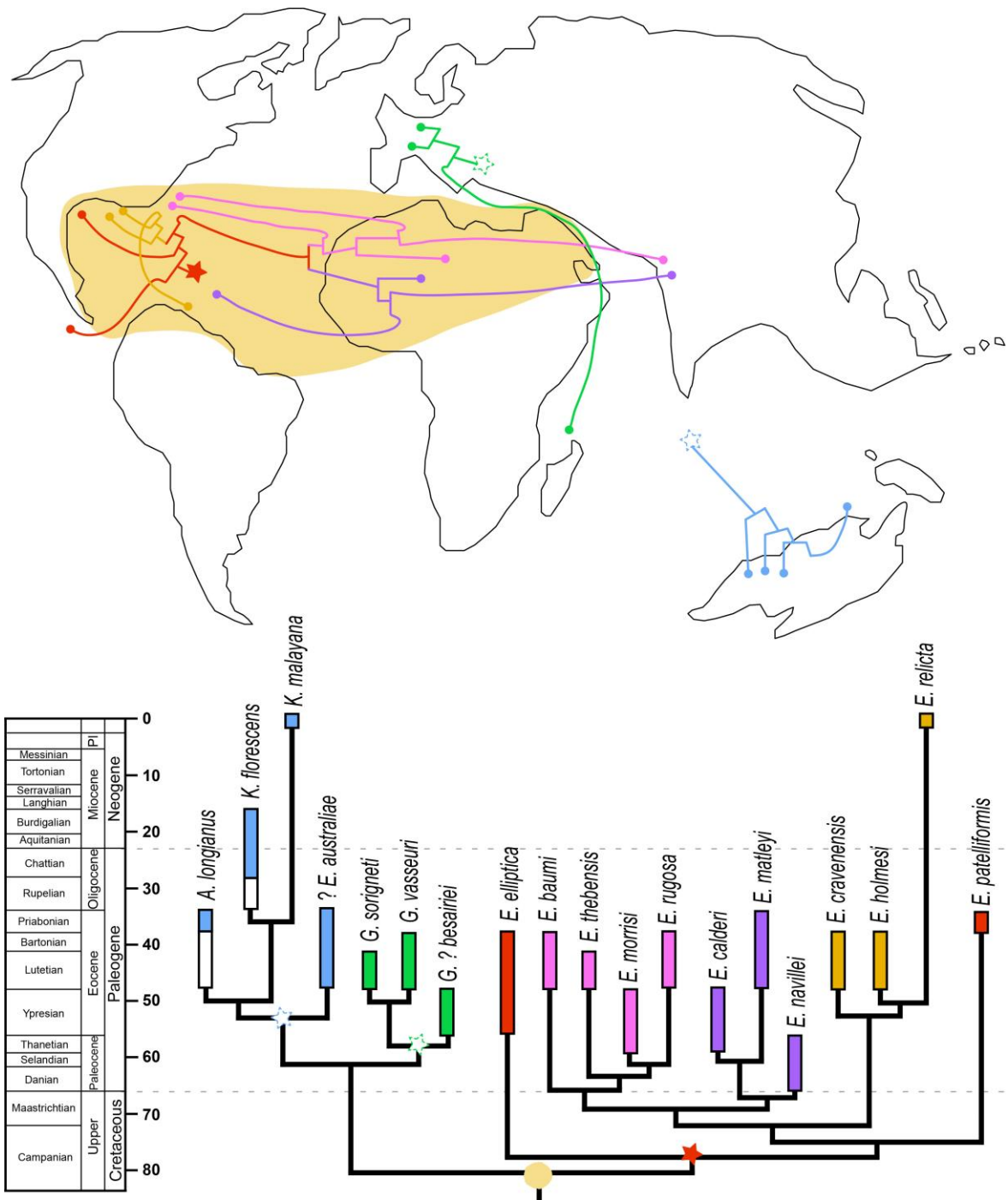
Within the crown *Cassidulus* clade, the DEC model estimated a long-range dispersal event from SWA to the IPA, via the EPA. Although, the range EPA + SWA was allowed in the model because there was no isthmus separating both regions for most of the time, this combination should not be allowed from the Pliocene onwards. Unfortunately, the DEC model does not allow for time-stratified area constraints. Disallowing the combination EPA+SWA resulted in an ancestral area SWA+STH and dispersal from STH to the IPA, which is also unlikely towards the Recent because of the closure of the Tethys Ocean. Explaining this disjunct distribution is not straightforward, especially without knowing when these species diverged. The four extant *Cassidulus* species are relicts from a Paleocene split. Also, they do not have a feeding larval stage and their young settle on the adults’ test, suggesting they have low dispersal capabilities. Although Young et al. (1997) noted that there are deep-sea lecitotrophic, echinoderms with a wider geographic range than planktotrophic species, the shallow-water

environment is more unstable than the deep sea and the distribution of cassiduloids is limited. Other dispersal routes not considered in this model because of the absence of species (e.g. South Africa and Southeast Pacific) could also be possible. Finding undiscovered fossil or extant species could fill up this gap in space and time. Several *Cassidulus* species have been described, but many were mistakenly placed into this genus; others were erroneously identified as *C. caribaeorum*, when they were actually new species (Mooi 1990a; Souto & Martins 2018). A revision of the described *Cassidulus* species is needed to gain a better understanding of its evolution. From my literature analyses, I could not reliably assign any species to improve the calibration within the *Cassidulus* clade and to my knowledge, its oldest species is *C. anceps* nov. comb. Also, some species described as a *Cassidulus* (e.g. *C. mercedensis* Anderson, 1958; *C. senni* Kier, 1966; *C. santolayae* Sillero in Santolaya & Sillero, 1994) do not belong to this genus.

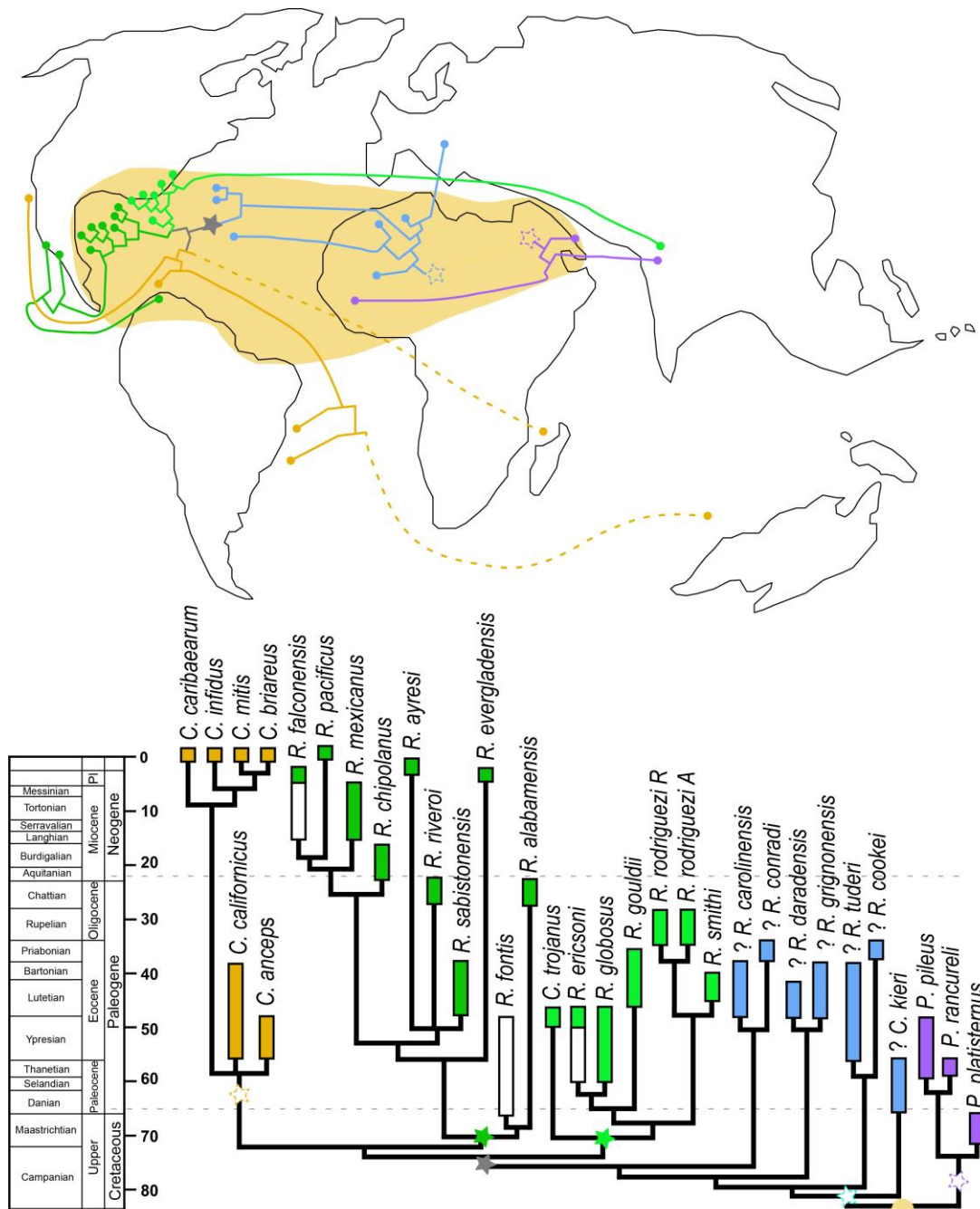
None of the geographic ranges of extant cassiduloid species overlap. The closest species are the Caribbean *C. caribaeorum* and *E. relictus*. However, their lineages have been separated since the Early Cretaceous and they live at different depths (1–18 m versus 57–112 m, respectively; Gladfelter 1978; Mooi 1990b; present paper). Although *K. malayana* and *C. briareus* are found in Australia, nothing is known about the precise location of the latter species (Souto & Martins 2018). The highest latitude cassidulids and faujasiids have lived is at about 30°N (modern day NC, U.S.A.) and 52°S (modern day SA, Australia) (paleolatitude estimated according to van Hinsbergen et al. 2015). These were achieved in the Eocene, when the global temperature was at its highest (Zachos et al. 2001). Of the seven extant species, five live in the tropics, one in a transitional latitude, and another in the subtropics.

Decreasing species richness indicates that the families Cassidulidae and Faujasiidae are in decline. There are several possible explanations for this decline, including climate change and competition. Whether one or multiple reasons apply, their inability to evolve new traits has probably made the cassiduloids ecologically restricted and less adaptable to changes. Also, because most cassiduloid species are gregarious and endemic to small areas, they are more susceptible to extinction than widespread taxa (Payne & Finnegan 2007). For example, populations of *C. caribaeorum* are frequently exposed to storms. However, our knowledge about this species is very poor and the only census ever conducted was in the 1970s (Gladfelter 1978). However, difficulties in collecting specimens and problems with classification may be leading us to biased conclusions. Focused analyses dealing with smaller subgroups, rather than broad-scale analyses at higher levels of universality will result in greater clarity of the taxonomic status of the clades involved. Also, studying the biology of species across the phylogeny (e.g. *K. malayana*, *E. relictus*, *O. epigonus* and the neolampadids) will give better insights into the evolutionary history of this neglected group.





**Figure 2.17.** Ancestral area reconstruction of clade F from best tree inferred by the dispersal-extinction-cladogenesis (DEC) model with range and time-stratified dispersal constraints. Above: map recovering the conditions of the Paleogene indicating the distribution range of the species included in the phylogeny below. Map was based on Scotese (1997). Below: phylogeny calibrated with the “basic” method. Black bars represent known stratigraphic ranges and white bars represent uncertain range. Solid stars indicate one ancestral area and white stars represent two areas. Large orange patch indicates ancestral area of clade F. Taxa follow classification proposed by this study.



**Figure 2.18.** Ancestral area reconstruction of clade I from best tree inferred by the dispersal-extinction-cladogenesis (DEC) model with range and time-stratified dispersal constraints. Above: map recovering the conditions of the Paleogene indicating the distribution range of the species included in the phylogeny below. Map was based on Scotese (1997). Below: phylogeny calibrated with the “basic” method. Black bars represent known stratigraphic ranges and white bars represent uncertain range. Solid stars indicate one ancestral area and white stars represent two areas. Large orange patch indicates ancestral area of clade I. Dotted lines indicate uncertainty regarding the route of long-dispersal. Taxa follow classification proposed by this study.

## CHAPTER 3

# Estimating echinoid diversity dynamics from open-access databases: pitfalls and evolutionary trends

### Introduction

Digitization efforts, including the development of open-access online databases, are revolutionizing research (Benton 1999; Nelson & Ellis 2018). Large amounts of data (e.g. classic literature, species occurrences and photographs, genomes, taxonomy) allow for large-scale analyses, and data accessibility facilitates research in institutions worldwide. Worryingly, regardless of the size and amount of funding, data quality varies broadly among databases (Baxevanis & Bateman 2015) and except for a handful that undergo constant update, most databases do not go under scrutiny and rely on volunteer revisions. However, expertise (especially taxonomic) to perform such revisions is often lacking, the data used are usually reviewed only upon publication and the researcher may never correct the inconsistencies in the online database itself. In addition, the amount of database information is rapidly increasing, and volunteer revision is often unmanageable. As a result, data quality is questionable, and researchers must pay attention to biases affecting their results.

Biases introduced in paleobiology databases include those related to taxonomic and stratigraphic favoritism (i.e. monographic effect inflating entries of a particular taxon or stratigraphic interval), research trends (e.g. oversampling of stages flanking major mass extinction events and localities with perfect fossil preservation [i.e. Lagerstätten]), and research funding (e.g. most research is performed in developed countries). But issues may also be a result of outdated/incorrect information in the literature, especially related to taxonomic classifications. These affect each entry individually and depending on the amount of inconsistencies, they may also introduce biases in the dataset as a whole.

There are about 20 online databases with paleobiologic data (not including museum databases), over 65% being focused on a particular taxon, time period, or geographic locality. Launched in 1998, the Paleobiology Database (PBDB) is currently the largest database with information from fossils and its relevance for the scientific community is unquestionable (Peters & McClennen 2016). The compilation of different sources of paleontological data and the development of analytical tools have allowed researchers to approach big questions in deep time, reviving the field of Paleontology. Since its development 20 years ago, 326 papers have been published using PBDB data, and these papers have been cited more than 30,000 times (up to November 1<sup>st</sup>, 2018).

Example of large-scale analyses that can be done using PBDB data are estimates of diversity curves and turnover rates (i.e. origination and extinction rates) of a certain taxon through geologic time. Diversity curves are fluctuations in taxonomic richness through time that provide insights on the evolutionary history of a certain group. Further, by knowing when the most prominent origination (peaks) and extinction (drops) events happened, researchers can analyze the major contributors to biodiversity change (gain and loss) and use these data to predict future changes in biodiversity (Erwin 2001; McInerney & Wing 2011; Willis & MacDonald 2011).

Diversity curves have been estimated since the late 1800s, but the methods used to estimate them only came under scrutiny a century later (e.g. Raup 1972; Bambach 1977; Signor 1978; Sepkoski et al. 1981). In addition to data simulation, Sepkoski's comprehensive dataset (Sepkoski 1981) allowed for empirical large-scale analyses of the marine biota's biodiversity trend. Since then, researchers have been pre-occupied in discussions about biases that could be affecting the patterns observed in the published diversity curves. Such discussions were driven by the recognition that the fossil record was incomplete and sampling was not uniform for various reasons. Some of the biases affecting diversity curves, in particular, are the following: (1) the volume of sedimentary rock varies and diversity tends to be higher when there is more rock; (2) our understanding of the modern biota is almost perfect, therefore, identifying younger fossils is easier than identifying older fossils with unique morphological characteristics; (3) the Pull of the Recent gives an inaccurate idea of increasing diversification towards the Recent (i.e. in addition to (1) and (2), older fossils have been subject to taphonomic processes for longer, therefore, fossils are better preserved towards the Recent); (4) an artificial drop in diversity may occur at the edges of diversity curves because the intervals at the beginning of the range are usually undersampled in relation to the others (especially upon the origination of a taxon, when it is still rare) and because the intervals at the end of the range may be affected by reduced sampling as a result of extinctions (Edge effect and Signor-Lipps effect); (5) stages have different length and longer stages tend to have higher diversity than shorter stages; and (6) taphonomic conditions vary from place to place and certain localities will not preserve fossils as well as others (Raup 1976; Marshall & Ward 1996; Foote 2000; Benton 2003; Wall et al. 2009; Smith 2001; Alroy 2010). The PBDB has been a major source of data to test how such biases affect paleontological analyses, and one of its primary goals is to accumulate enough data to recover reliable evolutionary trends in the evolution of life (Alroy et al. 2001).

Here I assess the quality of echinoid (Echinodermata) entries in the PBDB, compare echinoid diversity curves derived from the PBDB data with a new dataset composed by corrected PBDB data and additional data from the literature, and estimate the turnover rates of the echinoids throughout their evolutionary history. I chose echinoids because of my taxonomic expertise and their rich fossil record. Finally, next steps to improve the PBDB echinoid data are suggested.

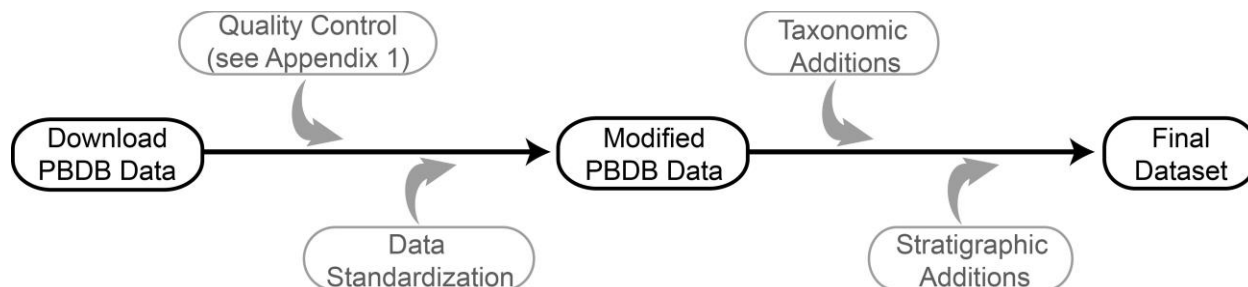
## **Methods**

### **Data retrieval, assessment of data quality, and data improvement**

Echinoid occurrences were downloaded from the PBDB on October 13<sup>th</sup>, 2018. This dataset was assessed for quality regarding data annotation accuracy (i.e. quality of each datum), satisfactory sampling (i.e. quality of the information as a whole), and taxonomic accuracy. Assessment of data quality was performed to the occurrence level; Figure 3.1 and Appendix 3.1 describe the workflow I used for data compilation, assessment steps and modifications done to improve the dataset. Thirty-five records that failed quality control (e.g. non-echinoid entries, inaccurate stratigraphic range, primary reference was uncertain about genus classification, among others) were removed. After data assessment, stratigraphic and temporal information was standardized.

### Smoothing sampling biases resulting from the PBDB dataset

Because the echinoid dataset was largely incomplete both taxonomically and temporally, I added the echinoid genera that have not been entered in the PBDB and extended the stratigraphic range of the genera whose entries did not include their first appearances (FAs) and/or last appearances (LAs). Missing genera were compiled from WoRMS (2018a), Smith & Kroh (2011) and the literature. Although this addition was comprehensive, valid extinct genera may be missing. Also, the phylogenetic analysis by Kroh & Smith (2010) is to the family level and some genus classifications in the dataset may still not be accurate.



**Figure 3.1.** Workflow followed to retrieve and assess the Paleobiology Database echinoid dataset.

### Generating diversity curves

Analyzes were performed to the genus level (unidentified echinoid genera composing 11% of the dataset were excluded) not only because most of the occurrences in the PBDB are classified to the genus level, but also because of taxonomic over-splitting is common in the fossil record. Over-splitting usually occurs when poorly preserved specimens cannot be accurately identified and are described as a new species, when specimens collected in different formations are not compared to each other and may be described as new, and also when specimens belonging to the same lineage but different time intervals (i.e. fossil record is interrupted) have slight morphological variations that are used to separate them into different species. Within the cassiduloid echinoids, a famous case of a genus with high species diversity and low morphological variability is the genus *Echinolampas*, composed of almost 300 species.

In the absence of a genus-level global phylogeny, ghost lineages of genera were not extended and their stratigraphic ranges reflect only the fossil record. Also, although most of the PBDB occurrences were restricted to one stage, the length of the stages pertinent to this study (i.e. from the Late Ordovician to the Holocene) varied from 0.01–18.5 millions of years. Therefore, instead of assuming that the occurrence lived throughout its entire assigned range, I randomly drew absolute ages within the stratigraphic range of each occurrence 100 times. The duration of the time intervals was then standardized by combining the stages into approximately 10 million-year bins (Appendix 3.2).

I used three counting methods to generate diversity curves (Appendix 3.3), following Alroy et al. (2001) and Quental & Marshall (2010). Sample in bin is the most straightforward method (SB), which is basically the sum of taxa found in each time interval. However, if there is an oversampled interval, it will have higher diversity and an apparent burst of origination. To account for this sampling bias, I used the boundary-crosser method (BC), the most conservative

method that includes only the taxa that crossed a boundary (i.e. genera that have been collected at least in two different time intervals, which, by definition, excludes single-interval taxa). This method also guarantees that the taxa coexisted (i.e. belonged to the same cohort), because they had to be together at the boundary. The third method used was the sample in bin corrected for the sampling completeness at each time interval (CC). This method provides the highest diversities and represents the upper boundary of the confidence interval produced by the three curves. To estimate the completeness of each time interval, I calculated the number of genera crossing both boundaries of the time interval and divided this estimate by the expected number of genera to be found in that time interval (i.e. genera that have been sampled before and after that interval but not at it). The diversity of each time interval was then estimated by dividing the number of genera found at the interval by its completeness. Because this method relies on occurrences to estimate completeness, the additional genera that were not in the PBDB were not included.

All three methods described above included the range-through assumption to reduce biases related to incomplete preservation and undersampled time intervals (SBrt, BCrt and CCrt from here onwards). This assumption dictates that if a genus occurred in interval A and interval D, it had to have occurred in the intervals in between (i.e. B and C) because taxa cannot go extinct and re-originate. A problem may arise if the taxon at interval A is actually different from a taxon at interval D, even though they have been called the same name because of morphological similarities (the opposite of over-splitting). However, this issue cannot be corrected without a proper morphological examination of both specimens. Although their goal is to reduce sampling biases, these methods introduce biases related to the way they count taxa (Alroy 2010). Unfortunately, because the additions made to the dataset were composed of FAs and LAs instead of occurrences, I could not perform analyses to the occurrence level. But by using different methods, I hoped for accounting for some of these method's inherent biases.

### **Estimating diversity dynamics**

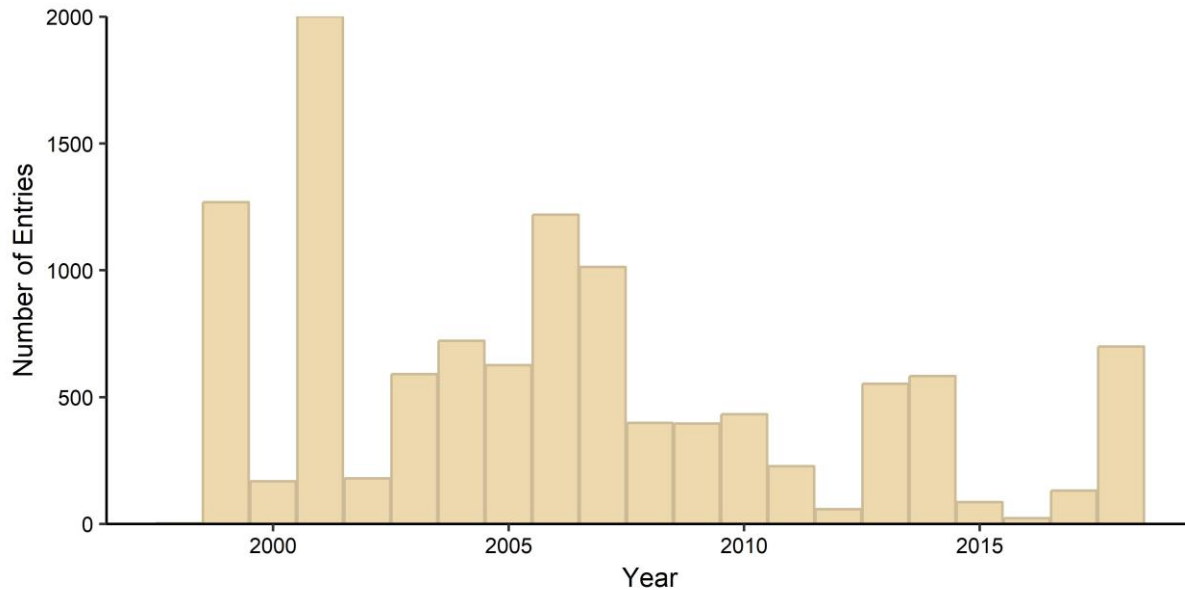
Per-capita origination ( $p$ ) and extinction ( $q$ ) rates at each time interval were estimated according to Foote (2000):  $p = \log(N_{bt} / [N_{bt} + N_t])$  and  $q = \log(N_{bt} / [N_{bt} + N_b])$ , where  $N_t$  is the number of taxa that originates in the interval and crosses its top boundary,  $N_b$  is the number of taxa that crosses the bottom boundary of the interval and goes extinct in it, and  $N_{bt}$  is the number of taxa that originates before an interval and crosses both of its boundaries. Rates were then normalized by the interval duration ( $T$ ):  $p = \log(N_{bt} / [N_{bt} + N_t]) / T$  and  $q = \log(N_{bt} / [N_{bt} + N_b]) / T$ . Single-interval taxa were excluded from the calculations because they are usually artifacts resulting from incomplete preservation (although some could be real short-lived genera).

## **Results and Discussion**

### **Quality of the echinoid PBDB dataset**

*Data retrieval.*—The echinoid PBDB dataset was derived from 1,099 references published between 1841 and 2018, and included *ca.* 9,500 occurrences (*ca.* 8,500 identified at least to the genus level) representing 445 genera, about 65% of the valid echinoid genera with a fossil record. About 60% of the occurrences were from publications from 1980–2009. Data entry in the PBDB was random in respect to time, the highest peaks being when the database was launched and then in 2006–2007, when the deadline for the initial project was approaching (Fig. 3.2). Table 3.1 shows a summary of the downloaded and modified datasets.

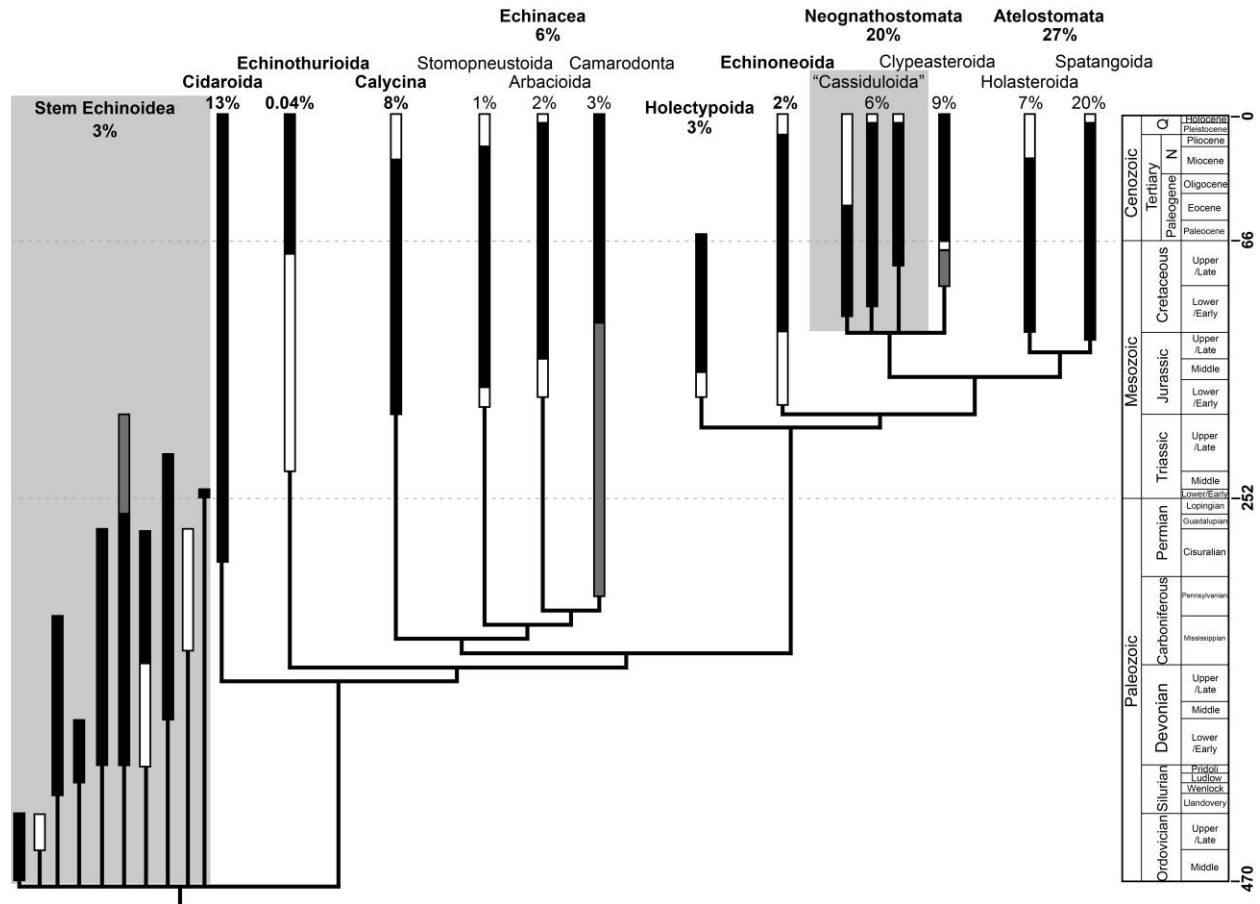
*Assessment of data quality.*—Genus classifications were mostly outdated (94 synonymies found), at least 67 species were misclassified and two non-echinoid genera (a gastropod and a crustacean) that were named with pre-occupied echinoid names were found in the database. Revising these taxonomic issues were very important to remove the artificial increase in diversity caused by synonymies. Also, higher taxonomic ranks (i.e. family and order) were often outdated or missing. Missing genera classifications are not an issue for global analyses focused beyond the class level, but they lower the power of analyzes at lower taxonomic ranks. Analyzes comparing families or orders, for example, may be hampered because they do not show up in the database even though some of their genera have been represented.



**Figure 3.2.** Number of Paleobiology Database entries per year since the beginning of the project, in 1998, until the data retrieval in Oct 13th, 2018.

Figure 3.3 shows the phylogenetic coverage of the PBDB dataset. The Irregularia composed 54% of the occurrences, an expected result given that this group is more likely to be fossilized than the “regular” echinoids because they live in direct contact with the sediment and often buried (Kier 1977). Also, although they originated in the Mesozoic, their current diversity is higher than the other echinoids combined. Within the Irregularia, the Atelostomata accounted for 27% of the occurrences: 20% of spatangoids and 7% of holasteroids. This result was also expected given the spatangoid’s Cenozoic diversification worldwide. However, 30% of the spatangoid data was derived from only one (out of 26) family, the Hemiasteridae. This family is composed by 12 genera and those occurrences account for only seven of these. The Neognathostomata accounted for 20% of the occurrences: 9% of clypeasteroids and 6% of “cassiduloids”. Although the clypeasteroids have dominated the Neognathostomata diversity from the Oligocene onwards, the “cassiduloids” attained *ca.* 40% of the echinoid diversity in the Eocene but they are underrepresented in the PBDB. Two stem group Echinoidea were not represented at all. Two stem group Echinoidea were not represented at all and another underrepresented group was the Echinothurioidea, a predominately deep-sea taxon with fragile tests. As Smith (2001) pointed out, the fossil record is biased with high diversity of shallow

water taxa; therefore, the low number of echinothurioid and holasteroid occurrences may be a reflect of that, though their current diversity is low.



**Figure 3.3.** Phylogenetic coverage of the echinoid Paleobiology Database (PBDB) occurrences up to Oct 13<sup>th</sup>, 2018. Percentages above bars are the relative number of occurrences per taxon in the PBDB. Taxa in bold are major clades but not necessarily in the same taxonomic rank. Echinacea includes Stomopneustida, Arbacioida and Camarodonta; Neognathostomata includes “Cassiduloida” and Clypeasteroida; Atelostomata includes Holasteroida and Spatangoida. Phylogenetic relationships were based on Kroh & Smith (2010) except for the stem group Echinozoa and for the “cassiduloids”, whose branches were collapsed because phylogenetic relationships are not well-resolved. Solid black bars indicate PBDB stratigraphic ranges, white bars indicate stratigraphic ranges missing in the PBDB, and dark grey solid bars indicate PBDB ranges that are probably erroneous (e.g., many occurrences were annotated in the PBDB as “Echinozoa indet.”, which would mean the order Echinozoa when they are actually unidentified echinoid spines, or “Echinozoa irr” instead of “Irregularia”). Collapsed branches (shaded in light grey) are the stem group Echinozoa (from left to right: Bothriocidaridae, Eothuriidae, Lepidocentridae, Echinocystitidae, Lepidesthidae, Archaeocidaridae, Palaechinidae, Proterocidaridae, Cravenechinidae and Lenticidaridae) and the “cassiduloids” (from left to right: Apatopygoida, Cassiduloida [including the Faujasiidae], Echinolampadoida).



**Table 3.1.** Characteristics of the echinoid dataset downloaded from the Paleobiology Database in 13 October 2018. Taxonomic Data also includes values for modified and final datasets.

<b>General Statistics</b>			
Number of entries		9539	
Number of data enterers/modifiers		98/54	
Number of references		1100 (22 thesis; 8 unpublished)	
Years with most number of publication		1990s and 2000s (226 each)	
Years with most number of occurrences		1990s (2180)	
Average number of occurrences per reference		9 (1860s had 50)	
<b>Geographic Data</b>			
Number of countries with occurrences		112	
Number of occurrences per continent			
Europe		4807 (50%)	
North America		2359 (25%)	
Asia <sup>1</sup>		830 (9%)	
Africa		738 (8%)	
South America		455 (5%)	
Oceania		331 (3%)	
Antarctica		18 (0.2%)	
Countries with higher number of occurrences per continent			
U.S.A. (1 <sup>st</sup> )		1896 (20%)	
France (2 <sup>nd</sup> )		1324 (14%)	
Egypt (5 <sup>th</sup> )		357 (4%)	
Saudi Arabia (8 <sup>th</sup> )		321 (3%)	
Brazil (11 <sup>th</sup> )		283 (3%)	
New Zealand (16 <sup>th</sup> )		148 (2%)	
<b>Stratigraphic Data</b> (Occurrences per interval)			
Mesozoic		5768 (60%)	
Cenozoic		2706 (28%)	
Paleozoic		633 (7%)	
<b>Taxonomic Data</b>			
	Raw PBDB data	Modified	Final <sup>2</sup>
Number of orders	23	21	21
Number of families	94	134	150
Number of genera	503	445	857
Number of accepted names	1068	1006	NA
Records to genus level (and below)	8010	8034	NA
Occurrences per major group			
Irregularia	46%	54%	NA
Non-Irregularia Euechinoidea	14%	19%	NA
Cidaroida	13%	13%	NA
Paleozoic echinoids	0.4%	3%	NA

<sup>1</sup> Because most of the Russian territory is in Asia, Russia was considered part of this continent.

<sup>2</sup> Taxa with fossil record.

Fossil occurrences in the PBDB were retrieved from 113 countries and an offshore location (Appendix 3.4); 50% of the occurrences were from Europe (14% of the total from France) and 25% from North America (20% of total from the U.S.A.). With over 75% of the data being from the northwest hemisphere, local events may be interpreted as global. Further, Allison & Briggs (1993) noted that diversity estimates have been underestimated by this geographic sampling bias. But if studies are regional or at short time-scales, such bias should not be an issue (Smith, 2001). In terms of temporal coverage, the dataset had occurrences ranging from the Late Ordovician to the Holocene (*ca.* 467 my range); most of them from the Mesozoic and 41% of the total from the Cretaceous alone (79 my range). Most major taxa did not have occurrences from the Holocene (Fig. 3.3) and this probably result from a sampling gap given that almost half of the living species do not have a fossil record. Although a higher number of occurrences were expected for the Late Cretaceous because of the bulk of research focusing on the end-Cretaceous mass extinction, occurrences were equally distributed between the Early and Late Cretaceous. However, the late Early and late Late Cretaceous had 5% more occurrences than the early Early and early Late Cretaceous.

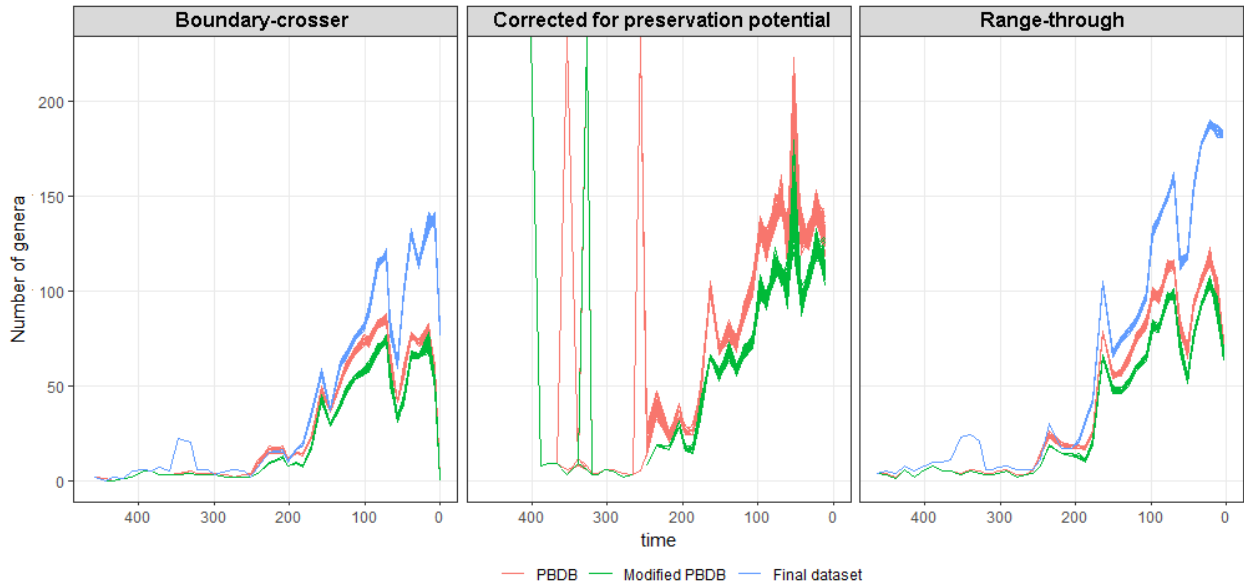
Less than 7% of the occurrences were from the Paleozoic and only four groups crossed the end-Permian boundary (although two are probably misclassified; Fig. 3.3). Phylogenetic studies indicate that crown group Echinoidea diverged before the end-Permian (Smith et al. 2006; Kroh & Smith 2010), though none of its stem group was thought to have crossed the boundary. However, Paleozoic echinoids have been severely understudied and recent discoveries have shown that stem lineages survived at least until the Late Triassic (Hagdorn 2018; Thompson et al. 2018).

### **Echinoid diversity through time**

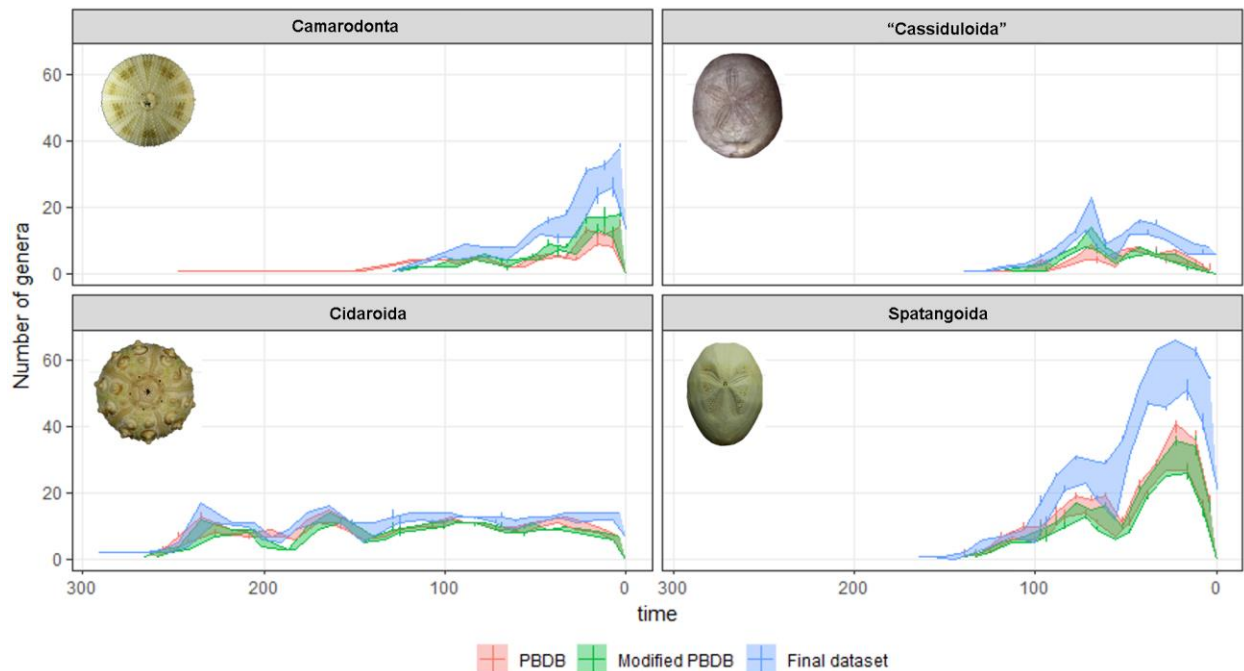
*PBDB versus final dataset.*—Overall, the diversification trend did not change much in the curves before and after the correction and addition of data (Fig. 3.4). However, the final dataset had higher genus diversity, especially from the Late Cretaceous to the Recent and during the Devonian through the Carboniferous, when the additional genera mattered the most because the PBDB did not have much data for the Paleozoic. Interestingly, the PBDB dataset had higher diversity than the modified dataset during the Mesozoic and Cenozoic, possibly because of the correction of synonymies that decreased the number of genera from 503 to 445 (Table 3.1).

At the order level, however, differences are more apparent (Fig. 3.5). Genus diversity of camarodonts and spatangoids increased significantly with the addition of data, which means that they are underrepresented in the PBDB, while the diversity of cidaroids and “cassiduloids” did not increase by much if at all, which indicates that their PBDB occurrences have more taxonomic errors. Although the amount of taxonomic errors varies from group to group, large datasets and analyses at high taxonomic ranks should minimize their impact on diversity estimates because the errors will be randomly distributed (Smith 2001).

The diversity curves in Figure 3.5 also show different evolutionary trends among echinoids: the camarodonts and the spatangoids showing a burst of diversification after the end-Cretaceous mass extinction; the cidaroids showing slight changes in genus diversity since its origination and not reaching 20 genera at any interval; and the “cassiduloids” (paraphyletic, *sensu* Kier [1962]) showing a steep increase in genus diversity and then two consecutive drops, an abrupt drop at the end-Cretaceous and then a slow but steady drop from the Oligocene onwards. In terms of species diversity, the rock-boring and epifaunal camarodonts and the deposit-feeding and infaunal spatangoids are the most successful echinoid groups in the Recent.



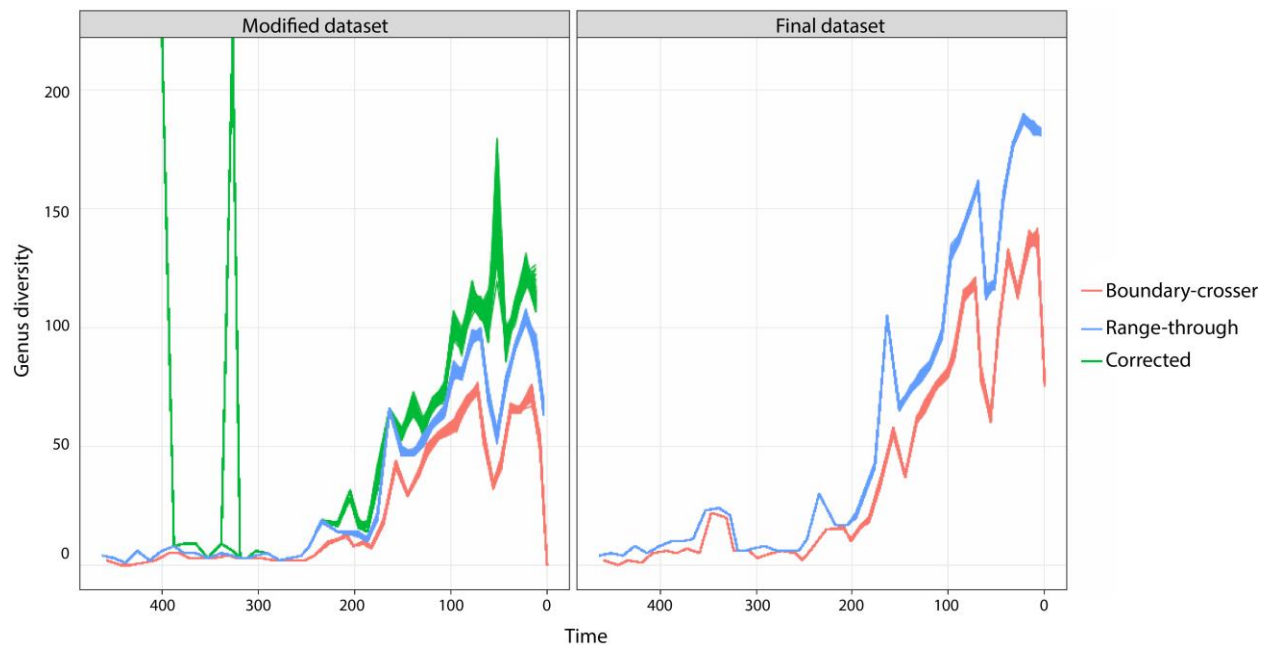
**Figure 3.4.** Comparison among echinoid diversity curves derived from the PBDB dataset (original; in red), the modified dataset (with taxonomic and stratigraphic corrections; in green), and the final dataset (with additional genera; in blue). Genus diversity was estimated with three different methods (see Appendix 3.3 for an explanation of the methods): boundary-crosser and sample in bin with range-through for all datasets, and sample in bin with the range-through assumption corrected for preservation potential for the PBDB and modified datasets.



**Figure 3.5.** Comparison among diversity curves of major echinoid groups derived from the PBDB dataset (original; in red), the modified dataset (with taxonomic and stratigraphic corrections; in green), and the final dataset (with additional genera; in blue). Genus diversity was

estimated with the sample in bin method with the range-through assumption. “Cassiduloida” refers to the paraphyletic order as defined by Kier (1962).

*The echinoid diversity dynamics.*—After correcting and adding the data, I generated diversity curves using different methods to account for sampling and preservation biases. Figure 3.6 shows the trend of echinoid genus diversity since its appearance in the fossil record. The first occurrences were retrieved from the Middle Ordovician (more specifically, from the Darriwilian at about 467–458 mya). Echinoids are the sister group to the clade composed by ophiocystoids and holothuroids (Smith & Reich 2013). Unequivocal holothuroid records dates from the Middle Ordovician (although uncertain records have been found in the Middle-Upper Cambrian) (Reich 2010) and the ophiocystoids records dates from the Early Ordovician (about 478–470 mya) (Reich & Haude 2004), indicating that we are missing at least the first 10 my of echinoid evolution.

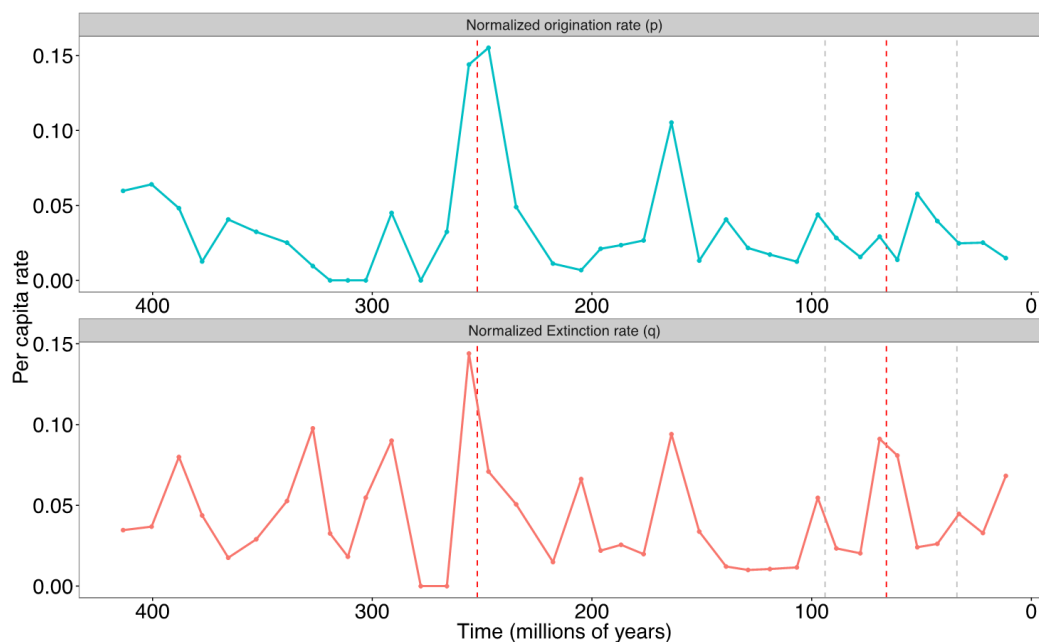


**Figure 3.6.** Echinoid diversity curve through time. Genus diversity was estimated with three different methods (see Appendix 3.3 for an explanation of the methods): boundary-crosser (in red) and sample in bin with range-through (in blue) for the modified and final datasets, and sample in bin with the range-through assumption corrected for preservation potential (in green) for the modified datasets.

Diversity was kept low throughout the Paleozoic, although the final dataset shows a burst of diversification in the Late Devonian followed by a sudden drop in the Late Carboniferous. The unusual peaks in diversity estimated using the modified dataset corrected for preservation potential are artifacts resulting from a high number of range-throughs within those time intervals, which would reduce their preservation potential and boost their genus diversity. A high number of range-throughs in the Paleozoic may be a result of gaps in the fossil record and/or wrong

taxonomic assignments resulting from poor preservation of morphological features. Unfortunately, Paleozoic echinoids are understudied making it challenging to interpret the observed trend.

Although the echinoderms were severely affected by the end-Permian mass extinction (Sprinkle 1983), the diversity curves estimated here do not show a decrease in echinoid genus diversity across the Permo-Triassic boundary; but they show an increase of diversity during the Triassic. Skeletonized invertebrates were apparently vulnerable to the end-Permian mass extinction (Erwin 1994), but its effect on echinoids deserves further investigations. There was certainly a morphological shift from tests with imbricating plates characteristic of the “Paleozoic” echinoids to rigid tests characteristic of the modern echinoids (Smith 2005). However, this shift could have happened over millions of years. It has long been recognized that two echinoid lineages crossed the Permo-Triassic boundary (Kier 1984; Smith 2007), but only recently we have discovered stem group echinoids in the Mesozoic (Shi-xue Hu et al. 2011; Hagdorn 2018; Thompson et al. 2018). The discovery of Paleozoic echinoids is especially challenging because their imbricated tests are easy to disarticulate and less likely to fossilize (Thompson & Ausich 2016), but with more studies focused on the stem group, their diversity could increase. In addition to the poor preservation, the outcrop area across the Permo-Triassic boundary is small (Smith 2007; Smith & McGowan 2007). With such a low genus diversity across the boundary, a decrease from four to two genera, for example, would represent 50% of the total diversity. Therefore, the trends and turnover rates (Fig. 3.7) observed here could be a result of the mass extinction, of bad luck for some of the few existing genera, or of incomplete sampling.



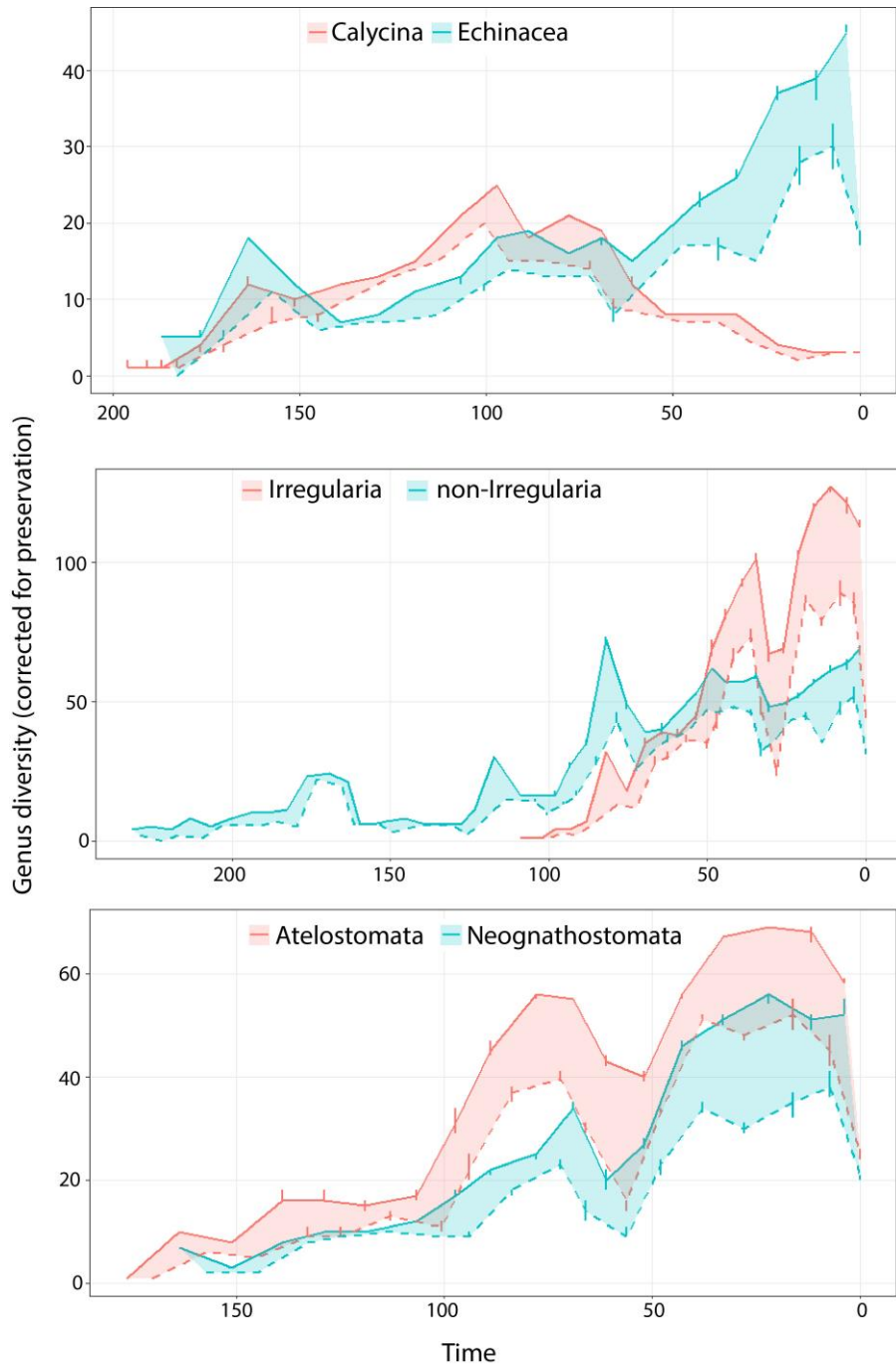
**Figure 3.7.** Echinoid per-capita origination (top, in blue) and extinction (bottom, in red) rates at each time interval. Red dotted lines indicate, from left to right, the Permo-Triassic and the Cretaceous-Paleogene boundaries; grey dotted lines indicate, from left to right, the Early-Late Cretaceous and the Eocene-Oligocene boundaries.

Diversification rates increased during the Mesozoic, especially from the Mid-Jurassic, possibly driven by the origin of the irregular urchins and infaunalization during the Marine Mesozoic Revolution (Vermeij 1977), although this increase could be a result of the poor Triassic fossil record (Smith 2007). Genus diversity dropped by the Late Jurassic when extinction rates were high (although the corrected curve in Figure 3.6 indicates that this drop could be a result of poor preservation), and then quickly recovered afterwards with a steady and sharp increase throughout the Cretaceous. Interestingly, although the extinction rate was high at the end of the Early Cretaceous, coinciding with an ocean anoxic event that caused the extinction of deep-sea echinothuroids, holasteroids and spatangoids (Smith & Stockley 2005), the diversity curves did not show a reduction in genus diversity. Equally high origination rates indicate that the genus extinctions were substituted by genus originations and the net diversity was kept unchanged despite the deep-sea extinctions.

The magnitude of the end-Cretaceous mass extinction varies among the curves, but the extinction rate was high (again, the corrected curve suggests low preservation in the Cretaceous). Also, extinction continued through the Danian indicating that the extinction was gradual for the echinoids. Smith & Jeffery (1998) suggested that a reduction in test size from the Maastrichtian to the Paleocene and a correlation between feeding strategy and survival indicate that the echinoid extinction at the end-Cretaceous was driven by low nutrient availability. In this scenario, deposit-feeder echinoids with penicillate tube-feet and generalist omnivores were more likely to survive because of their resourcefulness and flexibility, respectively, while the echinoids restricted to a certain kind of food because of strategy specialization (e.g. grazing herbivores) or lack of innovation (deposit-feeders with suctorial tube-feet) were more likely to perish. A peak in origination rate following the extinction indicates a faunal turnover, possibly with the diversification of clypeasteroids and spatangoids. The echinoids recovered quickly and reached about 125–180 genera in the Early Eocene. The diversity trajectory towards the Recent varied among curves and drops in diversity may be a result of Edge effects.

The analysis using the SBrt method with the final dataset indicates that the echinoid genus diversity has never been higher, with 255 genera in the Recent followed by 190 from the Late Oligocene to the Early Miocene (Cenozoic 5). High diversity during this interval was also obtained with the modified dataset using the SBrt method, which suggested about 110 genera. However, in the analysis using the CCrt method with the modified dataset, the Early Eocene has highest diversity, about 130 genera.

The comparison between the evolutionary trajectory of major, closely related, echinoid groups show different patterns (Fig. 3.8). While the Echinacea (group composed by camarodonts and arbacioids) have been steadily diversifying and currently representing most of the “regular” echinoid’s genus diversity, the Calycina (group currently composed by the salenioids) has been declining since the middle of the Cretaceous. Also, the diversity of “regular” echinoids has not changed much in the last 100 million-years, while the diversity of irregular echinoids has more than doubled. This great diversification was driven by both Atelostomata (e.g. heart urchins and holasteroids) and Neognathostomata (e.g. sand dollars and cassiduloids), although the former has been more diverse.



**Figure 3.8.** Comparison between diversity trajectories of major echinoid groups derived from the final dataset: the superorder Calycina (e.g. Salenioida) versus the superorder Echinacea (e.g. Camarodonta); the infraclass Irregularia versus the other (“regular”) echinoids; and the superorder Atelostomata (e.g. heart urchins) versus the superorder Neognathostomata (e.g. sand dollars). Genus diversity was estimated with the sample in bin method with the range-through assumption.

### **Echinoid PBDB data: moving forward**

Overall, the echinoid data from the PBDB reflected major trends observed in the evolution of the marine biota. However, spatial, temporal and taxonomic biases exist. Efforts should be put into increasing the taxonomic and geographic coverage of the PBDB echinoid data; stratigraphic biases will likely be reduced as a result.

Databases with paleontological data have been compiled by researchers for a long time, but they were restricted to small research groups and analyses by distinct research groups were likely to use other sources of data. Open-access results in widespread use of the same data to answer various questions. Having comprehensive open-access data is certainly beneficial to science and one of the advantages is that the data is under the scrutiny of hundreds of researchers with different expertise. However, errors and biases in the data will be propagated at a fast pace.

Cladistic rigor has revolutionized classification schemes and scientific names present in outdated literature should be checked; such practices benefit not only biodiversity research, but also conservation and management. Integrating information from databases that provide different sources of data has the potential to combine efforts, avoid data duplication and increase data quality. Also, having to use multiple databases and choosing from multiple databases can be overwhelming and do not facilitate the use and retrieval of information. At least for the echinoids, the World Register of Marine Species (WoRMS) database has been a reliable source of taxonomic information and although its focus is on extant taxa, data on extinct taxa has been entered as well. Integrating databases, however, is not a trivial task and funding is necessary to resolve conflicts between them.

In addition, including voucher numbers for occurrences could not only prevent duplicate information but also check and track taxonomic assignments. Digitization efforts are providing images of millions of specimens whose taxonomy could be coarsely checked online if needed. Museum specimens (especially marine invertebrates) are not all vouchered and voucher numbers are not available in all publications; however, some journals have been requiring this information and some collections are fully catalogued.

The scientific community can be divided into three categories according to their opinion and usage of open-access data: the ones that do not use online databases at all hoping that someday databases be comprehensive and correct, the ones that review the data before analyzing it (especially by means of collaborations), and the ones that recognize the problem but use the data anyway because revision may seem impossible or not doable in a reasonable time frame. Regardless of what kind of scientists we are, recognizing biases in the data we analyze is very important to an accurate understanding of our results. This awareness will not only facilitate the identification of spurious results but also the recognition that even with all the biases, the data is robust enough to reach reliable conclusions. For the better or for the worse, science progresses when data analyses are published, especially when there is the integration of knowledge by means of collaborations with specialists.



## Bibliography

- Adegoke, O. S. 1977. Stratigraphy and paleontology of the Ewekoro Formation (Paleocene) of southwestern Nigeria. *Bulletin of American Paleontology*, 71, 5–379.
- Afzal, J., Williams, M. & Aldridge, R. J. 2009. Revised stratigraphy of the lower Cenozoic succession of the Greater Indus Basin in Pakistan. *Journal of Micropalaeontology*, 28, 7–23.
- Agassiz A. 1869. Preliminary report on the Echini and star-fishes dredged in deep water between Cuba and the Florida Reef, by L. F. de Pourtalès, Assist. U.S. Coast Survey. *Bulletin of the Museum of Comparative Zoölogy at Harvard College*, 1, 253–308.
- Agassiz, A. 1863. List of the echinoderms sent to different institutions in exchange for other specimens, with annotations. *Bulletin of the Museum of Comparative Zoology*, 1, 17–28.
- Agassiz, A. 1872–1874. Revision of the echini. *Memoirs of the Museum of Comparative Zoology*, 3, 1–762.
- Agassiz, A. 1879. Preliminary report on the Echini of the Exploring Expedition of H.M.S "Challenger". *Proceedings of the American Academy of Arts and Sciences*, 6, 190–212.
- Agassiz, L. & Desor, E. 1847. Catalogue raisonné des espèces, des genres et des familles d'échinides. *Annales des Sciences Naturelles, Zoologie*, 3(7), 129–168.
- Agassiz, L. 1839. Description des Échinodermes fossiles de la Suisse. Première partie, Spatangoides et Clypéasteroides. *Mémoires de la Société Helvétique des Sciences Naturelles*, 3, i-viii + 1–101, 14 pls.
- Allison, P. A. & Briggs, D. E. G. 1993. Paleolatitudinal sampling bias, Phanerozoic species diversity, and the end-Permian extinction. *Geology*, 21, 65–68.
- Alroy, J. 2010. Fair sampling of taxonomic richness and unbiased estimation of origination and extinction rates. Pp. 55–80 in: Alroy, J. & Hunt, G. (eds) *Quantitative Methods in Paleobiology*. Paleontological Society, Denver.
- Alroy, J., Marshall, C. R., Bambach, R. K., Bezusko, K., Foote, M., Fursich, F. T., Hansen, T. A., Holland, S. M., Ivany, L. C., Jablonski, D., Jacobs, D. K., Jones, D. C., Kosnik, M. A., Lidgard, S., Low, S., Miller, A. I., Novack-Gottshall, P. M., Olszewski, T.D., Patzkowsky, M.E., Raup, D. M., Roy, K., Sepkoski, J. J., Jr., Sommers, M.G., Wagner, P. J., and Webber, A. 2001. Effects of sampling standardization on estimates of Phanerozoic marine diversification, *PNAS*, 98, 6261–6266.
- Alvarado, J. J., Solis-Marin, F. A. & Ahearn, C. 2008. Equinodermos (Echinodermata) del Caribe Centroamericano. *Revista de Biología Tropical*, 56 (Supl. 3), 37–55.
- Alvarado, J.J. 2011. Echinoderm diversity in the Caribbean Sea. *Marine Biodiversity*, 41(2), 261–285.
- Anderson, F. M. 1905. A stratigraphic study in the Mount Diablo Range of California. *Proceedings of the California Academy of Sciences*, series 3, 2, 155–248.
- Anderson, F. M. 1958. Upper Cretaceous of the Pacific coast. *The Geological Society of America*, 71, 1–378.
- Arnold, B. W. & Clark, H. L. 1927. Jamaican fossil Echini; with descriptions of new species of Cenozoic Echinoidea by H. L. Hawkins. *Memoirs of the Museum of Comparative Zoology*, 50, 1–84.
- Baker, A. N. 1983. A new apatopygid echinoid genus from New Zealand (Echinodermata: Cassiduloida). *National Museum of New Zealand Records*, 2, 163–173.

- Bambach, R. K. 1977. Species Richness in Marine Benthic habitats through the Phanerozoic. *Paleobiology*, 3(2), 152–167.
- Baxevanis, A. D. & Bateman, A. 2015. The importance of biological databases in biological discovery. *Current Protocols in Bioinformatics*, 50, 1.1.1–1.1.8.
- Bell, M. A. & Lloyd, G. T. 2015. strap: an R package for plotting phylogenies against stratigraphy and assessing their stratigraphic congruence. *Palaentology*, 58, 379–389.
- Benton, M. 1999. The history of life: large databases in Palaeontology. Pp. 249–283 in: Harper, D. A. T. (ed) *Numerical Paleobiology: computer-based modelling and analysis of fossils and their distributions*. John Wiley and Sons.
- Benton, M. J. & Storrs, G. W. 1994. Testing the quality of the fossil record: paleontological knowledge is improving. *Geology*, 22, 111–114.
- Benton, M. J. 2003. The quality of the fossil record. Pp 66–90 in: Donoghue, P. C. J. & Smith, M. P. (eds) *Telling the evolutionary time: molecular clocks and the fossil record*. CRC Press.
- Besaire, H. & Lambert, J. 1930. Notes sur quelques Échinides de Madagascar et du Zululand. *Bulletin de la Société Géologique de France*, series 4, 30, 107–117.
- Bittner, A. 1892) Über Echiniden des Tertiärs von Australien. *Sitzungsberichte der Kaiserlichen Akademie der Wissenschaften zu Wien (Math.-Naturw. Classe)*, 101(1), 331–371.
- Blainville, H. M. de 1830. *Zoophytes*. In: Dictionnaire des sciences naturelles, dans lequel on traite méthodiquement des différents êtres de la nature, considérés soit en eux-mêmes, d'après l'état actuel de nos connaissances, soit relativement à l'utilité qu'en peuvent retirer la médecine, l'agriculture, le commerce et les arts. Edited by F. G. Levrault. Volume 60. Le Normant, Paris, 631 pp.
- Blainville, H. M. de 1834. *Manuel d'Actinologie ou de Zoophytologie*. F.G. Levrault, Strasbourg, 694 pp.
- Bodenbender, B. E. & Fisher, E. C. 2001. Stratocladistic analysis of blastoid phylogeny. *Journal of Paleontology*, 75, 351–69
- Boivin, S., Saucède, T., Laffont, R., Steimetz, E. & Neige, P. 2018. Diversification rates indicate an early role of adaptive radiations at the origin of modern echinoid fauna. *PLoS ONE*, 13, e0194575.
- Bouvé, T. T. 1846. *Pygorhynchus goldii*, a new Echinus from the Millstone Grit of Georgia. *Proceedings of the Boston Society of Natural History*, 2, 39–41.
- Bouvé, T. T. 1851. New species of echinoderms from the lower tertiary rocks of Georgia. *Proceedings of the Boston Society of Natural History*, 4, 2–4.
- Bruguière, J. -G., Bory de Saint-Vincent, J. B. G. & Müller, O. F. 1827. *Tableau encyclopédique et méthodique des trois règnes de la nature: vers, coquilles, mollusques et polypiens*. Volume 2. Chez Mme veuve Agasse, Paris, plates 96–314.
- Brusatte, S. L. 2011. Calculating the tempo of morphological evolution: rates of discrete character change in a phylogenetic context. Pp. 53–74 in Elewa, A. M. T. (ed) *Computational Paleontology*. Springer-Verlag Publishers, Heidelberg.
- Bry, F. & Kröger, P. 2003. A computational Biology database digest: data, data analysis, and data management. *Distributed and Parallel Databases*, 13, 7–42.
- Bush, A. B. G. 1997. Numerical simulation of the Cretaceous Tethys circumglobal current. *Science*, 275, 807–810.

- Carbayo, F., Francoy, T. M. & Giribet, G. 2016. Non-destructive imaging to describe a new species of *Obama* land planarian (Platyhelminthes, Tricladida). *Zoologica Scripta*, 45, 566–578.
- Carrasco, J. F. 2016. *Rhyncholampas grignonensis* (Defrance, 1825) (Echinoidea, Eoceno) in Spain. Review of synonymy. *Batalleria*, 23, 35–41.
- Carter, B. D. & Beisel, T. H. 1987. "*Cassidulus trojanus*" belongs in the genus *Eurhodia* (Echinoidea) based upon new criteria. *Journal of Palaeontology*, 61, 1080–1083.
- Clark W. B. & Twitchell, M. W. 1915. The Mesozoic and Cenozoic Echinodermata of the United States. *Monographs of the United States Geological Survey*, 54, 1–341.
- Clark, H. L. 1917. Hawaiian and other Pacific echini. The Echinoneidae, Nucleolitidae, Urechinidae, Echinocorythidae, Calymnidae, Pourtalesiidae, Palaeostomatidae, Aeropsidae, Palaeopneustidae, Hemiasteridae, and Spatangidae. *Memoirs of the Museum of Comparative Zoology*, 46(2), 91–283.
- Coates, A. G. 1999. Lithostratigraphy of the Neogene strata of the Caribbean coast from Limon, Costa Rica, to Colon, Panamá. Pp. 17–38 in: Collins, L. S. & Coates, A. G. (eds) *A paleobiotic Survey of Caribbean faunas from the Neogene of the Isthmus of Panama*. Paleontological Research Institution, Ithaca.
- Cohen, K. M., Finney, S. C., Gibbard, P. L. & Fan, J. -X. 2013 (updated). The ICS International Chronostratigraphic Chart. V2017/02. *Episodes*, 36, 199–204.
- Conrad, T. A. 1850. Descriptions of one new Cretaceous and seven new Eocene fossils. *Journal of the Academy of Natural Sciences, Philadelphia*, 2, 39–41.
- Cooke, C. W. 1942. Cenozoic irregular echinoids of eastern United States. *Journal of Paleontology*, 16, 1–62.
- Cooke, C. W. 1953. American Upper Cretaceous Echinoidea. *Geological Survey Professional Paper*, 254–A, 1–44.
- Cooke, C. W. 1955. Some Cretaceous echinoids from the Americas. *Geological Survey Professional Paper*, 264–E, 1–112.
- Cooke, C. W. 1959. Cenozoic echinoids of eastern United States. *Geological Survey Professional Paper*, 321, 1–106.
- Cooke, C. W. 1961. Cenozoic and Cretaceous echinoids from Trinidad and Venezuela. *Smithsonian Miscellaneous Collections*, 142, 1–35.
- Costello, M. J., Bouchet, P., Boxshall, G., Fauchald, K., Gordon, D., Hoeksema, B. W., Poore, G. C. B., van Soest, R. W. M., Stohr, S., Walter, T. C., Vanhoorne, B., Decock, W., Appeltans, W. 2013. Global coordination and standardisation in marine biodiversity through the World Register of Marine Species (WoRMS) and related databases. *PLoS ONE*, 8(1), e51629.
- Cotteau, G. 1866. Échinides nouveaux ou peu connus. *Revue et magasin de zoologie pure et appliquée, série 2*, 18, 262–268.
- Cotteau, G. 1883. Échinides nouveaux ou peu connus, part II. *Bulletin de la Société zoologique de France*, 8, 450–464.
- Cotteau, G. 1885–1889. *Paléontologie française. Terrain Tertiaire. Échinides Eocènes*. Vol. 1. G. Masson, Paris, 672 pp., 200 pls.
- Cuvier, G. 1836. *Le Règne Animal, distribué d'après son organisation, pour servir de base à l'histoire naturelle des animaux, et d'introduction à la anatomie comparée. Echinodermes*. Fortin, Masson et Cie, Paris, 20 pls.

- d'Archiac, E. & Haime, J. 1853–1854. *Description des animaux fossiles du groupe nummulitique de l'Inde*. Gide et Baudry, Paris.
- Day, M. O.; Rubidge, B. S. & Abdala, F. 2016. A new mid-Permian burnetiamorph therapsid from the Main Karoo Basin of South Africa and a phylogenetic review of Burnetiamorpha. *Acta Palaeontologica Polonica*, 61, 701–719.
- de Loriol, P. 1880. Monographie des échinides contenus dans les Couches Nummulitiques de l'Égypte. *Memoires de la Societe Physique d' Histoire Naturelle, Geneve*, 27, 59–148.
- Defrance, M. 1825. Nucléolites. Pp. 212–215 in *Dictionnaire des Sciences Naturelles*, tome 35. Levrault, Strasbourg.
- Des Moulins, C. 1835–1837. Études sur les échinides. *Actes de la Société Linnéenne de Bordeaux*, 7/9, 1–518.
- Döderlein, L. 1906. Die Echinoiden der Deutschen Tiefsee-Expedition. Pp. 61–290 in C. Chun (ed) *Wissenschaftliche Ergebnisse der Deutschen Tiefsee-Expedition auf dem Dampfer "Valdivia" 1898–1899*. Gustav Fischer, Jena.
- Donohue, M. J., Doyle, J. A., Gauthier, J., Kluge, A. G. & Rowe, T. 1989. The importance of fossils in phylogeny reconstruction. *Annual review of Ecology and Systematics*, 20, 431–460.
- Donovan, S. K. 2004. Echinoderms of the mid-Cainozoic White Limestone group of Jamaica. *Cainozoic Research*, 3, 143–156.
- d'Orbigny, A. 1853–1860. *Paléontologie française. Description des animaux invertébrés. Terrains Crétacés. Échinoïdes irréguliers*. Vol. 6. G. Masson, Paris, 596 pp.
- Duncan, P. M. & Sladen, W. P. 1882–1886. A description of the fossil Echinoidea of western Sind. *Palaeontologica Indica*, series 14, 1, 1–382.
- Duncan, P. M. 1877. On the Echinodermata of the Australian Cenozoic (Tertiary) deposits. *Quarterly Journal of the Geological Society of London*, 33, 43–73.
- Duncan, P. M. 1889. A revision of the genera and great groups of the Echinoidea. *Journal of the Linnean Society, Zoology*, 23, 1–311.
- Eichwald, E. 1829. *Zoologia specialis quam expositis animalibus tum vivis, tum fossilibus potissimum Rossiae in universum et Poloniae in specie*. Volume 1. J. Zawadzki, Vilnius, 314 pp.
- Erwin, D. H. 1994. The Permo-Triassic extinction. *Nature*, 367, 231–236.
- Erwin, D. H. 2001. Lessons from the past: Biotic recoveries from mass extinctions. *PNAS*, 98, 5399–5403.
- Faulwetter, S., Vasileiadou, A., Kouratoras, M., Dailianis, T. & Arvanitidis, C. 2013. Micro-computed tomography: introducing new dimensions to taxonomy. *ZooKeys*, 263, 1–45.
- Felsenstein, J. 1985. Confidence limits on phylogenies: an approach using the bootstrap. *Evolution*, 39, 783–791.
- Fischer, D. C. 2008. Stratocladistics: integrating temporal data and character data in phylogenetic inference. *Annual Review of Ecology, Evolution, and Systematics*, 39, 365–85.
- Fisher, A. G. 1951. The echinoid fauna of the Inglis member, Moodys Branch formation. *Florida Geological Survey B*, 34, 49–101.
- Foellmi, K. B. & Delamette, M. 1991. Model simulation of Mid-Cretaceous ocean circulation-Technical Comments. *Science*, 251, 94.
- Foote, M. 2000. Origination and extinction components of taxonomic diversity: general problems. *Paleobiology*, 26(sp4), 74–102.

- Fourtau, R. 1899. Révision des échinides fossiles de l'Egypt. *Mémoires de l'Institut Egyptien (Le Caire)*, 3, 605–740.
- Fourtau, R. 1913. *Catalogue des Invertébrés fossiles de l'Egypte représentés dans les collections du Géological Museum au Caire. Terrains Tertiaires, Ière partie. Échinides Eocènes.* Gouv. Egyptien, Adm. Arpentages, Le Caire, 93 pp.
- Fox, D. L.; Fisher, D.C. & Leighton, L. R. 1999. Reconstructing phylogeny with and without temporal data. *Science*, 284, 1816–1819.
- Gauthier, J.; Kluge, A. G. & Rowe, T. 1988. Amniote phylogeny and the importance of fossils. *Cladistics*, 4, 105–209.
- Gauthier, V. 1889. Note sur les échinides crétacés recueillis par M. de Grossouvre. *Bulletin de la Société géologique de France, série 3*, 17, 525–532.
- Gladfelter, W. B. 1978. General ecology of the cassiduloid urchin *Cassidulus caribaeorum*. *Marine Biology*, 47, 149–160.
- Godefroid, S. & Vanderborght, T. 2011. Plant reintroductions: the need for a global database. *Biodiversity Conservation*, 20, 3683–3688.
- Gordon, W. A. 1973. Marine life and ocean surface currents in the Cretaceous. *The Journal of Geology*, 81, 269–284.
- Goubert, M. E. 1859. Quelques mots sur l'étage Eocène Moyen dans le bassin de Paris. *Bulletin de la Société Géologique de France, série 2*, 17, 137–148.
- Gray, J. E. 1851. Description of two new genera and some new species of Scutellidae and Echinolampadidae in the collection of the British Museum. *Proceedings of the Zoological Society, London*, 19, 34–38.
- Gray, J. E. 1855. *Catalogue of the Recent Echinida, or sea eggs, in the collection of the British Museum. Part I – Echinida Irregularia.* Order of the Trustees, London, 69 pp.
- Gregory, J. W. 1890. Some additions to the Australian Tertiary Echinoidea. *Geological Magazine*, 7, 481–492.
- Gregory, J. W. 1892. Further additions to Australian fossil Echinoidea. *Geological Magazine*, 9, 433–438.
- Hagdorn, H. 2018. Slipped through the bottleneck: *Lazarechinus mirabeti* gen. et sp. nov., a Paleozoic-like echinoid from the Triassic Muschelkalk (late Anisian) of East France. *PalZ*, 92, 267–282.
- Haq, B. U., Hardenbol, J. & Vail, P. R. 1987. Chronology of fluctuating sea levels since the Triassic. *Science*, 235, 1156–1167.
- Harzhauser, M., Kroh, A., Mandic, O., Piller, W. E., Gohlich, U., Reuter, M. & Berning, B. 2007. Biogeographic responses to geodynamics: a key study all around the Oligo–Miocene Tethyan Seaway. *Zoologischer Anzeiger*, 246, 241–256.
- Holmes, F. C. 2004. A new Late Eocene cassiduloid (Echinoidea) from Yorke Pensilvania, South Australia. *Memoirs of Museum Victoria*, 61, 209–216.
- Holmes, F.C. 1999. Australian Tertiary Apatopygidae (Echinoidea). *Proceedings of the Royal Society of Victoria*, 111, 51–70.
- Holthuis, L. B. 2002. The Indo-Pacific scyllarine lobsters (Crustacea, Decapoda, Scyllaridae). *Zoosystema*, 24, 499–683.
- Hu, S.X., Zhang, Q.Y., Chen, Z.Q., Zhou, C.Y., Lü, T., Xie, T., Wen, W., Huang, J.Y. and Benton, M.J., 2011. The Luoping biota: exceptional preservation, and new evidence on the Triassic recovery from end-Permian mass extinction. *Proceedings of the Royal Society of London B: Biological Sciences*, 278(1716), 2274–2282.

- Huelsenbeck J. P. 1991. When fossils are better than extant taxa in phylogenetic analysis. *Systematic Zoology*, 40, 458–469.
- Huelsenbeck, J. P. 1994. Comparing the stratigraphic record to estimates of phylogeny. *Paleobiology*, 20, 470–483.
- ICZN. 1999. *International Code of Zoological Nomenclature*. Fourth Edition. The International Trust for Zoological Nomenclature, London, 306 pp.
- Jeannet, A. 1928. Contribution à l'étude des échinides tertiaires de la Trinité et du Venezuela. *Mémoires de la Société Paléontologique Suisse*, 48, 1–49.
- Kellum, L. B. 1926. Paleontology and stratigraphy of the Castle Hayne and Trent Marls in North Carolina. *United States Geological Survey*, 143, 1–41.
- Kew, W. S. W. 1920. Cretaceous and Cenozoic Echinoidea of the Pacific Coast of North America. *University of California Publications in Geological Sciences*, 12, 22–236.
- Kier, P. M. & Lawson, M. H. 1978. Index of living and fossil echinoids 1924–1970. *Smithsonian Contributions to Paleobiology*, 34, 1–182.
- Kier, P. M. 1962. Revision of the cassiduloid echinoids. *Smithsonian Miscellaneous Collections*, 144, 1–262.
- Kier, P. M. 1963. Tertiary echinoids from the Caloosahatchee and Tamiami Formations of Florida. *Smithsonian Miscellaneous Collections*, 145, 1–63.
- Kier, P. M. 1966. Four new Eocene echinoids from Barbados. *Smithsonian Miscellaneous Collections*, 151, 1–28.
- Kier, P. M. 1972. Tertiary and Mesozoic echinoids of Saudi Arabia. *Smithsonian Contributions to Paleobiology*, 10, 1–242.
- Kier, P. M. 1974. Evolutionary trends and their functional significance in the post-Paleozoic echinoids. *Memoir (The Paleontological Society)*, 5, 1–95.
- Kier, P. M. 1975. The echinoids of Carrie Bow Cay, Belize. *Smithsonian Contributions to Zoology*, 206, 1–45.
- Kier, P. M. 1977. The poor fossil record of the regular echinoids. *Paleobiology*, 3(2), 168–174.
- Kier, P. M. 1980. The echinoids of the middle Eocene Warley Hill formation, Santee Limestone and Castle Hayne Limestone of North and South Carolina. *Smithsonian Contributions to Paleobiology*, 39, 1–102.
- Kier, P. M. 1984. Echinoids from the Triassic (St. Cassian) of Italy, their lantern supports, and a revised phylogeny of Triassic echinoids. *Smithsonian Contributions to Paleobiology* 56, 1–41.
- Krau L. 1954. Nova espécie de ouriço do mar: *Cassidulus mitis*, Ordem Cassiduloidea, Echinoidea, capturado na Baía de Sepetiba. *Memórias do Instituto Oswaldo Cruz*, 52, 455–475.
- Kroh, A. & Mooi, R. 2017. World Echinoidea Database at <http://marinespecies.org/Echinoidea/aphia.php?p=taxdetails&id=510501> on 2017-08-19.
- Kroh, A. & Smith, A. B. 2010. The phylogeny and classification of post-Palaeozoic echinoids. *Journal of Systematic Palaeontology*, 8, 147–212.
- Kroh, A. 2010. Index of living and fossil echinoids 1971–2008. *Annalen des Naturhistorischen Museums in Wien, Serie A*, 112, 195–470.
- Lamarck, J. B. P. A. d. M. d. 1801. *Système des animaux sans vertèbres, ou tableau général des classes, des ordres et des genres de ces animaux; présentant leurs caractères essentiels et leur distribution, d'après la considération de leurs rapports naturels et de leur organisation, et suivant l'arrangement établi dans les galeries du Muséum d'hist.*

- naturelle, parmi leurs dépouilles conservées; précédé du discours d'ouverture de cours de zoologie donné dans le Muséum national d'histoire naturelle l'an 8 de la République.* Chez l'auteur & Deterville, Paris, 432 pp.
- Lamarck, J. B. P. A. d. M. d. 1816. *Histoire naturelle des animaux sans vertèbres*. Vol. 3. Verdière, Paris, 586 pp.
- Lamarck, J. B. P. A. d. M. d. 1837. *Histoire naturelle des animaux sans vertèbres*. Volume 1. Meline, Cans et Compagnie, Bruxelles, 670 pp.
- Lamarck, J. B. P. A. d. M. d. 1840. *Histoire naturelle des animaux sans vertèbres*. Volume 3. J.B. Baillière, Paris, 770 pp.
- Lambert, J. & Thiéry, P. 1909–1925. *Essai de nomenclature raisonnée des échinides*. Librairie Septime Ferrière, Chaumont, 607 pp.
- Lambert, J. 1918. Considérations sur la classification des échinides atelostomes. *Mémoires de la Société Académique de l'Aube*, series 3, 82, 9–54.
- Lambert, J. 1929. Sur les Échinides éocènes de Madagascar. *Comptes rendus hebdomadaires des séances de l'Académie des sciences*, 189, 192–194.
- Lambert, J. 1931. Étude sur les échinides fossiles du Nord de l'Afrique. *Mémoires de la Société Géologique de France, Nouvelle Série (Mémoire No. 16)*, 7, 5–108.
- Lambert, J. 1933. Échinides de Madagascar communiqués par M. H. Besairie. *Annales Géologiques du Service des Mines*, 3, 1–49.
- Lambert, J. 1936. Quelques nouveaux échinides fossiles du Crétacé du Mexique. *Bulletin de la Société géologique de France*, 6, 3–6.
- Lambert, J. 1937. Échinides fossiles du Maroc. *Notes et Mémoires du Service des Mines et de la Carte Géologique du Maroc*, 39, 39–109.
- Lamouroux, M. M., Saint-Vincent, B. & Deslongchamps, E. 1824. *Encyclopédie méthodique: histoire naturelle des zoophytes, ou animaux rayonnés*. Volume 2. Chez Mme veuve Agasse, Paris, 819 pp.
- Leonelli, S. & Ankeny, R. A. 2012. Re-thinking organisms: The impact of databases on model organism biology. *Studies in History and Philosophy of Biological and Biomedical Sciences*, 43, 29–36.
- Leske, N. G. 1778. *Iacobi Theodori Klein naturalis dispositio echinodermatum. Accesserunt lucubratiuncula de aculeis echinorum marinorum et spicilegium de belemnitis. Edita et descriptionibus novisque inventis et synonymis auctorem aucta*. Officina Libraria Gleditschiana, Leipzig, 278 pp.
- Lieberman, B. S. 2003. Paleobiogeography: the relevance of fossils to Biogeography. *Annual Reviews of Ecology, Evolution and Systematics*, 34, 51–69.
- Lodeiros, C., Martín, A., Francisco, V., Noriega, N. Díaz, Y., Reyes, J., Aguilera, O. & Alió, J. 2013. Echinoderms from Venezuela: scientific recount, diversity and distribution. Pp. 235–275 in Alvarado, J. J. & Solís-Marín, F. A. (eds) *Echinoderm research and diversity in Latin America*. Springer, Berlin.
- Lovén, S. 1874. Études sur les échinoidées. *Kongelige Svenska Vetenskaps-Akademiens Handlingar*, 11, 1–91, 53 pls.
- Mansfield, W. C. 1932. Pliocene fossils from Limestone in Southern Florida. *Geological Survey Professional Paper*, 170–D, 43–56.
- Marshall, C. R. & Ward, P. D. 1996. Sudden and gradual molluscan extinctions in the latest Cretaceous of Western European Tethys. *Science* 274, 1360–1363.

- McCrary, J. 1859. Remarks on the Eocene Formation in the neighborhood of Alligator, Florida. *Proceedings of the Elliott Society of Natural History (Charleston, South Carolina)*, 1, 282–283.
- McInerney, F. A. & Wing, S. L. 2011. The Paleocene-Eocene Thermal Maximum: A perturbation of carbon cycle, climate, and biosphere with implications for the future. *Annual Review of Earth and Planetary Sciences*, 39, 489–516.
- McKinney, M. L. & Oyen, C. W. 1989. Causation and nonrandomness in biological and geological time series: temperature as a proximal control of extinction and diversity. *Palaios*, 4, 3–15.
- Meunier, S. 1906. Observation sur la Géologie du Sénégal. *Le Naturaliste*, 471, 233–235.
- Mihaljević, M., Klug, C., Aguilera, O., Lüthi, T. & Sánchez-Villagra, M. R. 2010. Paleodiversity of Caribbean echinoids including new material from the Venezuelan Neogene. *Palaeontologia Electronica*, 13, 13.3.20A.
- MNHN. 2017. Muséum national d’Histoire naturelle, Paris (France). Collection: Echinoderms (IE). Specimen MNHN-IE-2013-10590. Accessed at <http://coldb.mnhn.fr/catalognumber/mnhn/ie/2013-10590>.
- Mooi, R. 1990a. A new “living fossil” echinoid (Echinodermata) and the ecology and paleobiology of Caribbean cassiduloids. *Bulletin of Marine Science*, 46, 688–700.
- Mooi, R. 1990b. Living cassiduloids (Echinodermata: Echinoidea): a key and annotated list. *Proceedings of the Biological Society of Washington*, 103, 63–85.
- Mortensen, T. 1948a. *A monograph of the Echinoidea*. IV. 1. Holectypoida, Cassiduloida. C. A. Reitzel, Copenhagen, 371 pp.
- Mortensen, T. 1948b. New Echinoida (Cassiduloida; Clypeasteroida). *Videnskabelige Meddelelser Dansk Naturhistorisk Forening*, 111, 67–72.
- Nelson, G. & Ellis, S. 2018. The history and impact of digitization and digital data mobilization on biodiversity research. *Philosophical Transactions of the Royal Society of London B*, 374, 20170391.
- Néraudeau, D., Mazet, M. & Roman, J. 1997. La faune d’échinides du Lutétien de Cahaignes (Eure, France). *Cossmanniana*, 4, 29–38.
- Nixon, K. C., Carpenter, J. M. 1993. On outgroups. *Cladistics*, 9, 413–426.
- O’Dea, A., Lessios, H.A., Coates, A.G., Eytan, R.I., Restrepo-Moreno, S.A., Cione, A.L., Collins, L.S., Queiroz, A., Farris, D.W., Norris, R.D., Stallard, R.F., Woodburne, M.O., Aguilera, O., Aubry, M.-P., Berggren, W.A., Budd, A.F., Cozzuol, M.A., Coppard, S.E., Duque-Caro, H., Finnegan, S., Gasparini, G.M., Grossman, E.L., Johnson, K.G., Keigwin, L.D., Knowlton, N., Leigh, E.G., Leonard-Pingel, J.S., Marko, P.B., Pyenson, N.D., Rachello-Dolmen, P.G., Soibelzon, E., Soibelzon, L., Todd, J.A., Vermeij & G.J., Jackson, J.B.C. 2016. Formation of the Isthmus of Panama. *Science Advances*, 2, e1600883.
- Okanishi, M., Fujita, T., Maekawa, Y., Sasaki, T. (2017) Non-destructive morphological observations of the fleshy brittle star, *Asteronyx loveni* using micro-computed tomography (Echinodermata, Ophiuroidea, Euryalida). *ZooKeys*, 663, 1–19.
- O’Leary, M. A. & Kaufman, S. G. 2012. *MorphoBank 3.0: Web application for morphological phylogenetics and taxonomy*. Available at: <http://www.morphobank.org>, accessed 30 November 2018.
- Oliveira, J., Manso, C. L. C. & Andrade, E. J. 2013. *Petalobrissus* of the Jandaíra Formation’s Cretaceous. *Brazilian Journal of Geology*, 43, 661–672.



- Osborn, A. S. & Ciampaglio, C. N. 2014. *Rhyncholampas alabamensis* (Twitchell) (Echinoidea, Cassidulidae) from the Late Oligocene (Chattian) Chickasawhay Limestone of Mississippi and Alabama. *Southeastern Geology*, 50, 135–143.
- Osborn, A. S., Mooi, R. & Ciampaglio, C. N. 2016. Additions to the Eocene echinoid fauna of the southeastern United States, including a new genus and species of prenasterid heart urchin. *Southeastern Geology*, 52, 33–59.
- Oyen, C. W. & Portell, R. W. 1996. A new species of *Rhyncholampas* (Echinoidea: Cassidulidae) from the Chipola Formation: the first confirmed member of the genus from the Miocene of the southeastern USA and the Caribbean. *Tulane Studies in Geology and Paleontology*, 29, 59–66.
- Oyen, C. W. & Portell, R. W. 2002. Oligocene and Miocene echinoids. *Florida Fossil Invertebrates*, 2, 1–22.
- Patterson, D. J., Cooper, J., Kirk, P. M., Pyle, R. L. & Remsen, D. P. 2010. Names are key to the big new biology. *Trends in Ecology and Evolution*, 25(12), 686–691.
- Payne, J. L. & Finnegan, S. 2007. The effect of geographic range on extinction risk during background and mass extinction. *PNAS*, 104, 10506–10511.
- Peters, S. E. & McClennen, M. 2016. The Paleobiology Database application programming interface. *Paleobiology*, 42(1), 1–7.
- Philip, G. M. 1963. Two Australian Tertiary neolampadids, and the classification of the cassiduloid echinoids. *Palaeontology*, 6, 106–107.
- Pol, D. & Norell, M. A. 2001. Comments on the Manhattan stratigraphic measure. *Cladistics*, 17, 285–289.
- Poulsen, C. J., Seidov, D., Barronm E. J. & Peterson, W. H. 1998. The impact of paleogeographic evolution on the surface oceanic circulation and the marine environment within the mid-Cretaceous Tethys. *Paleoceanography*, 13, 546–559.
- Prevosti, F. J. & Chemisquy, M. A. 2010. The impact of missing data on real morphological phylogenies: influence of the number and distribution of missing entries. *Cladistics*, 26, 326–339.
- Quental, T. B. & Marshall, C. R. 2010. Diversity dynamics: molecular phylogenies need the fossil record. *Trends in Ecology & Evolution*, 25(8), 434–441.
- Raup, D. M. 1972. Taxonomic diversity during the Phanerozoic. *Science*, 177, 1065–1071.
- Raup, D. M. 1976. Species diversity in the Phanerozoic: an interpretation. *Paleobiology*, 2, 289–297.
- Ree, R. H. & Smith, S. A. 2008. Maximum likelihood inference of geographic range evolution by dispersal, local extinction, and cladogenesis. *Systematic Biology*, 57, 4–14.
- Ree, R. H., Moore, B. R., Webb, C. O. & Donoghue, M. J. 2005. A likelihood framework for inferring the evolution of geographic range on phylogenetic trees. *Evolution*, 59, 2299–2311.
- Reich, M. & Haude, R. 2004. Ophiocistioidea (fossil Echinodermata): an overview. Pp. 489–494 in Heinzeller, T. & Nebelsick, J. H. (eds) *Echinoderms*: München. Taylor & Francis, London.
- Reich, M. The early evolution and diversification of holothurians (Echinozoa). Pp. 55–59 in Harris, L. G., Boetger, S. A., Walker, C. W. & Lesser, M. P. (eds) *Echinoderms*: Durham. Taylor & Francis, London.
- Reyment, R. A. 1980. Biogeography of the Saharan Cretaceous and Paleocene Epicontinental Transgressions. *Cretaceous Research*, 1, 299–327.

- Rodríguez-Barreras, R., Sabat, A. M., Benavides-Serrato, M. & Bontemps, D. R. 2012. A new record for Puerto Rico of the irregular echinoid *Cassidulus caribaeorum*. *Marine Biodiversity Records*, 5, e85.
- Roman, J. & Gorodiski, A. 1959. Échinides Éocènes du Sénégal. *Notes du Service de Géologie et de Prospection Minière*, 3, 1–91.
- Roman, J. & Strougo, A. 1994. Echinoides du Libyen (Eocene Inférieur) d' Egypte. *Revue de Paleobiologie*, 13, 29–57.
- Rowe, T. 1988. Definition, diagnosis and origin of Mammalia. *Journal of Vertebrate Paleontology*, 8, 241–264.
- Ruta, M., Wagner, P. J. & Coates, M. I. 2006. Evolutionary patterns in early tetrapods. I. Rapid initial diversification followed by decrease in rates of character change. *Proceedings of the Royal Society B*, 273, 2107–2111.
- Samyn, Y., Smirnov, A. & Massin, C. 2013. Carl Gottfried Semper (1832–1893) and the location of his type specimens of sea cucumbers. *Archives of Natural History*, 40(2), 324–339.
- Sánchez Roig, M. 1926. Contribucion a la Paleontologia Cubana: Los equinodermos fosiles de Cuba. *Boletin de Minas*, 10, 1–179.
- Sánchez Roig, M. 1949. Los equinodermos fosiles de Cuba. *Paleontologia Cubana*, 1, 1–330.
- Sánchez Roig, M. 1952. Nuevos generos y especies de equinodermos fosiles cubanos. *Memorias de la Sociedad Cubana de Historia Natural "Felipe Poey"*, 21, 1–61.
- Santolaya, J. M. & Sillero, C. 1994. Guía ilustrada de los equinoideos fósiles de la Provincia de Alicante (I). *Cidaris*, 3/5, 4–43.
- Saucède, T. & Néraudeau, D. 2006. An "Elvis" echinoid, *Nucleopygus (Jolyclypus) jolyi*, from the Cenomanian of France: phylogenetic analysis, sexual dimorphism and neotype designation. *Cretaceous Research*, 27, 542–554.
- Saucède, T., Mooi, R. & David, B. 2003. Combining embryology and paleontology: origins of the anterior-posterior axis in echinoids. *Comptes Rendus Palevol*, 2, 399–412.
- Schindelin, J., Arganda-Carreras, I., Frise, E., Kaynig, V., Longair, M., Pietzsch, T., Preibisch, S., Rueden, C., Saalfeld, S., Schmid, B., Tinevez, J. -Y., White, D. J., Hartenstein, V., Eliceiri, K., Tomancak, P. & Cardona, A. 2012. Fiji: an open-source platform for biological-image analysis. *Nature Methods*, 9(7), 676–682.
- Scotese C. R. 1997. *Continental Drift flip book*. 7<sup>th</sup> edition. Paleomap project. University of Texas, Arlington.
- Sepkoski, J. J. 1981. A factor analytic description of the Phanerozoic marine fossil record. *Paleobiology*, 7, 36–53.
- Sepkoski, J. J., Bambach, R. K., Raup, D. M. & Valentine, J. W. 1981. Phanerozoic marine diversity and the fossil record. *Nature*, 293, 435–437.
- Siddall, M. E. 1998. Stratigraphic fit to phylogenies: a proposed solution. *Cladistics*, 14, 201–208.
- Signor, P. W. 1978. Species richness in the Phanerozoic: an investigation of sampling effects. *Paleobiology*, 4, 394–406.
- Smiser, J. S. 1935. A monograph of the Belgian Cretaceous Echinoids. *Mémoires du Musée Royal d'Histoire Naturelle de Belgique*, 68, 1–98.
- Smith, A. B. 1994. *Systematics and the Fossil Record*. Blackwell Scientific, London, 223 pp.
- Smith, A. B. 1995. Late Campanian-Maastrichtian echinoids from the United Arab Emirates-Oman border region. *Bulletin of the Natural History Museum, London (Geology)*, 51, 121–240.

- Smith, A. B. 2000. Stratigraphy in phylogeny reconstruction. *Journal of Paleontology*, 74, 763–766.
- Smith, A. B. 2001. Large-scale heterogeneity of the fossil record: implications for Phanerozoic biodiversity studies. *Philosophical Transactions of the Royal Society of London B*, 356, 351–367.
- Smith, A. B. 2001. Probing the cassiduloid origins of clypeasteroid echinoids using stratigraphically restricted parsimony analysis. *Paleobiology*, 27, 392–404.
- Smith, A. B. 2005. Growth and form in echinoids: the evolutionary interplay of plate accretion and plate addition. Pp. 181–195 in: Briggs, D. E. G. (ed) *Evolving form and function: fossils and development*. Yale University Press, New Haven, CT.
- Smith, A. B. 2007. Intrinsic versus extrinsic biases in the fossil record: contrasting the fossil record of echinoids in the Triassic and early Jurassic using sampling data, phylogenetic analysis, and molecular clocks. *Paleobiology*, 33(2), 310–323.
- Smith, A. B. & Jeffery, C. H. 1998. Selectivity of extinction among sea urchins at the end of the Cretaceous period. *Nature*, 392, 69–71.
- Smith, A. B. & Jeffery, C. H. 2000. Maastrichtian and Paleocene echinoids: a key to world faunas. *Special Papers Palaeontology*, 63, 1–406.
- Smith, A. B. & Kroh, A. (eds) 2011. The Echinoid Directory. World Wide Web electronic publication. <http://www.nhm.ac.uk/research-curation/projects/echinoid-directory> [accessed from 1 October to 15 November 2018].
- Smith, A. B. & McGowan, A. J. 2007. The shape of the Phanerozoic marine palaeodiversity curve: how much can be predicted from the sedimentary rock record of Western Europe? *Palaeontology*, 50(4), 765–774.
- Smith, A. B., Pisani, D., Mackenzie-Dodds, J. A., Stockley, B., Webster, B. L. & Littlewood, D. T. J. 2006. Testing the molecular clock: molecular and paleontological estimates of divergence times in the Echinoidea (Echinodermata). *Molecular biology and evolution*, 23(10), 1832–1851.
- Smith, A. B. & Reich, M. 2013. Tracing the evolution of the holothurian body plan through stem-group fossils. *Biological Journal of the Linnean Society*, 109, 670–681.
- Smith, A. B. & Wright, C. W. 2000. British Cretaceous echinoids. Part 6, Neognathostomata (Cassiduloids). *Monographs of the Palaeontographical Society*, 154, 391–429.
- Souto, C., Manso, C. L. C. & Martins, L. 2011a. Rediscovery and redescription of *Cassidulus infidus* (Echinoidea: Cassidulidae) from Northeastern Brazil. *Zootaxa*, 3095, 39–48.
- Souto, C. & Martins, L. 2018. Synchrotron micro-CT scanning leads to the discovery of a new genus of morphologically conserved echinoid (Echinodermata: Cassiduloida). *Zootaxa*, 4457, 70–92.
- Souto, C., Martins, L. & Menegola, C. 2011b. A perplexing genus *Cassidulus* Lamarck: what's in it? *Gulf of Mexico Science Journal*, 29, 155.
- Sprinkle, J. 1983. Patterns and problems in echinoderm evolution. Pp. 1–18 in: Jangoux, M. & Lawrence, J. M. (eds) *Echinoderm Studies I*. A.A. Balkema, Rotterdam.
- Squires, R. L. & Demetron, R. A. 1995. A new genus of cassiduloid echinoid from the Lower Eocene of the Pacific Coast of Western North America and a new report of *Cassidulus ellipticus* Kew, 1920, from the Lower Eocene of Baja California Sur, Mexico. *Journal of Paleontology*, 69, 509–515.

- Srivastava, D. K., Singh, A. P., Tiwari, R. P. & Jauhri, A. K. 2008. Cassiduloids (Echinoidea) from the Siju Formation (late Lutetian–early Bartonian) of the South Garo Hills, Meghalaya, India. *Revue de Paléobiologie, Genève*, 27, 511–523.
- Stille, P., Steinmann, M. & Riggs, S. R. 1996. Nd isotope evidence for the evolution of the paleocurrents in the Atlantic and Tethys Oceans during the past 180 Ma. *Earth and Planetary Science Letters*, 144, 9–19.
- Stock, S. R. 2009. *MicroComputed Tomography: methodology and applications*. CRC Press, Boca Raton, FL, 331 pp.
- Sullivan, J. 2007. *Australanthus florescens* (Gregory, 1892). In: Smith, A.B. & Kroh, A. (eds), *The Echinoid Directory*. Available at: <http://www.nhm.ac.uk/our-science/data/echinoid-directory/taxa/taxon.jsp?id=1875>.
- Sumrall, C. D. & Brochu, C. A. 2003. Resolution, sampling, higher taxa and assumptions in stratocladistic analysis. *Journal of Paleontology*, 77, 189–194.
- Suter, S. J. 1988. The decline of the cassiduloids: merely bad luck? Pp. 91–95 in R. D. Burke, P. V. Mladenov, P. Lambert & R. L. Parsley (eds) *Echinoderm biology*. Balkema, Rotterdam.
- Suter, S. J. 1994a. Cladistic analysis of cassiduloid echinoids: trying to see the phylogeny for the trees. *Biological Journal of the Linnean Society*, 52, 31–72.
- Suter, S. J. 1994b. Cladistic analysis of the living cassiduloids (Echinoidea), and the effects of character ordering and successive approximations weighting. *Zoological Journal of the Linnean Society*, 112, 363–387.
- Swofford, D. L. 2003. PAUP\*. Phylogenetic Analysis Using Parsimony (\*and Other Methods). Version 4.0a163. Sinauer Associates, Sunderland, Massachusetts.
- Tawadros, E. E. 2012. *Geology of North Africa*. CRC Press, Balkema, Leiden, 931 pp.
- Telford, M. & Mooi, R. 1996. Podial particle picking in *Cassidulus caribaeorum* (Echinodermata: Echinoidea) and the phylogeny of sea urchin feeding mechanisms. *Biological Bulletin*, 191, 209–223.
- Thompson, J. R., Hu, S.-x., Zhang, Q.-Y., Petsios, E., Cotton, L. J., Huang, J.-Y., Zhou, C.-y., Wen, W., Bottjer, D. J. 2018. A new stem group echinoid from the Triassic of China leads to a revised macroevolutionary history of echinoids during the end-Permian mass extinction. *Royal Society Open Science*, 5, 171548.
- Thompson, J. R. & Ausich, W. I. 2016. Facies distribution and taphonomy of echinoids from the Fort Payne Formation (late Osagean, early Viséan, Mississippian) of Kentucky. *Journal of Paleontology*, 90(2), 239–249.
- Tzompantzi, D. B., Solís-Marín, F. A., Laguarda-Figueras, A., Abreu-Pérez, M. & Durán-González, A. 1999. Echinoids (Echinodermata: Echinoidea) from the Mexican Caribbean: Puerto Morelos, Quintana Roo, Mexico. *Avicennia*, 10/11, 43–72.
- Vadon, C., De Ridder, C., Guille, A. & Jangoux, M. (1984) Les types d'échinides actuels (échinodermes) du Muséum National d'Histoire Naturelle de Paris. *Bulletin du Muséum National d'Histoire Naturelle*, 6(4), 1–38.
- van Hinsbergen D. J. J., de Groot, L. V., van Schaik, S. J., Spakman, W., Bijl, P. K., Sluijs, A., Langereis, C. J. & Brinkhuis, H. 2015. Paleolatitude calculator for paleoclimate studies. *PLoS ONE*, 10, e0126946.
- Vermeij, G. J. 1977. The Mesozoic marine revolution: evidence from snails, predators and grazers. *Paleobiology*, 3, 245–258.

- von Martens, E. 1865. Über neue ostasiatische Echiniden. *Monatsberichte der Königlichen Preussische Akademie des Wissenschaften zu Berlin*, 140–144.
- Wagner, P. J. 2000. Exhaustion of morphologic character states among fossil taxa. *Evolution*, 54, 365–386.
- Wall, P. D., Ivany, L. C. & Wilkinson, B. H. 2009. Revisiting Raup: exploring the influence of outcrop area on diversity in light of modern sample-standardization techniques. *Paleobiology*, 35, 146–167.
- Weisbord, N. E. 1934. Some Cretaceous and Tertiary echinoids from Cuba. *Bulletins of American Paleontology*, 20, 1–84.
- Wiens, J. J. 2003. Missing data, incomplete taxa, and phylogenetic accuracy. *Systematic Biology*, 52, 528–538.
- Wilkinson, M., Suter, S. J. & Shires, V. L. 1996. The Reduced Cladistic Consensus method and cassiduloid echinoid phylogeny. *Historical Biology*, 12, 63–73.
- Willis, K. J. & MacDonald, G. M. 2011. Long-term ecological records and their relevance to climate change predictions for a warmer world. *Annual Review of Ecology, Evolution and Systematics*, 42, 267–287.
- Wills, M. A. 1999. Congruence between stratigraphy and phylogeny: randomization tests and the gap excess ratio. *Systematic Biology*, 48, 559–580.
- Wills, M. A., Barrett, P. M. & Heathcote, J. F. 2008. The modified gap excess ratio (GER\*) and the stratigraphic congruence of dinosaur phylogenies. *Systematic Biology*, 57, 891–904.
- Winterer, E. L. 1991. The Tethyan Pacific during Late Jurassic and Cretaceous times. *Palaeogeography, Palaeoclimatology, Palaeoecology*, 87, 253–265.
- WoRMS. 2018a. *Echinoidea*. Accessed at: <http://www.marinespecies.org/aphia.php?p=taxdetails&id=123082> on 2018-11-15.
- WoRMS. 2018b. *Neognathostomata*. Accessed at: <http://www.marinespecies.org/aphia.php?p=taxdetails&id=510501>, accessed 23 September 2018.
- Young, C. M.; Sewell, M. A.; Tyler, P. A. & Metaxas, A. 1997. Biogeographic and bathymetric ranges of Atlantic deep-sea echinoderms and ascidians: the role of larval dispersal. *Biodiversity and Conservation*, 6, 15071–522.
- Yu, Y., Harris, A. J., Blair, C., He, X. J. 2015. RASP (Reconstruct Ancestral State in Phylogenies): a tool for historical biogeography. *Molecular Phylogenetics and Evolution*, 87, 46–49.
- Zachos, J., Pagani, M., Sloan, L., Thomas, E. & Billups, K. 2001. Trends, rhythms, and aberrations in global climate 65 Ma to present. *Science*, 292, 686–693.
- Zamora, S., Rahman, I. A. & Ausich, W. I. 2015. Palaeogeographic implications of a new iocrinid crinoid (Disparida) from the Ordovician (Darriwillian) of Morocco. *PeerJ*, 3, e1450.
- Ziegler, A. & Menze, B. H. 2014. Accelerated acquisition, visualization, and analysis of zoo-anatomical data. In: Zander, J. & Mosterman, P. J. (eds), *Computation for humanity: information technology to advance society*. CRC Press, Boca Raton, FL, pp. 235–263.
- Ziegler, A. 2012. Broad application of non-invasive imaging techniques to echinoids and other echinoderm taxa. *Zoosymposia*, 7, 53–70.
- Ziegler, A., Faber, C., Mueller, S. & Bartolomaeus, T. (2008) Systematic comparison and reconstruction of sea urchin (Echinoidea) internal anatomy: a novel approach using magnetic resonance imaging. *BMC Biology*, 6, 33.

Ziegler, A., Mooi, R., Rolet, G. & De Ridder, C. 2010. Origin and evolutionary plasticity of the gastric caecum in sea urchins (Echinodermata: Echinoidea). *BMC Evolutionary Biology*, 10, 313.

## Appendices

**Appendix 2.1.** Material examined. Arranged in alphabetical order and using nomenclature prior to the analyses performed herein. C, cotype; H, holotype; N, neotype; P, paratype; S, syntype. Genus and family classification following WoRMS (2018b).

**FAMILY APATOPYGIDAE Kier.** *Apatopygus recens*: AM G.2029, J.7107; NMNH E11084, E14626, E16325, E36767; Baker (1983). *Nucleolites scutatus*: CASG 66723, 67305, 67308, 67542; MNHN B49337 (S); NMNH 19546A; Kier (1962).

### ORDER CASSIDULOIDA CLAUS

**Family Cassidulidae Agassiz and Desor.** *Cassidulus briareus*: MP 1267 Holotype MNHWU (H), MP 1267 Paratype MNHWU (P); Souto & Martins (2018). *Cassidulus californicus*: UCMP 11348 (N), NMNH 165664. *Cassidulus caribaeorum*: CASIZ 112632, 112633, 112637, 112638, 112683, 222205 (N), NHMUK 87.6.27.7, NMNH E13755, E36150, UF 11786–11788, 11797–11798, 11825–11826, 11892, 11933; Mortensen (1948a), Kier (1962). *Cassidulus ellipticus*: UCMP 11346 (C), 11347 (C); Squires & Demettrion (1995). *Cassidulus falconensis*: NMB M589/2 (H); NMNH 629295, 638635; UCMP 123469–123470. *Cassidulus infidus*: SMNH-type-4859 (H); UFBA 314, 757; UFSITAB-ECH 123; Souto *et al.* (2011a). *Cassidulus kieri*: NMNH 174760–174762 (P). *Cassidulus mitis*: CASIZ 116110; MNRJ 3673, 3674; UFBA 756; ZUEC 11–12; Krau (1954). *Cassidulus trojanus*: CASG (not deposited); UF 3353, 41273, 47041, 48497, 66560; NMNH 498996 (H).

*Eurhodia australiae*: MV P146332, P146359, P146368, P317347; UCMP 318981. *Eurhodia baumi*: CASG 71844; NMNH 264043 (H). *Eurhodia calderi*: NHMUK EE1300 (H); UCMP 123431, 318982–318985; Duncan & Sladen (1882–1886). *Eurhodia cravenensis*: NMNH 353256 (H). *Eurhodia holmesii*: CASG 67852, 68450; UCMP 123468; LACMIP (not deposited); NMNH 264048–264049, 264592, 562303. *Eurhodia matleyi*: NHMUK EE5193, E17666 (H); NMNH Acc. 268939, 444301; NMNH 461428. *Eurhodia morrisi*: NHMUK E42344–E42345 (S), E741a; CASG 33195.1; UCMP 318986–318987; Duncan & Sladen (1882–1886); Kier (1962). *Eurhodia navillei*: MHNG GEPI 26743 (H); MNHN R66902, R66907–R66908. *Eurhodia patelliformis*: CASG 71847; MCZ 102066 (H), 102067–102069, IPEC-3868; UF 4932, 41265; NMNH 498988, 562299. *Eurhodia relictata*: NMNH E20480 (H), E12971 (P); Mooi (1990a). *Eurhodia rugosa*: CASG 67850, 68447, 68449, 71849; UCMP 318994–318995; NMNH 562300 (N), 461473, 264004–264005; Kier (1962). *Eurhodia thebensis*: MNHN R62170 (S).

(H). *Glossaster sorigneti*: MNHN R62478 (type). *Glossaster vasseuri*: MNHN J00620 (S). *Glossaster welschi*: MNHN J00696 (S).

*Paralampas pileus*: UCMP 318990–318991; Duncan & Sladen (1882–1886). *Paralampas rancureli*: MNHN R06427 (H).

*Rhyncholampas alabamensis*: NMNH 559493 (H); Osborn & Ciampaglio (2014). *Rhyncholampas anceps*: MNHN J01155 (S). *Rhyncholampas ayresi*: UF 62977, 63062, 185774; NMNH 648160 (H), 648161 (P), 460584. *Rhyncholampas carolinensis*: UF 230496; NMNH 264052, 599488 (H), 460867. *Rhyncholampas chipolanus*: UF 66633, 215089–215090, 235966; Oyen & Portell (1996). *Rhyncholampas conradi*: UF 117494, 278684, 278699, 278670, 278703; NMNH 460607, 562304. *Rhyncholampas daradensis* (?): MNHN R06029. *Rhyncholampas ericsoni*: UF 245016, 247899 (H), 247901–247902 (P); NMNH 560420–560421 (P).

*Rhyncholampas evergladensis*: UCMP 123435; UF 6069, 24524, 232256; NMNH 371329 (C), 371330 (P), 460887, 460891, 460893, 460896; 648147–648148. *Rhyncholampas globosus*: UF 12841, 115769, 165741, 245019, 248491 (H), 248492 (P), 252636, 252637 (P); NMNH 562307. *Rhyncholampas gouldii*: CASG 67775, 67903; UCMP 318989, 318992–318993; UF 5782, 67813, 156318. *Rhyncholampas grignonensis*: NMNH 633997. *Rhyncholampas mexicanus*: UCMP 11357 (H), 123471. *Rhyncholampas pacificus*: CASIZ 90704, 90706–90707, 90709, 106651, 106653; LACM E.1939-19.10, 1939-291.1; MCZ ECH-2714 (S), 2719 (S); MNHN-IE-2013-10554–2013-10556 (S); ZMB 2118; Mortensen (1948a). *Rhyncholampas riveroi*: UF 216884. *Rhyncholampas rodriguezii*: MNHN A22036 [*R. rodriguezii\_A*]; R66851[*R. rodriguezii\_R*]; UF 216778 [*R. rodriguezii\_R*]. *Rhyncholampas sabistonensis*: UF cat n. 2134, Acc no. 56; NMNH 562301. *Rhyncholampas tuderii*: MNHN A22037, R10086 (S).

**Family Neolampadidae Lambert.** *Neolampas rostellata*: NMNH 6790, E20529, E36132; ZMA.V.ECH.5461; ZMB 5847, 7249; Döderlein (1906), Mortensen (1948a).

*Studeria recens*: NHMUK 81.11.22.38 (C), 1949.2.4.61 (possibly C previously registered as NHMUK 87.11.22.38).

**Family Pliolampadidae Kier.** *Pliolampas elegantula*: MNHN R66890.

## ORDER CLYPEASTEROIDA Agassiz

**Family Faujasiidae Lambert.** *Australanthus longianus*: MV P19225, 19229, 20197, 146451ç146462, 146827; NHMUK E42428 (S); UCMP 318988; NMNH 96252, 460548.

*Faujasia apicalis*: CASG (not deposited); NMNH 131272, 460541; ZMA.ECH.E.7970. *Eurypetalum rancheriana*: UCMP 31218–31219 (P).

*Hardouinia mortonis*: CASG (not deposited); NMNH 464507, 464517, 464521, 464528; UCMP 123467. *Hardouinia bassleri*: NMNH 464461, 479787–479788, 979788.

*Petalobrissus cubensis*: CASG (not deposited); NMNH 131265, 131265A. *Petalobrissus setifensis*: NMNH 131261; Kier (1962).

*Procassidulus lapiscancri*: NMNH 131260, 131263, 460563–460564; UCMP 123466; ZMA.ECH.E.8178, 8180, 8184, 8185, 8874.

*Rhynchopygus arumaensis*: NMNH I170452 (H), I170453. *Rhynchopygus macari*: NMNH 461190. *Rhynchopygus marmini*: NMNH 131267.

*Stigmatopygus pulchellus*: NHMUK EE4314 (H) and EE4314 (P); NHMW 2015/0525/0001–2015/0525/0002.

## ORDER ECHINOLAMPADOIDA Kroh & Smith

**Family Echinolampadidae Gray.** *Echinolampas depressa*: CASIZ 174963; NHMUK 1892.2.25.23; NMNH E15144, E15565, E28085, E29737, E32937, E41070; UF 1246, 9027.

## INCERTAE SEDIS

*Kassandrina floescens*: CASG 71853; LACMIP 42070.1; MV P82080; NHMUK E3772–3773 (S). *Kassandrina malayana*: AM J.24441; ZMUC 236 (S), ZMUC 521 (S); Mortensen (1948a), Souto & Martins (2018).

*Oligopodia epigonus*: CASIZ 76289, 188760; UF 2490, 4662; ZMB 1433 (H); Mortensen (1948a). *Oligopodia tapeina*: MCZ 102037 (H).



**Appendix 2.2** Data matrix of 66 taxa and 98 characters. Partial uncertainty coded within curly brackets and polymorphism within brackets. Missing data indicated by “?” and inapplicability by “-”. Species nomenclature follows works prior to this analysis. Numbers in bold on top of column indicate the character in each block. NEXUS format available in MorphoBank (O’Leary & Kaufman 2012), project P3287.

	<b>1-5</b>	<b>6-10</b>	<b>11-15</b>	<b>16-20</b>	<b>21-25</b>	<b>26-30</b>	<b>31-35</b>	<b>36-40</b>	<b>41-45</b>
[Outgroups rooting the trees]									
<i>N. scutatus</i>	00000	00102	00 (01)00	00000	?0101	00000	0000 (01)	00000	00000
<i>A. recens</i>	11000	00002	01000	10010	00100	00002	00000	20000	00000
<i>E. depressa</i>	11110	10101	01200	00010	02113	20011	10121	20020	10020
[Additional outgroups]									
<i>F. apicalis</i>	01011	00200	01200	00010	22104	01000	12021	20220	10020
<i>F. rancheriana</i>	11000	00102	00100	00020	22104	01000	03021	00020	10020
<i>H. bassleri</i>	01001	01102	00{01}00	01000	22004	01000	??:121	(01)1210	00010
<i>H. mortonis</i>	01001	01102	00100	01010	22104	01000	03021	01010	00010
<i>A. longianus</i>	01010	00102	01 (12)00	00000	01002	00000	02120	20200	00000
<i>K. florescens</i>	10000	00102	01100	00000	01002	00001	01020	20200	00000
<i>K. malayana</i>	10000	00102	01100	00100	01002	00001	11020	20200	00000
<i>N. rostellata</i>	11110	10112	11010	101--	-----	-0----	1-010	21010	00000
<i>O. epigonus</i>	11010	10012	01000	10100	01103	00002	00010	21010	01000
<i>P. cubensis</i>	11000	00102	00200	00000	12103	01101	01010	01000	00000
<i>P. elegantula</i>	11110	10011	01110	10010	01000	00001	01?00	01010	10000
<i>P. lapiscancrri</i>	11000	00002	00 (01)01	00021	12104	01001	02020	20010	00010
<i>P. setifensis</i>	11000	00112	00{12}00	00000	02104	01001	00020	01010	00000
<i>R. arumaensis</i>	10000	00002	00 (12)00	00000	01103	01001	01010	01000	0??:00
<i>R. macari</i>	11000	00002	00101	00021	12104	01001	??:020	11010	0?:120
<i>R. marmini</i>	10000	00002	00100	00020	01{01}03	00002	01010	21011	0?:120
<i>S. pulchellus</i>	11000	00112	00 (12)00	00020	22204	01111	??:010	20010	0?:101
<i>S. recens</i>	11110	10112	11110	10020	01000	00001	12020	21110	00000
[Ingroup species]									
<i>C. briareus</i>	10010	00102	01000	000?0	02103	10011	11010	20011	10020
<i>C. californicus</i>	11000	00102	01100	00?:10	{01}2100	10011	??:010	21011	10020
<i>C. caribaeorum</i>	11000	00102	01000	00010	02103	10011	01010	20011	10020
<i>C. ellipticus</i>	21000	00{01}02	01{01}00	00000	11104	01001	??:?10	01010	0?:120
<i>C. falconensis</i>	11001	00102	01200	00010	12204	11011	02020	20111	10020
<i>C. infidus</i>	10010	00102	01000	00010	02103	10012	11010	20011	10020
<i>C. kieri</i>	11010	10112	01200	00010	02103	01001	00010	21010	10000
<i>C. mitis</i>	11010	00102	01000	00000	02203	10011	11010	20011	10020
<i>C. trojanus</i>	11000	00102	01100	00010	12103	11011	02110	00011	10020

Appendix 2.2. Continued.

	1-5	6-10	11-15	16-20	21-25	26-30	31-35	36-40	41-45
<i>E. australiae</i>	21100	00002	01100	00000	01002	01001	11010	11210	01100
<i>E. baumi</i>	11000	00102	01200	00010	11104	01000	12010	01010	0?120
<i>E. calderi</i>	11000	00102	01200	000(12)0	(01)1004	01101	02110	01210	0?120
<i>E. cravenensis</i>	11110	00112	01100	00010	12103	0100(12)	11010	01010	0?120
<i>E. holmesi</i>	11(01)10	00112	01100	00010	02104	01001	11010	01010	0?120
<i>E. matleyi</i>	11010	0?102	01200	00010	12104	01101	03110	00210	0?120
<i>E. morrissi</i>	21110	10011	01200	00000	01104	01100	11120	(12)0011	0?120
<i>E. navillei</i>	11000	00102	01200	00010	(12)210{34}	0110{01}	13110	00010	0?120
<i>E. patelliformis</i>	21100	00101	01(01)00	000(02)0	(01)2104	01001	01010	01210	0?120
<i>E. relicta</i>	01010	00012	01000	00110	02003	0100(12)	11010	01010	01120
<i>E. rugosa</i>	20000	00002	01200	00010	01104	01001	11010	01010	00120
<i>E. thebensis</i>	20000	00102	01?00	00?10	1210{34}	01?00	1?1?1?	00010	0?120
<i>G. sorigneti</i>	20000	00102	01200	00?20	0100{34}	01001	11?10	01000	0?001
<i>G. vasseuri</i>	20000	00102	01200	00020	1110{23}	01000	01010	20000	0?001
<i>G. welschi</i>	11000	0?102	0?200	??020	12104	01100	03?21	20000	0?001
<i>P. pileus</i>	11000	00102	01100	00010	12103	01001	10020	21010	10010
<i>P. rancureli</i>	11000	00112	01100	00000	12103	01001	00020	2101?	10010
<i>R. alabamensis</i>	01001	00102	01100	01010	{12}2104	11010	02010	10011	10020
<i>R. anceps</i>	11000	00102	01100	00010	02103	10011	??010	2?011	10020
<i>R. ayresi</i>	11010	10110	01100	01010	(12)2204	11011	03?10	00111	10020
<i>R. carolinensis</i>	11010	10111	01100	00010	(01)2103	11011	02010	00011	10020
<i>R. chipolanus</i>	01010	00102	01100	01010	22204	11011	0??20	10011	10020
<i>R. conradi</i>	11110	10011	01200	00010	02113	11011	12?11	20011	10020
<i>R. daradensis</i>	11000	10012	01200	00010	12104	01011	10010	11011	10020
<i>R. ericsoni</i>	01011	00200	01100	010?0	12204	11011	02?10	(12)0011	10020
<i>R. evergladensis</i>	11000	00102	01000	01010	(12)2204	11010	03010	10111	10020
<i>R. globosus</i>	01011	00210	01100	01010	12204	1101?	02110	00011	10020
<i>R. gouldii</i>	01011	00(12)00	01100	00010	(01)2204	11011	02?10	(01)0111	10020
<i>R. grignonensis</i>	11010	00112	01000	00010	02103	11011	00010	10011	00020
<i>R. mexicanus</i>	11000	01102	01200	00010	22204	11010	03?20	10111	10020
<i>R. pacificus</i>	11000	00102	01(12)00	00010	1220(34)	11010	02110	20111	10020
<i>R. riveroi</i>	11000	00102	01{01}00	0?020	?2204	11010	0??10	00111	10020
<i>R. rodriguezii_A</i>	01011	00210	01000	00010	12103	11011	03110	10111	10020
<i>R. rodriguezii_R</i>	11011	00110	01100	00010	02103	11011	0?110	(01)0011	10020
<i>R. sabistonensis</i>	11000	00102	01100	01000	{12}2204	11010	03?10	00111	10020
<i>R. tuderii</i>	11000	00112	01200	00010	1210{34}	?0011	00020	20?10	10020

**Appendix 2.2. Continued.**

	46-50	51-55	56-60	61-65	66-70	71-75	76-80	81-85	86-90	91-95	96-98
[Outgroups rooting the trees]											
<i>N. scutatus</i>	??003	10-00	00000	00000	00000	00010	-0000	00000	01000	?000?	???
<i>A. recens</i>	00000	10-00	00010	00000	00110	00010	00000	00000	11000	00010	100
<i>E. depressa</i>	21-53	11000	00010	00000	01000	00012	00001	00010	01000	00012	000
[Additional outgroups]											
<i>F. apicalis</i>	??-66	02110	00200	01001	10101	11101	11211	21201	20100	1111?	???
<i>F. rancheriana</i>	??-53	02110	01100	??010	00000	11002	11122	01000	20100	0211?	???
<i>H. bassleri</i>	?-2023	?-2023	0?200	01001	10110	21102	01121	01100	20100	02???	???
<i>H. mortonis</i>	?-2033	02110	02100	01001	10110	11101	11202	01201	10001	0211?	???
<i>A. longianus</i>	?-2021	02100	12100	01?01	01111	11102	11201	31200	00101	0211?	???
<i>K. florescens</i>	?-2022	02102	12000	11010	01000	01002	01211	31200	10?00	?211?	???
<i>K. malayana</i>	00031	02101	12000	01010	01000	01002	01211	31200	10?00	02111	000
<i>N. rostellata</i>	0015(34)	00-00	00210	01000	10101	01102	01201	31200	10000	12000	110
<i>O. epigonus</i>	00043	10-02	00210	00000	00001	00002	01001	21200	01000	12000	100
<i>P. cubensis</i>	?-2012	12100	02000	10100	01110	01002	01221	01000	21000	0211?	???
<i>P. elegantula</i>	?-20153	11000	00200	00000	10101	00002	01011	31200	11000	1101?	???
<i>P. lapiscancrini</i>	?-2013(56)	02101	122(01)0	10001	101?1	11101	11201	11200	20000	1211?	???
<i>P. setifensis</i>	?-2062	0210?	02000	?0100	01110	01002	01121	01000	21000	0?11?	???
<i>R. arumaensis</i>	?-2033	12000	02100	00000	00110	00002	01221	11100	21000	1201?	???
<i>R. macari</i>	?-201{123}{34}	02101	12210	??001	10111	?1002	11221	11200	1?00?	?211?	???
<i>R. marmini</i>	?-20133	02100	02210	??001	10111	11101	11201	31201	20?00	02?1?	???
<i>S. pulchellus</i>	?-20{34}2	02110	02200	01001	01101	11101	11202	11101	10101	0211?	???
<i>S. recens</i>	?-2055	10-00	00200	01010	10110	01002	01211	21200	21000	1200?	???
[Ingroup species]											
<i>C. briareus</i>	11134	02102	02000	10100	01000	01002	01201	11210	00010	1211?	?1?
<i>C. californicus</i>	?-201?4	02102	02000	?0000	0100?	01002	012{01}1	11200	?00?0	1211?	???
<i>C. caribaeorum</i>	1114(12)	02102	02000	10000	01000	01002	01201	21200	00010	12111	010
<i>C. ellipticus</i>	?-20133	02102	12200	??010	101?0	01002	012?1	11{12}?0	?0000	?211?	???
<i>C. falconensis</i>	?-20133	02101	02000	1?110	01000	01002	01211	01110	10010	0211?	???
<i>C. infidus</i>	11133	02102	02000	10000	01000	01002	01201	11200	00010	11111	011
<i>C. kieri</i>	?-2033	02001	02000	00000	01000	00002	01021	11100	10000	1101?	???
<i>C. mitis</i>	11133	02101	02000	10100	01000	01002	01201	11210	00010	02111	011
<i>C. trojanus</i>	?-20123	02102	12000	1?100	01000	01002	01211	11100	100?0	0211?	???
<i>E. australiae</i>	?-2041	02102	12200	??010	10110	01002	01211	11100	10100	0211?	???
<i>E. baumi</i>	?-20132	02102	12200	??010	10110	01002	01121	11100	20000	0211?	???
<i>E. calderi</i>	?-2024	02102	12200	01010	10110	01002	01121	01000	20100	0211?	???
<i>E. cravenensis</i>	?-20{23}4	02101	12200	??010	101?1	01002	01121	01100	20000	0211?	???
<i>E. holmesi</i>	?-2046	02101	12200	01010	10111	01002	01121	11100	20000	0211?	???

Appendix 2.2. Continued.

	46-50	51-55	56-60	61-65	66-70	71-75	76-80	81-85	86-90	91-95	96-98
<i>E. matleyi</i>	??023	02100	02200	?1010	10111	01002	01121	01000	20100	0211?	???
<i>E. morrisi</i>	??133	02101	02200	01010	10110	01002	01121	01000	20100	0211?	???
<i>E. navillei</i>	??044	02102	12200	??010	101?0	01002	01121	11100	20100	0211?	???
<i>E. patelliformis</i>	??03(56)	02102	12200	01010	10110	01002	01121	11100	?0000	?211?	???
<i>E. relicta</i>	00054	02101	12210	10010	10111	01002	01211	21200	10000	1201?	?10
<i>E. rugosa</i>	??124	02102	12200	01010	10110	01002	01221	01000	20100	0211?	???
<i>E. thebensis</i>	??1{123}{234}	02102	02200	??010	10110	01002	01121	11100	20100	0211?	???
<i>G. sorigneti</i>	??030	02102	12201	??010	10111	01002	012?1	11100	???:0?	?211?	???
<i>G. vasseuri</i>	??030	02102	12201	01010	10111	01002	01122	01000	20100	0211?	???
<i>G. welschi</i>	??0{12}0	?2???	02200	??001	00??1	?1?0?	?1121	01100	20100	0?11?	???
<i>P. pileus</i>	??(01)32	02010	02000	?0000	01000	00002	010{01}1	21210	01000	1201?	???
<i>P. rancureli</i>	??043	02001	02100	??010	01??1	01002	01011	21200	?1000	?200?	???
<i>R. alabamensis</i>	??1?{34}	02101	02000	?0100	01000	01002	01211	01000	10010	0211?	???
<i>R. anceps</i>	??1{34}{34}	02102	02000	?0000	01000	00002	01201	212?0	?0000	1211?	???
<i>R. ayresi</i>	??123	02001	02000	1?110	01000	01002	01211	01110	20010	?211?	???
<i>R. carolinensis</i>	??143	02001	02000	1?000	01000	00002	01011	21100	200?0	?101?	???
<i>R. chipolanus</i>	??1{34}2	02101	02000	1?110	01000	01002	01211	11110	2?010	0211?	???
<i>R. conradi</i>	??135	12001	01000	?0000	01010	00002	01211	11100	11000	1201?	???
<i>R. daradensis</i>	??152	02001	02000	?0000	0101?	01002	01221	11100	20000	1111?	???
<i>R. ericsoni</i>	??1{12}3	02110	02000	1?110	01000	01002	01211	11100	100?0	?211?	???
<i>R. evergladensis</i>	??125	02101	02000	10110	01000	01002	01211	11110	10010	?211?	???
<i>R. globosus</i>	??114	02110	02000	1?110	01000	01002	01211	11100	100?0	?211?	???
<i>R. gouldii</i>	??124	02111	02000(01)	1?110	01000	01002	01211	21100	10010	0211?	???
<i>R. grignonensis</i>	??144	0200?	02000	10000	01010	00012	012?1	11110	00010	?211?	???
<i>R. mexicanus</i>	??142	02101	02001	1?110	01000	01002	01211	01100	?00??	?211?	???
<i>R. pacificus</i>	11132	02101	02000	10110	01000	01002	01211	01110	20010	02111	010
<i>R. riveroi</i>	??1{123}3	0210?	02000	1?110	010?0	01002	012??	?1?10	??0?0	?211?	???
<i>R. rodriguezii_A</i>	??134	02101	02000	??000	01000	01002	01211	21??:0	?00?0	?211?	???
<i>R. rodriguezii_R</i>	??13{34}	02101	02000	??000	01000	01002	01211	21100	10010	0211?	???
<i>R. sabistonensis</i>	??1{234}{234}	02101	02001	1?100	010?0	01002	01211	01110	20010	0211?	???
<i>R. tuderii</i>	??133	02101	02000	?0000	010?0	00002	01021	11100	100?0	0211?	???

**Appendix 2.3.** Batch files for PAUP analyses (available in MorphoBank [O'Leary & Kaufman 2012], project P3287). Modifications between analyses in squared brackets. File names were also modified according to the analysis performed.

#### [ANALYSIS 1]

```
begin PAUP;
log file=hsearch_A1.log;
execute Cassidulids.nex; [ANALYSIS 3 ONLY: Cassidulids_NoPartialUncertainty.nex;]
[ANALYSIS 2 ONLY: exclude 46 47 95-98;]
[ANALYSIS 4 ONLY: delete 1 4-9 13-20 23 25 26 28 30-39 41-60 62-66;]
outgroup Nscutatus Arecens Edepressa; [ANALYSIS 4 ONLY: Arecens Edepressa;]
set criterion=parsimony;
pset mstaxa=variable; [ANALYSIS 3 ONLY: =polymorph;]
pset collapse=minbrlen;
set root=outgroup; set storebrlens=yes; set maxtrees=10000 increase=auto;
hsearch start=stepwise addseq=random randomize=addseq nreps=1000
savereps=yes hold=5 swap=tbr multrees=yes rstatus=yes;
savetrees file=hsearch_A1.all.tre brlen=yes;
filter best=yes permdel=yes;
savetrees file=hsearch_A1.best.tre brlen=yes;
pscores X/tl ci ri rc hi; [X was replaced with chosen tree]
describe X/plot=phylogram brlens=yes chglist=yes apolist=yes diag=yes; [X was replaced with
    chosen tree(s)]
contree all/majrule cutoff=50 file=hsearch_A1_majrule.tre;
bootstrap nreps=1000 search=heuristic/addseq=random nreps=10;
savetrees from=1 to=1 file=hsearch_A1_bootstrap.trees brlens=yes savebootp=NodeLabels
MaxDecimals=0;
log stop;
quit;
```

**Appendix 2.4.** Dispersal constraint Q-matrices used in the DEC analyses. Dispersal probabilities reflect connectivity between areas as a result of distance, currents and barriers. For example, high rates ( $10^0 = 1$ ) in the early Cenozoic result from the high connectivity promoted by the circum-equatorial current; intermediate rates ( $10^{-1} = 0.1$ ) in the Late Oligocene result from the disruption of the circum-equatorial current system that reduced the connectivity between disjunct areas; and finally, low rates ( $10^{-2} = 0.01$ ) from the Pliocene to the Recent result from the formation of the Isthmus of Panama and the closure of the Tethys seaway, which almost stopped the exchange between disjunct areas (Stille et al. 1996; Harzhauser et al. 2007; O’Dea et al. 2016). Faujasiids did not occur in area SWA.

<b>Recent</b>	EPA	IND	IPA	MAD	NWA	SWA	NTH	STH
EPA	1	0.01	0.1	0.01	0.01	0.01	0.01	0.01
IND	0.01	1	1	1	0.01	0.01	0.1	0.1
IPA	0.1	1	1	1	0.01	0.01	0.01	0.01
MAD	0.01	1	1	1	0.01	0.01	0.01	0.01
NWA	0.01	0.01	0.01	0.01	1	1	0.1	0.01
SWA	0.01	0.01	0.01	0.01	1	1	0.01	0.01
NTH	0.01	0.1	0.01	0.01	0.1	0.01	1	1
STH	0.01	0.1	0.01	0.01	0.01	0.01	1	1

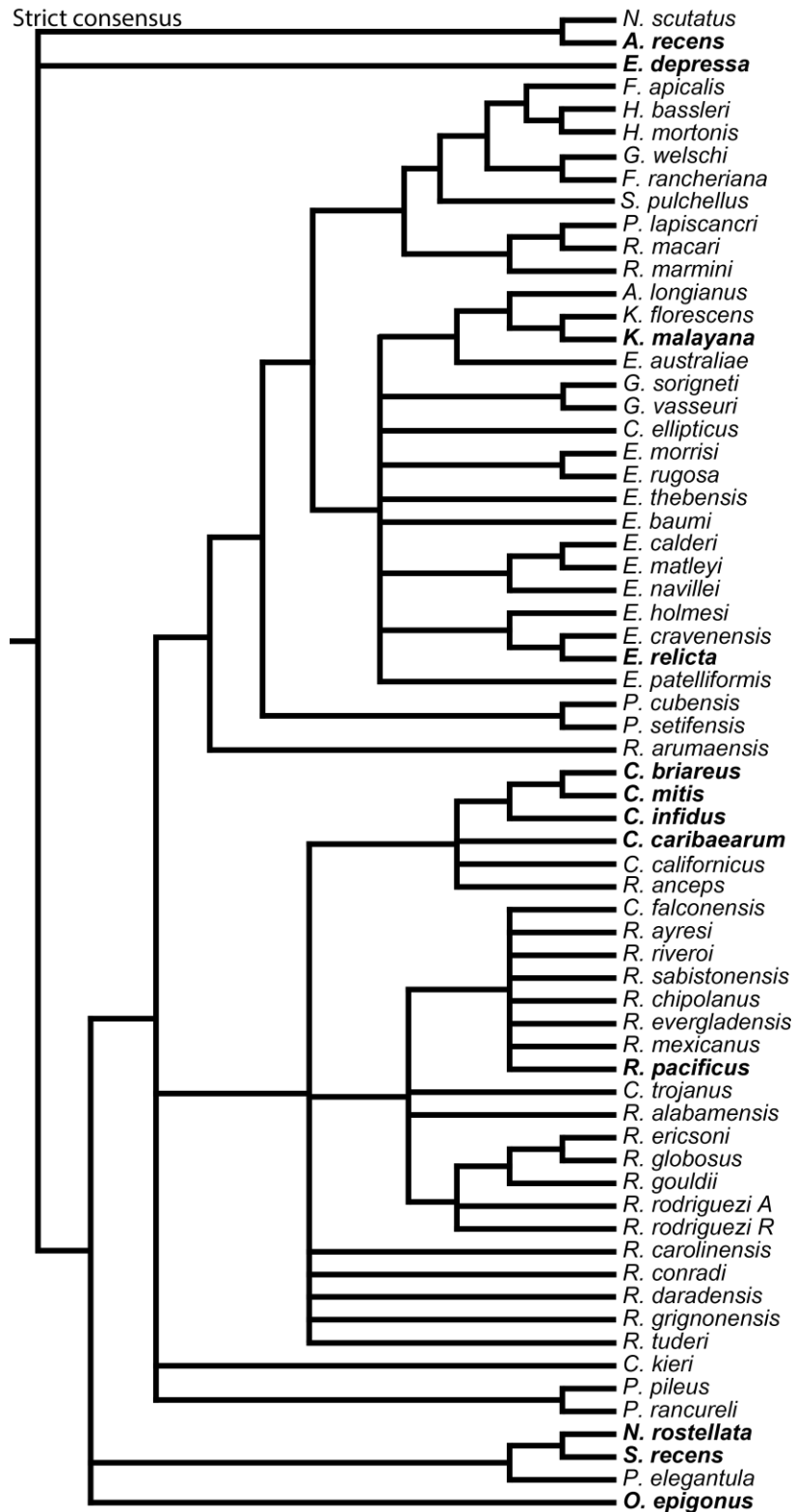
<b>5.3 My</b>	EPA	IND	IPA	MAD	NWA	SWA	NTH	STH
EPA	1	0.1	0.1	0.1	1	1	0.1	0.1
IND	0.1	1	1	1	0.1	0.1	1	1
IPA	0.1	1	1	1	0.1	0.1	0.1	0.1
MAD	0.1	1	1	1	0.1	0.1	0.1	1
NWA	1	0.1	0.1	0.1	1	1	1	1
SWA	1	0.1	0.1	0.1	1	1	0.1	1
NTH	0.1	1	0.1	0.1	1	0.1	1	1
STH	0.1	1	0.1	1	1	1	1	1

<b>28.1 My</b>	EPA	IND	IPA	MAD	NWA	SWA	NTH	STH
EPA	1	1	1	1	1	1	1	1
IND	1	1	1	1	1	1	1	1
IPA	1	1	1	1	1	1	1	1
MAD	1	1	1	1	1	1	1	1
NWA	1	1	1	1	1	1	1	1
SWA	1	1	1	1	1	1	1	1
NTH	1	1	1	1	1	1	1	1
STH	1	1	1	1	1	1	1	1

**Appendix 2.5.** Range constraints used in the DEC analyses were based on the distance and presence of barriers between areas. Adjacent areas were generally allowed (“1”), while disjunct areas were not (“0”). Faujasiids did not occur in area SWA.

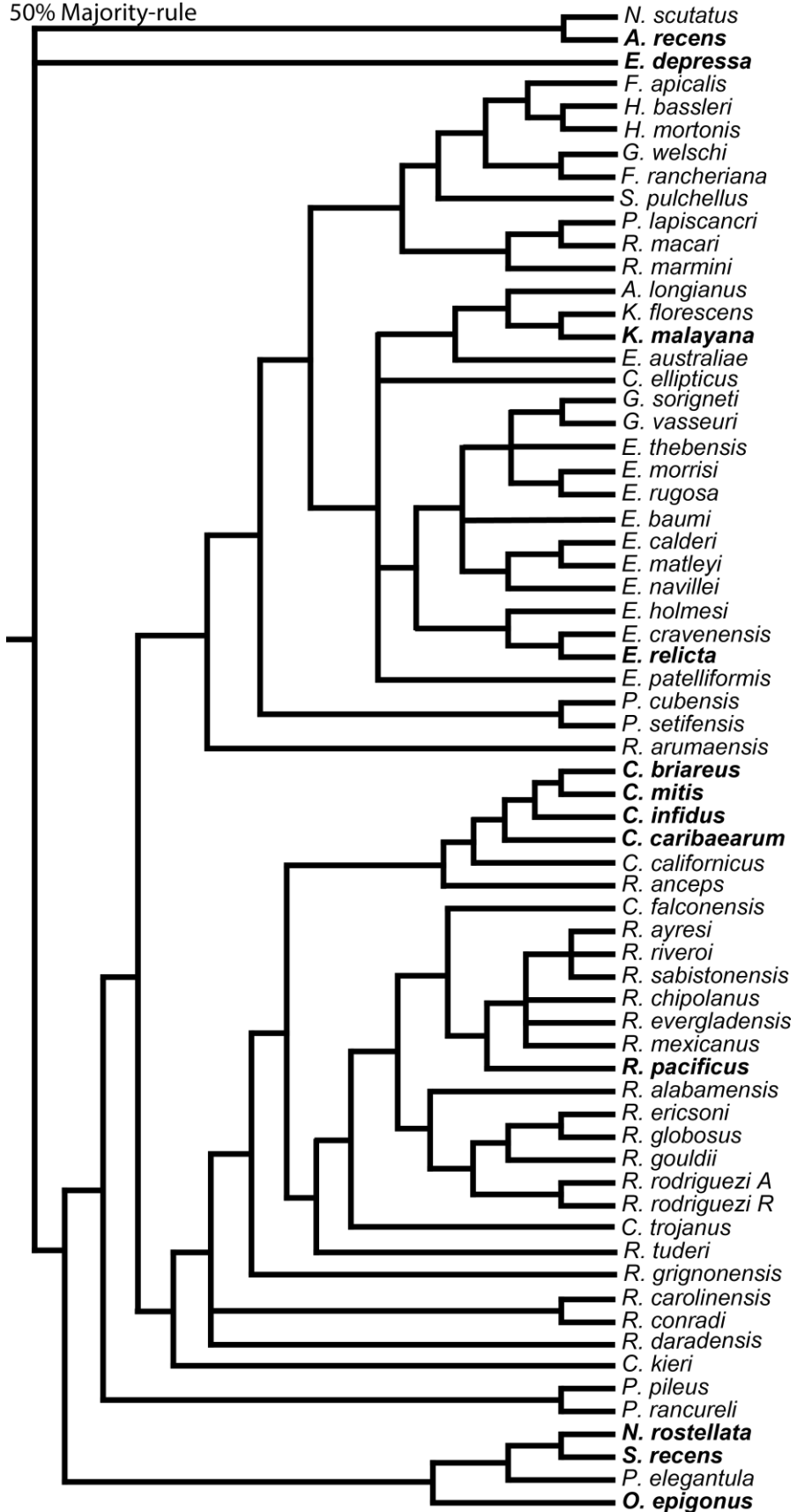
	EPA	IND	IPA	MAD	NWA	SWA	NTH	STH
EPA	-	0	1	0	1	1	0	0
IND		-	1	1	0	0	1	1
IPA			-	1	0	0	0	1
MAD				-	0	0	1	1
NWA					-	1	1	1
SWA						-	0	1
NTH							-	1
STH								-

**Appendix 2.6.** Strict consensus and 50% majority-rule consensus of 900 MPTs recovered by Analysis 1 (including all taxa, all characters and partial uncertainty) with unordered characters (724 steps, CI 0.246, RI 0.610). Extant taxa in bold.





50% Majority-rule



**Appendix 2.7.** Stratigraphic fit for each MPT estimated by the following metrics: the Gap Excess Ratio (GER; Wills 1999; Wills et al. 2008), the modified Manhattan Stratigraphic Measure (MSM\*; Siddall 1998; Pol & Norell 2001), the Relative Consistency Index (RCI; Benton & Storrs 1994), and the Stratigraphic Consistency Index (SCI; Huelsenbeck 1994). Estimated p-values for each metric (est.p.) are also included. Best fit values for each metric in bold.

Tree	SCI	RCI	GER <sup>1</sup>	MSM*	est.p.SCI	est.p.RCI	est.p.GER	est.p.MSM*
1	<b>0.557</b>	<b>-145.92</b>	<b>0.846</b>	<b>0.120</b>	2.12E-08	3.03E-08	6.20E-07	2.33E-11
2	0.541	-150.41	0.843	0.118	1.69E-06	1.26E-07	1.86E-06	1.80E-10
3	<b>0.557</b>	-156.06	0.839	0.116	6.88E-08	6.01E-08	1.25E-06	4.36E-10
4	<b>0.557</b>	<b>-145.92</b>	<b>0.846</b>	<b>0.120</b>	1.11E-07	2.97E-08	2.83E-07	7.28E-12
5	<b>0.557</b>	<b>-145.92</b>	<b>0.846</b>	<b>0.120</b>	3.60E-07	2.85E-08	1.53E-07	1.58E-12
6	0.541	-160.54	0.836	0.114	1.22E-06	1.98E-08	1.63E-06	3.88E-10
7	0.541	-150.41	0.843	0.118	9.63E-07	8.46E-08	6.81E-07	4.45E-11
8	0.541	-150.41	0.843	0.118	7.18E-07	7.60E-08	1.13E-06	6.43E-11
9	<b>0.557</b>	-156.06	0.839	0.116	2.47E-07	6.06E-08	2.66E-06	1.15E-09
10	<b>0.557</b>	-156.06	0.839	0.116	2.58E-07	8.07E-09	7.57E-07	1.54E-10
11	0.541	-160.54	0.836	0.114	6.51E-07	7.40E-08	2.84E-06	1.62E-09
12	0.541	-160.54	0.836	0.114	1.74E-06	9.55E-08	5.23E-06	2.41E-09
13	0.525	-167.58	0.831	0.111	7.72E-06	8.23E-08	6.12E-06	7.15E-09
14	0.525	-157.44	0.838	0.115	2.12E-06	6.25E-08	3.23E-06	9.05E-10
15	0.508	-172.06	0.828	0.109	4.18E-05	2.98E-07	1.14E-05	2.89E-08
16	0.525	-167.58	0.831	0.111	1.87E-05	9.22E-08	8.21E-06	1.41E-08
17	0.525	-167.58	0.831	0.111	9.92E-06	1.12E-07	6.42E-06	1.30E-08
18	0.508	-161.93	0.835	0.113	4.08E-05	5.73E-08	3.69E-06	1.59E-09
19	0.525	-157.44	0.838	0.115	1.12E-05	2.11E-07	3.15E-06	1.60E-09
20	0.525	-157.44	0.838	0.115	1.58E-05	6.55E-08	9.99E-07	1.64E-10
21	0.508	-172.06	0.828	0.109	0.000129	2.18E-07	1.54E-05	5.64E-08
22	0.508	-172.06	0.828	0.109	6.63E-05	1.65E-07	1.66E-05	3.56E-08
23	0.508	-161.93	0.835	0.113	4.41E-05	8.82E-08	2.57E-06	8.23E-10
24	0.508	-161.93	0.835	0.113	4.77E-05	1.23E-07	6.54E-06	5.34E-09

<sup>1</sup> The modified GER (GER\*) and topological GER (GER<sub>t</sub>) were also calculated; result for all trees was “1”.

**Appendix 2.8.** Apomorphy list for the clades labeled in Figure 2.11. Single arrows (--->) indicate ambiguous synapomorphies and double arrows (==>) indicate unambiguous synapomorphies.

Clade	Character r	Change	Clade	Character	Change	Clade	Character	Change		
A	9	0 ---> 1	D	9	1 ---> 0	H	21	0 ==> 1		
	13	0 ---> 1		12	1 ==> 0		36	2 ---> 0		
	34	0 ---> 1		19	1 ==> 0		43	0 ==> 1		
	37	0 ==> 1		32	0 ==> 1	I	41	0 ==> 1		
	39	0 ---> 1		36	2 ---> 0		46	0 ---> 1		
	74	1 ==> 0		68	0 ==> 1		47	0 ---> 1		
	77	0 ==> 1		69	0 ==> 1		55	0 ---> 1		
	81	0 ==> 1		78	0 ==> 2	67	0 ==> 1			
	82	0 ==> 1		86	0 ==> 2	J	26	0 ---> 1		
	83	0 ==> 1		E	19		0 ---> 2	29	0 ==> 1	
	91	0 ==> 1			34		1 ---> 2	37	1 ==> 0	
	92	0 ==> 2			65	0 ==> 1	44	0 ==> 2		
	97	0 ---> 1			70	0 ---> 1	48	0 ==> 1		
	B	4			0 ---> 1	71	0 ==> 1	61	0 ---> 1	
6		0 ---> 1	73		0 ==> 1	93	0 ==> 1			
8		1 ---> 0	75		2 ==> 1	K	9	1 ==> 0		
16		0 ==> 1	76		0 ==> 1		53	0 ==> 1		
22		2 ==> 1	F		1		1 ==> 2	72	0 ==> 1	
49		3 ---> 4			12	0 ==> 1	89	0 ---> 1		
58		0 ==> 2			22	2 ---> 1	L	27	1 ==> 0	
70		0 ==> 1			55	0 ==> 2		32	2 ---> 1	
81		1 ==> 2			56	0 ==> 1		55	1 ==> 2	
83		1 ==> 2			64	0 ==> 1		79	1 ==> 0	
94		1 ---> 0		G	23	1 ---> 0	83	1 ==> 2		
96		0 ---> 1			25	4 ---> 2	86	1 ---> 0		
C		27			0 ==> 1	39	1 ---> 0	M	21	0 ---> 1
		51			1 ---> 0	44	2 ---> 0		36	2 ==> 1
	52	0 ==> 2			50	3 ==> 1	49		3 ==> 2	
	57	0 ==> 2			88	0 ==> 1	63		0 ==> 1	
	79	0 ==> 2			97	1 ---> 0	91		1 ==> 0	
	95	0 ==> 1								

**Appendix 2.9.** Character attributes: character number (Ch.), number of character states (#states), percentage of missing data (MD; lower values, when present, consider partial uncertainty as missing data), number of steps (#steps), and consistency index (CI). Characters shaded in grey have high percentage of missing data and were removed from Analysis 2.

Ch.	# states	MD (%)	# steps	CI	Ch.	# states	MD (%)	# steps	CI	Ch.	# states	MD (%)	# steps	CI
1	3	100	13	0.154	21	3	93–97	22	0.409	41	2	100	5	0.200
2	2	100	9	0.111	22	3	100	9	0.222	42	2	74	3	0.333
3	2	100	8	0.250	23	3	98.5–100	10	0.200	43	2	98.5	5	0.200
4	2	100	14	0.071	24	2	100	2	0.500	44	3	100	8	0.250
5	2	100	5	0.200	25	5	92–100	15	0.333	45	2	100	2	0.500
6	2	100	7	0.143	26	3	98.5	3	0.667	46	3	16.7	2	1.000
7	2	97	2	0.500	27	2	100	5	0.200	47	2	16.7	2	0.500
8	3	98.5–100	14	0.214	28	2	98.5	4	0.250	48	2	100	7	0.286
9	2	100	11	0.091	29	2	100	3	0.333	49	7	82–97	35	0.171
10	3	100	8	0.250	30	3	97–99	17	0.235	50	7	91–100	44	0.227
11	2	100	1	1.000	31	2	91	12	0.083	51	2	97	5	0.200
12	2	98.5	4	0.250	32	4	85	16	0.188	52	3	98.5	3	0.667
13	3	92–98.5	25	0.360	33	2	80	7	0.143	53	2	97	4	0.250
14	2	100	1	1.000	34	3	100	14	0.143	54	2	97	3	0.333
15	2	100	1	1.000	35	2	98.5	5	0.400	55	3	92	14	0.143
16	2	98.5	2	0.500	36	3	100	23	0.304	56	2	100	6	0.167
17	2	97	4	0.250	37	2	98.5	12	0.083	57	3	98.5	4	0.500
18	2	95.5	4	0.250	38	3	98.5	10	0.200	58	3	100	8	0.250
19	3	97	17	0.235	39	3	100	8	0.250	59	2	100	7	0.286
20	2	100	1	1.000	40	2	98.5	3	0.333	60	2	100	4	0.500

**Appendix 2.9.** Continued...

Ch.	# states	MD (%)	# steps	CI	Ch.	# states	MD (%)	# steps	CI	Ch.	# states	MD (%)	# steps	CI
61	2	65	5	0.200	74	2	100	2	0.500	87	2	94	4	0.250
62	2	62	4	0.250	75	3	98.5	5	0.400	88	2	94	5	0.200
63	2	98.5	4	0.250	76	2	98.5	3	0.333	89	2	86	3	0.333
64	2	100	8	0.125	77	2	100	1	1.000	90	2	94	3	0.333
65	2	100	3	0.333	78	3	100	12	0.167	91	2	76	8	0.125
66	2	100	5	0.200	79	3	91-94	14	0.143	92	3	97	7	0.286
67	2	100	5	0.200	80	3	98.5	5	0.400	93	2	97	4	0.250
68	2	97	5	0.200	81	4	98.5	27	0.111	94	2	98.5	4	0.250
69	2	86	7	0.143	82	2	100	1	1.000	95	3	14	2	1.000
70	2	97	10	0.100	83	3	95.5-97	15	0.133	96	2	14	2	0.500
71	3	97	3	0.667	84	2	95.5	6	0.167	97	2	17	3	0.333
72	2	100	6	0.167	85	2	100	4	0.250	98	2	15	1	1.000
73	2	98.5	5	0.200	86	3	86	17	0.118					

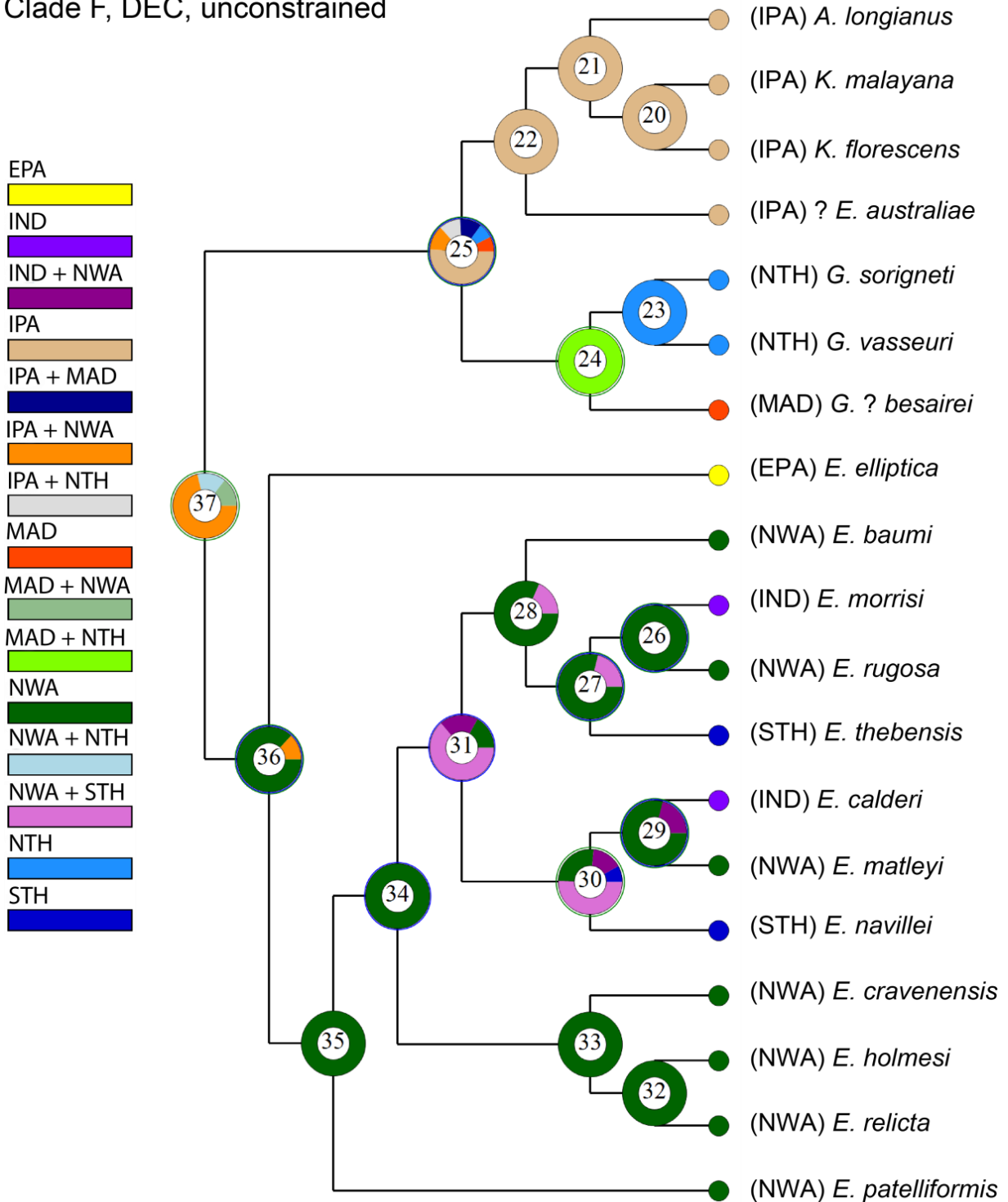
**Appendix 2.10.** Biogeographic events inferred by the different scenarios of the dispersal-extinction-cladogenesis (DEC) model.

<b>CLADE F</b>	Global dispersal	Global vicariance	Global extinction
Unconstrained	13	8	0
Range Constraint	14	6	3
Dispersal Constraint	12	8	1
Both Constraints	13	6	3

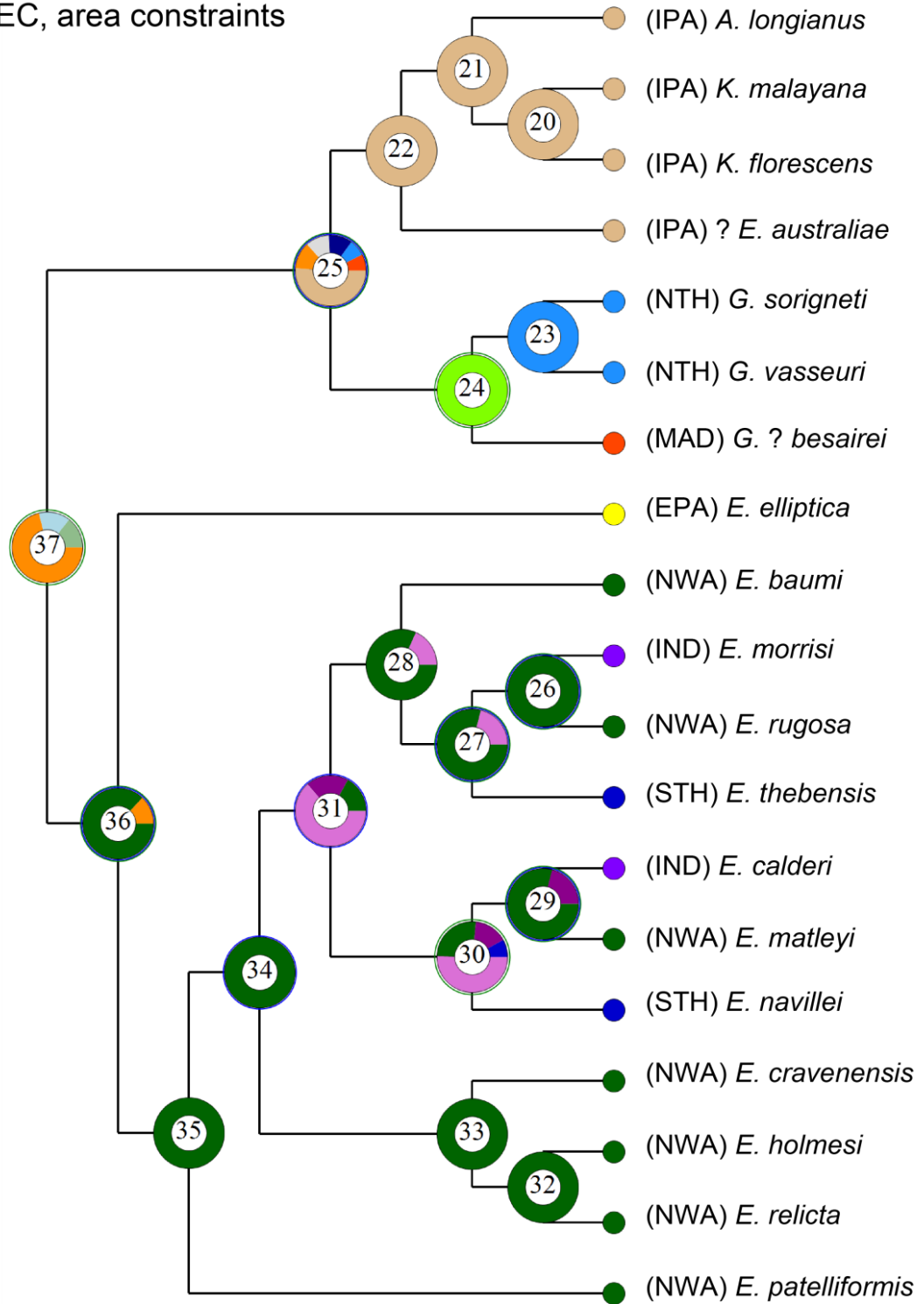
<b>CLADE I</b>	Global dispersal	Global vicariance	Global extinction
Unconstrained	17	10	0
Range Constraint	19	10	1
Dispersal Constraint	17	10	0
Both Constraints	19	10	2

**Appendix 2.11.** Ancestral area reconstructions of clade F inferred by the dispersal-extinction-cladogenesis (DEC) model with various scenarios. Taxa follow classification proposed by this study. Pie charts at each node indicate the relative probability of ancestral area(s); colors for areas indicated in legend.

Clade F, DEC, unconstrained

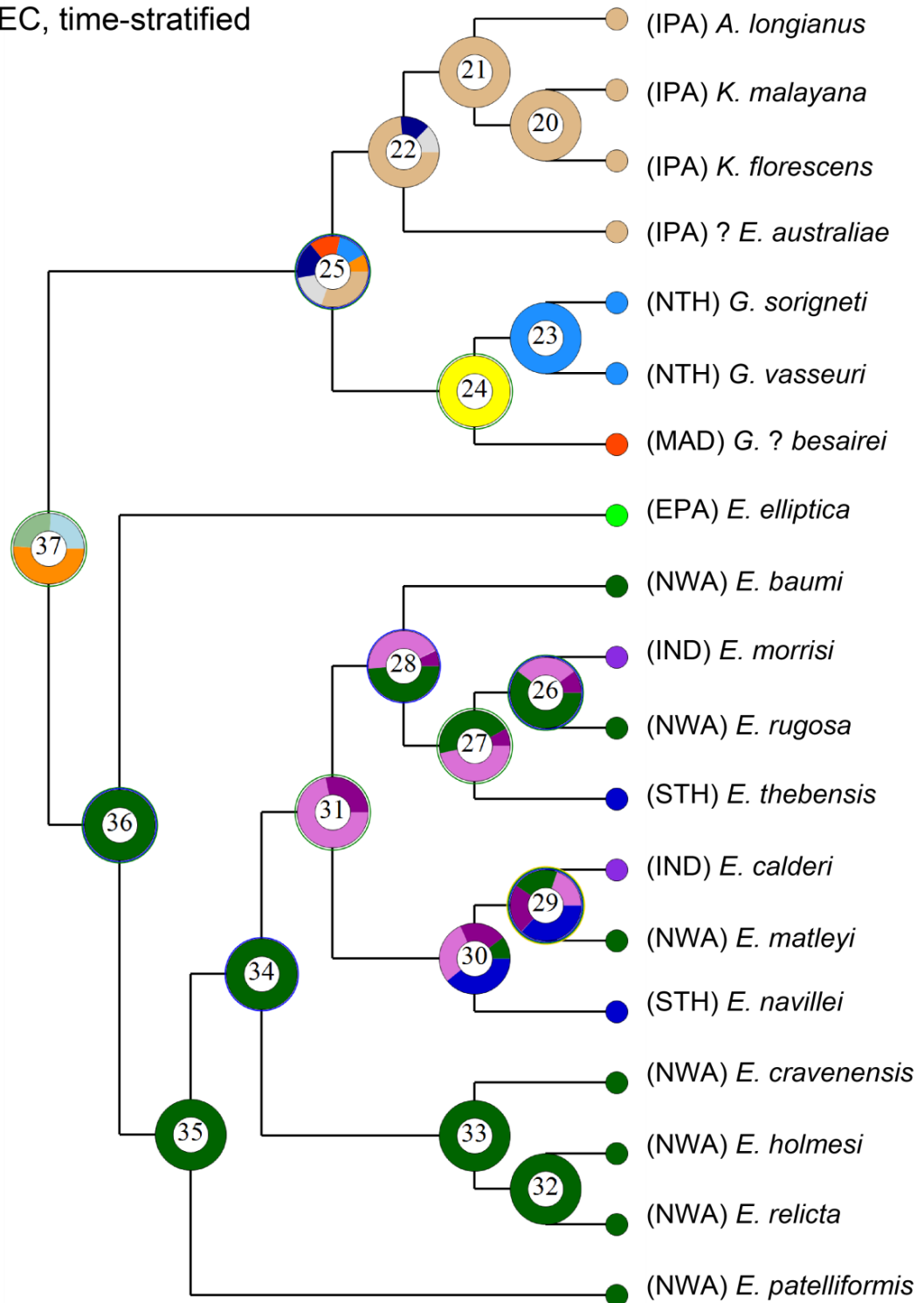


Clade F, DEC, area constraints

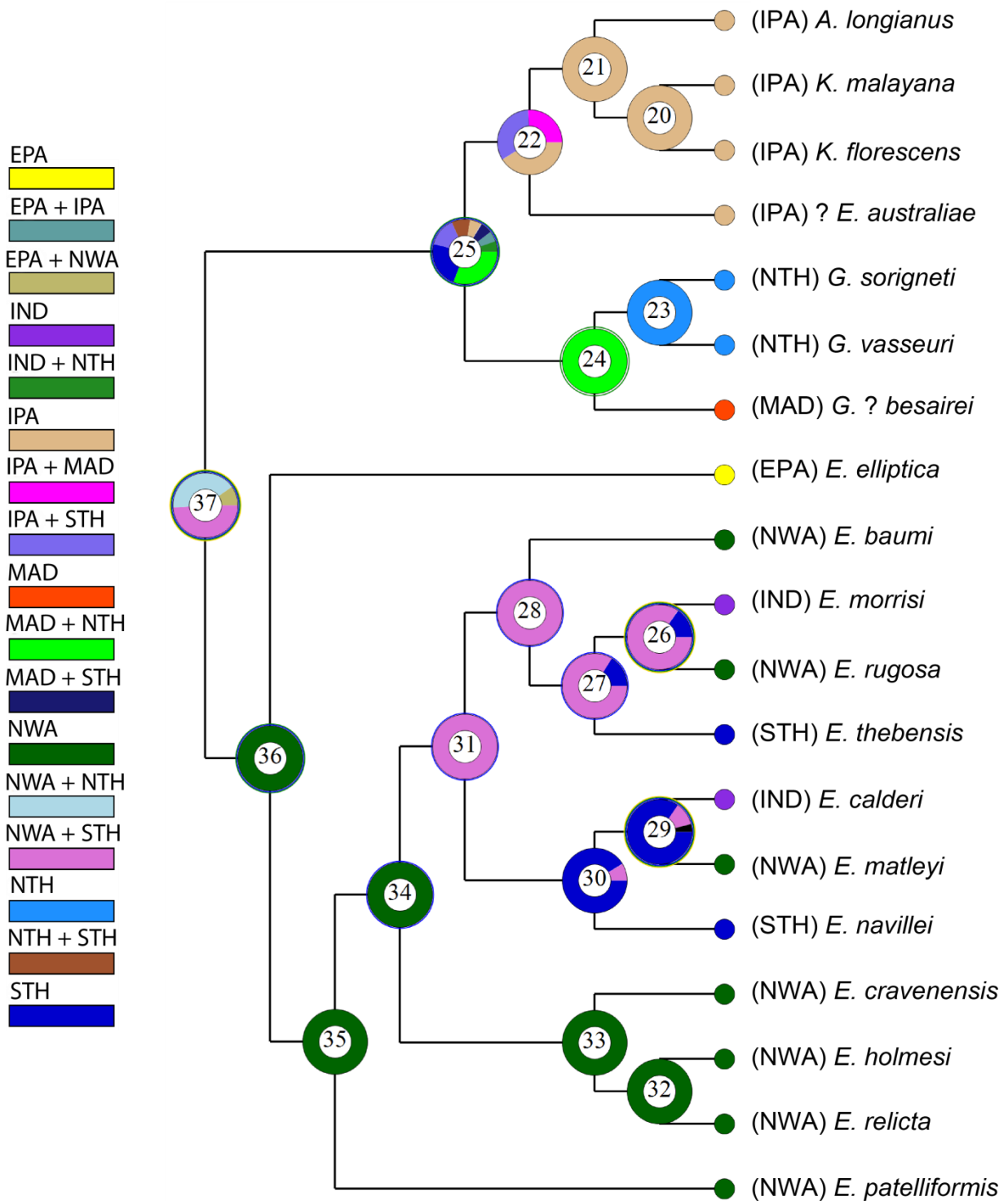




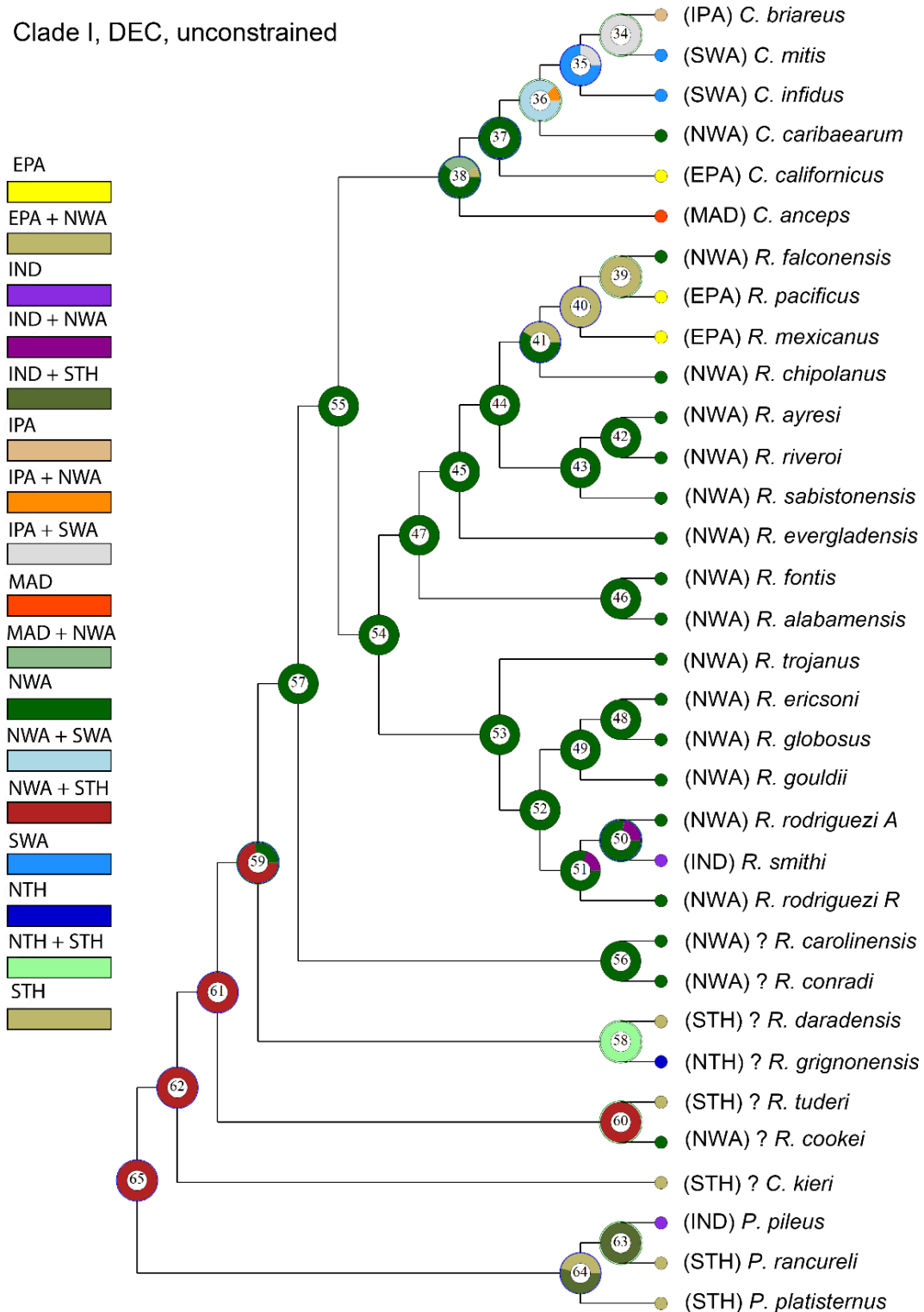
Clade F, DEC, time-stratified



Clade F, DEC, time-stratified and area constraints



**Appendix 2.12.** Ancestral area reconstructions of clade I inferred by the dispersal-extinction-cladogenesis (DEC) model with various scenarios. Taxa follow classification proposed by this study. Pie charts at each node indicate the relative probability of ancestral area(s); colors for areas indicated in legend.



Clade I, DEC, area constraints

EPA



EPA + NWA



EPA + SWA



IND



IND + STH



IPA



MAD



NWA



NWA + SWA



NWA + NTH



NWA + STH



SWA



SWA + STH



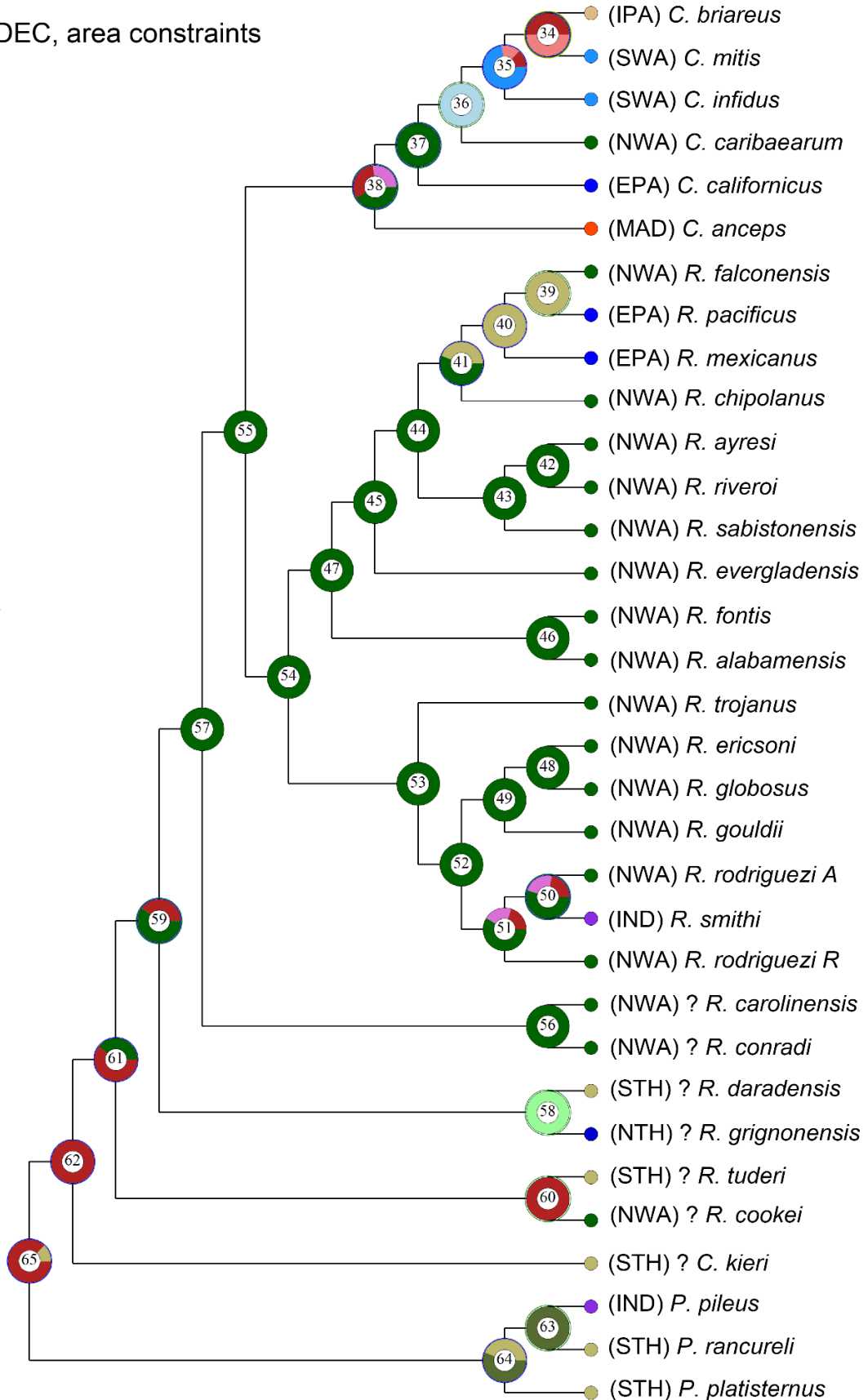
NTH



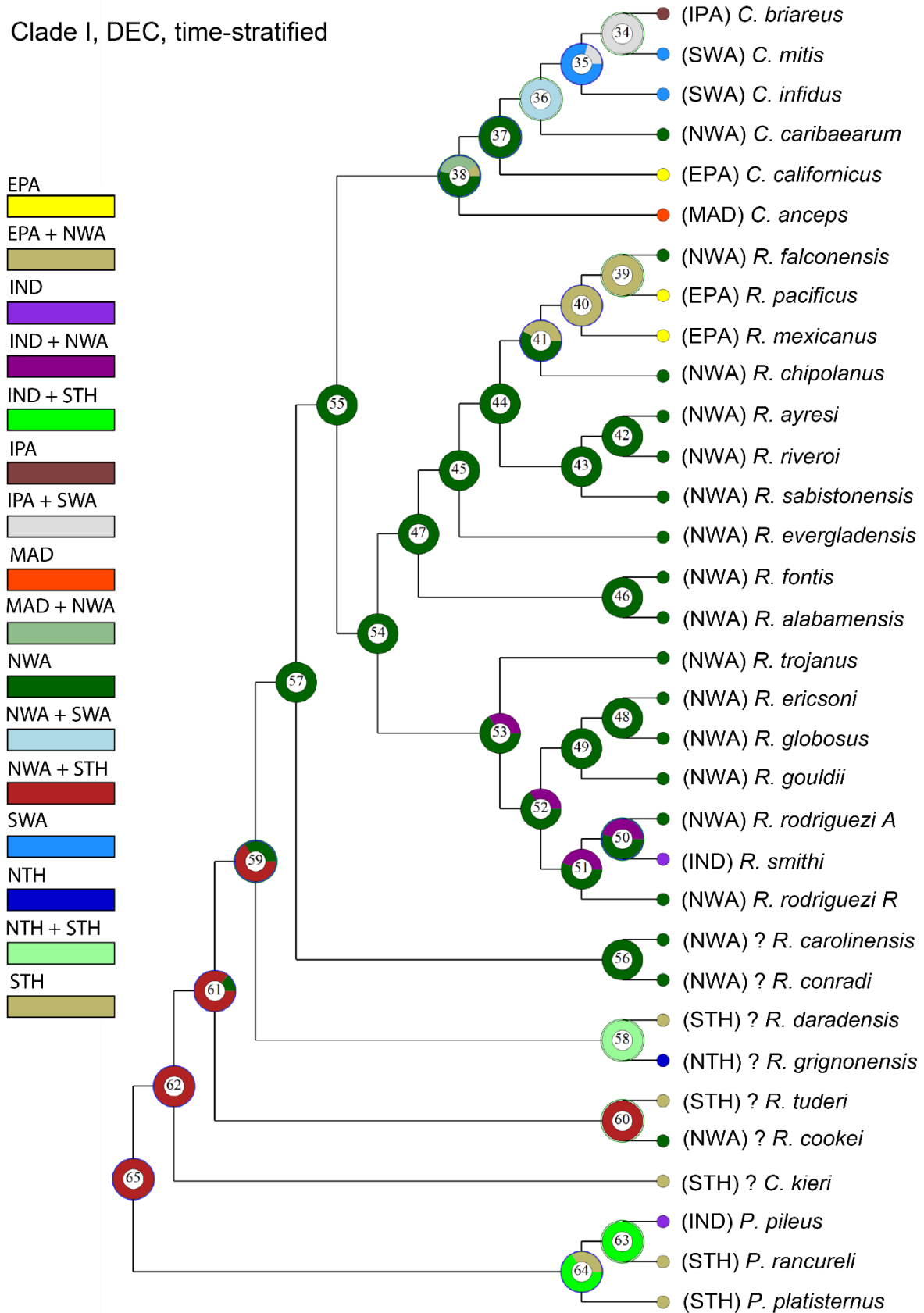
NTH + STH



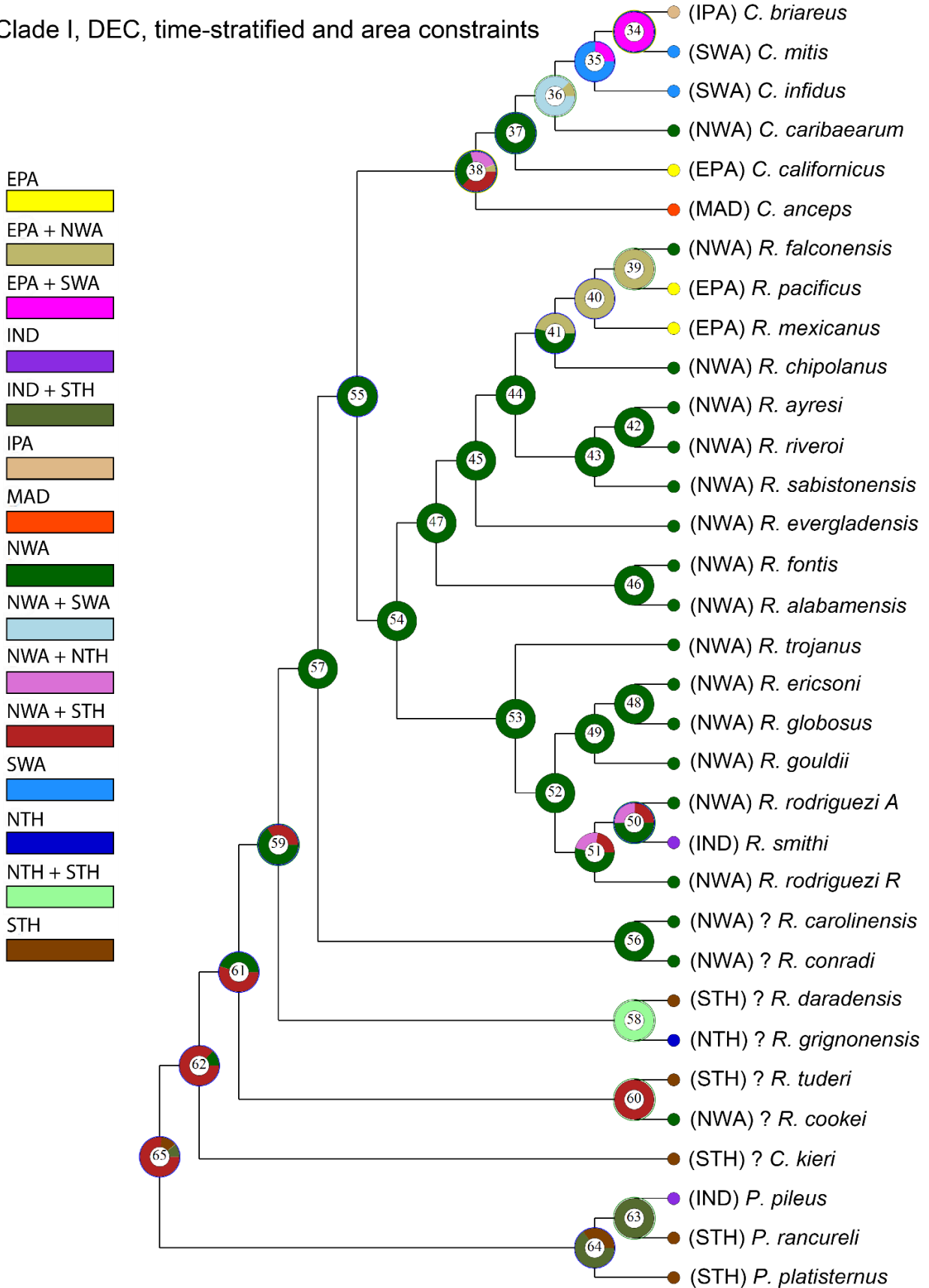
STH



Clade I, DEC, time-stratified



Clade I, DEC, time-stratified and area constraints



**Appendix 2.13:** Biogeographic scenario inferred by the dispersal-extinction-cladogenesis (DEC) model with range and time-stratified dispersal constraints.

## CLADE F

- node 20 (anc. of terminals 2–3): IPA 100  
Event Route: IPA->IPA^IPA->IPA|IPA  
Dispersal:0, Vicariance:0, Extinction:0, Probability: 1.0000
- node 21 (anc. of terminals 1–3): IPA 100  
Event Route: IPA->IPA^IPA->IPA|IPA  
Dispersal:0, Vicariance:0, Extinction:0, Probability: 1.0000
- node 22 (anc. of terminals 1–5): IPA 41.02; IPA+STH 33.07; IPA+MAD 25.91.  
Event Route: IPA->IPA^IPA->IPA|IPA  
Dispersal:0, Vicariance:0, Extinction:0, Probability: 0.4102
- node 23 (anc. of terminals 17–18): NTH 100  
Event Route: NTH->NTH^NTH->NTH|NTH  
Dispersal:0, Vicariance:0, Extinction:0, Probability: 1.0000
- node 24 (anc. of terminals 17–19): MAD+ NTH 100  
Event Route: MAD+NTH->MAD|NTH  
Dispersal:0, Vicariance:1, Extinction:0, Probability: 1.0000
- node 25 (anc. of terminals 1–19): MAD+NTH 30.85; STH 23.03; IPA+STH 14.50; NTH+STH 9.23; IPA 5.96; MAD+STH 5.79; EPA+IPA 5.47; IND+NTH 5.16  
Event Route: MAD+NTH->IPA+MAD+NTH->MAD+NTH|IPA  
Dispersal:1, Vicariance:1, Extinction:0, Probability: 0.1265
- node 26 (anc. of terminals 11–15): NWA+STH 84.59; STH 15.41  
Event Route: NWA+STH->NWA->IND+NWA->IND|NWA  
Dispersal:1, Vicariance:1, Extinction:1, Probability: 0.8459
- node 27 (anc. of terminals 11–16): NWA+STH 83.98; STH 16.02  
Event Route: NWA+STH->NWA+STH^STH->STH|NWA+STH  
Dispersal:1, Vicariance:0, Extinction:0, Probability: 0.7104
- node 28 (anc. of terminals 6–16): NWA+STH 100  
Event Route: NWA+STH->NWA+STH^NWA->NWA|NWA+STH  
Dispersal:1, Vicariance:0, Extinction:0, Probability: 0.8398
- node 29 (anc. of terminals 7–10): STH 84.58; NWA+STH 11.62; IND+STH 3.80  
Event Route: STH->->IND+NWA->IND|NWA  
Dispersal:3, Vicariance:1, Extinction:1, Probability: 0.8458
- node 30 (anc. of terminals 7–12): STH 91.26; NWA+STH 8.74  
Event Route: STH->STH^STH->STH|STH  
Dispersal:0, Vicariance:0, Extinction:0, Probability: 0.7719
- node 31 (anc. of terminals 6–12): NWA+STH 100  
Event Route: NWA+STH->NWA+STH^STH->STH|NWA+STH  
Dispersal:1, Vicariance:0, Extinction:0, Probability: 0.9126
- node 32 (anc. of terminals 9–14): NWA 100  
Event Route: NWA->NWA^NWA->NWA|NWA  
Dispersal:0, Vicariance:0, Extinction:0, Probability: 1.0000
- node 33 (anc. of terminals 8–14): NWA 100

Event Route: NWA->NWA^NWA->NWA|NWA  
 Dispersal:0, Vicariance:0, Extinction:0, Probability: 1.0000  
 node 34 (anc. of terminals 6–14): NWA 100  
 Event Route: NWA->NWA^NWA->NWA+STH^NWA->NWA|NWA+STH  
 Dispersal:1, Vicariance:0, Extinction:0, Probability: 1.0000  
 node 35 (anc. of terminals 6–13): NWA 100  
 Event Route: NWA->NWA^NWA->NWA|NWA  
 Dispersal:0, Vicariance:0, Extinction:0, Probability: 1.0000  
 node 36 (anc. of terminals 4–13): NWA 100.00  
 Event Route: NWA->EPA+NWA->EPA|NWA  
 Dispersal:2, Vicariance:1, Extinction:0, Probability: 1.0000  
 node 37 (anc. of terminals 1–13): NWA+STH 48.92; NWA+NTH 41.37; EPA+NWA 9.71  
 Event Route: NWA+STH->NWA->MAD+NWA+NTH->NWA|MAD+NTH  
 Dispersal:2, Vicariance:1, Extinction:1, Probability: 0.1509

**Dispersal Between Areas.** MAD->IPA: 0.5; NWA->EPA: 1; NWA->IND: 0.5; NWA->MAD: 0.5; NWA->NTH: 0.5; NWA->STH: 1; NTH->IPA: 0.5; STH->IND: 1.5; STH->MAD: 0.5; STH->NWA:1; STH->NTH: 0.5.

**Speciation Within Areas.** IPA: 3, NWA: 5, NTH: 1, STH: 3.

**Dispersal Table:**

	from	to	within
EPA	0.00	1.00	0
IND	0.00	2.00	0
IPA	0.00	1.00	3
MAD	0.50	1.00	0
NWA	3.50	1.00	5
NTH	0.50	1.00	1
STH	3.50	1.00	3

**CLADE I**

node 34 (anc. of terminals 1–7): EPA+SWA 100  
 Event Route: EPA+SWA->SWA->IPA+SWA->IPA|SWA  
 Dispersal:1, Vicariance:1, Extinction:1, Probability: 1.0000  
 node 35 (anc. of terminals 1–5): SWA 75.50; EPA+SWA 24.50  
 Event Route: SWA->SWA^SWA->EPA+SWA^SWA->SWA|EPA+SWA  
 Dispersal:1, Vicariance:0, Extinction:0, Probability: 0.7550  
 node 36 (anc. of terminals 1–3): NWA+SWA 87.49; EPA+NWA 12.51  
 Event Route: NWA+SWA->NWA|SWA  
 Dispersal:0, Vicariance:1, Extinction:0, Probability: 0.6605  
 node 37 (anc. of terminals 1–2): NWA 100  
 Event Route: NWA->EPA+NWA+SWA->EPA|NWA+SWA



Dispersal:3, Vicariance:1, Extinction:0, Probability: 0.8749  
 node 38 (anc. of terminals 1–12): NWA+STH 37.30; NWA 33.11; NWA+NTH 23.70;  
 EPA+NWA 5.89  
 Event Route: NWA+STH->NWA->MAD+NWA->MAD|NWA  
 Dispersal:1, Vicariance:1, Extinction:1, Probability: 0.3730  
 node 39 (anc. of terminals 4–24): EPA+NWA 100  
 Event Route: EPA+NWA->NWA|EPA  
 Dispersal:0, Vicariance:1, Extinction:0, Probability: 1.0000  
 node 40 (anc. of terminals 4–23): EPA+NWA 100  
 Event Route: EPA+NWA->EPA+NWA^EPA->EPA|EPA+NWA  
 Dispersal:1, Vicariance:0, Extinction:0, Probability: 1.0000  
 node 41 (anc. of terminals 4–15): NWA 53.95; EPA+NWA 46.05  
 Event Route: NWA->NWA^NWA->EPA+NWA^NWA->NWA|EPA+NWA  
 Dispersal:1, Vicariance:0, Extinction:0, Probability: 0.5395  
 node 42 (anc. of terminals 13–25): NWA 100  
 Event Route: NWA->NWA^NWA->NWA|NWA  
 Dispersal:0, Vicariance:0, Extinction:0, Probability: 1.0000  
 node 43 (anc. of terminals 13–28): NWA 100  
 Event Route: NWA->NWA^NWA->NWA|NWA  
 Dispersal:0, Vicariance:0, Extinction:0, Probability: 1.0000  
 node 44 (anc. of terminals 4–28): NWA 100  
 Event Route: NWA->NWA^NWA->NWA|NWA  
 Dispersal:0, Vicariance:0, Extinction:0, Probability: 0.5395  
 node 45 (anc. of terminals 4–19): NWA 100  
 Event Route: NWA->NWA^NWA->NWA|NWA  
 Dispersal:0, Vicariance:0, Extinction:0, Probability: 1.0000  
 node 46 (anc. of terminals 11–31): NWA 100  
 Event Route: NWA->NWA^NWA->NWA|NWA  
 Dispersal:0, Vicariance:0, Extinction:0, Probability: 1.0000  
 node 47 (anc. of terminals 4–31): NWA 100  
 Event Route: NWA->NWA^NWA->NWA|NWA  
 Dispersal:0, Vicariance:0, Extinction:0, Probability: 1.0000  
 node 48 (anc. of terminals 18–20): NWA 100  
 Event Route: NWA->NWA^NWA->NWA|NWA  
 Dispersal:0, Vicariance:0, Extinction:0, Probability: 1.0000  
 node 49 (anc. of terminals 18–21): NWA 100  
 Event Route: NWA->NWA^NWA->NWA|NWA  
 Dispersal:0, Vicariance:0, Extinction:0, Probability: 1.0000  
 node 50 (anc. of terminals 26–32): NWA 49.73; NWA+ NTH 25.78; NWA+STH 24.48  
 Event Route: NWA->IND+NWA->NWA|IND  
 Dispersal:2, Vicariance:1, Extinction:0, Probability: 0.4973  
 node 51 (anc. of terminals 26–27): NWA 53.62; NWA+ NTH 23.81; NWA+STH 22.57  
 Event Route: NWA->NWA^NWA->NWA|NWA  
 Dispersal:0, Vicariance:0, Extinction:0, Probability: 0.2667  
 node 52 (anc. of terminals 18–27): NWA 100  
 Event Route: NWA->NWA^NWA->NWA|NWA

Dispersal:0, Vicariance:0, Extinction:0, Probability: 0.5326  
 node 53 (anc. of terminals 8–27): NWA 100  
 Event Route: NWA->NWA^NWA->NWA|NWA  
 Dispersal:0, Vicariance:0, Extinction:0, Probability: 1.0000  
 node 54 (anc. of terminals 4–27): NWA 100  
 Event Route: NWA->NWA^NWA->NWA|NWA  
 Dispersal:0, Vicariance:0, Extinction:0, Probability: 1.0000  
 node 55 (anc. of terminals 1–27): NWA 100  
 Event Route: NWA->NWA^NWA->NWA+STH^NWA->NWA|NWA+STH  
 Dispersal:1, Vicariance:0, Extinction:0, Probability: 0.3730  
 node 56 (anc. of terminals 14–16): NWA 100  
 Event Route: NWA->NWA^NWA->NWA|NWA  
 Dispersal:0, Vicariance:0, Extinction:0, Probability: 1.0000  
 node 57 (anc. of terminals 1–16): NWA 100  
 Event Route: NWA->NWA^NWA->NWA|NWA  
 Dispersal:0, Vicariance:0, Extinction:0, Probability: 1.0000  
 node 58 (anc. of terminals 17–22): NTH +STH 100  
 Event Route: NTH+SHT->STH|NTH  
 Dispersal:0, Vicariance:1, Extinction:0, Probability: 1.0000  
 node 59 (anc. of terminals 1–22): NWA 65.62; NWA+STH 34.38  
 Event Route: NWA->NWA+NTH+STH->NTH+STH|NWA  
 Dispersal:3, Vicariance:1, Extinction:0, Probability: 0.6562  
 node 60 (anc. of terminals 29–30): NWA+STH 100  
 Event Route: NWA+STH->STH|NWA  
 Dispersal:0, Vicariance:1, Extinction:0, Probability: 1.0000  
 node 61 (anc. of terminals 1–30): NWA+STH 54.63; NWA 45.37  
 Event Route: NWA+STH->NWA+STH^NWA->NWA+STH|NWA  
 Dispersal:1, Vicariance:0, Extinction:0, Probability: 0.3585  
 node 62 (anc. of terminals 1–6): NWA+STH 86.97; NWA 13.03  
 Event Route: NWA+STH->NWA+STH^STH->STH|NWA+STH  
 Dispersal:1, Vicariance:0, Extinction:0, Probability: 0.4751  
 node 63 (anc. of terminals 9–10): IND +STH 100  
 Event Route: IND+STH->IND|STH  
 Dispersal:0, Vicariance:1, Extinction:0, Probability: 1.0000  
 node 64 (anc. of terminals 9–33): IND +STH 65.27; STH 34.73  
 Event Route: IND+STH->IND+STH^STH->STH|IND+STH  
 Dispersal:1, Vicariance:0, Extinction:0, Probability: 0.6527  
 node 65 (anc. of terminals 1–33): NWA+STH 76.51; STH 12.87; IND+STH 10.62  
 Event Route: NWA+STH->NWA+STH^STH->IND+NWA+STH^STH->  
 IND+STH|NWA+STH  
 Dispersal:2, Vicariance:0, Extinction:0, Probability: 0.4343

**Dispersal Between Areas.** EPA->IPA: 0.5; NWA->EPA: 2; NWA->IND: 1.5; NWA->MAD: 0.5; NWA->SWA: 1; NWA->NTH: 1; NWA->STH: 2; SWA->EPA: 1; SWA->IPA: 0.5; STH ->IND: 0.5; STH->MAD: 0.5.

**Speciation Within Areas.** EPA: 1; NWA: 17; SWA: 1; STH: 3.

**Dispersal Table:**

	from	to	Within
EPA	0.50	3.00	1
IND	0.00	2.00	0
IPA	0.00	1.00	0
MAD	0.00	1.00	0
NWA	8.00	1.00	1
STH	1.50	1.00	1
NTH	0.00	1.00	0
STH	1.00	2.00	3

**Appendix 3.1.** Steps taken to assess and standardize the quality of the Paleobiology Database dataset.

#### DATA ANNOTATION ACCURACY AND COMPLETENESS

- Remove duplicated references.

##### Stratigraphy

- Correct stage (“early\_interval” and “late\_interval”) misspellings.
- Check primary reference to check the possibility of narrowing down coarse age assignments (e.g. Cretaceous).
- Check primary reference for occurrences that span for more than 40 my.

##### Geography

- If country (“cc”) field is blank, use primary reference to locate country where specimens were found. If occurrence is not located nearby a landmass, use NA.

##### Taxonomy

- Include higher classification for unclassified genera.
- Correct misspellings for all taxonomic ranks.

#### SAMPLING BIASES

- Stratigraphic bias: estimate percentage of occurrences per time interval (Eras, Periods and Epochs and Stages).
- Geographic bias: estimate percentage of occurrences per country and continent.
- Taxonomic bias: estimate percentage of occurrences per major taxonomic groups.

#### TAXONOMIC ACCURACY (following WoRMS and Chapter 2)

- Check higher classification of each genus.
- Check status of families, genera and species.
- If occurrence is to species level, check species classification.
- Check if temporal information for each genus is accurate using Kroh & Smith (2010), Smith & Kroh (2011), and additional literature. Then, if 30 my beyond the FAD or LAD, check primary reference and additional literature.

#### DATA STANDARDIZATION

- Substitute regional stages (“early\_interval” and “late\_interval”) for overlapping international stages.
- Standardize minimum and maximum ages (“min\_ma” and “max\_ma”) following the International Chronostratigraphic Chart 2018.

**Appendix 3.2.** Assignment of geologic stages into approximately 10 million-year bins.

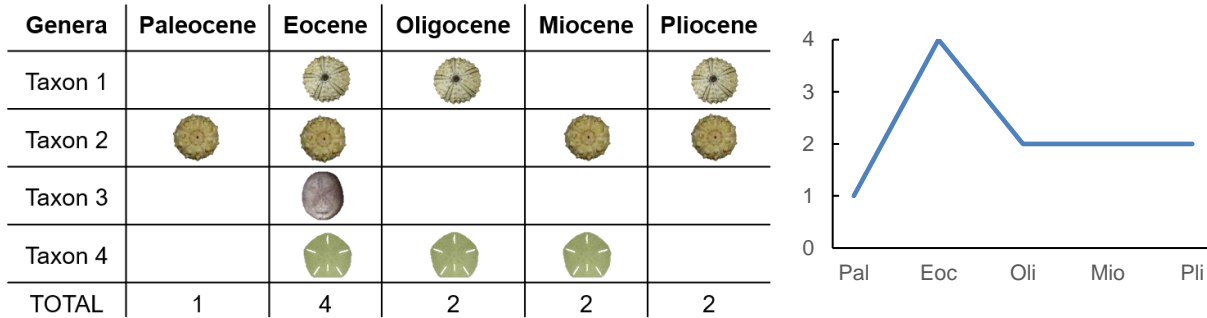
<b>10 my bins</b>	<b>Duration (my)</b>	<b>Stages</b>
Cenozoic 7	7.25	Holocene Pleistocene Calabrian Gelasian Piacenzian Pliocene Zanclean Messinian
Cenozoic 6	8.72	Tortonian Serravallian Langhian
Cenozoic 5	11.85	Burdigalian Aquitanian Chattian
Cenozoic 4	9.98	Rupelian Priabonian
Cenozoic 3	10	Bartonian Lutetian
Cenozoic 2	8.2	Ypresian
Cenozoic 1	10	Thanetian Selandian Danian
Cretaceous 8	6.1	Maastrichtian
Cretaceous 7	11.5	Campanian
Cretaceous 6	10.3	Santonian Coniacian Turonian
Cretaceous 5	6.6	Cenomanian
Cretaceous 4	12.5	Albian
Cretaceous 3	12	Aptian
Cretaceous 2	7.9	Barremian Hauterivian
Cretaceous 1	12.1	Valanginian Berriasian
Jurassic 5	12.3	Tithonian Kimmeridgian
Jurassic 4	13	Oxfordian Callovian Bathonian Bajocian
Jurassic 3	12.4	Aalenian Toarcian
Jurassic 2	8.1	Pliensbachian
Jurassic 1	10.5	Sinemurian Hettangian
Triassic 4	7.2	Rhaetian
Triassic 3	18.5	Norian

**Appendix 3.2.** Continued.

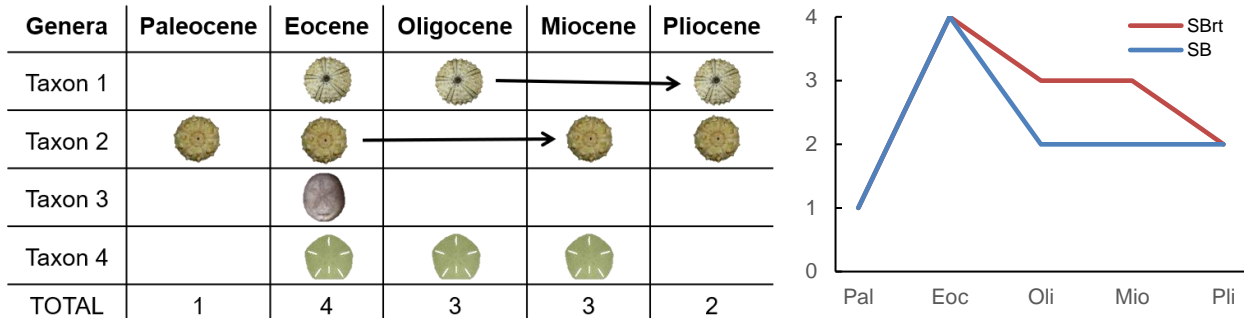
<b>10 my bins</b>	<b>Duration (my)</b>	<b>Stages</b>
Triassic 2	15	Carnian Ladinian
Triassic 1	10	Anisian Olenekian
Triassic 1		Induan
Permian 4	7.1	Changhsingian Wuchiapingian
Permian 3	13.85	Capitanian Wordian Roadian
Permian 2	10.55	Kungurian
Permian 1	15.4	Artinskian Sakmarian Asselian
Carboniferous 6	8.1	Gzhelian Kasimovian
Carboniferous 5	8.2	Moscovian
Carboniferous 4	8	Bashkirian
Carboniferous 3	7.7	Serpukhovian
Carboniferous 2	15.8	Visean
Carboniferous 1	12.2	Tournaisian
Devonian 5	13.3	Famennian
Devonian 4	10.5	Frasnian
Devonian 3	10.6	Givetian Eifelian
Devonian 2	14.3	Emsian
Devonian 1	11.6	Pragian Lochkovian
Silurian 2	14.2	Pridoli Ludfordian Gorstian Homerian Sheinwoodian
Silurian 1	10.4	Telychian Aeronian Rhuddanian
Ordovician 5	14.6	Hirnantian Katian Sandbian
Ordovician 4	8.9	Darriwilian

**Appendix 3.3.** Illustration of the methods used to estimate the diversity curves and the range-through assumption. Eoc, Eocene; Mio, Miocene; Oli, Oligocene; Pal, Paleocene; Pli, Pliocene.

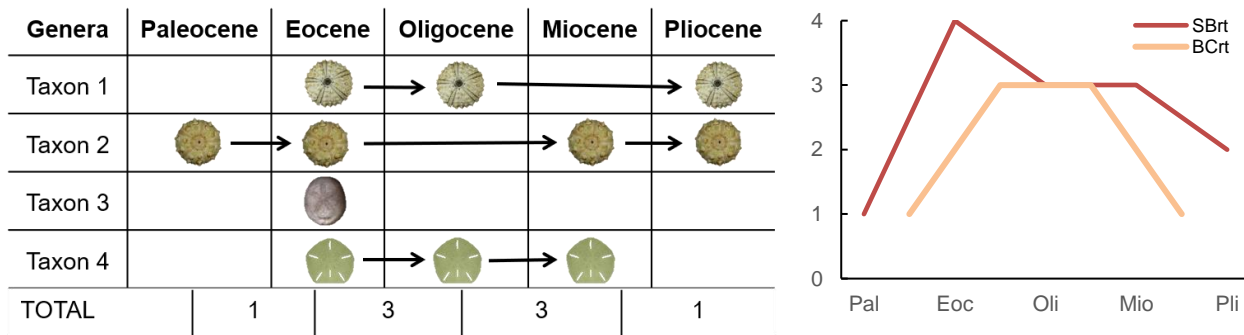
Sample in bin method (SB): total is the number of taxa found in each time interval.












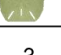

Range-through assumption (rt): assumes that if a taxon has been found in the Eocene and in the Miocene, it must have occurred in the Oligocene. Range-throughs are indicated by an arrow.












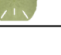

Boundary-crosser method (BC): total is the number of taxa crossing a boundary; therefore, it is estimated at each boundary. It includes the range-through assumption and, by definition, it excludes singletons (e.g. Taxon 3).



Sample in bin method corrected for the sampling completeness (CC): total is an estimation of the sampled in bin (SB) diversity with the range-through (RT) assumption corrected for the sampling completeness at each time interval.

Genera	Paleocene	Eocene	Oligocene	Miocene	Pliocene
Taxon 1				→	
Taxon 2			→		
Taxon 3					
Taxon 4					
TOTAL (SB + RT)	1	4	3	3	2

First and last occurrences are excluded from the calculation because their existence is certain; therefore, their inclusion would increase the completeness of their respective time intervals.

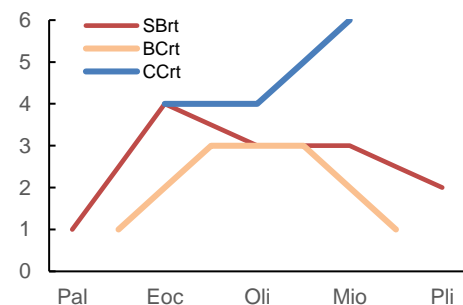
Genera	Paleocene	Eocene	Oligocene	Miocene	Pliocene
Taxon 1				→	
Taxon 2			→		
Taxon 3					
Taxon 4					

Preservation potential is calculated by dividing the number of range-through taxa (excluding the first and last occurrences) by the number of taxa that expected to be found in that time interval (unsampled taxa).

Range-through taxa	0	1	2	1	0
Expected taxa	0	1	3	2	0
Preservation potential	0	1	0.67	0.5	0

The corrected diversity is then obtained by dividing the sampled in bin diversity with the range-through assumption by the completeness of each time interval. First and last time intervals will not have a diversity measure because no taxon range-through them.

TOTAL (SB + RT)	1	4	3	3	2
Preservation potential	-	1	0.67	0.5	-
TOTAL corrected diversity	-	4	4	6	-





**Appendix 3.4.** Geographic distribution of the Paleobiology Database entries (in black). Distribution is by country (not specific localities within countries), except for Antarctica.

